#370 4/30/80

DO NOT MICROFILM COVER

Lib. 1411

SAN-20500-1(Vol.5)

CONCEPTUAL DESIGN OF ADVANCED CENTRAL RECEIVER POWER SYSTEMS

Volume 5. Final Technical Report

By
A. S. Brower
J. F. Doyle
E. E. Gerrels
A. C. Ku
B. D. Pomeroy
J. M. Roberts
R. M. Salemme

MASTER

June 29, 1979

Work Performed Under Contract No. EM-78-C-03-1725

General Electric Company
Schenectady, New York

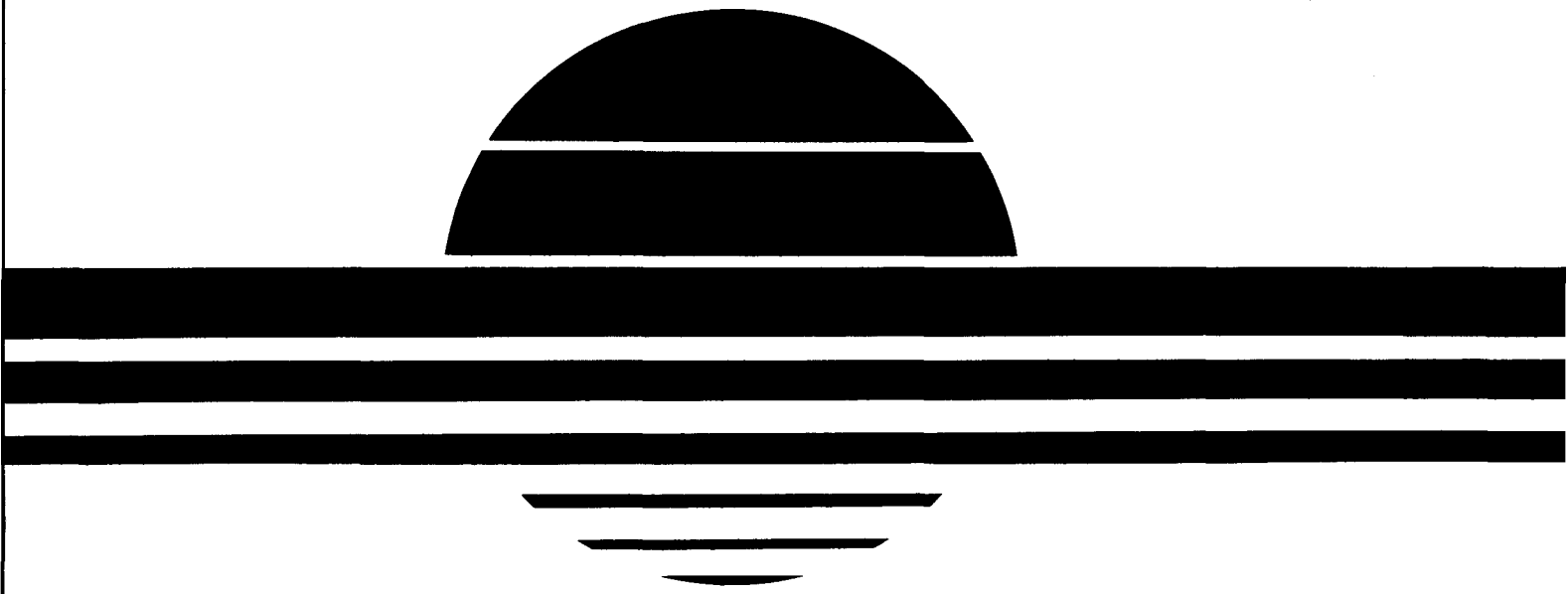

U.S. Department of Energy

Solar Energy

DISTRIBUTION OF THIS DOCUMENT IS UNLIMITED

DISCLAIMER

This report was prepared as an account of work sponsored by an agency of the United States Government. Neither the United States Government nor any agency thereof, nor any of their employees, makes any warranty, express or implied, or assumes any legal liability or responsibility for the accuracy, completeness, or usefulness of any information, apparatus, product, or process disclosed, or represents that its use would not infringe privately owned rights. Reference herein to any specific commercial product, process, or service by trade name, trademark, manufacturer, or otherwise does not necessarily constitute or imply its endorsement, recommendation, or favoring by the United States Government or any agency thereof. The views and opinions of authors expressed herein do not necessarily state or reflect those of the United States Government or any agency thereof.

DISCLAIMER

Portions of this document may be illegible in electronic image products. Images are produced from the best available original document.

DISCLAIMER

"This book was prepared as an account of work sponsored by an agency of the United States Government. Neither the United States Government nor any agency thereof, nor any of their employees, makes any warranty, express or implied, or assumes any legal liability or responsibility for the accuracy, completeness, or usefulness of any information, apparatus, product, or process disclosed, or represents that its use would not infringe privately owned rights. Reference herein to any specific commercial product, process, or service by trade name, trademark, manufacturer, or otherwise, does not necessarily constitute or imply its endorsement, recommendation, or favoring by the United States Government or any agency thereof. The views and opinions of authors expressed herein do not necessarily state or reflect those of the United States Government or any agency thereof."

This report has been reproduced directly from the best available copy.

Available from the National Technical Information Service, U. S. Department of Commerce, Springfield, Virginia 22161.

Price: Paper Copy $15.00
Microfiche $3.50

DO NOT MICROFILM
COVER

SAN-20500-1(Vol.5)
Distribution Category UC-62d

CONCEPTUAL DESIGN OF ADVANCED CENTRAL RECEIVER POWER SYSTEMS

Volume V

U.S. Department of Energy

Contract No. DE-AC03-78ET20500

Final Technical Report

June 29, 1979

GENERAL ELECTRIC

NOTICE
PORTIONS OF THIS REPORT ARE ILLEGIBLE.
It has been reproduced from the best available copy to permit the broadest possible availability.

DISTRIBUTION OF THIS DOCUMENT IS UNLIMITED

ACKNOWLEDGMENTS

This report has been prepared by General Electric Corporate Research and Development for the Department of Energy. The principal authors are:

A.S. Brower, GE
J.F. Doyle, Kaiser Engineers
E.E. Gerrels, GE
A.C. Ku, GE
B.D. Pomeroy, GE
J.M. Roberts, GE
R.M. Salemme, GE

B.D. Pomeroy was Technical Manager for this study, R.M. Salemme was Deputy Program Manager, and G.R. Fox was Program Manager.

Other General Electric components participating in this program were the Energy Systems Programs Department, the Advanced Reactor Systems Department, the Electric Utility Systems Engineering Department, and the Medium Steam Turbine Department. Kaiser Engineers, Foster Wheeler Development Corporation, and the University of Houston Energy Laboratory were subcontractors.

This report is based upon work performed by the authors and the following technical contributors:

J.C. Amos, GE
G. Carli, Foster Wheeler
D.H. Hall, GE
V. Kadambi, GE
F.V. Kahle, Kaiser Engineers
W.L. Kuhre, Kaiser Engineers
R.G. Livingston, GE
F.W. Lipps, Univ. of Houston
W.D. Marsh, GE
T.V. Narayanan, Foster Wheeler
J.J. Reilly, GE
C.N. Spalaris, GE
L.L. Vant Hull, Univ. of Houston
M.D. Walzel, Univ. of Houston

The authors would also like to thank the following people for their assistance and advice:

S.C. Bialy, GE
E. Brooks, GE
D.H. Brown, GE
K. Chen, GE
R.N. Clayton, GE
A.V. Curinga, GE
K.J. Daniel, GE
J.A. Elsner, GE
F.N. Mazandarany, GE
G. Oganowski, GE
F. Tippets, GE

TABLE OF CONTENTS

Volume I, Part 1

Volume I, Part 2

TABLE OF CONTENTS (Cont'd)

TABLE OF CONTENTS (Cont'd)

Volume II

TABLE OF CONTENTS (Cont'd)

Volume III

TABLE OF CONTENTS (Cont'd)

Volume IV

TABLE OF CONTENTS (Cont'd)

Volume V

TABLE OF CONTENTS (Cont'd)

LIST OF ILLUSTRATIONS

Volume V

LIST OF ILLUSTRATIONS (Cont'd)

LIST OF TABLES

LIST OF TABLES (Cont'd)

LIST OF TABLES (Cont'd)

LIST OF TABLES (Cont'd)

Appendix A

EFFICIENCY AND COST ESTIMATES FOR CAVITY RECEIVERS - PARAMETRIC ANALYSIS

EFFICIENCY

Consider the receiver cavity shown in Figure A-1 with incident solar flux of q_s. The absorbed thermal power is given by

$$Q_{sol} = q_s \alpha_\epsilon a \qquad \text{(A-1)}$$

where q_s = incident solar flux (MW/m^2)

α_ϵ = effective absorptivity of the aperture

$a = S^2$, area of aperture

If the solar absorption process inside the cavity is assumed diffuse, then

$$\alpha_\epsilon = \left[1 - \frac{a}{A}\left(1 - \frac{1}{\alpha}\right)\right]^{-1} \qquad \text{(A-2)}$$

where A = area to tubed surface = $S^2 + 4Sd$

α = tubed surface absorptivity

The average surface temperature in the cavity can be approximated by

$$T = \frac{T_H + T_L}{2} + q_s\left(\frac{a}{A}\right)\frac{1}{U_T} \qquad \text{(A-3)}$$

where T_H = sodium peak temperature

T_L = sodium inlet temperature

U_T = tube wall conductance

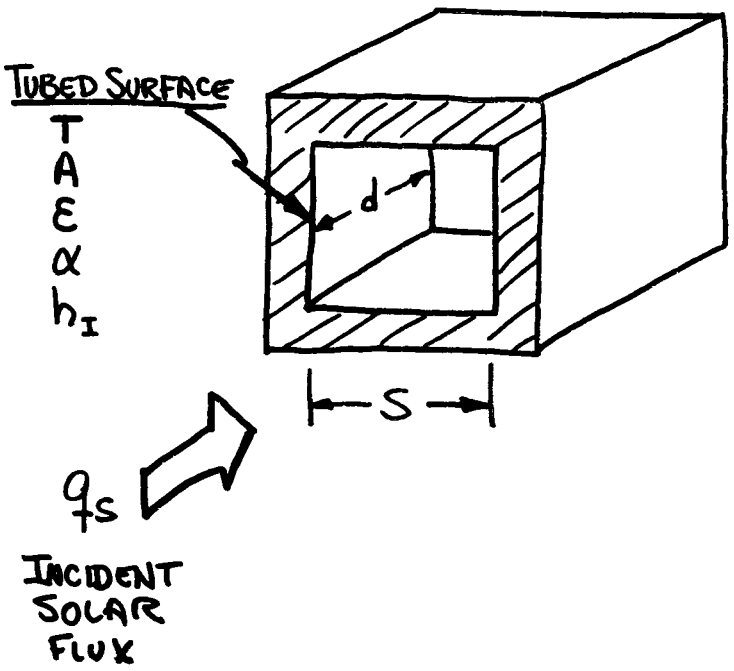

Figure A-1. Cavity Receiver Model

The tube wall conductance is given by

$$\frac{1}{U_T} = \frac{1}{h_N}\left(\frac{1}{1-2\delta/d_o}\right) + \frac{d_o}{2K_W}\ln\left[\frac{1}{1-2\delta/d_o}\right] \quad \text{(A-4)}$$

where h_N = sodium heat transfer coefficient

δ = tube wall thickness

d_o = tube OD

K_W = thermal conductivity of wall

The average surface temperature is used to compute the radiation losses as follows:

$$Q_{RAD} = \sigma \varepsilon_\epsilon a \left[T^4 - T_A^4\right] \quad \text{(A-5)}$$

where σ = Stefan Boltzmann constant

$\varepsilon_\epsilon = \left[1 - \frac{a}{A}\left(1 - \frac{1}{\varepsilon}\right)\right]^{-1}$ = effective emissivity

T_A = air temperature

similarly the connection losses are given by

$$Q_{CONV} = h_I A (T - T_A) \quad \text{(A-6)}$$

The total thermal power transferred to the sodium is

$$Q_T = Q_{SOL} - Q_{RAD} - Q_{CONV} \quad \text{(A-7)}$$

Receiver efficiency is given by

$$\eta = \frac{Q_T}{q_s a} \quad \text{(A-8)}$$

Tables A-1 and A-2 show the application of these equations to the flat receiver, glass heliostat case.

As the depth of the receiver increases, panels are added to cover the four sides of the box (d x s). The cost of each panel including insulation is approximately $90,000 and each panel requires an additional EM pump for flow control ($200,000). The structure to support these panels also increases in size. These costs increase the receiver/collector system cost as shown in Tables A-3 and A-4.

Table A-1

CAVITY RECEIVER PERFORMANCE INPUT DATA

FLAT RECEIVER, GLASS HELIOSTAT (ref. table 3.2-4)

INCIDENT POWER	401.29	MWt
CONVECTION LOSS	-3.92	
RADIATION LOSS	-11.40	
REFLECTION LOSS	-20.06	
HEAT TO SODIUM	365.91	
PUMP THERMAL INPUT .9×6.78	+ 6.10	
TOWER BASE	372.01	MWt

$q''_s = 401.29/(20.81)^2 = .927\ MW/m^2$

$S = 20.81\ m$

$\sigma = .1714E-8\ Btu/ft^2 hr\ ^\circ R^4$

$h_z = 2.90\ Btu/hr\ ft^2\ ^\circ F$

$T_A = 82.6\ ^\circ F$

$T_H = 1100^\circ F$

$T_L = 725^\circ F$

$\alpha = .95$

$\varepsilon = .90$

$\delta = .035''$

$d_o = 1.00''$

$h_W = 7000\ Btu/hr\ ft^2 ^\circ F$

$K_W = 10\ Btu/hr\ ft\ ^\circ F$

$U_T = 2172\ Btu/hr\ ft^2 ^\circ F$

Table A-2

CAVITY RECEIVER PERFORMANCE SUMMARY

d	(m)	0	5	10	15	20.81
T	(°F)	1048	981	959	947.4	939.6
α_ϵ	(%)	95.0	97.4	98.2	98.7	99.0
ϵ_ϵ	(%)	90.0	94.6	96.3	97.2	97.8
Q_{SOL}	(MWt)	381.4	391.0	394.3	396.1	397.3
Q_{RAD}	(MWt)	10.7	9.4	8.9	8.7	8.6
Q_{CONV}	(MWt)	3.8	7.0	10.1	13.3	17.0
Q_{TOT}	(MWt)	366.8	374.6	375.3	374.1	371.7
η	(%)	91.4	93.3	93.5	93.2	92.6

Table A-3

CAVITY RECEIVER COST MODEL

FLAT RECEIVER, GLASS HELIOSTAT (ref. table 3.2-4)

C_o = 70.398 M# (Rec'r, tower, riser/downcomer, pumps, field, land, wire & fixed cost)

Q_o = .846E6 MWth annual tower base energy

Cost of panels 1.535 / 17 = .09029 M#

$$C_{PANEL} = .09029\,(17 + 4n)$$

n = number of panel widths in depth
= d / 1.2241 m

Cost of structure assume this scales as diagonal

$$C_{STRUCT} = .908 \text{ M\#} \frac{\sqrt{d^2 + 2(17)^2}}{\sqrt{2(17)^2}} = .0378\sqrt{d^2 + 578}$$

Cost of pumps 200,000# for each additional 6m pump

$$C_{PUMPS} = 3.39 + [2.507 + .0341(T+H)]\left(\frac{Q_N}{376}\right) + (4n)\,.20 \text{ M\#}$$

$$\Delta C = C_{PANEL} - C^o_{PANEL} + C_{STRUCT} - C^o_{STRUCT} + C_{PUMP} - C^o_{PUMP}$$

$$\boxed{\Delta C = .29029\,(4n) + .908\left(\sqrt{1 + d^2/578} - 1\right) + 9.9955\left(\eta/\eta_o - 1\right)}$$

$$\boxed{C = C_o + \Delta C}$$

$$\boxed{Q = Q_o\,(\eta/\eta_o)}$$

$$\boxed{FOM = C/Q}$$ Figure of Merit

Table A-4

CAVITY RECEIVER COST AND PERFORMANCE SUMMARY

d (m)	0	4.90	9.79	14.69	20.81
n	0	4	8	12	17
η (%)	91.4	93.3	93.5	93.2	92.6
ΔC (M$)	0	4.871	9.591	14.287	20.164
C (M$)	70.398	75.269	79.989	84.685	90.562
Q (TWth)	.846	.864	.865	.863	.857
Form ($/MWh)	83.2	87.1	92.4	98.1	105.7

$Q_o = .846$ TWth

$C_o = 70.398$ M$

$\eta_o = 91.4$ %

Appendix B

ABSORBER LOSS CALCULATIONS FOR PARAMETRIC ANALYSIS

Temperature distributions are shown in Figures B-1 through B-4 for the four cases of flat and cylindrical receivers at 1100 F and 1300 F. The inset in these figures gives the data used to compute the temperatures in nodes 1 and 9; the temperatures in nodes 2 through 8 were obtained by linear interpolation. The panel flowrate, W, was obtained by summing the heat input for all nodes and dividing by the product of Cp ΔT.

$$W = \sum_{n=1}^{N} q_s \Delta x \Delta y / C_p / (T_H - T_c) \qquad \text{(B-1)}$$

where

q_s = heat flux from flux plots

C_p = sodium specific heat

T_H = sodium peak temperature

T_c = sodium inlet temperature

The losses computed from these temperature distributions are given in Tables B-1 through B-4.

All calculations were performed on the Hewlett Packard-65 programmable calculator using the equations described in Section 3.3.2.

The tube sizes selected are not standard. The size was set to fill the space provided by the panel width and to provide a pressure drop in the hot panel (No. 1) of less than 10 psi.

NODE	T_{Na}	N_T	K_N	C_P	δ	d_o	K_W
9	1100	39	36.1	.300	.035	1.009	10.7
1	725	39	41.8	.307	.035	1.009	9.6

$\Delta x = \Delta y = 1$ m

TEMPERATURES (°F) - Two

PANEL No. \ NODE No.	9	8	7	6	5	4	3	2	1
1	1133	1138	1144	1148	1151	1155	1155	1155	1155
2	1098	1107	1119	1131	1143	1156	1163	1167	1163
3	1062	1075	1094	1114	1135	1156	1170	1179	1177
4	1027	1045	1069	1097	1127	1157	1178	1191	1190
5	991	1014	1045	1081	1120	1158	1186	1203	1203
6	956	982	1020	1064	1112	1158	1193	1214	1215
7	920	951	995	1047	1104	1159	1201	1226	1230
8	885	920	970	1030	1096	1159	1208	1238	1243
℄ 9	849	889	945	1013	1088	1160	1216	1250	1261
W(lb/hr) $\times 10^{-6}$	.2542	.3668	.4412	.5674	.7071	.8429	.9531	1.022	1.046

Figure B-1. Flat Absorber - 1100 F Case - Temperature Distribution

NODE	T_{INL}	N_T	K_N	G_P	δ	d_o	K_W
9	1300	51	33.4	.300	.035	.772	11.5
1	680	51	42.5	.308	.035	.772	9.6

$\Delta x = \Delta y = 1$ m

TEMPERATURES (°F) - T_{WO}

PANEL No. \ NODE No.	9	8	7	6	5	4	3	2	1
1	1330	1336	1341	1345	1348	1350	1352	1353	1353
2	1263	1274	1285	1297	1309	1320	1328	1334	1335
3	1197	1211	1229	1248	1270	1298	1305	1314	1317
4	1130	1149	1172	1200	1230	1259	1281	1295	1219
5	1063	1087	1116	1152	1191	1228	1258	1275	1281
6	996	1024	1060	1103	1152	1198	1234	1256	1263
7	930	962	1004	1055	1113	1167	1210	1237	1245
8	863	899	947	1006	1073	1137	1187	1217	1227
℄ 9	796	837	891	958	1034	1106	1163	1198	1209
W (lb/hr) $\times 10^{-5}$	1.539	2.039	2.672	3.436	4.282	5.105	5.772	6.188	6.329

Figure B-2. Flat Absorber - 1300 F Case - Temperature Distribution

Node	T_{Na}	N_T	K_N	C_P	δ	d_o	K_W
9	725	129	41.8	.3065	.035	.5993	9.58
1	1100	129	36.1	.3000	.035	.5993	10.67

TEMPERATURES (°F) – T_{WO}

$\Delta X = 1.9635$ m

$\Delta y = .88235$ m

Panel No. \ Node No.	12	11	10	9	8	7	6	5	4	3	2	1
1	1101	1101	1102	1103	1105	1109	1112	1114	1118	1121	1123	1125
2	1064	1064	1065	1068	1072	1078	1084	1088	1093	1097	1100	1102
3	1027	1027	1029	1032	1039	1048	1056	1061	1068	1073	1077	1079
4	990	990	992	997	1006	1017	1027	1035	1042	1048	1053	1056
5	953	953	955	962	973	986	999	1009	1017	1024	1030	1034
6	915	916	918	926	939	955	971	983	992	1000	1007	1011
7	878	879	882	891	906	925	943	956	967	976	984	988
8	841	842	845	855	873	894	914	930	941	956	960	965
9	804	805	808	820	840	863	886	903	916	927	937	942
W(lb/hr) x 10^{-6}	.1932	.2015	.2207	.2623	.3216	.4412	.5189	.5836	.6523	.7104	.7541	.7812

NORTH FACE ℄

Figure B-3. Cylindrical Absorber - 1100 F Case - Temperature Distribution

GENERAL ELECTRIC

NODE	T_{N_2}	N_T	K_N	C_P	δ	d_o	K_w
9	680	165	42.5	.3075	.035	.4685	9.58
1	1300	165	33.4	.3000	.035	.4685	11.50

TEMPERATURES (°F) - T_{WO}

$\Delta x = 1.9635$ m

$\Delta y = .88235$ m

NODE NO. → / PANEL NO. ↓	12	11	10	9	8	7	6	5	4	3	2	1
1	1301	1301	1302	1303	1305	1308	1311	1313	1317	1319	1322	1323
2	1233	1233	1234	1237	1241	1246	1252	1256	1261	1264	1268	1269
3	1165	1165	1166	1170	1177	1185	1193	1198	1205	1209	1214	1216
4	1096	1097	1098	1104	1112	1123	1133	1141	1148	1154	1160	1162
5	1028	1029	1031	1037	1048	1061	1074	1084	1092	1099	1106	1109
6	960	960	963	971	984	999	1015	1026	1036	1044	1051	1055
7	892	892	895	904	920	938	956	969	980	989	997	1001
8	823	824	827	838	855	876	896	911	923	934	943	948
9 (℄)	755	756	759	771	791	814	837	854	867	879	889	894
W (lb/hr) $\times 10^{-5}$	1.1727	1.2201	1.3369	1.5885	1.9478	2.6719	3.1424	3.5346	3.9504	4.3024	4.5668	4.7310

SOUTH FACE — NORTH FACE ℄

Figure B-4. Cylindrical Absorber - 1300 F Case - Temperature Distribution

GENERAL ELECTRIC

Table B-1

SUMMARY - NORTH FIELD - 1100 F

Panel No.		Convective Losses MW_t	Radiative Losses MW_t
2		0.1758	0.6319
3		0.1731	0.6072
4		0.1692	0.5684
5		0.1635	0.5194
6		0.1580	0.4735
7		0.1524	0.4349
8		0.1479	0.4036
9		0.1447	0.3827
		1.2846	4.0216
		x 2	x 2
		2.5692	8.0432
1		0.1757	0.6338
	Totals	2.7449	8.6770

Table B-2

SUMMARY - NORTH FIELD - 1300 F

Panel No.		Convective Losses MW_t	Radiative Losses MW_t
2		0.1883	0.7669
3		0.1856	0.7391
4		0.1813	0.6971
5		0.1758	0.6448
6		0.1701	0.5950
7		0.1647	0.5539
8		0.1604	0.5214
9		0.1570	0.4967
		1.3832	5.0149
		x 2	x 2
		2.7664	10.0298
1		0.1890	0.7757
	Totals	2.9554	10.8055

Table B-3

SUMMARY - 360° FIELD 1100 F

Panel No.		Convective Losses MW_t	Radiative Losses MW_t
1		0.0745	0.7293
2		0.1757	0.7230
3		0.2198	0.7123
4		0.2332	0.6999
5		0.2312	0.6852
6		0.2114	0.6693
7		0.1158	0.6484
8		0.0685	0.6269
9		0.0705	0.6104
10		0.0757	0.6009
11		0.0951	0.5977
12		0.1118	0.5971
		1.6832	7.9004
		x 2	x 2
	Totals	3.3664	15.8008

Table B-4

SUMMARY 360° FIELD 1300 F

Panel No.		Convective Losses MW_t	Radiative Losses MW_t
1		0.0809	0.9361
2		0.1906	0.9299
3		0.2385	0.9166
4		0.2533	0.9033
5		0.2513	0.8862
6		0.2300	0.8689
7		0.1261	0.8453
8		0.0748	0.8227
9		0.0772	0.8044
10		0.0828	0.7935
11		0.1040	0.7900
12		0.1222	0.7893
		1.8317	10.2862
		x 2	x 2
	Totals	3.6634	20.5724

Appendix C

SMALL ELECTROMAGNETIC PUMPS FOR PARAMETRIC ANALYSIS

The small electromagnetic (EM) pump heads were calculated using the analytical model detailed in Figure C-1. The pressure between any two points A and B (where flow is assumed to go from B to A) is given by

$$P_B - P_A = \frac{.02517}{\rho}\left(\frac{W_A^2}{d_A^4} - \frac{W_B^2}{d_B^4}\right)\frac{1}{144} + (z_A - z_B)\frac{\rho}{144} + \Delta P_{FRICT} \qquad \text{(C-1)}$$

$$\Delta P_{FRICT} = f\left(\frac{L_e}{D}\right)\frac{V^2}{2g}\frac{\rho}{144}$$

where

ρ = fluid density

W = mass flowrate

d = pipe diameter

z = elevation (see Figure a)

f = friction factor

L_e = equivalent length of pipe

g = constant

V = fluid speed

This method is the same as that used in Task 4 (see Section 5.3.4 for more details). The calculated values used in Task 2 are contained in Tables C-1 and C-2 for the north field configuration at 1100 F and 1300 F respectively. Pressure losses in the 360° field cases were assumed equal to the corresponding north field cases.

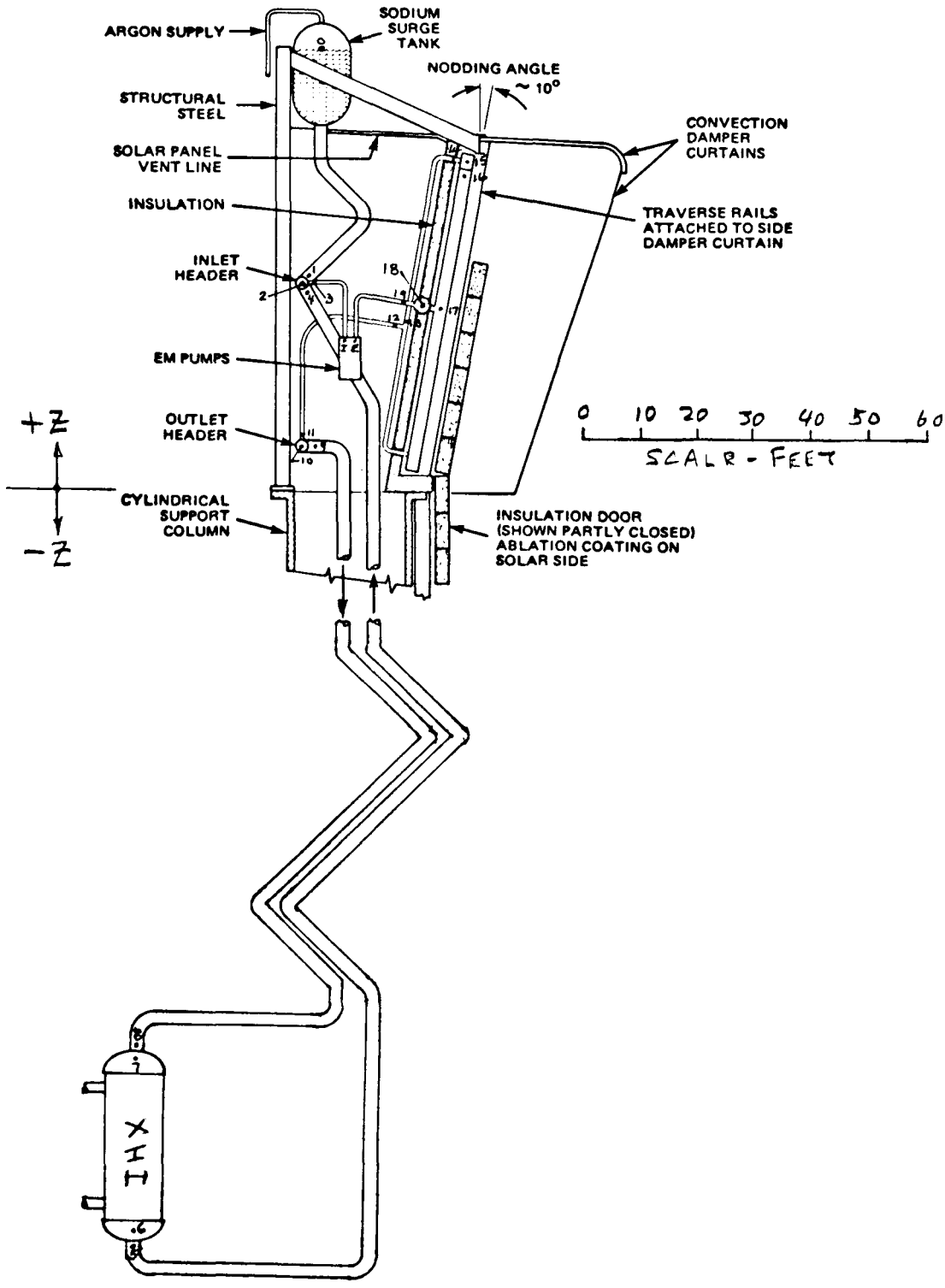

Figure C-1. Analytical Model for Receiver Subsystem Pressure Estimates

Table C-1

RECEIVER SUBSYSTEM PRESSURES - NORTH FIELD - 1100 F

SEGMENT		d_A	d_B	W_A	W_B	L_{EQ}	Z_A	Z_B	$\Delta P_{FRCT.}$	P_A	P_B
A	B	ID-INCH	ID-INCH	#/HR x 10^{-6}	#/HR x 10^{-6}	FT.	FT.	FT.	psid	psig	psig
0	1	48.0	10.25	0	0	40	+75	+35	0	0	14.92
1	2	10.25	27.0	0	11.223	0	+35	+35	0	14.92	13.68
3	2	8.125	27.0	1.045	11.223	10	+35	+35	.23	13.68	13.98
I	3	8.125	8.125	1.045	1.045	30	+15	+35	.68	13.98	7.20
2	4	27	23.25	11.223	11.223	130	+35	+35	1.43	13.98	14.40
4	5	23.25	23.25	↓	↓	1596	+35	-492	17.57	14.46	228.49
5	6	23.25	48.0	↓	↓	35	-492	-490	.39	228.49	230.25
6	7	48.0	48.0	↓	↓	0	-490	-443	10	230.25	223.24
7	8	48.0	23.25	↓	↓	62	-443	-441	.69	223.24	220.97
8	9	23.25	23.25	↓	↓	1486	-441	+5	16.51	220.97	80.92
9	10	23.25	27.0	↓	↓	130	+5	+5	1.44	80.92	83.44
10	11	27.0	8.125	↓	1.045	42	+5	+5	.96	83.44	84.32
11	12	8.125	8.125	1.045	1.045	50	+5	+30	1.14	84.32	76.68
12	13	8.125	6.125	1.045	.523	32	+30	+30	.80	76.68	77.80
13	14	6.125	6.125	.523	.523	35	+30	+60	.88	77.80	68.15
14	15	6.125	12.25	.523	.523	9.5	+60	+60	.24	68.15	69.39
15	16	12.25	.9395	.523	.0134	2.6	+60	+60	.67	69.39	68.85
16	17	19395	.9395	.0134	.0134	38	+60	+30	10	68.85	89.72
17	18	.9395	15.375	.0134	1.045	1.3	+30	+30	.33	89.72	91.15
18	19	15.375	8.125	1.045	1.045	43	+30	+30	.97	91.15	90.92
19	E	8.125	8.125	1.045	1.045	30	+30	+15	.68	90.92	97.19

Table C-2

RECEIVER SUBSYSTEM PRESSURES - NORTH FIELD - T300 F

SEGMENT		d_A	d_B	W_A	W_B	L_{EQ}	Z_A	Z_B	$\Delta P_{FRCT.}$	P_A	P_B
A	B	ID-INCH	ID-INCH	#/HR x 10^6	#/HR x 10^6	FT.	FT.	FT.	psid	psig	psig
0	1	48	10.25	0	0	40	+75	+35	0	0	15.02
1	2	10.25	23.25	0	6.80	0	+35	+35	0	15.02	14.20
3	2	6.125	23.25	.633	6.80	7.5	+35	+35	.26	14.20	15.12
I	3	6.125	6.125	.633	.633	30	+15	+35	1.06	15.12	.67
2	4	23.25	17.375	6.80	6.80	102	+35	+35	1.83	15.12	15.15
4	5	17.375	17.375	↓	↓	1596	+35	-492	28.75	15.15	241.81
5	6	17.375	48.0	↓	↓	25	-492	-490	.45	241.81	244.09
6	7	48.0	48.0	↓	↓	0	-490	-443	10	244.09	237.28
7	8	48.0	17.375	↓	↓	47	-443	-441	.87	237.28	234.62
8	9	17.375	17.375	↓	↓	1486	-441	+5	27.6	234.62	110.90
9	10	17.375	23.25	↓	↓	102	+5	+5	1.88	110.90	114.79
10	11	23.25	6.125	↓	.633	34	+5	+5	1.24	114.79	115.31
11	12	6.125	6.125	.633	.633	50	+5	+30	1.81	115.31	108.63
12	13	6.125	4.09	.633	.316	22	+30	+30	1.57	108.63	109.79
13	14	4.09	4.09	.316	.316	35	+30	+60	2.50	109.79	102.11
14	15	4.09	10.25	↓	↓	5.8	+60	+60	.42	102.11	104.52
15	16	10.25	.702	↓	.00620	1.8	+60	+60	.47	104.52	104.14
16	17	.702	.702	.00620	.00620	32	+60	+30	10	104.14	124.87
17	18	.702	12.25	.00620	.633	1.1	+30	+30	.28	124.87	125.88
18	19	12.25	6.125	.633	↓	35	+30	+30	1.24	125.88	125.74
19	E	6.125	6.125	↓	↓	30	+30	+15	1.06	125.74	132.43

The pressure differential calculated across the EM pumps $\Delta P_E = (P_E - P_I)$ and other components corresponds to full flow in the hot panel flow. Corrections must be made to this reference value to account for:

- Changes in system temperature
- Changes in flowrate from panel to panel in the receiver
- Changes in tower height which directly affect the riser downcomer friction and density head terms

These changes were made by applying appropriate corrections and the pump heads for all of the parametric cases were calculated. The flowrates in each individual panel were established in the receiver loss calculations. With flows and heads known, the required pumping power can be calculated by the following relation:

$$MW_e = \frac{W \Delta p}{\rho \eta} \times 5.423E-8 \qquad \text{(C-2)}$$

where $W =$ mass flow of fluid

$\Delta p =$ pressure drop across pump

$\rho =$ fluid density

$\eta =$ pump efficiency (50%)

Part of this electrical input is lost to stator cooling air (20%); the rest goes into the sodium as mechanical work and thermal heating.

Figure C-2 was used to establish the capital costs for the EM pumps. The cost of the pumps is obtained by entering with the gpm flowrate and interpolating for the pump head. Table C-3 lists the detailed results of these calculations and shows the total receiver pumping power and pump cost for each of the parametric cases.

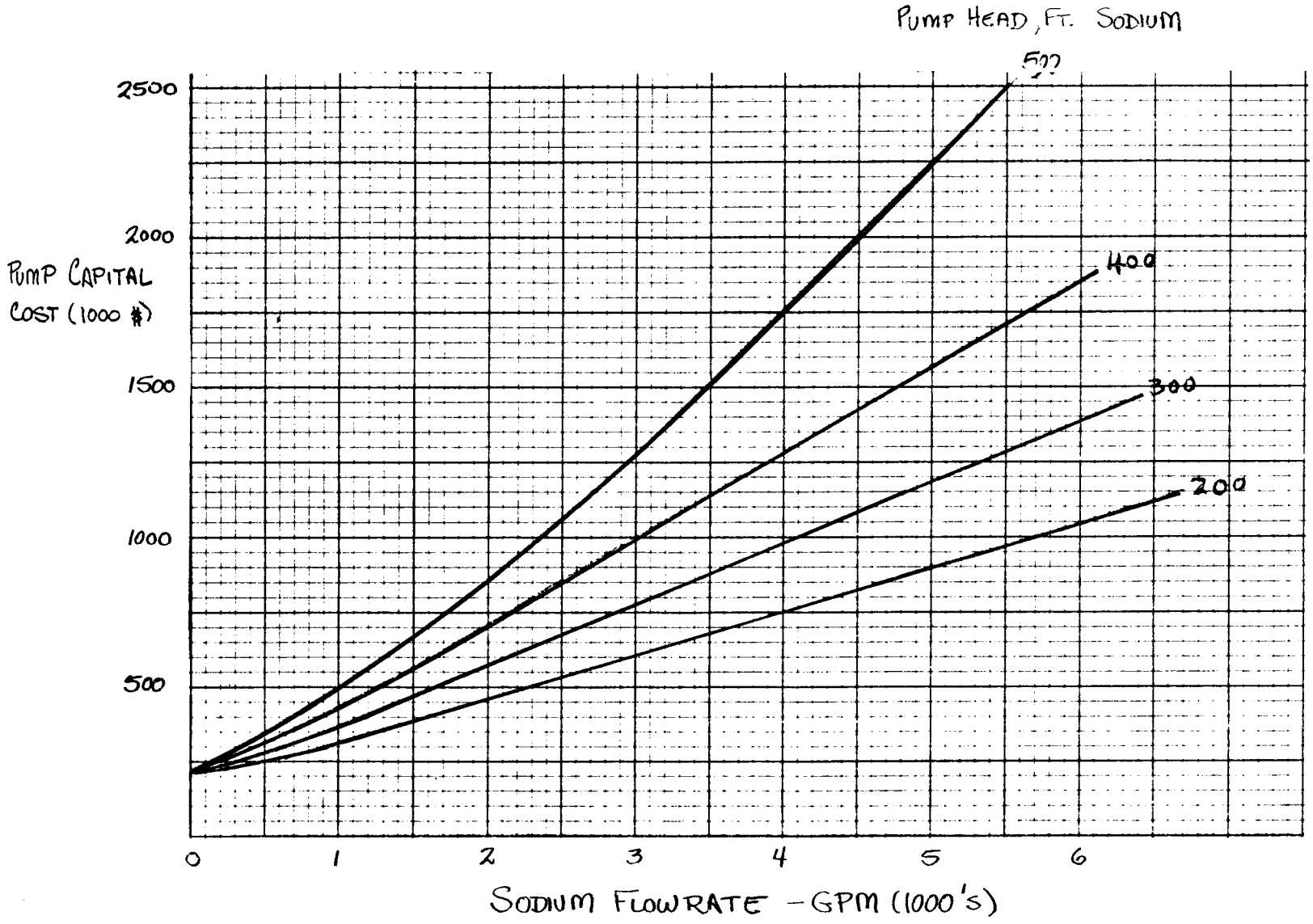

Figure C-2. Small Electromagnetic Pump Capital Costs

Table C-3

PUMPING POWER AND PUMP COST FOR RECEIVER SUBSYSTEM

FIELD 360° MAX. SODIUM TEMP. 1100 °F TOWER 150 M

PUMP NO.	NO. REQD	GPM	FT. HEAD	POWER MWe	CAPITAL $
1	2	1813	241	.142	.996 x 10^6
2		1750	240	.136	.960 x 10^6
3		1649	237	.127	.924 x 10^6
4		1514	234	.115	.840 x 10^6
5		1355	230	.101	.790 x 10^6
6		1204	227	.089	.730 x 10^6
7		1024	224	.074	.670 x 10^6
8		746	220	.053	.560 x 10^6
9		609	218	.043	.526 x 10^6
10		512	217	.036	.500 x 10^6
11		468	217	.033	.490 x 10^6
12		449	217	.032	.485 x 10^6
		(1.962 MWe)		TOTAL $	8.471 x 10^6 (24 PUMPS)

FIELD 360° MAX. SODIUM TEMP. 1100 °F TOWER 225 M

PUMP NO.	NO. REQD	GPM	FT. HEAD	POWER MWe	CAPITAL $
1	2	1815	270	.159	1.004 x 10^6
2		1750	269	.153	1.000 x 10^6
3		1649	266	.142	.940 x 10^6
4		1514	263	.129	.880 x 10^6
5		1355	259	.114	.830 x 10^6
6		1204	256	.100	.750 x 10^6
7		1024	253	.084	.700 x 10^6
8		746	249	.060	.596 x 10^6
9		609	247	.049	.550 x 10^6
10		512	246	.041	.524 x 10^6
11		468	246	.037	.510 x 10^6
12		449	246	.036	.504 x 10^6
		(2.208 MWe)		TOTAL $	8.788 x 10^6 (24 PUMPS)

Table C-3 (Cont'd)

FIELD 360° MAX. SODIUM TEMP. 1100 °F TOWER 300 m

PUMP NO.	NO. REQD	GPM	FT. HEAD	POWER MW	CAPITAL $
1	2	1813	299	.176	1.08 x10^6
2		1750	298	.169	1.04 x10^6
3		1649	295	.158	.998 x10^6
4		1514	292	.143	.930 x 10^6
5		1355	288	.127	.880 x 10^6
6		1204	285	.111	.790 x10^6
7		1024	282	.094	.730 x10^6
8		746	278	.067	.620 x10^6
9		609	276	.055	.570 x10^6
10		512	275	.046	.530 x10^6
11		468	275	.042	.520 x10^6
12		449	275	.040	.518 x10^6

(2.456 MWe) TOTAL $ 9.206 x10^6 (24 PUMPS)

FIELD 360° MAX. SODIUM TEMP. 1300 °F TOWER 150 m

PUMP NO.	NO. REQD	GPM	FT. HEAD	POWER MW	CAPITAL $
1	2	1091	324	.116	.840 x10^6
2		1054	323	.111	.820 x10^6
3		992	320	.104	.760 x10^6
4		911	317	.094	.730 x 10^6
5		815	313	.083	.690 x 10^6
6		725	310	.073	.660 x10^6
7		616	307	.062	.610 x10^6
8		449	303	.044	.536 x10^6
9		366	301	.036	.508 x10^6
10		308	300	.030	.484 x 10^6
11		281	300	.028	.470 x10^6
12		271	300	.027	.476 x10^6

(1.616 MWe) TOTAL $ 7.594 x10^6 (24 PUMPS

Table C-3 (Cont'd)

FIELD 360° MAX. SODIUM TEMP. 1300°F TOWER 225M

PUMP NO.	NO. REQD	GPM	FT. HEAD	POWER MWe	CAPITAL $
1	2	1091	369	.131	$.860 \times 10^6$
2		1054	367	.126	$.850 \times 10^6$
3		992	364	.118	$.820 \times 10^6$
4		911	361	.107	$.760 \times 10^6$
5		815	358	.095	$.740 \times 10^6$
6		725	355	.084	$.685 \times 10^6$
7		616	552	.071	$.640 \times 10^6$
8		449	347	.051	$.560 \times 10^6$
9		366	346	.041	$.524 \times 10^6$
10		308	345	.035	$.504 \times 10^6$
11		281	344	.032	$.494 \times 10^6$
12		271	344	.030	$.488 \times 10^6$

(1.842 MWe) TOTAL $ 7.925×10^6 (24 PUMPS)

FIELD 360° MAX. SODIUM TEMP. 1300 °F TOWER 300 M

PUMP NO.	NO. REQD	GPM	FT. HEAD	POWER MWe	CAPITAL $
1	2	1091	412	.147	$.920 \times 10^6$
2		1054	411	.141	$.910 \times 10^6$
3		992	408	.132	$.880 \times 10^6$
4		911	405	.120	$.860 \times 10^6$
5		815	402	.107	$.800 \times 10^6$
6		725	399	.094	$.740 \times 10^6$
7		616	395	.080	$.670 \times 10^6$
8		449	391	.057	$.582 \times 10^6$
9		366	390	.047	$.540 \times 10^6$
10		308	389	.039	$.516 \times 10^6$
11		281	388	.036	$.504 \times 10^6$
12		271	388	.034	$.500 \times 10^6$

(2.068 MWe) TOTAL $ 8.422×10^6 (24 PUMPS)

Table C-3 (Cont'd)

FIELD NORTH MAX. SODIUM TEMP. 1100 °F TOWER 150 M

PUMP NO.	NO. REQD	GPM	FT. HEAD	POWER MWe	CAPITAL $
1	1	2430	241	.190	.580×10⁶
2	2	2376	240	.185	1.140×10⁶
3		2216	237	.171	1.080×10⁶
4		1960	233	.148	.960×10⁶
5		1644	228	.121	.860×10⁶
6		1319	223	.096	.740×10⁶
7		1026	220	.073	.670×10⁶
8		783	218	.055	.546×10⁶
9		591	217	.042	.520×10⁶

(1.972 MWe) TOTAL $ 7.096×10⁶ (17 PUMPS)

FIELD NORTH MAX. SODIUM TEMP. 1100 °F TOWER 225 M

PUMP NO.	NO. REQD	GPM	FT. HEAD	POWER MWe	CAPITAL $
1	1	2430	270	.213	.630×10⁶
2	2	2376	269	.205	1.220×10⁶
3		2216	266	.191	1.150×10⁶
4		1960	262	.166	1.040×10⁶
5		1644	257	.137	.920×10⁶
6		1319	252	.108	.830×10⁶
7		1026	249	.083	.710×10⁶
8		783	247	.063	.600×10⁶
9		591	246	.047	.544×10⁶

(2.219 MWe) TOTAL $ 7.644×10⁶ (17 PUMPS)

Table C-3 (Cont'd)

FIELD NORTH MAX. SODIUM TEMP. 1100 °F TOWER 300M

PUMP NO.	NO. REQD	GPM	FT. HEAD	POWER MWe	CAPITAL $
1	1	2430	299	.236	.660 x 10^6
2	2	2376	298	.230	1.310 x 10^6
3	|	2216	295	.212	1.210 x 10^6
4	|	1960	291	.185	1.120 x 10^6
5	|	1644	286	.152	.970 x 10^6
6	|	1319	281	.120	.830 x 10^6
7	|	1026	278	.094	.740 x 10^6
8	|	783	276	.070	.632 x 10^6
9	↓	591	275	.053	.562 x 10^6

(2.468 MWe) TOTAL $ 8.034 x 10^6 (17 PUMPS)

FIELD NORTH MAX. SODIUM TEMP. 1300 °F TOWER 150 M

PUMP NO.	NO REQD	GPM	FT. HEAD	POWER MWe	CAPITAL $
1	1	1465	324	.155	.490 x 10^6
2	2	1433	323	.151	.960 x 10^6
3	|	1337	320	.136	.740 x 10^6
4	|	1182	316	.122	.830 x 10^6
5	|	992	311	.101	.750 x 10^6
6	|	796	307	.080	.680 x 10^6
7	|	619	303	.061	.600 x 10^6
8	|	472	301	.046	.540 x 10^6
9	↓	356	300	.035	.500 x 10^6

(1.619 MWe) TOTAL $ 6.29 x 10^6 (17 PUMPS)

Table C-3 (Cont'd)

FIELD NORTH MAX. SODIUM TEMP. 1300 °F TOWER 225 M

PUMP NO.	NO. REQD	GPM	FT. HEAD	POWER MWe	CAPITAL $
1	1	1465	368	.176	.535×10⁶
2	2	1433	367	.172	1.040×10⁶
3		1337	364	.159	.970×10⁶
4		1182	360	.139	.880×10⁶
5		992	355	.115	.770×10⁶
6		796	351	.091	.720×10⁶
7		619	347	.070	.660×10⁶
8		472	345	.053	.570×10⁶
9		356	344	.040	.524×10⁶

(1.854 MWe) TOTAL $ 6.669×10⁶ (17 PUMPS)

FIELD NORTH MAX. SODIUM TEMP. 1300 °F TOWER 300 M

PUMP NO.	NO. REQD	GPM	FT. HEAD	POWER MWe	CAPITAL $
1	1	1465	412	.197	.575×10⁶
2	2	1433	411	.192	1.100×10⁶
3		1337	408	.178	1.060×10⁶
4		1182	404	.156	1.000×10⁶
5		992	399	.129	.820×10⁶
6		796	395	.103	.750×10⁶
7		619	391	.079	.670×10⁶
8		472	389	.060	.590×10⁶
9		356	388	.045	.536×10⁶

(2.081 MWe) TOTAL $ 7.121×10⁶ (17 PUMPS)

Appendix D

TOWER COST ESTIMATES FOR PARAMETRIC ANALYSIS

In Task 2 Kaiser Engineers designed three receiver towers on the basis of the receiver weights estimated by GE (Section 3.3.2). Cost estimates for these towers were developed by Kaiser Engineers; the details of these estimates are listed in Tables D-1 through D-3.

Table D-1

COST OF 150 METER TOWER

DESCRIPTION	QUANTITY	UNIT COST		LABOR	MATERIAL	TOTAL
		LABOR	MAT'L			
492' TOWER (150 METERS)						
Foundations, Price includes forms, rebar, concrete, misc. embeds	2700 CY	65 -	85 -	176000	230000	406000
Tower, 92'Ø Base, All-in price based on similar tower, slipforming assumed	4900 CY	180 -	225 -	882000	1103000	1985000
Elevated Slabs at 406', 472', & 492', all-in rate for concrete	1200 CY	165 -	250 -	198000	300000	498000
Misc Steel for Core and Maint. Platforms at 150' & 300'	45 TN	500 -	700 -	23000	32000	55000
Service Elevator, 2.5 Ton, 8'x10' Cab, Includes hoist, cable & counterweight ass'y	1 EA	150,000	50,000	50000	150000	200000
S/T, Directs Only				1329000	1815000	3144000
Taxes on Mat'l @6%						109000
Contractor Indirects						979000
Total Cost						4232000
USE						4300000

Table D-2

COST OF 225 METER TOWER

DESCRIPTION	QUANTITY	UNIT COST		LABOR	MATERIAL	TOTAL
		LABOR	MAT'L			
738' TOWER (225 METERS)						
Foundations, Price includes forms, rebar, concrete, misc. embeds.	5100 CY	65 -	85 -	332000	434000	766000
Tower, 120.5' Base, All-in price factored from similar tower, slipforming assumed.	9600 CY	190 -	240 -	1824000	2304000	4128000
Elevated slabs at 652', 718', & 738', all-in rate for concrete	1200 CY	170 -	260 -	204000	312000	516000
Misc. Steel for Core and Maint. Platforms at 150', 300', 450', & 600'	71 TN	525 -	735 -	37000	52000	89000
Service Elevator, 25 Ton, 8'x10' Cab, Includes hoist, cable, & counterweight ass'y	1 EA	170000	55000	55000	170000	225000
S/T, Directs Only				2452000	3272000	5724000
Taxes on Mat'l @6%						196000
Contractor Indirects						1799000
Total Cost						7719000
USE						$ 7700000

Table D-3

COST OF 300 METER TOWER

DESCRIPTION	QUANTITY	UNIT COST LABOR	UNIT COST MAT'L	LABOR	MATERIAL	TOTAL
984' TOWER (300 METERS)						
Foundations, Price includes forms, rebar, concrete, misc. embeds.	11500 CY	65 -	85 -	748 000	978 000	1726000
Tower, 165' Base, All-in price factored from similar tower, slipforming assumed.	18200 CY	200 -	250 -	3640000	4550000	8190 000
Elevated Slabs at 898', 964', & 984', all-in rate for concrete	1200 CY	180 -	275 -	216 000	330 000	546000
Misc. Steel for Core and Maint Platforms at 150', 300', 450', 600', 4750'	97 TN	550 -	770 -	53000	75 000	128 000
Service Elevator, 2.5 Ton, 8'x10' Cab, Includes hoist, cable, & counterweight ass'y	1 EA	185,000	65,000	65000	185000	250000
S/T, Directs Only				4722000	6118 000	10840000
Taxes on Mat'l @ 6%						367 000
Contractor Indirects						3445000
Total Cost						14652000
USE						14700 000

Appendix E

RISER/DOWNCOMER COST ESTIMATES FOR PARAMETRIC ANALYSIS

In Task 2 Kaiser Engineers designed and cost estimated six riser/downcomer combinations corresponding to the 1100 F/1300 F temperature levels and the three tower heights (150 meters, 225 meters, and 300 meters). The details of these cost estimates are given in Tables E-1 through E-6.

Table E-1

RISER/DOWNCOMER COST - 1300 F, 150 METERS

DESCRIPTION	QUANTITY	UNIT COST LABOR	UNIT COST MAT'L	LABOR	MATERIAL	TOTAL
1300° F SYSTEM 492' TOWER (150 METERS)						
Downcomer Inconel 625, 5/16" Walls 18" Ø, Helical Run	578 LF	9 40	403 —	6000	233000	239000
Riser A335, ¼" Walls, 18" Ø, Helical Run	578 LF	7 12	67 20	4000	39000	43000
Hangers Spring-Type, @ 50' on Pipe Run	13 EA	125 —	1000 —	2000	13000	15000
Insulation Thermal 12, 12" Thick, w/ Aluminum Jacket	1156 LF	22 52	53 —	26000	61000	87000
S/T, Directs Only				38000	346000	384000
Taxes on Mat'l @6%						21000
Contractor Indirects						58000
Total Cost						463000
USE						± 500000

Table E-2

RISER/DOWNCOMER COST - 1300 F, 225 METERS

DESCRIPTION	QUANTITY	UNIT COST LABOR	UNIT COST MAT'L	LABOR	MATERIAL	TOTAL
1300°F SYSTEM 738' TOWER (225 METERS)						
Downcomer Inconel 625, 3/8" Walls 18" Ø, Helical Run	866 LF	11 60	453 -	10000	392000	402000
Riser A335, 5/16" Walls, 18" Ø, Helical Run	866 LF	9 25	83 20	8000	73000	81000
Hangers Spring-Type, @ 50' on Pipe Run	19 EA	125 -	1000 -	2000	19000	21000
Insulation Thermal 12, 12" Thick, w/ Aluminum Jacket	1732 LF	22 50	53 -	39000	92000	131000
S/T Directs Only				59000	576000	635000
Taxes on Mat'l @ 6%						35000
Contractor Indirects						93000
Total Cost						763000
USE						$ 800000

Table E-3

RISER/DOWNCOMER COST - 1300 F, 300 METERS

DESCRIPTION	QUANTITY	UNIT COST LABOR	UNIT COST MAT'L	LABOR	MATERIAL	TOTAL
1300°F SYSTEM 984' TOWER (300 METERS)						
Downcomer Inconel 625, 7/16" Walls 18"Ø, Helical Run	1155 LF	13.50	524 -	16000	605000	621000
Riser A335, 3/8" Walls 18"Ø, Helical Run	1155LF	11.50	101 -	13000	117000	130000
Hangers Spring-Type @ 50' on Pipe Run	25 EA	125 -	1000 -	3000	25000	28000
Insulation Thermal 12, 12" Thick, w/ Aluminum Jacket	2310 LF	22.50	53 -	52000	123000	175000
S/T, Directs Only				84000	870000	954000
Taxes on Mat'l @ 6%						52000
Contractor Indirects						138000
Total Cost						1144000
USE					$	1200000

Table E-4

RISER/DOWNCOMER COST - 1100 F, 150 METERS

DESCRIPTION	QUANTITY	UNIT COST LABOR	UNIT COST MAT'L	LABOR	MATERIAL	TOTAL
1100°F SYSTEM 492' TOWER (150 METERS)						
Downcomer 316 SS, ½" Walls, 24"Ø, Helical Run	578 LF	21	613	13000	354000	367000
Riser A335, 3/8" Walls, 24"Ø, Helical Run	578 LF	15	132	9000	76000	85000
Hangers Spring-Type, @ 50' on Pipe Run	13 EA	125	1000	2000	13000	15000
Insulation Thermal 12, 12" Thick, w/ Aluminum Jacket	1156 LF	29	70	34000	81000	115000
S/T, Directs Only				58000	524000	582000
Taxes on Mat'l @ 6%						32000
Contractor Indirects						87000
Total Cost						701000
USE						$ 700000

Table E-5

RISER/DOWNCOMER COST - 1100 F, 225 METERS

DESCRIPTION	QUANTITY	UNIT COST		LABOR	MATERIAL	TOTAL
		LABOR	MAT'L			
1100°F SYSTEM 738' TOWER (225 METERS)						
Downcomer 316SS, 5/8" Walls, 24" Ø, Helical Run	866 LF	28.90	635 -	25000	550000	575000
Riser A335, 7/16" Walls, 24" Ø, Helical Run	866 LF	18.60	157 -	16000	136000	152000
Hangers Spring-Type, @ 50' on Pipe Run	19 EA	125 -	1000 -	2000	19000	21000
Insulation Thermal 12, 12" Thick, w/ Aluminum Jacket	1732 LF	29 -	70 -	50000	121000	171000
S/T, Directs Only				93000	826000	919000
Taxes on Mat'l @ 6%						50000
Contractor Indirects						139000
Total Cost						1108000
Use						$1100000

Table E-6

RISER/DOWNCOMER COST - 1100 F, 300 METERS

DESCRIPTION	QUANTITY	UNIT COST LABOR	UNIT COST MAT'L	LABOR	MATERIAL	TOTAL
1100°F System 984' Tower (300 Meters)						
Downcomer 316 SS, 3/4" Walls, 24"Ø, Helical Run	1155 LF	39 -	712 -	45000	822000	867000
Riser A335 1/2" Walls 24"Ø, Helical Run	1155 LF	22 -	180 -	26000	208000	234000
Hangers Spring-Type, @ 50' on Pipe Run	25 EA	125 -	1000 -	3000	25000	28000
Insulation Thermal 12, 12" Thick, w/ Aluminum Jacket	2310 LF	29 -	70 -	67000	162000	229000
S/T, Directs Only				141000	1217000	1358000
Taxes on Mat'l @ 6%						73000
Contractor Indirects						206000
Total Cost						1637000
USE						SL 1700000

Appendix F

TRANSIENT THERMAL ANALYSIS OF SODIUM/IRON STORAGE

As a result of this study, a paper has been prepared on the transient thermal behavior of sodium/iron storage for submission to Solar Energy Journal. The text of this paper is reproduced in full in this appendix.

THERMAL ENERGY STORAGE IN A PACKED BED OF IRON SPHERES WITH LIQUID SODIUM COOLANT

B.D. Pomeroy

Corporate Research and Development
General Electric Company
Schenectady, New York

ABSTRACT

In sodium/iron storage three principal factors cause broadening of the thermocline. They are:

1. Conduction resistance in the iron
2. Convective resistance between the sodium and the iron
3. Axial conduction in the sodium and iron

It is assumed that a uniform fluid velocity profile is achieved in the storage tank by appropriate flow distributor design and that heat losses through the tank wall are negligible in comparison with the thermal power extracted from the tank.

This paper identifies the major design parameters which control thermocline broadening, and a procedure is described for estimating the tank outlet temperature as a function of time.

These relations show that it is possible to design a sodium/iron storage device which limits thermocline spreading to less than 20% of the nominal discharge time.

1. INTRODUCTION

Sodium has been identified as an attractive heat transfer medium for solar central receiver power plants because of its high temperature capabilities and high convective heat transfer coefficient. If sodium is used to cool the receiver, it would seem advantageous from the viewpoint of system simplicity to use it for heat storage as well. The disadvantage of this approach is the high cost of the storage vessels and sodium required. One solution to this problem is to fill the tanks with iron spheres, which would improve the volumetric heat capacity by a factor of three or four, and would greatly reduce the sodium inventory.

It is generally understood that during the discharge of packed bed storage devices the hot and cold regions of the vessel are separated by a transition zone called the thermocline. A narrow thermocline is desirable because it permits delivery of peak temperature liquid to the electrical power generation subsystem (EPGS) throughout the discharge cycle. A wide thermocline results in lower average temperatures, and a correspondingly lower efficiency in the EPGS.

In sodium/iron storage three principal factors cause broadening of the thermocline. They are:

1. Conduction resistance in the iron
2. Convective resistance between the sodium and the iron
3. Axial conduction in the sodium and iron

It is assumed that a uniform liquid velocity profile is achieved in the storage tank by appropriate flow distributor design, and that heat losses through the tank walls are negligible in comparison with the thermal power extracted from the tank.

This paper identifies the major design parameters which control thermocline broadening, and a procedure is described for estimating the tank outlet temperature as a function of time.

2. ANALYSIS

Consider the storage tank pictured in Fig. 1 during a discharge cycle. Initially it is filled with sodium and iron at a uniform temperature T_0. At time t = 0 flow is initiated which injects cold sodium at temperature T_i into the bottom of the tank. What is the liquid outlet temperature $T_L(L,t)$ as a function of time?

As might be expected, the complete mathematical formulation of this problem, which includes all three factors cited above, cannot be solved analytically. Schmidt and Szego [1] have plotted numerical solutions for the complete formulation over a range of parameters appropriate to water/rock systems; however, the sodium/iron system parameters are generally outside the range of these solutions because of the very high sodium heat transfer coefficients. The inapplicability of these solutions has motivated the present study in which several special cases have been investigated to identify the major design variables for the sodium/iron system.

Case 1 - Ideal Heat Transfer. Assume that the spheres are perfectly conducting and that there is no convective resistance or axial conduction; then the liquid and solid temperatures are identical and the governing equation is

$$\frac{\partial \theta}{\partial \tau} + \frac{\partial \theta}{\partial \xi} = 0 \tag{1}$$

with initial and boundary conditions

$$\theta(\xi, 0) = 0 \tag{2}$$

$$\theta(0, \tau) = 1 \tag{3}$$

The solution can be obtained with Laplace transform techniques, and when evaluated at $\xi = 1$ the tank outlet temperature is found to be a step function.

$$\theta(1,\tau) = \begin{cases} 0 & 0 < \tau < 1 \\ 1 & \tau \geq 1 \end{cases} \tag{4}$$

This is the ideal thermocline; it moves through the tank at a speed which is slower than the average fluid speed, and it exits from the tank at time

$$t^* = \frac{L}{u}\left[1 + \left(\frac{\rho_S C_S V_S}{\rho_L C_L V_L}\right)\right] \tag{5}$$

In the more complex formulations of the problem this time constant remains the basic scaling parameter. Even when the thermocline is dispersed, the spread is roughly centered about this time as shown in Fig. 2. Thus t* can be used as a first approximation for the duration of the storage discharge cycle.

Case 2 - Convective Resistance Effects. Assume that there is a finite convective resistance but that the spheres have uni-

form temperature and there is no axial conduction; then the governing equations for the liquid and solid are:

$$\frac{\partial \theta_L}{\partial \tau} - b_1 t^* (\theta_S - \theta_L) + \frac{ut^*}{L} \frac{\partial \theta_L}{\partial \xi} = 0 \tag{6}$$

$$\frac{\partial \theta_S}{\partial \tau} + b_2 t^* (\theta_S - \theta_L) = 0 \tag{7}$$

while the initial and boundary conditions are

$$\theta_L (\xi, 0) = \theta_S (\xi, 0) = 0 \tag{8}$$

$$\theta_L (0, \tau) = 1 \tag{9}$$

Laplace transform techniques are applicable to these equations and result in the solutions quoted by Yang [2] . Evaluating the liquid solution at $\xi = 1$ yields the tank outlet temperature as a function of time:

$$\theta_L(1, \tau) = 0 \qquad \text{for } [0 < \tau < (L/ut^*)] \tag{10a}$$

$$= e^{-s} \{ e^{-q} I_0 [2(sq)^{1/2}] + \psi_2^{**} \} \quad \text{for } [\tau \geq L/ut^*] \tag{10b}$$

where:

$$s = b_1 L/u$$

$$q = b_2 (t^* \tau - L/u)$$

$$\psi_2^{**} = \int_0^q e^{-\phi} I_0 [2(s\phi)^{1/2}] \, d\phi$$

The function ψ_2^{**} has been evaluated numerically and plotted by Rizika [3] . However, the graphs obtained were intended to be used for estimating dynamic performance of heat exchangers and piping systems and are not really applicable to most thermal

storage devices. Rizika considered $0 \leq s \leq 5$ whereas the sodium/iron storage has s values in the order of 5000.

Fortunately, for $s > 500$, eqn (10) can be simplified considerably, yielding a very compact expression for the time dependence of the outlet temperature. From this it is possible to deduce a closed form expression for the thermocline spread ($2\Delta\tau$) shown in Fig. 2.

For large values of s the first term in eqn (10b) can be shown to be vanishingly small. The integral in the second term can be simplified by noting that, for large values of s, the integrand is very small everywhere except in the vicinity of $\tau = 1$, where the argument of the Bessel function is very large, and the following approximation holds

$$I_0(X) = \frac{e^X}{(2\pi X)^{1/2}} \qquad (11)$$

Substituting this into the integral and changing the integration variable yields ψ_2^{**} in terms of an error integral. In fact the tank outlet temperature can be seen to be closely approximated by

$$\theta_L(1,\tau) = \begin{cases} \frac{1}{2}\,[1 - \mathrm{erf}(|Z|)] & Z \leq 0 \quad (12a) \\ \frac{1}{2}\,[1 + \mathrm{erf}(Z)] & Z \geq 0 \quad (12b) \end{cases}$$

where: $Z = q^{1/2} - s^{1/2}$

Inspection of tabulated values for the error function shows that the entire thermocline in (12) is contained between $Z = -2$ and $Z = +2$. Relating this back to the dimensionless time τ yields

$$2\Delta\tau = \frac{8\gamma}{(1+\gamma)\sqrt{s}} \tag{13}$$

Thus s and γ are the design parameters controlling thermocline spread due to convective resistance.

Case 3 - Axial Conduction Effects. Assume that there is axial conduction, but that the spheres have uniform temperatures and there is no convective resistance. Then the temperatures of the liquid and the spheres are identical at every point and the governing equation is:

$$\frac{\partial\theta}{\partial\tau} = a \frac{\partial^2\theta}{\partial\xi^2} - \frac{\partial\theta}{\partial\xi} \tag{14}$$

The initial condition is

$$\theta(\xi,0) = 0 \tag{15}$$

The inlet condition is evaluated by postulating a very small mixing zone whose temperature is determined by the energy balance between heat added by the cold liquid at temperature T_i and the heat outflow due to convection and conduction into the packed bed. This yields:

$$a \frac{\partial\theta}{\partial\xi}(0,\tau) = \theta(0,\tau) - 1 \tag{16}$$

At the outlet heat is extracted only by hot fluid leaving the tank; that is, no heat is conducted out of the tank at $\xi = 1$. This translates into

$$\frac{\partial\theta}{\partial\xi}(1,\tau) = 0 \tag{17}$$

These equations are very difficult to solve exactly because of the outlet condition (17). In a well-designed storage system the axial heat flow will be small compared with the axial energy transported by liquid flow. Under these conditions the effect of (17) on the outlet temperature is likely to be small. That is, the solution at $\xi = 1$ for (14) (15) (16) and (17) will be approximately the same as the solution for an infinitely long tank where we require only that

$$\theta(\xi, \tau) = \text{finite as } \xi \to \infty \tag{18}$$

Cabelli [4] gives the solution to (14) (15) (16) and (18), which yields the following expression for the outlet fluid temperature

$$\theta(1,\tau) = \int_0^\tau \left\{ \frac{1}{(\pi a \phi)^{1/2}} \exp\left[\frac{-1}{4a} \left(\sqrt{\phi} - \frac{1}{\sqrt{\phi}} \right)^2 \right] \right. \tag{19}$$

$$\left. - \frac{e^{1/a}}{2a} \operatorname{erfc}\left[\frac{1}{2\sqrt{a}} \left(\sqrt{\phi} + \frac{1}{\sqrt{\phi}} \right) \right] \right\} d\phi$$

In the sodium/iron system the parameter a is very small, and this leads to a simplification of (19) similar to that demonstrated in Case 2. First, note that the function

$$\sqrt{\phi} + \frac{1}{\sqrt{\phi}}$$

has a minimum value of 2 for $0 < \phi < \infty$; thus, the argument of the complementary error function in (19) is everywhere large when a is small. This permits the approximation

$$\operatorname{erfc}(X) = \frac{\exp[-X^2]}{\sqrt{\pi}\ X}$$

Substituting this into (19) and noting that the integrand peaks sharply near $\phi = 1$ and is almost zero elsewhere yields the following approximation for the outlet temperature:

$$\phi(1,\tau) = \begin{cases} \frac{1}{2} \left[1 - \text{erf}\left(|y|\right)\right] & \text{for } (\tau < 1) \quad (20a) \\ \frac{1}{2} \left[1 - \text{erf}\,(Y)\right] & \text{for } (\tau > 1) \quad (20b) \end{cases}$$

where $$y = (\tau - 1)/(4a)^{1/2}$$

As in Case 2, we note that in (20) the entire thermocline is contained between y = -2 and y = +2. Converting this to the equivalent values of τ yields

$$2\,\Delta\tau = 8a^{1/2} \quad (21)$$

This demonstrates that a is the primary design parameter which controls thermocline spreading due to axial conduction.

Case 4 - Effect of Nonuniform Temperature in Solid Spheres.

The question to be answered here is, "How small must a sphere be to achieve 99% heat extraction in the time it takes for the thermocline to pass the sphere?"

The problem of one-dimensional transient conduction in a sphere is well known and the solutions are given in numerous textbooks. Based on the solution given by Arpaci [5] the fraction of heat extracted in time t is

$$\frac{Q}{Q_i} = 6 \sum_{n=1}^{\infty} \frac{(\sin \mu_n - \mu_n \cos \mu_n)^2}{\mu_n^3 \,(\mu_n - \sin \mu_n \cos \mu_n)} \left(1 - \exp\left[-\mu_n^2\, Fo\right]\right) \quad (22)$$

where μ_n are the zeros of

$$\mu_n \cos \mu_n = (1 - Bi) \sin \mu_n \tag{23}$$

In the sodium/iron system the Biot number (Bi) is usually quite large. In the limit of infinite Bi (23) gives the eigenvalues

$$\mu_n = n\pi, \quad n = 1, 2, \ldots, \infty$$

and (22) reduces to

$$\frac{Q}{Q_i} = 6 \sum_{n=1}^{\infty} \frac{1 - \exp\left[-(n\pi)^2 Fo\right]}{(n\pi)^2} \tag{24}$$

This relation gives $Q/Q_i \geq 0.99$ when $Fo \geq 0.42$; thus the size of sphere which delivers 99% of its energy in time t is given by

$$R^2 \leq \frac{k_S}{\rho_S C_S} \left(\frac{t}{0.42}\right) \tag{25}$$

Given the thermocline speed as computed in Case 1, the time required for the thermocline to travel one sphere diameter is

$$t = \frac{2R(1+\gamma)}{u} \tag{26}$$

Combining (25) and (26) gives the relation of sphere radius to the other design parameters

$$R \leq 4.8 \frac{k_S}{\rho_S C_S} \frac{(1+\gamma)}{u} \tag{27}$$

3. EXAMPLE OF SODIUM/IRON STORAGE DESIGN PROCEDURE

Table 1 shows these relations applied to a sodium/iron storage unit designed for operation over the range of temperatures from 588 K (600 F) to 977 K (1300 F).

First it is necessary to select a discharge time which establishes the value of t* according to the analysis in Case 1. Then the liquid flow speed, u, is computed using (5).

After u is computed the next step is to estimate the sphere size required to prevent thermocline spreading due to internal conductive resistance in the spheres. This maximum allowable radius given by equation (27) is shown in Table 1 to be 0.012 m (0.47 inch). The design radius selected is 0.0065 m (0.26 inch).

Finally (13) and (21) give estimates of the thermocline spread which results from convective resistance and axial conduction effects during the discharge cycle. Convection alone would cause a thermocline spread ($2\Delta\tau$) that is 9% of the nominal discharge time. Axial conduction alone would account for a spread of 11%. Both effects are driven by temperature gradients in the region of the thermocline. Thus when both act, the convection effect would be decreased because of the decrease in temperature gradients caused by the axial conduction effect and vice versa. Thus the thermocline spreading when both effects act should be less than 9% + 11% = 20%.

4. CONCLUSION

It is possible to identify the major design parameters for a sodium/iron packed bed thermal storage device by considering several simple mathematical models for the transient heat transfer effects. These models give estimates for the maximum allowable sphere size, equation (27), and the storage discharge time constant, equation (5). Equations (13) and (21) provide estimates of the thermocline spreading due to convective resistance and axial conduction.

The relations show that it is possible to design a sodium/iron storage device which limits thermocline spreading to less than 20% of the total discharge time.

NOMENCLATURE

a = $\bar{k}A/(u\rho_L C_L V_L$

A = $A_S + A_L$

A_L = (V_L/L)

A_S = (V_S/L)

A^* = total surface area of spheres in bed

b_1 = $hA^*/(\rho_L C_L V_L)$

b_2 = $hA^*/(\rho_S C_S V_S)$

Bi = Biot Number = hR/k_S

C_L = average specific heat of liquid

C_S = average specific heat of solid

Fo = Fourier Number = $\dfrac{k_S}{\rho_S C_S} \quad \dfrac{t}{R^2}$

h = heat transfer coefficient between solid and liquid

k_L = average thermal conductivity of liquid

k_S = average thermal conductivity of solid

$\bar{k}$ = $(k_S A_S + k_L A_L)/A$ = average axial conductivity

L = length of tank

q = $b_2\ (t^*\ \tau - L/u)$

R = radius of solid spheres

s = $b_1 L/u$

t = time

t^* = tank time constant (equation (5)) = $\frac{L}{u}(1+\gamma)$

$T_L(X,t)$ = temperature of liquid in tank

$T_S(X,t)$ = temperature of solid in tank

T_0 = $T_L(X,0)$ = $T_S(X,0)$ = initial temperature

T_i = inlet liquid temperature

u = liquid speed in bed

V_L = volume of liquid in tank

V_S = volume of solid in tank

W = liquid mass flow = $\rho_L A_L u$

X = axial distance from inlet of tank

Y = $(\tau-1)/2a^{1/2}$

Z = $q^{1/2} - s^{1/2}$

γ = $\rho_S C_S V_S/(\rho_L C_L V_L)$

θ = $(T - T_0)/(T_i - T_0)$ = dimensionless temperature

ξ = X/L = dimensionless distance

ρ_L = average density of liquid

ρ_S = average density of solid

τ = t/t^* = dimensionless time

$$\psi_2^{**} = b_2 \int_0^{t-x/u} \exp\left[-b_2\sigma\right] I_0\left[2\left(\frac{Xb_1b_2\sigma}{w}\right)^{1/2}\right] d\sigma$$

ACKNOWLEDGEMENTS

This work was performed as part of a conceptual design study of advanced central receiver power plants sponsored by the United States Department of Energy (contract No. EG-77-C-03-1725). The author would also like to acknowledge the valuable assistance of Dr. Sudhir Savkar and Dr. Anthony Ku, both of the General Electric Company.

REFERENCES

1. F.W. Schmidt and J. Szego, "Transient Response of Solid Sensible Heat Thermal Storage Units - Single Fluid," J. Heat Transfer, ASME Transactions, 471-477 (August 1976).

2. W.J. Yang and C.P. Lee, "Dynamic Response of Solar Heat Storage Systems," ASME Paper 74-WA/HT-22, ASME Winter Annual Meeting, Nov. 17-22, 1974.

3. J.W. Rizika, "Thermal Lags in Flowing Systems Containing Heat Capacitors," ASME Transactions, 76, 411 (1954).

4. A. Cabelli, "Storage Tanks - A Numerical Experiment," Solar Energy, 19, 45-54 (1977).

5. V.S. Arpaci, Conduction Heat Transfer, Addison Wesley (1966).

Table 1. Sodium/Iron Storage Example

Tank Size 5 m (dia) x 20 m (L)

Material Properties (at 800 K)

		Sodium	Iron
Density	(kg/m^3)	800	7880
Thermal Conductivity	(W/m·K)	70	35
Specific Heat	(J/kg·K)	1250	630
Volume Fraction†	(%)	26	74
Heat Transfer Coeff.	(W/m^2K)	11,000	--

Design Procedure

Equation Number	Function Performed	Result
-	Select nominal discharge time	t* = 2 hours
(5)	Estimate liquid flow speed	u = 0.042 m/S
(27)	Estimate maximum sphere size	$R \leq 0.012$ m
	Select sphere size	R = 0.0055 m
(13)	Estimate convection effect on thermocline spread	$2 \Delta \tau = 0.09$
(21)	Estimate axial conduction effect on thermocline spread	2Λ ı 0.11

†assumes hexagonal close packing of spheres

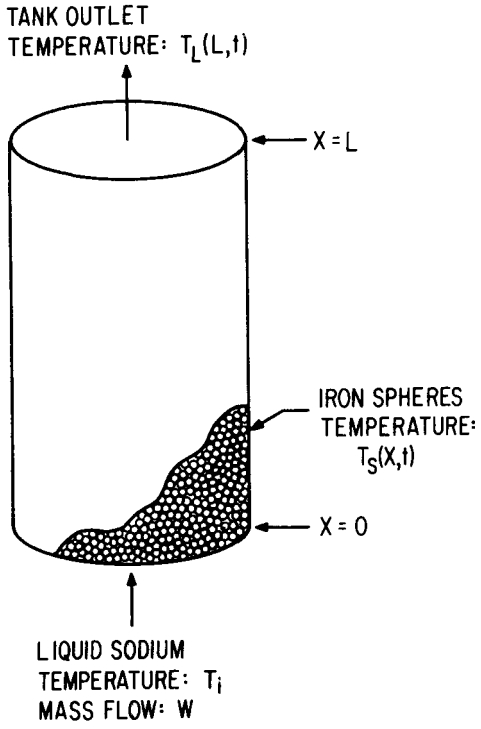

Fig. 1. Packed Bed Storage Device

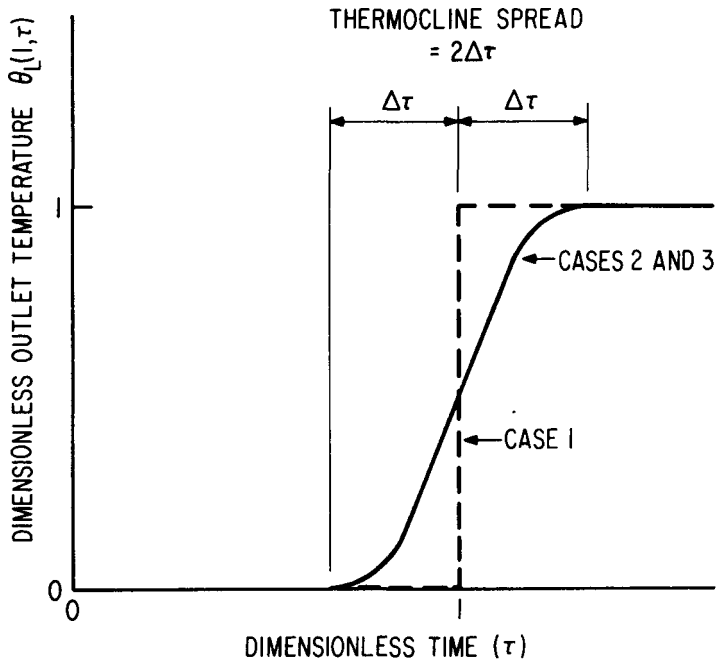

Fig. 2. Tank Outlet Temperature vs Time

Appendix G

DETAILS OF FIELD FABRICATED STORAGE VESSEL COST ESTIMATES FOR PARAMETRIC ANALYSIS

Tables G-1 through G-6 are the original tank price estimates prepared by Kaiser Engineers. These tables have been modified as shown to account for several design changes made during the parametric analysis. In Tables G-1, G-2, G-5, and G-6, the packing density of the iron storage medium was increased to 75 percent by volume. The price of iron was also increased to $0.45/pound to reflect the change from cast iron, which is not compatible with sodium, to carbon steel which is compatible.

In Tables G-3 and G-4, the design pressure was changed from 150 psig to 50 psig based on a design change which allowed the tanks to operate at pump inlet pressure rather than pump discharge pressure.

Tables G-7 and G-8 describe the scaling performed to generate estimates for Concepts 3 and 4.

Table G-1

TANK PRICING - CASE IIa

DESCRIPTION	QUANTITY	UNIT COST LABOR	UNIT COST MAT'L	LABOR	MATERIAL	TOTAL
CASE IIa						
TANK "A" 1100°F						
45.5' ø X 90.25' L.						
Tank, Cylindrical, Incoloy 800, 630 Tons, Includes Freight and Field Fabrication	1 EA			3 327 000	5 503 000	8 830 000
Steel Balls, 20,165 ← Correction for packing density & unit price (.45$/lb) No Scrap, ~~17,415~~ Tons, Includes Freight and Field Installation	1 LT			46 300 ~~40000~~	18 148 500 ~~7837000~~	18 194 800 ~~7877000~~
Tank Insulation, 12" KAYLO-10, 12,900 s.f., Includes Freight and Field Instal.	1 LT			161 000	101 000	262 000
Support Cradle, Carbon Steel, 45 Tons, Includes Field Erection and Cradle Insulation	1 EA			11 000	46 000	57 000
Heat Tracing, GE Pricing, Includes Thermocouples, 375 W/Ft Rated, 3100 LF	1 LT			54 000	112 000	166 000
S/T, Directs Only				~~3 593 000~~ 3 699 300	~~13 591 000~~ 23 910 500	~~17 192 000~~ 27 509 800
Taxes on Mat'l @ 6%						1 434 600 ~~816 000~~
Contractor Indirects		(.10 × mat'l + .60 × labor)				4 550 600 ~~3516000~~
Total Cost						33 495 000 ~~21 524 000~~
USE						~~21 500 000~~

Table G-2

TANK PRICING - CASE IIb

DESCRIPTION	QUANTITY	UNIT COST LABOR	UNIT COST MAT'L	LABOR	MATERIAL	TOTAL
CASE IIb TANK "B" 1100°F 35.7'Ø x 71.5' L.						
Tanks, Cylindrical, Incoloy 800, 312 Tons, Includes Freight and Field Fabrication	2 EA	1,300,000	2,502,000	2600000	5004000	7604000
Steel Balls, 1008Z ← No Scrap, ~~3910~~ Tons, Includes Freight and Field Installation	2 LT	29,000	4,010,000	54300 ~~48000~~	18 148 500 ~~8020000~~	18 202 800 ~~8068000~~
Tank Insulation, 12" KAYLO-10, 8000 s.f., Includes Freight and Field Instl	2 LT	100,000	63,000	200000	126000	326000
Support Cradles, Carbon Steel, 22 Tons, Includes Field Erection and Cradle Insulation	2 EA	6,000	23,000	12000	46000	58000
Heat Tracing, GE Pricing, Includes Thermocouples, 375 W/Ft. Rated, 1800'/Tnk	2 LT	32,000	65,000	64000	130000	194000
S/T, Directs Only				~~2924000~~ 2 930 300	~~13326000~~ 23 454 500	~~16250000~~ 26 384 800
Taxes on Mat'l @ 6%,						1407 300
						~~800000~~
Contractor Indirects						4 103 600
						~~3087000~~
Total Cost						31 895 700
						~~20137000~~
UTE						~~2220000~~

Table G-3

TANK PRICING - CASE IVa

DESCRIPTION	QUANTITY	UNIT COST LABOR	UNIT COST MAT'L	LABOR	MATERIAL	TOTAL
Case IVa Tank "C" 1100°F 59' Ø						
Tanks, Spherical, Incoloy 800, ~~45~~ 152 Tons, Includes Freight and Field Fabrication ← Correction for pressure (50/150)	5 EA	1,666,000	3,474,000	2 776 700 ~~8 330 000~~	5 790 000 ~~17 370 000~~	8 566 700 ~~25 700 000~~
Steel Balls None						
Tank Insulation, 12" KAYLO-10, 10,800 s.f., Includes Freight & Field Instl.	5 LT	135,000	85,000	675 000	425 000	1 100 000
Support Cradles, Carbon Steel, 20 Tons, Includes Field Erection and Cradle Insulation	5 EA	5,000	21,000	25 000	105 000	130 000
Heat Tracing, GE Pricing, Includes Thermocouples, 375 W/Ft. Rated, 2500 LF	5 LT	43,800	90,500	219 000	453 000	672 000
S/T, Directs Only				~~9 299 000~~ 3 695 700	~~18 353 000~~ 6 773 000	~~27 652 000~~ 10 468 700
Taxes on Mat'l @ 6%						406 400 ~~1 101 000~~
Contractor Indirects						2 894 700 ~~7 365 000~~
Total Cost			Single tank: 2,753,960 ←			13 769 800 ~~45 068 000~~
Use						~~26 [illegible]~~

Table G-4

TANK PRICING - CASE Va

DESCRIPTION	QUANTITY	UNIT COST LABOR	UNIT COST MAT'L	LABOR	MATERIAL	TOTAL
CASE Va TANK "D" 1300°F 51'Ø						
Tanks, Spherical, 120 ← correction for pressure (50/150) Inconel 625, ~~760~~ Tons; Includes Freight and Field Fabrication	5 EA	1,164,200	4,938,200	1 941 300 ~~5 824 000~~	8 231 300 ~~24 674 000~~	10 172 600 ~~30 498 000~~
Steel Balls None						
Tank Insulation, 12" KAYLO-10, 8250 s.f. Includes Freight & Field Instal.	5 LT	103,100	64,700	516 000	324 000	840 000
Support Cradles Carbon Steel, 15 Tons Includes Field Erection and Cradle Insulation	5 EA	3,800	16,000	19 000	80 000	99 000
Heat Tracing, GE Pricing, Includes Thermocouples, 375 W/Ft. Rated, 1900 LF	5 LT	33,300	66,800	167 000	344 000	511 000
S/T Directs Only				~~6 526 000~~ 2 643 300	~~25 442 000~~ 8 979 300	~~31 968 000~~ 11 622 600
Taxes on Mat'l @ 6%						538 700 ~~1 527 000~~
Contractor Indirects						2 483 900 ~~6 460 000~~
Total Cost				Single tank: 2,929,000	←	14 645 200 ~~37 955 000~~
USC					$1	~~40 000 000~~

Table G-5

TANK PRICING - CASE VIIa

DESCRIPTION	QUANTITY	UNIT COST LABOR	UNIT COST MAT'L	LABOR	MATERIAL	TOTAL
CASE VIIa TANK "E" 1300°F 40'ID x 78' L.						
Tank, Cylindrical, Inconel 625, 495 Tons, Includes Freight and Field Fabrication	1 EA			2191000	7762000	9953000
Steel Balls, 13443 ← correction for packing density & unit price (.45 $/LB) → No Scrap, ~~11,880~~ Tons, Includes Freight and Field Installation	1 LT			37 300 ~~33 000~~	12 098 700 ~~5 346 000~~	12 136 000 ~~5 379 000~~
Tank Insulation, 12" KAYLO-10, 9900 s.f., Includes Freight and Field Instal.	1 LT			124 000	78000	202000
Support Cradle, Carbon Steel, 40 Tons, Includes Field Erection and Cradle Insulation	1 EA			10000	42000	52000
Heat Tracing, GE Pricing, Includes Thermocouples, 375 W/Ft Rated, 2700 LF	1 LT			47000	98000	145000
S/T, Directs Only				~~2405000~~ 2 409 300	~~13326000~~ 20 078 700	~~15 731 000~~ 22 488 000
Taxes on Mat'l @6%						1 204 700 ~~800 000~~
Contractor Indirects						3 463 400 ~~2 776 000~~
Total Cost						27 146 100 ~~19 307 000~~
USE						~~19 307 000~~

Table G-6

TANK PRICING - CASE VIIb

DESCRIPTION	QUANTITY	UNIT COST LABOR	UNIT COST MAT'L	LABOR	MATERIAL	TOTAL
Case VIIb TANK "F" 1300°F 32'Ø x 62'L.						
Tanks, Cylindrical, Inconel 625, 250 Tons, Includes Freight and Field Fabrication	2 EA	1,292,600	4,229,300	2585000	8459000	11044000
Steel Balls, 6721 ← correction for packing density & unit price (.45 #/LB) → No Scrap, ~~5710~~ Tons, Includes Freight and Field Installation	2 LT	16,000	2,659,000	36 400 ~~32000~~	12 098 700 ~~5 318 000~~	12 135 100 ~~5 350 000~~
Tank Insulation, 12" KAYLO-10, 6,250 s.f., Includes Freight and Field Instal.	2 LT	78,000	49,000	156 000	98 000	254000
Support Cradles, Carbon Steel, 20 Tons, Includes Field Erection and Cradle Insulation	2 EA	5,000	21,000	10000	42000	52000
Heat Tracing GE Pricing, Includes Thermocouples, 375 W/Ft. Patch, 1500'/Tank.	2 LT	26,000	54000	52000	108000	160000
S/T, Directs Only				~~2835000~~ 2 839 400	~~20 805 000~~ 20 805 700	~~23 640 000~~ 23 645 100
Taxes on Mat'l @6%						1 248 300 ~~842 000~~
Contractor Indirects						3 784 200 ~~3 110 000~~
Total Cost						28 677 600 ~~20 112 300~~
Use						$ ~~20866~~

Table G-7

SCALING OF CASES IVa and Va
FOR CONCEPT 3

CASE No.	IVc			Vc		
	LABOR	MATL	TOTAL	LABOR	MATL	TOTAL
TANK	2776700	1679100	(a)	1941300	1317008	(b)
INSULATION	675000	450000		516000	324000	
SUPPORTS	25000	105000		19000	80000	
HEAT TRACING	219000	453000		167000	344000	
S/T, DIRECTS	3695700	2687100	6382800	2643300	2065008	4708308
TAXES, MATL			161226			123900
INDIRECTS			2486130			1792480
TOTAL($)			9030156			6624689
No. OF TANKS			5			5
SINGLE TANK($)			1806031			1324938

(a) SCALED FROM CASE IVa 2¼Cr-1Mo/INCOLLOY 800H = 1.10/3.80
(b) SCALED FROM CASE Va 2¼Cr-1Mo/INCONEL 625 = 1.10/6.86

Table G-8

SCALING OF CASES
FOR CONCEPT 4

CASE No.	IVd (2)			IVe (3)			Vd (4)			Ve (5)		
	LABOR	MATL	TOTAL	LABOR	MATL	TOTAL	LABOR	MATL	TOTAL	LABOR	MATL	TOTAL
TANK	2 776 700	5 790 000	x 1.333	2 776 700	1 679 000	x 1.333	1 941 300	8 231 300	x 1.333	1 941 300	1 317 008	x 1.333
INSULATION	675 000	475 000	x 1.211	675 000	450 000	x 1.211	516 000	324 000	x 1.211	516 000	324 000	x 1.211
SUPPORTS	25 000	105 000		25 000	105 000		19 000	80 000		19 000	80 000	
HEAT TRACING	219 000	453 000		219 000	453 000		167 000	344 000		167 000	344 000	
S/T, DIRECTS	3 695 700 x 1.211 = 4,475,493	8 910 220	13 385 713	3 695 770 x 1.211 = 4 475 493	3 458 928	7 934 421	2 643 300 x 1.211 = 3 201 036	11 880 620	15 081 656	2 643 300 x 1.211 = 3 201 036	2 661 775	5 862 831
TAXES, MAT'L			534 613			207 536			712 837			159 708
INDIRECTS			3 576 318			3 031 189			3 108 684			2 186 801
TOTAL ($)			17 496 643			11 173 145			18 190 340			8 209 340
No. OF TANKS			5			5			5			5
SINGLE TANK ($)			3 499 329			2 234 629			3 638 038			1 641 868

(1) TANK MATERIAL COST SCALED AS VOLUME OF TANK $(V/V_0) = 1.333$
ALL OTHER COSTS SCALED AS AREA OF TANK $A/A_0 = 1.211$

(2) SCALED FROM CASE IVa
(3) SCALED FROM CASE IVc
(4) SCALED FROM CASE Va
(5) SCALED FROM CASE Vc

Appendix H

STEAM GENERATOR HEAT BALANCES FOR PARAMETRIC ANALYSIS

The analytical model used to obtain the steam generator heat balances in Section 3.4.6 is illustrated in Figure H-1.

The enthalpy of the water entering the evaporator is obtained from a heat balance on the water side mixing tee where the return feedwater joins the recirculation flow leaving the steam drum:

$$[W_E - (W_S + W_B)]\, h_f + (W_S + W_B)\, h_{FW} = W_E\, h_{EO}$$

Dividing through by W_S and letting $R = W_E/W_S$ the water inlet enthalpy h_{EO} becomes:

$$h_{EO} = \left[1 - \frac{1}{R}\left(1 + \frac{W_B}{W_S}\right)\right] h_f + \left(1 + \frac{W_B}{W_S}\right)\frac{1}{R}\, h_{FW} \qquad \text{(H-1)}$$

Values for all of the water side flows, temperatures, enthalpies, and pressures in Task 2 were taken from the turbine heat balance which is detailed in Figure H-2. In addition, note that $R = 1.15$, $W_B/W_S = 0.10$, $h_f = 743.08$ Btu/hour and $h_{FW} = 524.9$* from which $h_{EO} = 534.4$ Btu/pound and $T_{EO} = 539.2$ F.

The sodium side heat input must balance the steam side output in the superheater/reheater:

$$W_N C_P (T_{N1} - T_{N4}) = W_S (h_{S1} - h_{SO}) + W_R (h_{R1} - h_{RO})$$

where: C_P = specific heat of sodium. Solving for T_{N4}:

$$T_{N4} = T_{N1} - \frac{W_S}{W_N C_P}(h_{S1} - h_{SO}) - \frac{W_R}{W_N C_P}(h_{R1} - h_{RO}) \qquad \text{(H-2)}$$

The evaporator heat balance between sodium and steam requires that:

$$W_N C_P (T_{N4} - T_{NS}) = W_E (h_{E1} - h_{EO})$$

*Blow-down flow is used to heat feedwater before going to condenser.

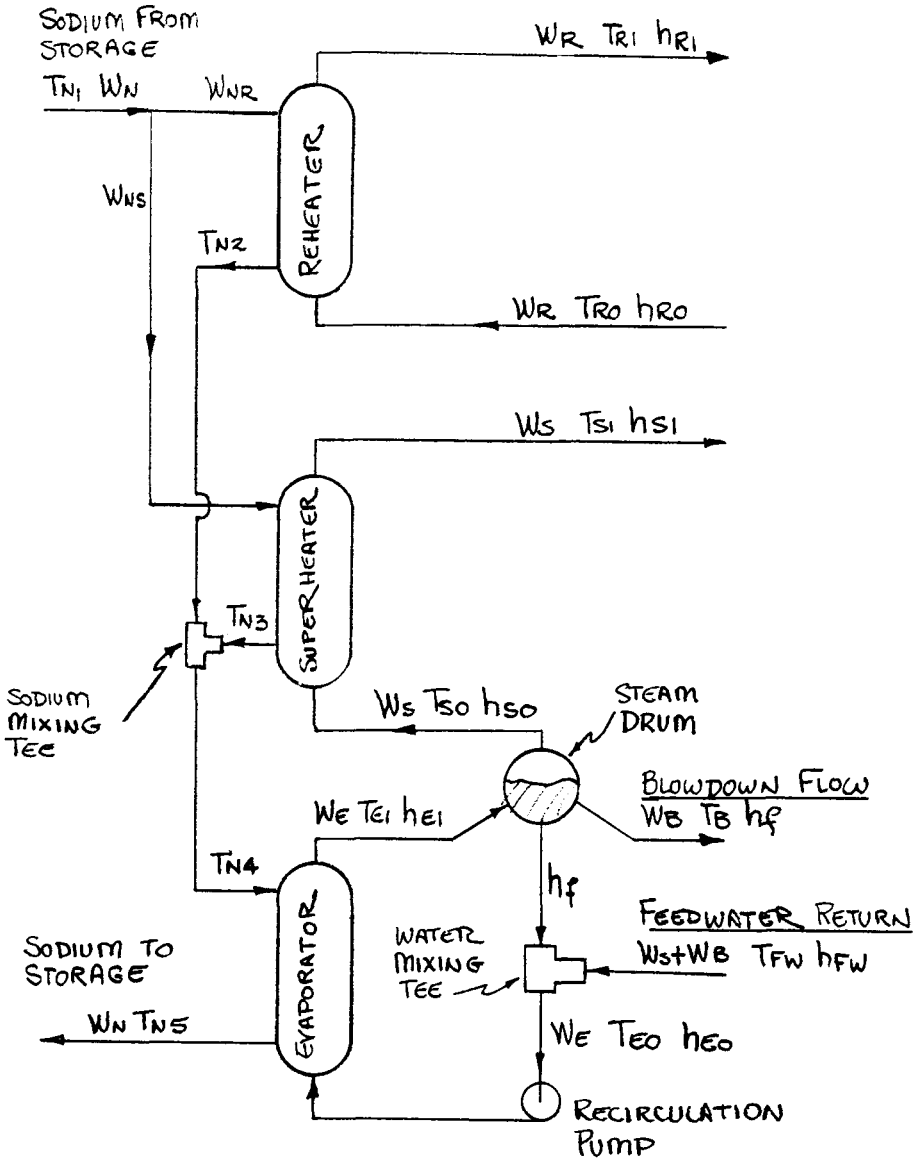

Where: W = fluid flowrate (LB/HR.)
T = temperature (°F)
h = enthalpy (BTU/LB)

Figure H-1. Analytical Model for Steam Generator Heat Balance

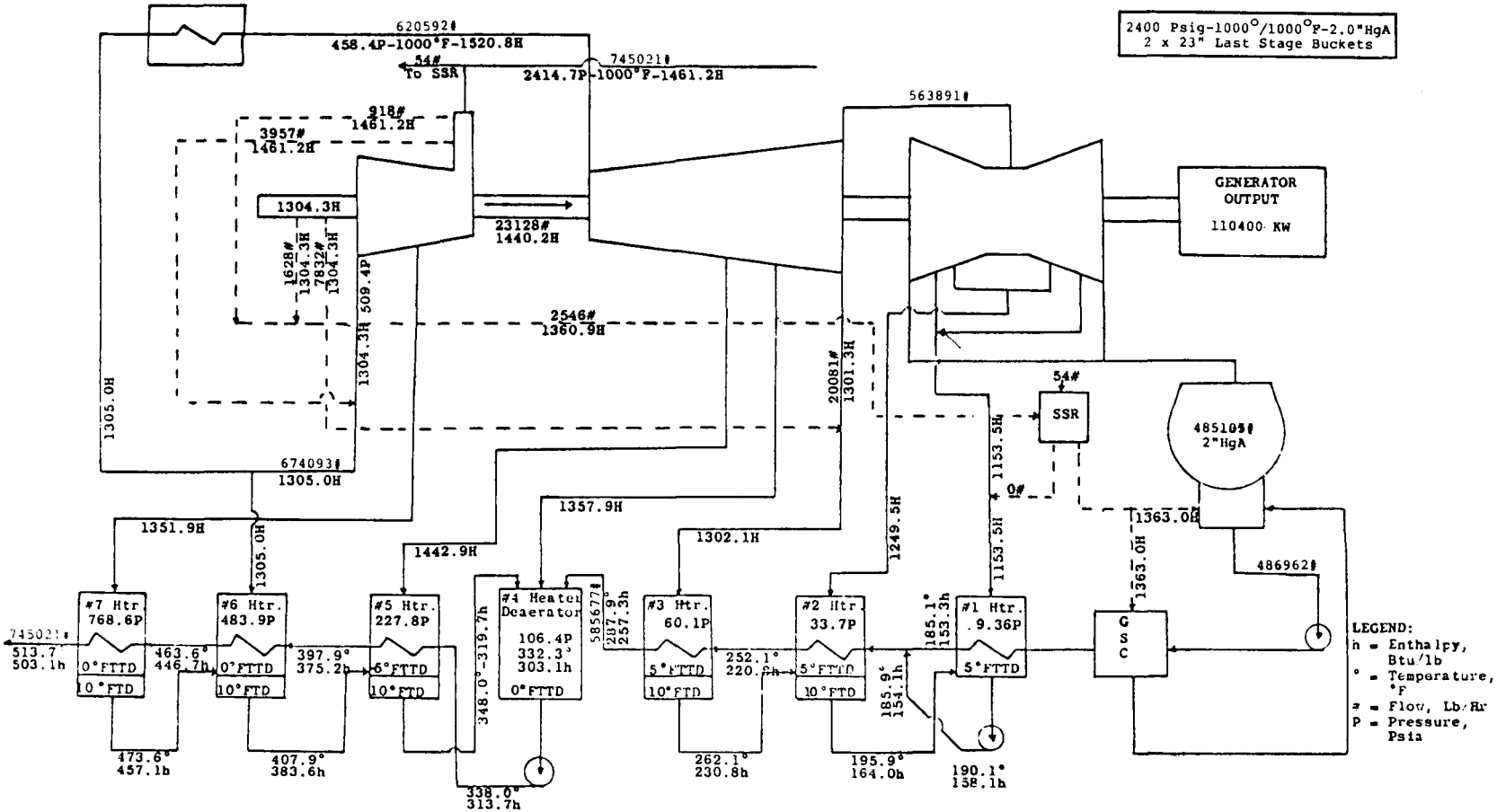

$$\text{Gross Heat Rate} = \frac{745021(1461.2-503.1)+620592(1520.8-1305.0)}{110400} = 7679 \text{ Btu/Kw-hr..}$$

Net Heat Rate = 7810 Btu/Kw-hr (43.7%)

Figure H-2. Approximate Steam Cycle Heat Balance

Solving for T_{N5}:

$$T_{N5} = T_{N4} - \frac{W_E}{W_N C_P}(h_{E1} - h_{E0}) \qquad \text{(H-3)}$$

Figure H-3 shows a plot of sodium and water temperatures vs. steam enthalpy. Using the slope of the sodium temperature line:

$$\frac{T_{N4} - T_{N5}}{h_{E1} - h_{E0}} = \frac{T_{NP} - T_{N5}}{h_f - h_{E0}} \qquad \text{(H-4)}$$

But from Figure H-3, $T_{NP} = T_{EI} + \Delta T$. Using this and Equation (H-4) to solve for T_{N4}:

$$T_{N4} = T_{N5}\left(1 - \frac{h_{E1} - h_{E0}}{h_f - h_{E0}}\right) + (T_{E1} + \Delta T)\left(\frac{h_{E1} - h_{E0}}{h_f - h_{E0}}\right) \qquad \text{(H-5)}$$

Substituting T_{N5} from Equation (H-3) into Equation (H-5):

$$T_{N4} = (T_{E1} + \Delta T) + \frac{W_E}{C_P W_N}(h_{E1} - h_f) \qquad \text{(H-6)}$$

But

$$h_{E1} = h_f + x\,h_{fg} = h_f + \frac{1}{R}\,h_{fg} \qquad \text{(H-7)}$$

where h_{fg} = heat of vaporization of water at the drum pressure.

$$T_{N4} = (T_{E1} + \Delta T) + \frac{W_E}{C_P W_N}\frac{h_{fg}}{R} \qquad \text{(H-8)}$$

Setting T_{N4} from Equation (H-8) equal to T_{N4} from Equation (H-5) and solving for the sodium flow W_N:

$$W_N = \frac{W_S(h_{S1} - h_{S0}) + W_R(h_{R1} - h_{RO}) + W_e h_{fg}/R}{C_P[T_{N1} - (T_{E1} + \Delta T)]} \qquad \text{(H-9)}$$

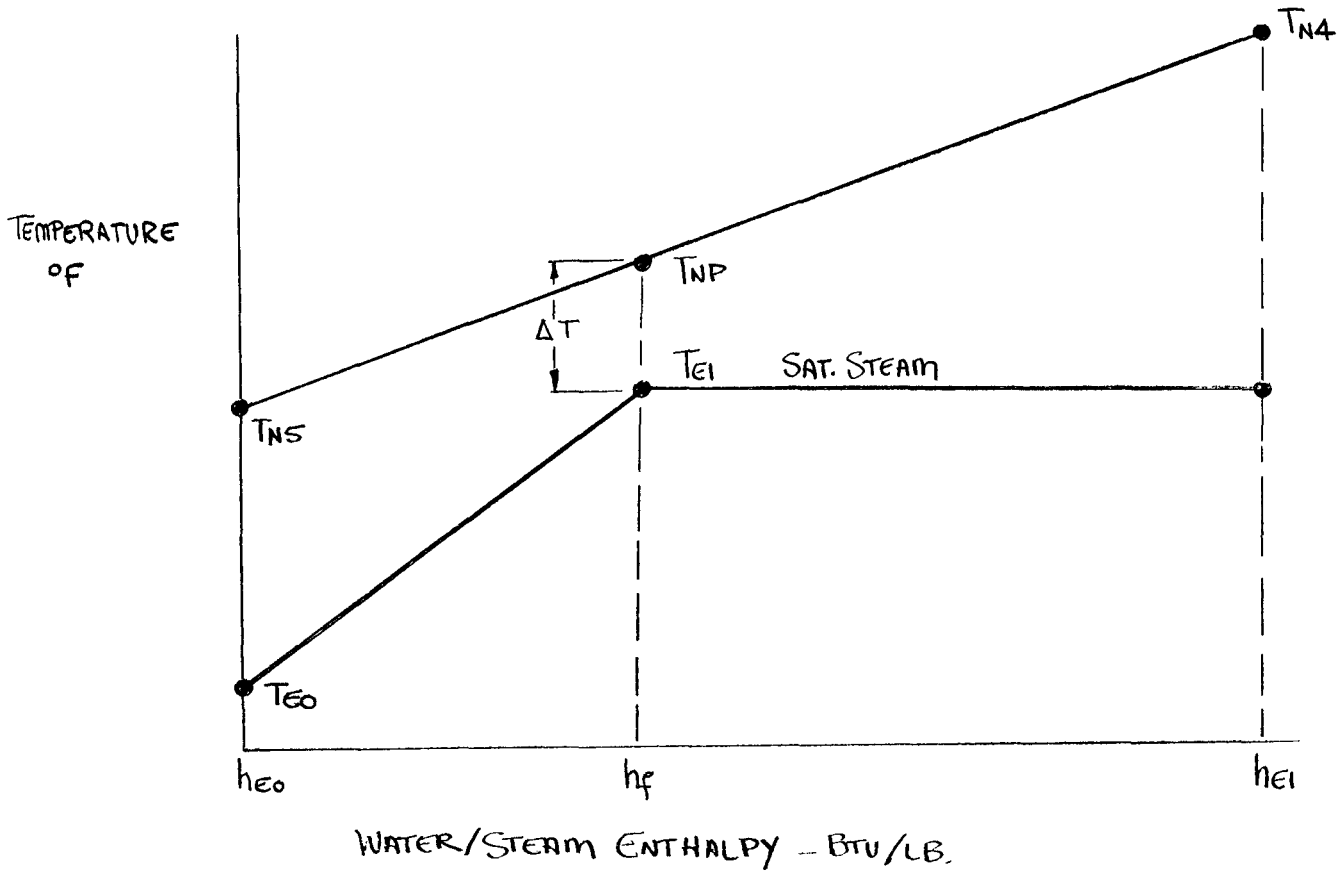

Figure H-3. Pinch Point Temperature Differential

In Task 2 an evaporator pinch point temperature of $\Delta T = 40$ F was selected. Small values of ΔT led to large evaporator surface area requirements but also result in a large temperature differential and low flow rates on the sodium side. Large differential sodium temperatures led to small storage requirements, so the selection of the pinch point should be the subject of an optimization of evaporator cost vs. storage cost; however, this subject was not addressed in Task 2 because of time limitations.

In Equation (H-9) the numerator represents steam side conditions, all of which are known from the turbine heat balance. Once the inlet sodium temperature T_{N1} is selected the sodium flow rate, W_N, can be calculated. Two operating conditions were studied in the parametric evaluations of Task 2, namely:

$$T_{N1} = 1050 \text{ F from which } W_N = 6.606 \times 10^6 \text{ pounds/hour}$$

$$T_{N1} = 1250 \text{ F from which } W_N = 4.157 \times 10^6 \text{ pounds/hour}$$

To avoid thermal unbalance at the sodium mixing tee, the superheater and reheater outlet temperatures were made equal:

$$T_{N2} = T_{N3} = T_{N4} \qquad \text{(H-10)}$$

Using the respective values of sodium flow rate and sodium inlet temperature from above, the following calculations are possible in the order listed:

from Equation (H-7),

$$h_{E1} = 1080.2 \text{ Btu/pound for } T_{N1} = 1050 \text{ F}$$

$$h_{E1} = 1080.2 \text{ Btu/pound for } T_{N1} = 1250 \text{ F}$$

from Equation (H-6),

$$T_{N2} = T_{N3} = T_{N4} = 840.1 \text{ F for } T_{N1} = 1050 \text{ F}$$

$$T_{N2} = T_{N3} = T_{N4} = 915.2 \text{ F for } T_{N1} = 1250 \text{ F}$$

from Equation (H-3),

$$T_{N5} = 627.5 \text{ F for } T_{N1} = 1050 \text{ F}$$

$$T_{N5} = 577.1 \text{ F for } T_{N1} = 1250 \text{ F}$$

The sodium flow rates in the superheater and reheater can be calculated from the respective heat balances:

$$W_{NR} C_P (T_{N1} - T_{N2}) = W_R (h_{R1} - h_{R0})$$

$$W_{NR} = \frac{W_R}{C_P}\left[\frac{h_{R1} - h_{R0}}{T_{N1} - T_{N2}}\right] \quad \text{(H-11)}$$

$$W_{NS} C_P (T_{N1} - T_{N3}) = W_S (h_{S1} - h_{S0}) \quad \text{(H-12)}$$

$$W_{NS} = \frac{W_S}{C_P}\left[\frac{h_{S1} - h_{S0}}{T_{N1} - T_{N3}}\right]$$

from which:

W_{NR} = 2.118 x 10^6 pounds/hour for T_{N1} = 1050 F

W_{NR} = 1.333 x 10^6 pounds/hour for T_{N1} = 1250 F

W_{NS} = 4.488 x 10^6 pounds/hour for T_{N1} = 1050 F

W_{NS} = 2.824 x 10^6 pounds/hour for T_{N1} = 1250 F

With the data obtained above, the steam generator heat balance calculations are complete.

IHX HEAT BALANCE

For simplicity, insulation losses and pump power inputs to the storage subsystem were ignored. Thus the inlet and outlet temperatures to the shell side of the IHX are the same as the steam generator shell side temperatures.

	1100 F System	1300 F System
T_{N5}-IHX shell inlet temperatures	627.5 F	577.1 F
T_{N1}-IHX shell outlet temperature	1050 F	1250 F
W_N IHX shell side sodium flow*	9.909 x 10^6 lb/hr	6.235 x 10^6 lb/hr
T_{T1} IHX tube inlet temperature (by definition)	1100 F	1300 F

*IHX flow = steam generator flow x 1.5 (solar multiple)

Except for the unknown tube side outlet temperature T_{T2}, a heat balance would be possible.

$$W_N C_P (T_{N1} - T_{NS}) = W_T C_P (T_{T1} - T_{T2})$$

which becomes

$$W_T = W_N \frac{(T_{N1} - T_{NS})}{(T_{T1} - T_{T2})} \qquad \text{(H-13)}$$

where

T_{T1} = temperature of sodium at the downcomer connection to the IHX

T_{T2} = temperature of sodium at the riser connection to the IHX

The tube side outlet temperature T_{T2} must be arbitrarily selected. A high value increases the log mean temperature difference (LMTD) which leads to a small surface area requirement. But a high value means that the tower flow rate will increase and a higher pump power will increase and a higher pump power will be required. Optimization of T_{T2} was beyond the scope of this study; therefore, the following values were arbitrarily selected:

T_{T1} = 725 F for 1100 F system

T_{T1} = 680 F for 1300 F system

Using these numbers in Equation (H-13) gives the following values for tower flow rate:

W_T = 11.223 x 10^6 pounds/hour for 1100 F system

W_T = 6.235 x 10^6 pounds/hour for 1300 F system

System losses were set equal to zero between the IHX and the absorber panels in Task 2. Therefore the flows and temperatures in the absorber panels are the same as listed above for the IHX, i.e.,

Total flow through the absorber panels (pounds/hour) = W_T

Absorber panel outlet temperature (^oF) = T_{T1}

Absorber panel inlet temperature (^oF) = T_{T2}

Appendix I

HEAT EXCHANGER COST ESTIMATES FOR PARAMETRIC ANALYSIS

COST OF MATERIALS

Table I-1 shows a material cost breakdown for ten identical steam generator modules assuming that these are the first ten modules of this type ever built. The estimate was prepared on 20 February 1976. The design is the same hockey stick design used in the study and has the following characteristics:

Vessel diameter, $D = 49$ in.

Number of tubes, $N_T = 757$

Tube pitch to diameter ratio, $P/d = 1.95$

Tubing outside diameter, $d = 0.625$ in.

Tubing wall thickness, $\delta = 0.109$ in.

Shell design pressure, $P_{SS} = 500$ psi

Tube design pressure, $P_{TS} = 2600$ psi

Active tube length, $L_A = 46$ ft

Since the Advanced Central Receiver System steam generators differ from the characteristics above, the material costs in Table I-1 must be adjusted. In general the cost adjustments were made on the basis of weight. Table I-1 contains columns labeled $N_T/757$, $P_{SS}/500$, $P_{TS}/2600$, $(D/49)$, $(D/49)^2$, $(D/49)^3$, and $L_A/46$. These headings refer to the scaling characteristics of each cost item. If a design remains the same as the reference design in all respects except length, then the cost of materials affected by length would be multiplied by $(L_A/46)$. Those components in Table I-1 affected by length are identified with an X in the $(L_A/46)$ column. The total cost effect of length can be obtained by adding all the costs with X in the $(L_A/46)$ column and multiplying the sum by $(L_A/46)$. Similar logic was applied to the other design parameters listed. Omitting for the moment the pressure effects, $P_{SS}/500$ and $P_{TS}/2600$, the resulting tabulation is:

$$\$M_B = 366890\,(D/49) + 294559\,(D/49)^2 + 3764098\,(D/49)^3 + 300\,(N_T/757) + 1059075\,(D/49)^2\,(L_A/46) \qquad \text{(I-1)}$$

The escalation factor for costs between 2/76 and 6/78 is:

$$(1.06)^2\,(1 + 0.06\,(4/12)) = 1.146 \quad (2YR-4\,Mo) \qquad \text{(I-2)}$$

A general overhead adder of 18% must also be applied. Correcting Equation (I-1) for this and for escalation and dividing by ten to obtain the single module cost results in:

$$\$M_o = 1013\,D + 16.59\,D^2 + 4.327\,D^3 + 0.0536\,N_T + 1.2967\,D^2 L_A + 11.65\,N_T L_A + 0.172\,D\,L_A \qquad \text{(I-3)}$$

This equation needs further adjustments to account for different tube size, different design pressures, and materials other than the 2-1/4 Cr - Mo used throughout the reference cost estimate. To do this, the following cost breakdown was used:

		% of Total Material Cost
$4.0568 x 10^5 = Total Tubing Cost		
$4.0568 x 10^5 x 30%	= $1.217 x 10^5 (Material))	10.6
$4.0568 x 10^5 x 50%	= $2.0284 x 10^5 (Manufacturing)	17.7
$4.0568 x 10^5 x 20%	= $0.8114 x 10^5 (Administration)	7.1
$7.4216 x 10^5 = Total Remaining Material Cost		
$7.4216 x 10^5 x 50%	= $3.7108 x 10^5 (Material)	32.3
$7.4216 x 10^5 x 20%	= $1.4843 x 10^5 (Manufacturing)	12.9
$7.4216 x 10^5 x 30%	= $2.2265 x 10^5 (Administration)	19.4
	Total %	100.0

Any change in material will therefore impact on the material fractions of the total component part cost plus the cost impact of using a material which is more difficult to machine weld, etc. In the latter case, an adder to the manufacturing cost is required.

The tubing incremental cost is calculated as follows:

where:

$$\frac{\Delta\$}{\$} = 0.106\left[\left(\frac{A}{A_R}\right)C_m - 1\right] \qquad \text{(I-4)}$$

C_M = ($/lb) for new material/($/lb) for 2-1/4 Cr - 1 Mo

A/A_R = tubing cross sectional area ratio = $17.78\,(\delta d - \delta^2)$

$\Delta\$/\$$ = incremental cost adder for tubing material change

Table I-1

PRODUCTION MATERIAL LIST
FOR TEN STEAM GENERATOR MODULES
(Date of Estimate: 20 February 1976)

QUANTITY	DESCRIPTION Page 1 of 3	ESTIMATED COST	$\frac{N_T}{757}$	$\frac{P_{ss}}{500}$	$\frac{P_{TS}}{2600}$	$\left(\frac{D}{49}\right)$	$\left(\frac{D}{49}\right)^2$	$\left(\frac{D}{49}\right)^3$	$\frac{LA}{40}$
22	FLANGES	327,435			X			X	
44	TRUNIONS	38,563						X	
24	CYLINDERS 19-3/4	74,192		X			X		X
12	CYLINDERS 27-1/2	68,689		X			X		X
12	RINGS	268,917		X			X		
22	STEAM HEADS	472,552			X			X	
13	REDUCERS	390,512		X				X	
13	REDUCERS	388,828		X				X	
21	OUTLET NOZZLES	74,775		X				X	
21	DRAIN NOZZLES	19,664		X				X	
11	INLET NOZZLES	67,380		X				X	
20	SWEEPOLETS	142,828		X				X	
2	SWEEPOLETS	14,542		X				X	
20	SWEEPOLETS	148,288		X				X	
2	SWEEPOLETS	15,090		X				X	
1 lot	BARE WELD WIRE & FLUX	121,249		X			X		X
1 lot	INCO 718 BAR	235,090		X			X		X
1 lot	PIPE	148,529		X				X	
21	RDT WELD CAPS 18"	66,698						X	
21	RDT WELD CAPS 8"	39,796						X	
21	RDT WELD CAPS 6"	33,011						X	
1 lot	BAR FOR UPPER T/S BAFFLE	16,095						X	
52	SHELL PL 2-1/4 X 80 X 163	340,895		X			X		X
11	UPPER SHELL PL 3-1/2 X 12 X 168	17,159		X				X	

GENERAL ELECTRIC

Table I-1 (Cont'd)

QUANTITY	DESCRIPTION Page 2 of 3	ESTIMATED COST	$\frac{N_T}{757}$	$\frac{P_{ss}}{500}$	$\frac{P_{TS}}{2600}$	$\left(\frac{D}{49}\right)$	$\left(\frac{D}{49}\right)^2$	$\left(\frac{D}{49}\right)^3$	$\frac{LA}{40}$
22	HEADER PL 4-1/4 X 96 X 102	179,646		X				X	
20	HEADER PL 4-4 1/4 X 96 X 94	165,572		X				X	
66	ELBOW 3-1/2 X 46 X 95	223,510		X				X	
20	TUBESHEETS 48" dia.	318,000						X	
10 lots	TUBING 5/8 dia.	3,000,000	X						X
10 lots	PLATE ASME SA-387 GR22 (Internals)	198,852		X				X	
10 lots	GAS CUTTING of ASME Plate	32,727		X				X	
11	TEMPORY WELD CAPS 26" dia x 1" tk	16,264						X	
40	FLEXITALLIC GASKETS	2,621			X		X		
5550	HELICOIL INSERTS	10,920			X		X		
1 lot	PINS & DOWELS	600		X			X		X
1 lot	WASHERS	300	X	X					
10	PLATES for ELBOW LINER 120x30x1/2	2,621		X				X	
1 lot	INSPECTION TRACKS	3,730				X			
10	SUPPORT RINGS (SUPPORT ASSY) NO364100M5	364,160		X		X			
1 lot	PLATE ASME SA-387 GR22	130,073		X				X	
1 lot	WELD ROD 16000#	27,312		X			X		X
2100 ft²	INSULATION BLANKET	9,618					X		X
60 Gal	PAINT (PRIMER & finish)	2,863				X			X
	GASES-ARGON	30,000					X		X
2	TEST HEADS 41" Ø X 11" TK	11,794		X				X	
20	GASKETS 18-2500# RF	1,145			X		X		
54	STUDS 2" Ø X 30" lg. w/2 nuts	10,998			X		X		
11	WELD CAPS 2"	2,266						X	

Table I-1 (Cont'd)

QUANTITY	DESCRIPTION Page 3 of 3	ESTIMATED COST	$\frac{N_T}{757}$	$\frac{P_{ss}}{500}$	$\frac{P_{TS}}{2600}$	$\left(\frac{D}{49}\right)$	$\left(\frac{D}{49}\right)^2$	$\left(\frac{D}{49}\right)^{\frac{1}{2}}$	$\frac{LA}{40}$
11	WELD CAPS 1"	3,172						X	
1 lot	CLEANING MATL'S	16,875					X		X
30	TEST PL 24x36x(2-1/4 - 3-1/2 - 4-1/4)	20,037						X	
	FREIGHT-CUDAHY to L.A 1,137,000# FORGINGS	55,122		X				X	
	FREIGHT-PITTS., PA. to L.A. 280,000# Plate	15,355		X			X		X
1 lot	COATED ELECTRODES	80,000		X			X		X
1 lot	CR MO BAR	9,605		X			X		X
1 lot	INCO BAR	16,000		X			X		X
	FREIGHT-GARY, IND., to L.A 500,000# PLATE	20,200		X			X		X

The associated increase in tubing manufacturing cost was set equal to the following expression:

$$\frac{\Delta\$}{\$} = 0.177\left[\left(\frac{d}{.625}\right)^{1/4}\left(\frac{0.109}{\delta}\right)^{1/4} C_{MF} - 1\right] \qquad \text{(I-5)}$$

where: C_{MF} = cost of manufacturing new material divided by cost for 2-1/4 Cr - 1 Mo.

It was arbitrarily decided that manufacturing costs for thicker or thinner wall tubes should be larger but as a weak function. Therefore the (1/4) exponent was chosen.

Adding Equations (I-4) and (I-5), a final expression is obtained. This can then be applied as a correction to Equation (I-3).

$$\$_{MT} = \$_{M_0}\left(1 + \left(\frac{\Delta\$}{\$}\right)_T\right)$$

and

$$\left(\frac{\Delta\$}{\$}\right)_T = 1.88\left(\delta d - \delta^2\right)C_M + 0.03087\left(d/\delta\right)C_{MF} - 0.282746 \qquad \text{(I-6)}$$

For the remainder of the material, the following correction was applied:

$$\left(\frac{\Delta\$}{\$}\right)_R = 0.323\left(C_M - 1\right) + 0.129\left(C_{MF} - 1\right) \qquad \text{(I-7)}$$

The effect of pressure levels on material cost was estimated to follow the following general rules:

1. Roughly one-quarter of the material will increase in thickness and weight by the factor $P_{TS}/2600$.
2. Roughly three-quarters of the material will increase in thickness and weight by the factor $P_{SS}/500$.

$$\left(\frac{\Delta\$}{\$}\right)_P = 0.323 \times \frac{1}{4}\left[P_{TS}/2600 - 1\right] + 0.323 \times \frac{3}{4}\left[P_{SS}/500 - 1\right]$$

thus $$\left(\frac{\Delta\$}{\$}\right)_P = 3.11 \times 10^{-5} P_{TS} + 4.85 \times 10^{-4} P_{SS} - 0.32336 \qquad \text{(I-8)}$$

Summing $(\Delta\$/\$)_T$ plus $(\Delta\$/\$)_R$ plus $(\Delta\$/\$)_P$,

$$\left(\frac{\Delta\$}{\$}\right)_M = 1.88(\delta d - \delta^2)\,C_m + 0.114\,(d/\delta)^{1/4}\,C_{MF} + 0.323\,C_m + 0.129\,C_{MF} + 3.11\times10^{-5}\,P_{TS} + 4.85\times10^{-4}\,P_{SS} - 1.0575 \qquad \text{(I-9)}$$

This correction is applied to the cost estimate as follows using $\$M_0$ from Equation (I-3):

$$\$_M = \$_{M0}\,(1 + (\Delta\$/\$)_M)$$

COST OF FABRICATION AND INSPECTION

Fabrication and inspection costs were not detailed in the 20 February 1976 cost estimate, but the total costs for subassemblies were given. A breakdown for these costs is detailed in Table I-2. Figure I-1 shows a learning curve applied to the reference units. Note that the cost of the Nth unit shipped is 0.729 times the cost of the fourth unit shipped. The reference costs are based on the fourth unit shipped; therefore, the 0.729 factor applies.

Using these overall cost numbers as a rough guide the fabrication and inspection, labor costs were detailed further using rough percentages of total cost for each operation. The results for one module escalated to June 1978 and corrected for the learning curve out to the Nth unit are detailed in Table I-3. Upon summation of all factors in the table, the fabrication and inspection labor costs became:

$$\$_{FI} = 1000\,[235(D/49)^2 + 30(D/49)^3 + 10(D/49) + 5(L_A/46) + 403(N_T/757) + 165(D/49)^2(L_A/46) + 295(D/49)(L_A/46) + 170(L_A/46)(N_T/757) + 50(D/49)^2(N_T/757) + 20(D/49)(L_A/46)(N_T/757) + 100(D/49)(N_T/757) \qquad \text{(I-10)}$$

which reduces to

$$\$_{FI} = 204D + 97.9D^2 + 0.255D^2 + 109\,L_A + 532\,N_T + 1.49\,D^2L_A + 131\,DL_A + 4.88\,L_AN_T + 0.0275D^2N_T + 0.01172\,DL_AN_T + 2.7DN_T$$

Table I-2

FABRICATION AND INSPECTION COST BREAKDOWN
FOR TEN HOCKEY STICK STEAM GENERATORS
(Date of Estimate: 20 February 1976)

Component Subassembly	Man-hours	Cost
Shroud Assembly	47,722	$ 1,551,753
Shroud/Shell Assembly	42,507	3,487,195
Tube Bundle	144,806	5,243,988
Loose Equipment	8,283	1,717,377
Final Assembly	154,229	5,104,839
Test	21,450	631,119
Totals	418,997	$17,736,271

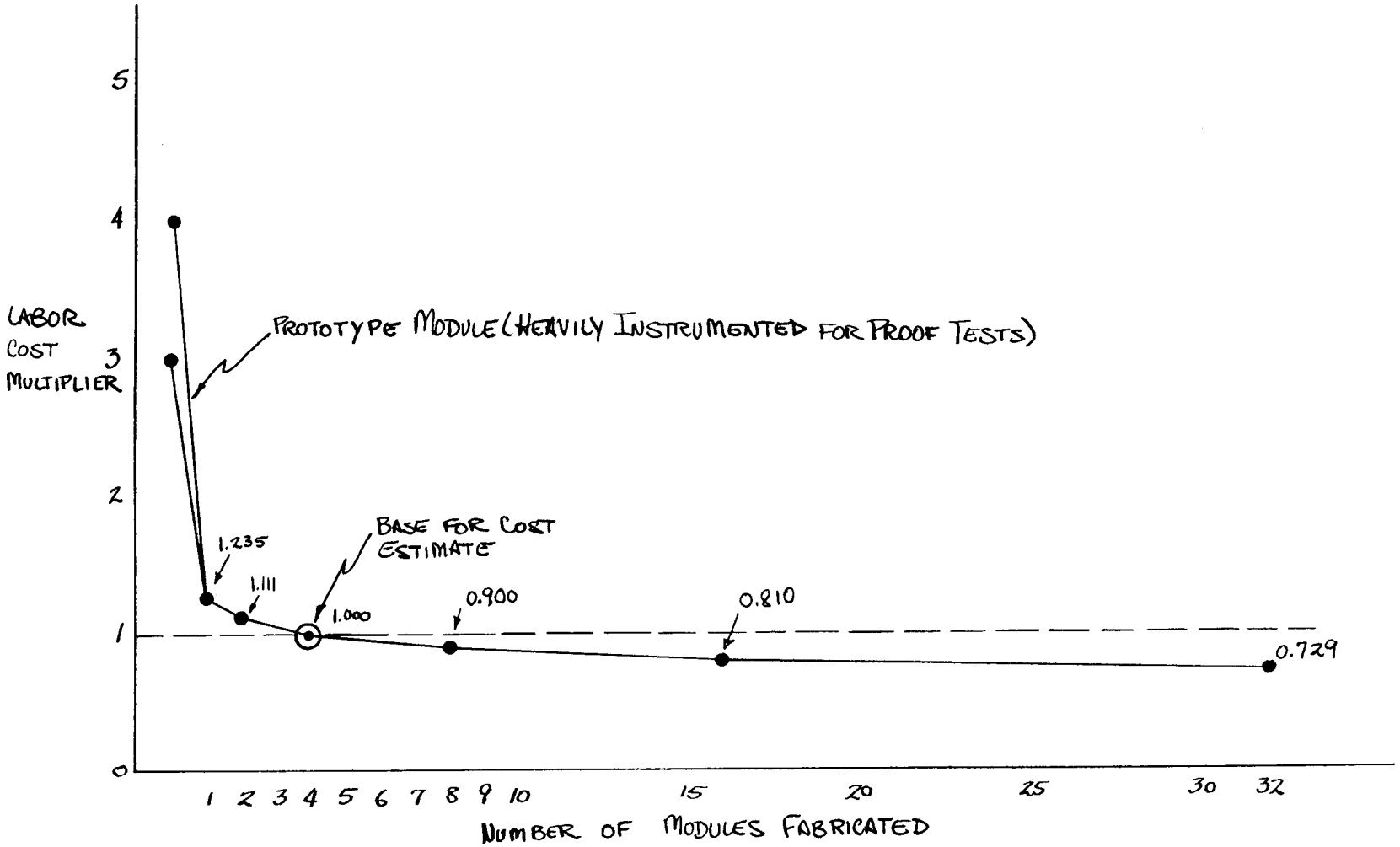

Figure I-1. Effect of Learning Curve on Steam Generator Labor Costs

Table I-3

REFERENCE LABOR COSTS FOR FABRICATION AND INSPECTION OF ONE MODULE

	$ x 10^-3	DESIGN CORRECTION FACTORS $(D/49)^3$	$(D/49)^2$	$D/49$	$LA/46$	$N/757$
TUBE SPACERS - 21 REQD						
CUT PLATES	5.0	XX			XX	
DRESS UP	5.0	XX			XX	
DRILL HOLES	120.0				XX	XX
CHAMFER HOLES	50.0				XX	XX
MISC.	5.0	XX			XX	
INSPECTION	20.0			XX	XX	XX
SHROUD LABOR						
PLATE PREP	15.0	XX			XX	
ROLLING PLATE	20.0			XX	XX	
PLATE WELDS	50.0			XX	XX	
FORGING WELDS	15.0	X				
SUPPORT PLATE FIXTURES	35.0			XX	XX	
INSTALL SUPPORT PLATES	20.0			XX	XX	
INSPECTION	20.0			XX	XX	
TUBE SHEETS						
FACING	5.0	X				
TUBE WELD PREPS	50.0					X
SHELL WELD PREPS	10.0	X				
TUBE HOLES	100.0			XX		XX
BOLT HOLES - THREADED	30.0	X				
INSPECTION	50.0	XX				XX
TUBE - TUBE SHEET WELDS						
TUBE WELD PREPS	20.0					X
TUBE BENDING	10.0					X
TUBE INSERTION	15.0					X
TUBE WELDS	118.0					X
INSPECTIONS	150.0					X

NOTE: COSTS ARE FOR ONE MODULE CORRECTED FOR N^{TH} UNIT (.73) AND CORRECTED FOR INFLATION (2/76 - 6/78) (1.146)

Table I-3 (Cont'd)

	$ x 10^-6	DESIGN CORRECTION FACTORS $(\frac{D}{49})^3$	$(\frac{D}{49})^2$	$\frac{D}{49}$	$\frac{LA}{46}$	$\frac{N}{757}$
SHELL LABOR						
PLATE PREP	15.0		XX		XX	
ROLL PLATES	15.0			XX	XX	
PLATE WELDS - LONGITUDINAL	20.0			XX	XX	
FORGING WELDS	20.0		X			
NOZZLE WELDS	20.0		X			
CYLINDRICAL WELD PREP	10.0		XX		XX	
CYLINDRICAL WELDS	20.0		XX		XX	
ASSEMBLY	15.0			XX	XX	
INSPECTION	50.0			XX	XX	
STEAM HEADS						
MACHINE FLANGES & HEADS	20.0	X				
BOLT HOLES - DRILL	10.0	X				
WELD PREPS	20.0		X			
WELD	30.0		X			
INSPECTION	40.0		X			
FINAL ASSEMBLY & INSPECTION	50.0			XX	XX	
MISCELLANEOUS						
THERMAL BAFFLES/LINERS	30.0		XX		XX	
INLET & OUTLET PLENUMS	50.0		XX		XX	
UPPER BAR SUPPORTS	45.0		X			
SHROUD STANDOFFS	5.0				X	
X-RAY FILM RACK	10.0			X		
FLOW RESTRICTORS	10.0					X
ORIFICING	30.0					X
MISC.	10.0		XX		XX	
	1483.0					

As the unit sizes increase, the cost of fabrication decreases because overhead costs are spread out and overall handling cost percentages decrease. This effect is not included in Equation (I-10). The logic developed for incorporating this effect is as follows.

Let $$R = \$_F / \$_{FI} \quad \text{(I-11)}$$

where $\$_{FI}$ = reference fabrication cost.

Let $$\$_{F_O} = \$_{FI} + (\$_{FI} - \$_F)(F/F_R) \quad \text{(I-12)}$$

where F, F_R = extrapolation factors for new design and old design respectively, e.g., (D/49), (N/757), (L_A/46), etc.

Equation I-12 indicates that the new cost of fabrication is some base cost at zero size factor (F/F_R) and this is increased with size by the difference ($\$_{FI} - \$_F$). Combining Equations I-11 and I-12:

$$\$_{F_O} = R\$_{FI} + \$_{FI}(1-R)\,F/F_R \quad \text{(I-13)}$$

A value of R=0.333 was chosen as the zero intercept value. Using this value and applying Equation I-13 to Equation I-10,

$$\$_{F_O} = 493840 + 65.5D^2 + 0.17D^3 + 136D + 73L_A + 355N_T + 0.994D^2L_A + 87.4DL_A + 3.26L_AN_T + 0.0183D^2N_T + 0.0078DL_AN_T + 1.8DN_T \quad \text{(I-14)}$$

Equation I-14 still remains uncorrected for tube size effects, design pressures (massiveness of parts), and material changes on the fabrication costs. The details of these correction factors are contained in Table I-4. The result is:

$$\Delta\$_F = 691200d^2 + 316800d + 200P_{SS} + 91.92P_{SS} + 753000C_{MF} - 1.56\times10^6 \quad \text{(I-15)}$$

Table I-4

EFFECTS OF TUBE SIZE, DESIGN PRESSURE,
AND MATERIAL TYPE ON FABRICATION COST

1- TUBE SIZE EFFECTS

TUBE SPACERS

DRILL HOLES	$120{,}000 \times \left(\frac{d}{.625}\right)^2$
CHAMFER HOLES	$50{,}000 \times (d/.625)$

TUBE SHEETS

TUBE WELD PREPS	$50{,}000 \times (d/.625)^2$
TUBE HOLES	$100{,}000 \times (d/.625)^2$

TUBE-TUBESHEET WELDS

TUBE WELD PREPS	$20{,}000 \times (d/.625)$
TUBE BENDING	$10{,}000 \times (d/.625)$
TUBE WELDS	$118{,}000 \times (d/.625)$

$$\Delta\$_F = 270{,}000\left(d/.625\right)^2 + 198{,}000(d/.625) - 4.68\times10^5$$

$$\Delta\$_F = 691200\, d^2 + 3.168\times10^5 d - 4.68\times10^5$$

2- DESIGN PRESSURES

SHROUD

PLATE PREP	$15{,}000\ (P_{ss}/500)$
ROLLING PLATE	$20{,}000\ (P_{ss}/500)$
PLATE WELDS	$50{,}000\ (P_{ss}/500)$
FORGING WELDS	$15{,}000\ (P_{ss}/500)$

SHELL

ALL BUT INSPECTION	$135{,}000\ (P_{ss}/500)$

Table I-4 (Cont'd)

TUBE SHEETS	
TUBE HOLES	100,000 (P_{TS}/2600)
BOLT HOLES	30,000 (P_{TS}/2600)
TUBE-TUBESHEET WELDS	
TUBE WELDS	118,000/2 (P_{TS}/2600)
STEAM HEADS	
MACHINING	20,000 (P_{TS}/2600)
BOLT HOLES - DRILL	10,000 (P_{TS}/2600)
WELD PREPS & WELD	20,000 (P_{TS}/2600)

$$\Delta \$_F = 100{,}000\,(P_{SS}/500) + 239{,}000\,(P_{TS}/2600) - 339{,}000$$

$$\Delta \$_F = 200\,P_{SS} + 91.92\,P_{TS} - 339{,}000$$

3- MATERIAL IMPACT ON $\$_F$

ADDING ALL MACHINING & WELDING OPERATIONS $\$ = 753{,}000$

$$\Delta \$_F = 753{,}000 \times C_{MF} - 753{,}000$$

4- TOTAL $\Delta \$_F$

$$\Delta \$_F = 691200\,d^2 + 316800\,d + 200\,P_{SS} + 91.92\,P_{TS} + 753{,}000 \times C_{MF} - 1.56 \times 10^6$$

WHERE; C_{MF} = FABRICATION COST MULTIPLE FOR MATERIAL OTHER THAN 2¼Cr-1Mo

ADDITIONAL COSTS FOR TOOLING CHARGES AND HANDLING

The additional charges listed below were also included in the 20 February 1976 cost estimate:

Rate Tooling	Man-hours	Cost
Tooling Design	810	$ 21,083
Tooling Fabrication (including materials)	57,096	1,847,320
Tooling Maintenance	6,749	206,465
Totals	64,655	$2,074,868
Materials Handling		
Fabrication (including materials)	12,900	$ 490,739
Handling Labor	17,228	488,494
Handling Equipment and Maintenance	4,343	97,614
Packaging and Shipping	1,845	252,465
Manufacturing and QC Equipment	-0-	234,315
Totals	36,316	$1,563,627

Dividing these total costs by 10, applying the Nth module factor, and escalating costs to June 1978, the following equations were developed to express tooling and handling charges.

$$\$_{TL} = 0.0658\,(\$_F + \$_M) \qquad \text{(I-16)}$$

$$\$_H = 0.0498\,(\$_F + \$_M) \qquad \text{(I-17)}$$

Equations I-16 and I-17 assume that the costs associated with tooling and handling are a fixed percentage of the total cost of the module.

SUMMARY OF HEAT EXCHANGER COST ESTIMATING PROCEDURE

In summation, a cost estimate for any Advanced Central Receiver System steam generator or IHX of the general hockey stick configuration is given with a reasonable degree of accuracy by solving the following equations in order;

$$\$_{MO} = 1013D + 16.59D^2 + 4.327D^3 + 0.0536\,N_T + 1.2967\,D^2L_A + 11.65\,N_TL_A + 0.172\,DL_A$$

$$(\Delta\$/\$)_M = 1.88(\delta d - \delta^2)C_M + 0.114\,(d/\delta)^{1/4}\,C_{MF} + 0.322\,C_M + 0.129\,C_{MF} + 3.11\times10^{-5}\,P_{TS} + 4.85\times10^{-5}P_{SS} - 1.0575$$

$$\$_M = \$_{MO}\,(1 + (\Delta\$/\$)_M)$$

$$\$_{FO} = 493840 + 65.5D^2 + 0.17D^3 + 136D + 73L_A + 355\,N_T + 0.994\,D^2L_A + 87.4\,DL_A + 3.26\,L_AN_T + 0.0183D^2N_T + 0.0078\,DL_AN_T + 1.8\,DN_T$$

$$\Delta\$_F = 691200\,d^2 + 316800\,d + 200\,P_{SS} + 91.92\,P_{SS} + 753000\,C_{MF} - 1.56\times10^6$$

$$\$_F = \$_{FO} + \Delta\$_F$$

$$\$_{TL} = 0.0658\,(\$_F + \$_M)$$

$$\$_H = 0.0498\,(\$_F + \$_M)$$

Equation (I-18) provides the total delivered cost of the heat exchanger being designed and tested.

$$\$_T = \$_M + \$_F + \$_{TL} + \$_H \qquad \text{(I-18)}$$

PARAMETRIC STEAM GENERATOR COSTS

The eight steam generators required for the Task II parametric study were evaluated for cost using Equation (I-18) and the design data from Section 3.4.6. The values for material cost adders were assumed to be as shown in Table I-5.

Table I-5

MATERIAL COST FACTORS

	Material Used	Material Cost Multiple (C_M)	Material Labor Cost Multiple (C_{MF})
Evaporator - 1100 F System	2-¼ Cr - 1 Mo	1.0	1.0
Evaporator - 1300 F System	2-¼ Cr - 1 Mo	1.0	1.0
Superheater - 1100 F System	I-800	5.1	1.25
Superheater - 1300 F System	I-625	6.0	1.25
Reheater - 1100 F System	I-800	5.1	1.25
Reheater - 1300 F System	I-625	6.0	1.25
IHX - 1100 F System	I-625	6.0	1.25
IHX - 1300 F System	316SS	3.82	1.25

Appendix J

COMPARISON OF MOLTEN SALT AND SODIUM AS SECONDARY LOOP FLUIDS

To assess the potential of using draw salt as a storage medium, a detailed comparison of sodium and salt was made using the Concept 3 storage configuration. The particular salt used in this comparison is described in Table J-1. It was assumed that this salt would cost $0.20/pound FOB in the Southwestern United States based on a verbal quote from Park Chemical Company.

The components analyzed in this comparison are shown in Figure J-1, and the results of performing a heat balance on the steam generators for both sodium and salt are presented in Table J-2.

A preliminary design for the sodium heat exchangers yielded the tube sizes and heat transfer coefficients listed in Table J-3. To estimate the changes in heat transfer for salt, the correlations given by Fraas and Ozisik* were used. For sodium:

$$Nu_N = 7 + .025 (Re_N Pr_N)^{.8} \qquad \text{(J-1)}$$

$$Nu_S = .023 Pr_S^{.4} Re_S^{.8} \qquad \text{(J-2)}$$

where Nu = Nusselt Number

Re = Reynolds Number

Pr = Prandtl Number

If we assume the salt heat exchangers are designed to have the same tube diameters and flow speeds as the heat exchangers using sodium, then

$$\frac{Nu_S}{Nu_N} = \frac{h_S k_N}{h_N k_S} \qquad \text{(J-3)}$$

Substituting Equations (J-1) and (J-2) into this relation gives

$$\frac{h_S}{h_N} = \left(\frac{k_S}{k_N}\right) \frac{.023 Pr_S^{.4}}{7 Re_N^{-.8} + .025 Pr_N^{.8}} \left(\frac{v_N}{v_S}\right)^{.8} \qquad \text{(J-4)}$$

*A.P. Fraas and M.N. Ozisik, Heat Exchanger Design, John Wiley and Sons, New York, 1965.

Table J-1
PROPERTIES OF DRAW SALT

Chemical Composition	54% KNO_3, 46% $NaNO_3$
Melting Point	484 K (430°F)
Special Heat (solid)	0.32 cal/gm-K (Btu/lb-°F)
(liquid)	0.37 cal/gm-K (Btu/lb-°F)
Thermal Conductivity	0.49 Kcal/h-m-K (0.33 Btu/h-ft-°F)
Heat of Fusion	19.3 cal/gm (35.0 Btu/lb)

Temperature K (°F)	Density gm/cm^3 (lb/ft^3)	Viscosity Centipoise
533 (500)	1.93 (120.5)	4.00
589 (600)	1.89 (118.0)	2.80
644 (700)	1.85 (115.5)	2.05
700 (800)	1.82 (113.6)	1.65
755 (900)	1.78 (111.1)	1.45
811 (1000)	1.74 (108.6)	1.00

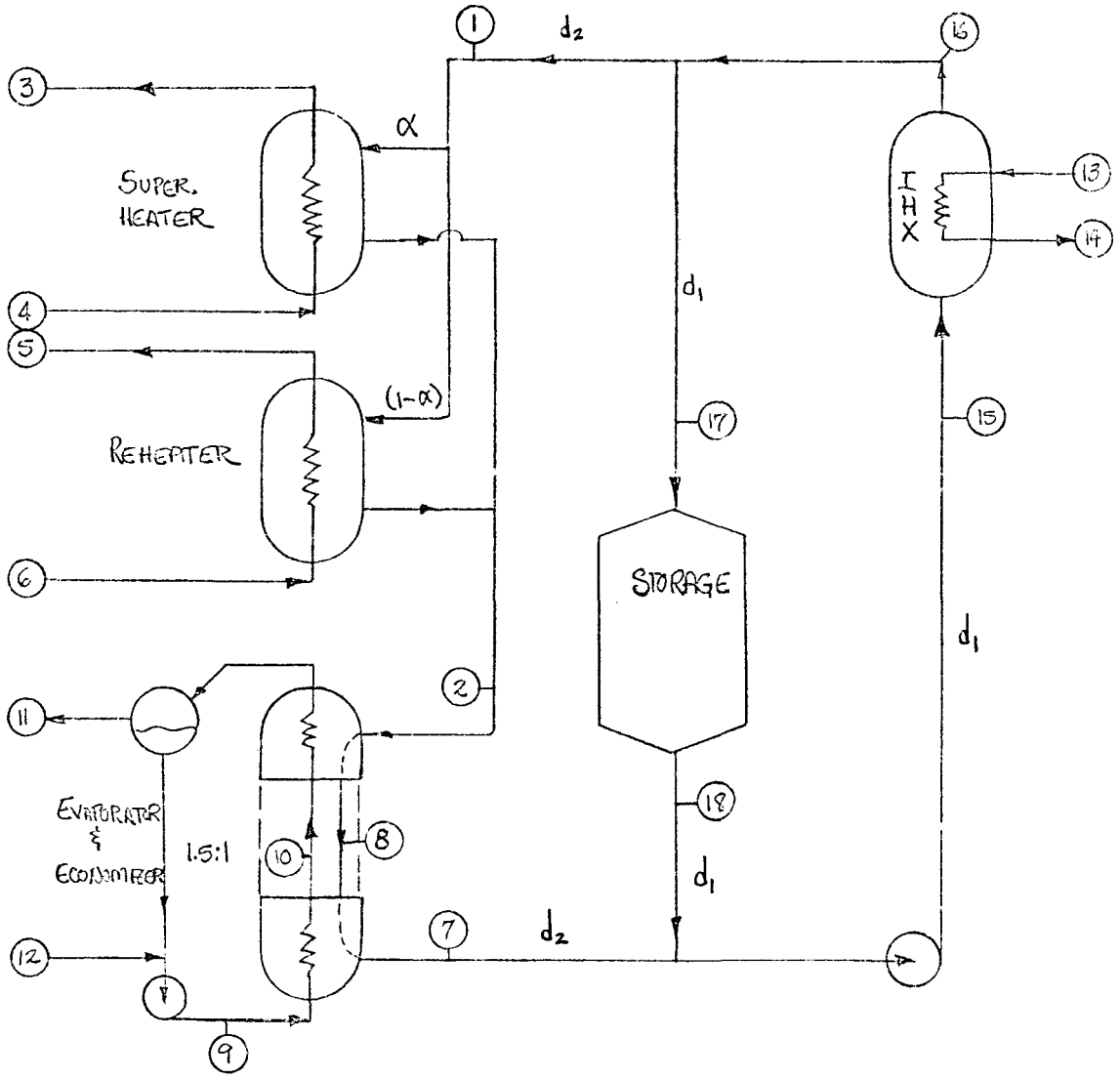

Figure J-1. System Configuration Used in Comparing Sodium with Molten Salt

Table J-2

SYSTEM STATE POINTS BASED ON STEAM GENERATOR HEAT BALANCE

STATE POINT	TEMP °F	PRESS psia	FLOWRATE lb/hr	ENTHALPY Btu/lb.
STEAM				
3	1000	2415	745021	1461.2
4	685	2800	745021	1054.8
5	1000	455	620592	1520.8
6	610	509	620592	1305.0
11	685	2800	745021	1054.8
12	514	2800	"	503.1
9	580	2800	1,117,532	591.8
10	685	2800	"	770.1
LOOP FLUID			FLOWRATE SODIUM	FLOWRATE SALT
1	1050		6.2819SE6	5.09347E6
2	818		"	"
8	706		"	"
7	600		"	"
17	1050		3.14097E6	2.54674E6
18	600		"	"
15	600		9.42292E6	7.64021E6
16	1050		"	"
RECEIVER FLUID				
13	1100			
14				

$\alpha = .6933$

Table J-3

HEAT TRANSFER CHARACTERISTICS OF SODIUM SYSTEM HEAT EXCHANGERS

Heat Exchanger	Tube OD (in.)	Wall (in.)	h_o Btu/hr-ft^2-°F	h_i Btu/hr-ft^2-°F	U_{wall} Btu/hr-ft^2-°F	U Btu/hr-ft^2-°F
			(Na)	(H_2O)		
Superheater	0.625	0.407	6046	2765	965	569
Reheater	1.050	0.950	2861	384	2557	276
Evaporator	0.625	0.407	6838	19260*	1208**	949
Economizer	0.625	0.407	7033	3860	1217**	734
			(Na)	(Na)		
IHX	0.970	0.88	4097	8236	2785	1357

h_o = heat transfer coefficient on outside of tube

h_i = heat transfer coefficient on inside of tube

U_{wall} = tube wall conductance

U = total tube conductance

*Assumes 50/50 split between nucleate/film boiling.

**Includes $U_{fouling}$ = 3721 and U_{tube} = 1810 econ./1790 evap.

where k = thermal conductivity

ν = viscosity

h = heat transfer coefficient

Applying this relation to the heat transfer coefficients in Table J-3 yields the coefficients for comparable salt heat exchangers listed in Table J-4.

These data were then used to estimate heat exchanger surface area required for both the salt and sodium systems. These results are summarized in Table J-5.

Pressure drops were then evaluated for both loops by scaling from the sodium results. In the heat exchangers (Table J-5), where most of the pressure drop is caused by momentum effects, the scaling was done by

$$\frac{\Delta P_S}{\Delta P_N} = \frac{\rho_S}{\rho_N} = 2.26 \qquad \text{(J-5)}$$

where ΔP = pressure drop

ρ = fluid density

which assumes the same flow speed in salt and sodium exchangers.

In piping runs, the pipe diameter was allowed to vary in order to maintain the same flow speed for salt and sodium. Pipe sizes, lengths, and numbers of fittings are listed in Table J-6, along with the pressure drops computed. The loop ΔP shown in this table includes gravity head effects due to the height of the storage tanks, and the heat exchanger pressure drops.

Pumping powers shown in Table J-6 assume an electromagnetic pump for the sodium (50% efficiency) and a centrifugal pump for the salt (81% efficiency).

The storage volume for $3MW_eh/MW_e$ was found to be 392,145 cubic feet for sodium and 140,719 cubic feet for salt. This includes two percent allowance for cover gas. The mass of storage medium required was 19.22×10^6 pounds for sodium and 15.59×10^6 pounds for salt, which includes a two percent adder for thermal losses and turbine startup.

These comparisons are summarized in Table J-7 where the relative sizes of salt equipment have been expressed as ratios with respect to the sodium case. The material selection shows that the salt case is identical to the sodium case except in the cold leg storage tank and piping. Incoloy 800 must be used in the superheater and reheater of both systems to avoid water side stress corrosion.

The factors in Table J-7 were used to scale the costs of Case S3 (Section 3.4.7). Costs for the salt and heat exchangers as well as the pipe, fittings, and valves

Table J-4

HEAT EXCHANGER CHARACTERISTICS OF SALT SYSTEM HEAT EXCHANGERS

Heat Exchanger	Tube OD (in.)	Tube ID (in.)	h_o $\left(\frac{Btu}{hr\text{-}ft^2\text{-}°F}\right)$ (Salt)	h_i $\left(\frac{Btu}{hr\text{-}ft^2\text{-}°F}\right)$ (H_2O)	U_{wall} $\left(\frac{Btu}{hr\text{-}ft^2\text{-}°F}\right)$	U $\left(\frac{Btu}{hr\text{-}ft^2\text{-}°F}\right)$
Superheater	0.625	0.407	907	2765	965	371
Reheater	1.050	0.950	429	384	2557	178
Evaporator	0.625	0.407	1026	19260	1208	461
Economizer	0.625	0.407	1055	3860	1217	531
IHX	0.970	0.88	614 (Salt)	8236 (Na)	2785	471

Table J-5

HEAT EXCHANGER SURFACE REQUIREMENTS

Heat Exchanger	Surface Area (ft^2) (Sodium)	Surface Area (ft^2) (Salt)	Effectiveness (%)	Pressure Drop (psi) (Sodium)	Pressure Drop (psi) (Salt)
Superheater	6271	9615	86	9.6	21.7
Reheater	4373	6767	89	3.9	8.8
Economizer	13,238	21,071	83	12.7	28.7
Evaporator	3684	6579	84		
IHX	10,299	26,650	90	7.2	16.3

Table J-6

PIPING AND LOOP PRESSURE DROP AND PUMPING POWER

	Pipe Diameter D_i (in.)	Pipe Diameter D_z (in.)	Length L_i (ft)	Length L_z (ft)	No. of Valves
Sodium	24.0	18.0	400	900	4
Salt	14.4	10.8	400	900	4

	Piping ΔP (psi)	Loop ΔP* (psi)	Volume Flow (gpm)	Pump Power (MW)
Sodium	112	144-165	23,499	2.292
Salt	288	360-407	8448	1.310

*Range shows effect of storage tank fluid level variations.

Table J-7

COMPARISON OF SODIUM TO MOLTEN SALT

1100 F CASE

		Sodium Storage	Molten Salt Storage
Secondary Loop Schematic		Concept 3	Concept 3
Containment:	Hot Leg	316SS	316SS
	Cold Leg	2-1/4 Cr-1 Mo	Carbon Steel
	Hot Tank	316SS	316SS
	Cold Tank	2-1/4 Cr-1 Mo	Carbon Steel
	Superheater	Incoloy 800	Incoloy 800
	Reheater	Incoloy 800	Incoloy 800
	Evaporator	2-1/4 Cr-1 Mo	2-1/4 Cr-1 Mo
	IHX	316SS	316SS
Equipment Sizes:			
	Storage Volume	1	0.359
	Area: Superheater	1	1.533
	Reheater	1	1.547
	Evaporator	1	1.634
	IHX	1	2.879
	Storage Material	Sodium	Salt
	Weight	1	0.813
	Cost ($/lb)	0.33	0.20
	Main Pump		
	Type	EM	Centrifugal
	Volume Flow	1	0.360
	Head	1	2.571
	Power (Electric)	1	0.572
	Cost	-	$2.77/gpm/psi
	Pipe Length	1	1
	Diameter	1	0.6

were obtained by applying the Table J-7 factors directly to the Case S3 costs of Section 3.4.7. The pump cost for salt was estimated using previous data for sodium centrifugal pumps. Salt storage vessel costs were scaled from the field assembled tank cases IVa and IVc in Appendix G. This scaling is shown in Table J-8.

Table J-8

COST OF MOLTEN SALT STORAGE TANKS - SCALING FROM SODIUM CASE S3

(IVf) HOT TANK 149,344 ft³ scale from IVa V/Vo = 1.436

(IVg) COLD TANK 149,344 ft³ scale from IVc V/Vo = 1.436

also carbon stl. # / 2¼Cr-1Mo # = .545

ratio of tank areas $A/A_o = (V/V_o)^{2/3} = 1.273$

	IVa → (IVf)			IVc → (IVg)		
TANK	2 776 700	5 790 000 x 1.436		2776 700	1679 000 x 1.436 x .545	
INSULATION	675 000	425 000 } x 1.273		675 000	450 000 } x 1.273	
SUPPORTS	25 000	105 000 }		25 000	105 000 }	
TRACE HEATING	219 000	453 000 }		219 000	453 000 }	
	3695 700			3695 700		
	x1.273			x1.273		
	4 704 626	9 585 799	14 290 425	4 704 625	2599 281	7 301 906
S/T, DIR.			573 948			155 837
TAX			3 779 356			3 082 503
INDIR.			18 623 729			10 540 246
			÷ 5			÷ 5
COST PER TANK			# 3 724 746			# 2 108 049

Appendix K

PARAMETRIC ANALYSIS OF STEAM CYCLES

STEAM GENERATOR HEAT BALANCES

The analytical models for both single and double reheat steam cycles are described in Figures K-1 and K-2. The $10^{o}F$ jump in the steam curve at the onset of nucleate boiling is an approximation to account for the fact that boiling starts while the water is still somewhat subcooled. Solving Equations 1 through 5 in Figure K-1 yields the boxed expressions for the unknown flows and temperatures. Similarly Equations 1 through 6 in Figure K-2 can be solved to derive the results listed.

These equations were programmed for the Hewlett Packard-67 calculator and were used to derive the output listed in the lower part of Table K-1. The upper part of this table gives the steam cycle input data for these calculations.

COST AND PERFORMANCE MODELS

The cost and performance models are described in Section 3.5. The equations for these models are shown in Figure K-3.

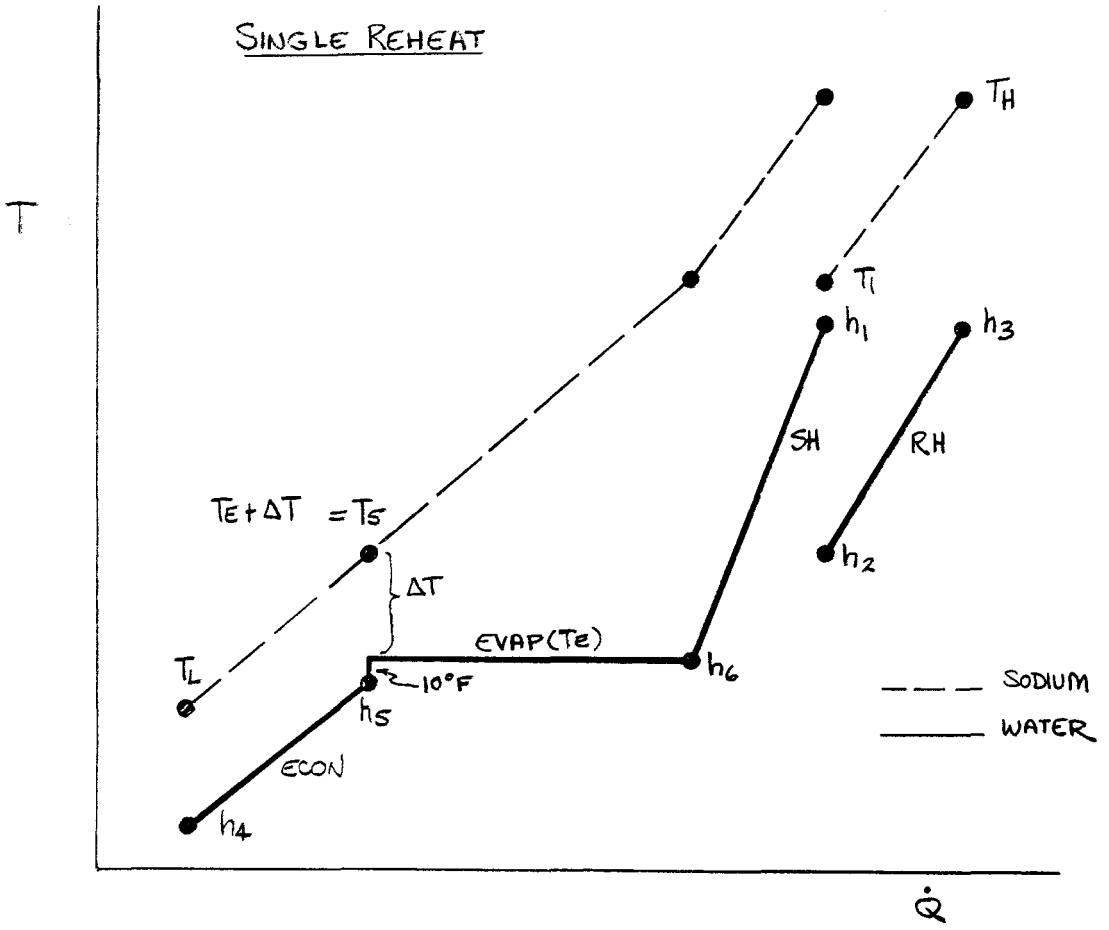

$$\dot{Q}_{SH} = y\, C_N \dot{m}_N (T_H - T_1) = \dot{m}_S (h_1 - h_6) \quad (1)$$

$$\dot{Q}_{RH} = (1-y)\, C_N \dot{m}_N (T_H - T_1) = \dot{m}_S \chi_{RH} (h_3 - h_2) \quad (2)$$

$$\dot{Q}_{EVAP} = C_N \dot{m}_N (T_1 - T_5) = \dot{m}_S (h_6 - h_5) \quad (3)$$

$$\dot{Q}_{ECON} = C_N \dot{m}_N (T_5 - T_L) = \dot{m}_S (h_5 - h_4) \quad (4)$$

$$P = \dot{m}_S [h_1 - h_4 + \chi_{RH} (h_3 - h_2)] / HR \quad (5)$$

$$\boxed{\dot{m}_S} = \frac{P \cdot HR}{h_1 - h_4 + \chi_{RH} (h_3 - h_2)}$$

Figure K-1. Steam Generator - Single Reheat Cycles

SINGLE REHEAT – cont'd

$$\boxed{\dot{m}_N} = \frac{\dot{Q}_{SH} + \dot{Q}_{RH} + \dot{Q}_{EVAP}}{C_N(T_N - T_E - \Delta T)}$$

$$\boxed{T_I} = T_H - \frac{(\dot{Q}_{SH} + \dot{Q}_{RH})}{C_N \dot{m}_N}$$

$$\boxed{y} = \frac{\dot{Q}_{SH}}{C_N \dot{m}_N (T_H - T_I)}$$

$$\boxed{T_L} = T_E + \Delta T - \frac{\dot{Q}_{ECON}}{C_N \dot{m}_N}$$

where:

$\dot{Q}_{SH}$ = heat to superheater
$\dot{Q}_{RH}$ = " " reheater
$\dot{Q}_{EVAP}$ = " " evaporator
$\dot{Q}_{ECON}$ = " " economizer

C_N = specific heat of sodium
$\dot{m}_N$ = sodium flowrate
y = sodium flow split between SH/RH

$\dot{m}_S$ = steam flowrate
h = enthalpy
T = temperature
P = electric output of generator (MWe)
HR = steam cycle heat rate
x_{RH} = steam flow fraction in RH

Figure K-1 (Cont'd)

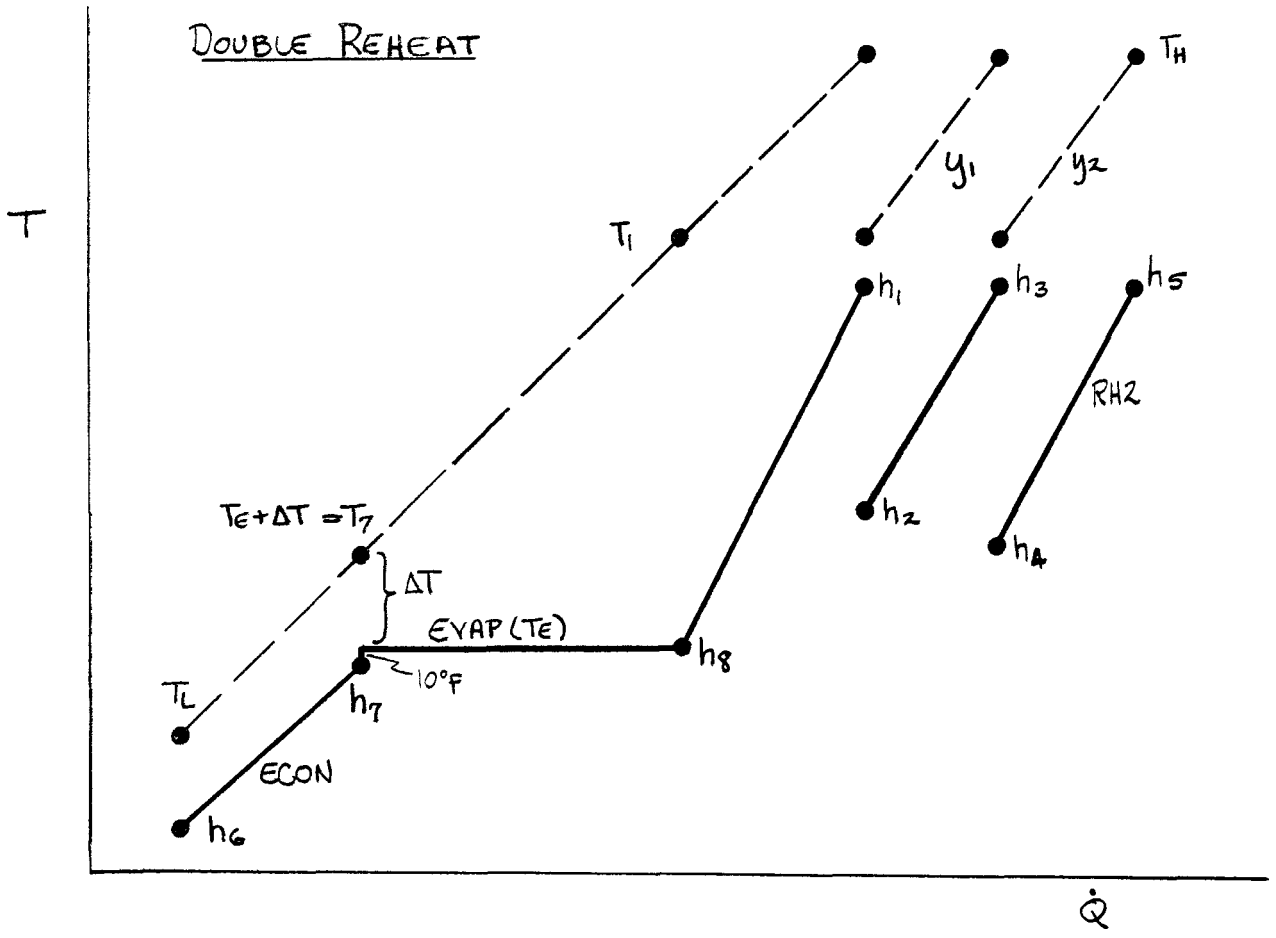

$$\dot{Q}_{SH} = (1-y_1-y_2)\,C_N\,\dot{m}_N\,(T_H-T_1) = \dot{m}_s\,(h_1-h_8) \qquad (1)$$

$$\dot{Q}_{RH_1} = y_1\,C_N\,\dot{m}_N\,(T_H-T_1) = x_1\,\dot{m}_s\,(h_3-h_2) \qquad (2)$$

$$\dot{Q}_{RH_2} = y_2\,C_N\,\dot{m}_N\,(T_H-T_1) = x_2\,\dot{m}_s\,(h_5-h_4) \qquad (3)$$

$$Q_{EVAP} = C_N\,\dot{m}_N\,(T_1-T_7) = \dot{m}_s\,(h_8-h_7) \qquad (4)$$

$$Q_{ECON} = C_N\,\dot{m}_N\,(T_7-T_L) = \dot{m}_s\,(h_7-h_6) \qquad (5)$$

$$P = \frac{\dot{m}_s}{HR}\left[h_1-h_6 + x_1(h_3-h_2) + x_2(h_5-h_4)\right] \qquad (6)$$

Figure K-2. Steam Generator - Double Reheat Cycle

DOUBLE REHEAT – cont'd.

$$\boxed{\dot{m}_S} = \frac{P \cdot HR}{h_1 - h_6 + x_1(h_3 - h_2) + (h_5 - h_4)}$$

$$\boxed{\dot{m}_N} = \frac{\dot{Q}_{SH} + \dot{Q}_{RH1} + \dot{Q}_{RH2} + \dot{Q}_{EVAP}}{C_N(T_H - T_E - \Delta T)}$$

$$\boxed{T_L} = T_E + \Delta T - \frac{\dot{Q}_{ECON}}{C_N \dot{m}_N}$$

$$\boxed{T_I} = T_E + \Delta T + \frac{\dot{Q}_{EVAP}}{C_N \dot{m}_N}$$

where: y_1 = sodium flow split to reheater #1
y_2 = " " " " " #2

x_1 = steam flow fraction in RH1
x_2 = " " " " RH2

Figure K-2 (Cont'd)

Table K-1

STEAM CYCLE PARAMETRIC HEAT BALANCES

CASE No	EP1		EP2		EP3		EP4		EP5		EP6	
CYCLE DESCRIPT.	1450/1000/1000		1800/1000/1000		2400/1000/1000		2400/1000/1000 HARP		2400/1050/1050 HARP		2400/1050/1050/1050	
$\dot{m}_s$ [a] (MLB/HR)											.7264	
x_{RH} or x_1	.8605		.8613		.8623		.8111		.8109		.8487	
x_2	—		—		—		—		—		.7393	
HR (BTU/KWH)	8152		8016		7856		7662		7543		7548	
h_1 (BTU/LB)	1491.6		1480.8		1461.7		1460.4		1493.2		1493.2	
h_2 "	1358.0		1339.0		1314.0		1289.6		1321.1		1401.3	
h_3 "	1526.9		1525.2		1522.4		1523.8		1549.7		1536.2	
h_4 "	429.0		446.9		472.9		512.8		494.7		1405.9	
h_5 "	595.8		639.1		704.8		724.0		724.0		1553.1	
h_6 "	1168.7		1145.8		1096.4		1079.0		1079.0		542.3	
h_7 "	—		—		—		—		—		724.0	
h_8 "	—		—		—		—		—		1079.0	
T_E (°F)	595		625		665		674		674		674	
$\dot{Q}_{SH}$ (MW_t)	72.14		74.45		81.31		85.06		87.37		88.15	
$\dot{Q}_{RH1}$ "	32.46		35.63		39.99		42.34		39.12		24.36	
$\dot{Q}_{RH2}$ "	—		—		—		—		—		23.16	
$\dot{Q}_{EVAP}$ "	128.04		112.60		87.17		79.17		74.89		75.56	
$\dot{Q}_{ECON}$ "	37.27		42.60		51.63		47.11		48.37		38.68	
T_H (°F)	1100	1300	1100	1300	1100	1300	1100	1300	1100	1300	1100	1300
$\dot{m}$ [b] (MLB/HR)	5.347	3.808	5.449	3.809	5.581	3.795	5.649	3.815	5.506	3.719	5.777	3.901
y_1 y	.6896		.6764		.6703		.6676		.6909		.1796	
y_2	—		—		—		—		—		.1707	
T_1 (°F)	877	987	870	971	853	936	843	920	839	913	833	904
T_L (°F)	526	494	546	508	570	520	589	543	584	536	608	571

a. P = 113 MWe b. C_N = .3 BTU/LB °F C. ΔT = 10°F

$$\boxed{C(m\$)} = 121.40\left(\frac{HR}{HR_o}\right) + 58.21\left(\frac{\dot{m}_N}{\dot{m}_{N_o}}\right) + 11.41$$

$$+ 20.24 + \Delta C_{EPGS}$$

where: $HR_o = 8016$ BTU/KWH

$\dot{m}_{N_o} =$ 5.449 MLB/HR @ 1100°F
3,809 MLB/HR @ 1300°F

$\Delta C_{EPGS} =$

−.19 M$	EP1
0	EP2
+ .40	EP3
+ 1.76 M$	EP4
+ 2.29	EP5
+ 4.44	EP6

$$\boxed{P(MWe)} = 113\ MWe - 1.78\left(\frac{HR}{HR_o}\right) - 5.89\left(\frac{\dot{m}_N}{\dot{m}_{N_o}}\right) - 5.33$$

Figure K-3. Power Plant Cost and Performance Models

Appendix L

MATERIALS EVALUATION AND SELECTION

Cost comparisons in the parametric analysis were made on the basis of the preliminary materials selection summarized in Table L-1. This selection was reviewed in Task 2 with respect to the following criteria:

a. Alloys must possess documented mechanical properties which form a sound basis for design. Materials approved by the ASME Code or Code Cases are regarded as preferred candidates. Materials which lack a widespread data base may be considered as candidates for a future cost improvement program, but will not be selected for the first commercial plant.

b. Alloys must be compatible with system working fluids.

c. Alloys selected must be readily available and not overly difficult to fabricate. Preference will be given to metals which are frequently used in industry, and (or) which are available in a wide variety of product forms.

Applying these criteria to materials considered resulted in the recommendations indicated in Table L-2. In summary, state-of-the-art commercially available, code approved materials have been selected for the 1100 F design. These materials are Incoloy 800H for the superheater, reheater, and absorber panel tubing; type 316 stainless steel for the hot-leg piping and the hot storage tanks; carbon steel for the cold-leg piping and the cold storage tanks; and 2-1/4 Cr - 1 Mo for the evaporator tubing. For the 1300 F concept, Incoloy 800H is not suitable for the hot components in contact with sodium due to excessive corrosion at 1300 F. Type 316SS has adequate sodium corrosion resistance at 1300 F, is code approved and, therefore, is a qualified candidate for all hot components with the exception of the steam generators due to susceptibility to water-side stress-corrosion cracking (SCC). The use of type 316 SS for the hot storage tanks may prove too costly due to its very low strength at 1300 F, requiring excessively thick sections. Inconel 617 has been identified as a potential candidate material for the hot components of the 1300 F design, but no data are available on its compatibility with sodium.

The evaluation and analysis that led to the above recommendations is detailed below:

STAINLESS STEEL

Type 316 (Grades 316 and 316H)* stainless steel is a qualified material under the ASME Boiler and Pressure Vessel Codes, and its creep and fatigue properties have been established (Table L-3). Although its strength decreases rapidly between 1100 F and 1300 F, there are no mechanical reasons why this alloy cannot be used at 1300 F, so long as thicker sections can be tolerated.

*Type 316SS in this appendix is used in a generic sense to include grades 316 and 316H.

Table L-1

MATERIALS INITIALLY CONSIDERED IN THE PARAMETRIC ANALYSIS

	Peak Sodium Temperature	
Component	1100 F	1300 F
Cold Leg Piping	2-1/4 Cr - 1 Mo	2-1/4 Cr - 1 Mo
Hot Leg Piping	316SS	Inconel 625
Absorber Panels	316SS	Inconel 625
Storage Tanks (Hot)	316SS	Inconel 625
Storage Tanks (Cold)	2-1/4 Cr - 1 Mo	2-1/4 Cr - 1 Mo
IHX	316SS	Inconel 625
Evaporator	2-1/4 Cr - 1 Mo	2-1/4 Cr - 1 Mo
Superheater	Incoloy 800	Inconel 625
Reheater	Incoloy 800	Inconel 625

Table L-2

MATERIALS SELECTION
CONCEPTUAL DESIGN ANALYSIS

Component	Peak Sodium Temperature[a] 1100 F	1300 F	Status of Material Selected
Cold Leg Piping	Carbon Steel	Carbon Steel	Qualified[b]
Hot Leg Piping	316SS	316SS Inconel 617	Qualified Test Program Required
Absorber Panels[c]	Incoloy 800H	316SS Inconel 617	Qualified Test Program Required
Storage Tanks (Hot)	316SS	316SS Inconel 617	Qualified Test Program Required
Storage Tanks (Cold)	Carbon Steel	Carbon Steel	Qualified
Superheater[d] and Reheater	Incoloy 800H	-- Inconel 617	Qualified Test Program Required
Evaporator	2-1/4 Cr - 1Mo	2-1/4 Cr - 1Mo	Qualified

(a) Selected temperature is 1100 F; however, system cost may be reduced if 1300 F can be achieved with Inconel 617. Type 316SS is suitable for all components at 1300 F except storage tanks (too costly, low strength) and superheater and reheater modules (water-side corrosion).

(b) Qualified means that there are sufficient strength and compatibility data available to assure that the indicated components can be successfully designed and operated. Additional test programs will be necessary in some cases to define and verify the required design data base.

(c) Incoloy 800H selected at 1100 F because of superior creep/fatigue resistance relative to type 316SS; type 316SS or Inconel 617 must be used at 1300 F because Incoloy is incompatible with sodium at 1300 F.

(d) 300 series stainless steels are not recommended because of water-side stress corrosion.

Table L-3

ABSORBER TUBES

Maximum Allowable Stress Values in Tension
(Section 8-Div. 1)* (in kpsi)

Temperature (°F)	800	800H	316	316H
1100	13.0	10.0	12.4	12.4
1150	9.8	9.8	9.8	9.8
1300	2.0	5.4	4.1	4.1

Design Fatigue Values, Code Case 1592

Tables T-1420-1C Incoloy 800H
Tables T-1420-1A, 1B 316, 304

Allowable Cycles	ε_t(Strain Range)	Temperature (°F)	Alloy
10^4	0.0021	1100	800H
10^4	0.00221	1100	316
10^6	0.00112	1100	800H
10^6	0.000963	1100	316
10^4	0.00159	1300	800H
10^4	0.00186	1300	316
10^6	0.000937	1300	800H
10^6	0.000834	1300	316

*ASME Boiler and Pressure Vessel Code

Table L-4

CORROSION RATE OF VARIOUS ALLOYS
IN FLOWING SODIUM

Alloy	1300 F (mils/year)	1150 F (mils/year)
304	0.70	0.15
316	0.55	0.15
Incoloy 800*	1.0	0.25
347	0.75	0.2

Oxygen in Na: Less than 10 ppm (3-4 ppm)
Velocities : 10-17 ft/sec
ΔT : 445 to 500 F
Specimen Geometry: (a) 0.5-in. OD x 0.035-in. wall
(b) 0.875 in. OD x 0.035 in. wall
(c) 0.250 in. OD x 0.015 in. wall

*Al = 0.30, Ti = 0.44 w/o

Reference: L-4

Type 316 has been used in sodium systems which have operated successfully for a number of years. Test loops with 316SS piping were operated for up to 30,000 hours with no evidence of deterioration. Smaller scale experiments have demonstrated low corrosion rates for type 316 at temperatures up to 1300 F (Table L-4). At these temperatures, type 316SS has lower corrosion rates than the other stainless steels tested, and is therefore the preferred candidate.

However, these alloys (300 series) are not compatible with water/steam. Type 316 is subject to stress corrosion cracking in both chlorine-containing and caustic media (Ref. L-7, paper 4.2.1), Refs. L-12, L-13A) and therefore is not recommended for the superheater and reheater design. The most recent (and dramatic) example is the failure of sodium-heated superheater and reheater units at the United Kingdom's Prototype Faster Reactor (PFR) facility. The tubing in these units was constructed from 316 stainless steel and failed because of severe water-side stress corrosion.

Stainless steels are frequently used in large industrial equipment, and are available in all of the shapes required for the Advanced Central Receiver plant, i.e., pumps, valves, and pipe fittings. A variety of 316SS components have been manufactured and used successfully in sodium, e.g., the core internals, pumps, and large diameter piping and valves now in operation at the PFR facility and the Phenix reactor (France).

Thus type 316 stainless steel is recommended for all hot-leg components at both 1100 F and 1300 F and 1300 F except the steam generators. Stainless steel storage vessels constructed for 1300 F service would probably be so thick-walled if made of type 316 as to be uneconomical, but there are no critical materials problems with such a design.

INCOLOY 800/800H*

Information regarding the mechanical properties of Incoloy 800H has been adequately developed and documented in the ASME code (Cases 1325-9 and 1592-10). From the viewpoint of ASME Code allowable stresses, Incoloy 800H is about equal to 316 stainless steel (Table L-3). However, it is well known that the strength of type 316 deteriorates by as much as a factor of eight when held in tension for long periods of time during low cycle fatigue testing (Refs. L-8, L-9). The mechanisms that lead to this behavior are believed to be less effective in Incoloy 800H. In low cycle fatigue tests in air, Incoloy 800H has been found to be slightly better than 316 stainless steel (Ref. L-13B). It remains to be demonstrated that this superiority is maintained in sodium with long hold times.

Long term general corrosion test data for Incoloys 800 and 800H in water/steam environments have been available for some time, including data under heat transfer conditions at very high heat fluxes (Ref. L-11). This information has been verified by workers at GFK, Karlsruhe, Germany. Although Incoloys 800 and 800H are not immune to stress corrosion in water/steam, they are much more resistant to this kind of attack than the 300 series stainless steels (Refs. L-2, L-6, L-10, L-14).

*Incoloy 800 has 0.10% (max.) carbon; Incoloy 800H has 0.05-0.10% carbon and average grain size coarser than ASTM No. 5.

The corrosion rate for Incoloy 800 in sodium was measured at 1300 F in a 15,000 hour test and found to be equivalent to a uniform loss of one mil/year (Table L-4). This result is somewhat misleading however, because the sodium selectively leaches out the grain boundary constituents, thus greatly reducing strength and fatigue resistance. In less than 5000 hours at 1300 F, the corrosion had penetrated along the grain boundaries to a depth of three mils. Similar tests at 1150 F (Table L-4) showed material losses of 0.25 mils/year with no indications of grain boundary attack. Although there are no data on corrosion of Incoloy 800H in sodium, its behavior is expected to be similar to Incoloy 800.

Incoloy 800 is more resistant to carburization in sodium than are the 300-series austenitic stainless steels (Ref. L-13). This is an important consideration when ferritic materials such as 2-1/4 Cr - 1 Mo and carbon steel are to be used in the same sodium loop with austenitics.

Incoloys 800 and 800H have had many years of successful experience in superheated steam. General Electric used Incoloy 800 in the mid-1960s to fabricate nuclear fuel elements for service in superheated steam (Refs. L-1 and L-2). General Atomic Company replaced the superheater section of the Peach Bottom Unit I gas-cooled reactor with Incoloy 800 in 1966, following SCC failure of the original 304H tubing which occured prior to reactor startup. This plant was operated trouble-free for seven years. Beginning about 1960, trial installation of Incoloy 800 and 800H were placed in the superheaters of Philadelphia Electric, Wisconsin Edison, Baltimore Gas and Electric, several American Electric Power Corporation plants, Ohio Power (Muskingum), Electric Energy (Joppa, Illinois), and Southern California Edison (Huntington Beach). All of these installations have demonstrated trouble-free service, and many were followed by full superheater sections of Incoloy 800 or 800H (Ref. L-13C). Superheater and reheater sections of the Fort St. Vraine (Colorado) gas-cooled reactor power plant are tubed with Incoloy 800.

The selection of Incoloy 800H over Incoloy 800 was primarily based on the former's inclusion in Code Gas 1592.

European reactor manufacturers (Kraftwerk Union) have used Incoloy 800 for their pressurized water reactor steam generators. Canadian vendors are also using this material for their steam generators, although their field experience in this application is limited. The fact that Incoloy 800 is rapidly being considered to replace other alloys for constructing water reactor steam generators means that vigorous activity will be maintained to expand the design data base. This additional information would benefit not only nuclear plants but would improve solar plant reliability as well.

Incoloy 800 is available in a variety of wrought product forms, including forgings and castings. Recently, 15 tons of this material were purchased in the form of forged rings up to 26 inches in diameter by 2 inches thick. Based on the experience gained regarding its weldability, a test was devised and used successfully as part of the purchasing specifications with no price penalties.

Due to severe intergranular corrosion by sodium, Incoloy 800H cannot be considered a candidate for 1300 F service. However, this material exhibits acceptable sodium corrosion behavior at 1100 F, and provides the water-side

stress corrosion resistance needed for a successful steam generator design. It has also been selected for the absorber panel design, based on early indications that its low cycle fatigue strength is superior to that of 316H stainless steel.

INCONELS

Initially, Inconel 625 seemed a logical candidate for the 1300 F application because of its use by U.S. industry since 1962, good weldability, availability of a fair data base, and acceptance by the ASME code, Section VIII. However, a review of the available information revealed that this alloy suffers from excessive loss of ductility after exposure at 1000 to 1400 F for long periods (Ref. L-14). Corroborative findings have been obtained in test runs of Inconel 625 tubing at the Eddystone Power Plant. On this basis Inconel 625 has been dropped as a potential candidate for the 1300 F design.

Inconel 617 (Nickel-base alloy), which was developed for high temperature strength and oxidation resistance to 1800 F has been selected as a potential candidate material for the 1300 F design. The thermal stability of this alloy has been studied and found to be adequate. Soaking at 1100 - 1500 F for times in excess of 20,000 hours shows that the early drop in ductility begins to recover after about 4000 hours (Ref. L-16A). The minimum toughness observed was about 40 foot-pounds (Charpy V-notch), which increased after 4000 hours. This compares with about two foot-pounds for Inconel 625, which showed no evidence of recovery.

The corrosion rate of Inconel 617 in sodium has not been measured. Its behavior might prove to be similar to other high nickel alloys tested in sodium, such as Incoloy 800 cited earlier. Other nickel-base alloys such as Inconel 718, Inconel 706, and PE-16, when exposed to sodium at 1300 F, displayed corrosion to 1-1.5 mils after 2000 hours (Refs. L-15 and L-16). However, because Inconel 617 offers the promise of significant plant cost reductions, it should not be eliminated from consideration until its corrosion rate in sodium is established from actual measurements. The use of Inconel 617 will require ASME Code qualification as well as vendor qualification for production of tubing. Most of the current production experience with this alloy is for plate, sheet, and bar products. However, based on the limited experience in production of Inconel 617 tubing and related experience from similar materials, production of Inconel 617 tubing is not expected to present problems.

LOW ALLOY AND CARBON STEELS

The evaporator module will be constructed from 2-1/4 Cr - 1 Mo steel. A sizeable data base has been established for this alloy (Refs. L-17, L-18, L-19), and it is accepted by the ASME boiler and pressure vessel codes.

Compatibility with sodium at the temperatures of interest (600-950 F) has been established, and large components have been constructed and operated successfully. These components include the steam generator for the Experimental Breeder Reactor II (14 years operation in the U.S.), steam generators, and piping for the Prototype Fast Reactor (4 years operation in Great Britain), steam generators for the KNK reactor (4 years operation in Germany), and evaporators for the BN350 reactor (4 years operation in the USSR). Steam generator prototypes made of 2-1/4 Cr - 1 Mo are now under test at Henglo, Holland (50 MW_t),

Les Remardieres, France (49 MW_t), Oarai, Japan (50 MW_t) and at General Electric (2 MW_t). Smaller experimental facilities in the United States, Germany, Russia, Japan, Great Britain, and France have operated for as long as five years, successfully demonstrating the compatibility of 2-1/4 Cr - 1 Mo with flowing sodium.

For cold-leg components not exceeding 650 F, lower grades of steels can be selected to reduce costs. This is particularly advantageous in the cold storage vessels which require large quantities of metal, and where the more rigorous welding practices required by 2-1/4 Cr - 1 Mo could complicate field assembly. For 2-1/4 Cr - 1 Mo, welds must be preheated to 350 F and post-treated at 1300 F with no cooldown between welding passes. Carbon steel, on the other hand, requires about 300 F preheat with no limitation on cooldown between passes; in addition, the post weld heat treatment at 1100 F can sometimes be eliminated on sections less than 1.5 inches thick.

Tests at temperatures in excess of 1100 F with carbon steel and 2-1/4 Cr - 1 Mo indicated that decarburization and corrosion rates were about the same for the two materials. Since 2-1/4 Cr - 1 Mo is acceptable at lower temperatures, carbon steel is expected to be acceptable also.

Carbon steel has been used in the construction of the sodium dump tank for the Clinch River Breeder Reactor (CRBR). This component is 28 feet in diameter, 24 feet high, and is made of one inch thick SA515 grade 60 (0.27 percent max.) carbon steel. Other major sodium service components made of carbon steel include the sodium/water reaction products tanks along with connecting piping about 18 inches in diameter. Experiments were performed at General Electric's Advanced Reactor Systems Department to ascertain whether the base or weld material graphitization (Ref. L-20). Using a Larson/Miller extrapolation, it is estimated that the material can be operated at 950 F for at least 3000,000 hours without graphitization. The maximum cold-leg and cold storage tank design temperature for the Advanced Central Receiver concept is about 640 F.

The specific grade of carbon steel to be used will be determined during Phase II after in-depth evaluation of existing data. SA515, grades 60 and 70 and SA637, class 1 will be included in this evaluation. Cost estimates in Phase I were based on SA515, grade 70.

REFERENCES

Incoloy 800 and Type 316SS

L-1. Materials for Nuclear Superheat Applications, GEAP-3875, January 5, 1962.

L-2. Nucleonics, Vol. 21, No. 9, September 1963.

L-3. Microstructural Evaluation, Aging, Mechanical Properties, GEAP-4794 and GEAP-4751, January and February 1965.

L-4. Effects of Sodium Exposure on the Corrosion and Strength of Stainless Steel, GEAP-10394, August 1971.

L-5. Data for Use in Design of Gas Cooled and LMFBRs - Huntington Alloys, October 1975.

L-6. Review of the Behavior of Alloy 800 for Use in LMFBR Steam Generators, WNET-115-R1, February 1976.

L-7. Petten International Conference on Alloy 800, The Netherlands, March 1978. (all topics: corrosion, low cycle fatigue, stress corrosion).

L-8. G.J. Zema and D.L. Smith, "Low Cycle Fatigue Behavior of Types 304 and 316 Stainless Steel Tested in Sodium at 500°C," Argonne National Laboratory.

L-9. D.R. Dierks, "A Compilation of Elevated Temperature, Strain Controlled Fatigue Data on Type 316 Stainless Steel," ANL/MSD-77-8, October 1977.

L-10. P. Bergeand and J. Donati, INCO Power Conference, October 4-7, 1977, Lausanne, Switzerland, paper No. 1, Figures 8 and 9.

L-11. W.L. Pearl, E.G. Brush, G.G. Gaul, G.P. Wozadlo, "Corrosion of Incoloy 800 in Simulated Superheat Reactor Environment," Journal of Nuclear Applications, June 1965, p. 235.

L-12. W.L. Pearl, G.G. Gaul, G.P. Wozadlo, Nuclear Science and Engineering, Vol. 19 (1964), p. 274.

L-13. LMFBR Heat Exchanger Materials Development Program, GEAP-13919-2, December 1972, pp. 3-4.

L-13A. P.P. Snowden, Journal of Iron and Steel Inst., Vol. 197, (1961), p. 136.

L-13B. C.E. Taske, W.T. O'Donnel, Trans. ASME, November 1977, p. 548.

L-13C. F.N. Mazandarany and R.L. Rittenhouse, "Effects of Service Environments on the Behavior of HTGR Steam Generator Sturctural Materials," GA-A13553, July 1975.

Inconel 625 and Inconel 718

L-14. Effects of Elevated Temperature Aging on the Mechanical Properties and Ductility of Ni-Cr-Mo-Cb Alloy 625, Gulf-GA-A12683, October 1, 1973.

L-15. Corrosion Considerations in Alloy Development, Trans. International Conference on Liquid Metal Technology in Energy Production, Seven Springs, Pennsylvania, May 2, 1976, p. 738.

L-16. W.G. Brehm and R.P. Anantatmula, "Corrosion Considerations in Alloy Development," International Conference on Liquid Metal Technology in Energy Production, Seven Springs, Pennsylvania, May 2, 1976, p. 738.

L-16A. O.F. Kimball, G. Lai, and G. Reynolds, Met. Trans., Vol. 7A, Dec. 1976, p. 1951 and private communication with G. Lai of General Atomic Co., San Diego, Ca.

Alloy 2-1/4 Cr - 1 Mo

L-17. J.S. Armijo, J.L. Krankota, C.N. Spalaris, K.M. Horst, and F.E. Tippets, "Materials Selection and Expected Performance in Near Term LMFBR Steam Generators," British Nuclear Energy Society Meeting, March 1974, London, United Kingdom.

L-18. C.N. Spalaris, K.D. Challenger, D. Dutina, and P.J. Ring, "Sodium Heated Steam Generators - Near Term and Projected Information Needs - Ferritic Steels," BNES, May-June Meeting 1977.

L-19. G.J. Licina and J.F. Copeland, "A Review of 2-1/4 Cr - 1 Mo Steel for Steam Generator Applications in CRBRP," GEAP-20589, October 1974.

Carbon Steel

L-20. L.V. Hampton, "Final Report Graphitization Experiments," ARSD, Materials Engineering Internal Memorandum, April 6, 1978.

Appendix M

HYDRAULIC ANALYSIS OF ABSORBER CONCEPT

EFFECT OF GROSS AIMING ERRORS ON SOLAR FLUX

This analysis was performed to determine the sensitivity of the absorber panel performance to displacements of the heat flux along the panel length due to gross aiming errors. The heat flux step function values given along the length of the panel (Figure M-1) were used as a starting point, but were found to be much too coarse for such a study. Therefore, the coarse grid for the hot absorber panel was revised as shown in Figure M-2. The average values of heat flux over each meter of length in Figure M-2 were made to agree with the coarse one-meter length increments shown in the original flux plot.

Method of Solution

It is assumed in Figure M-2 that the flux plot is symmetrical about the panel centerline. If the solar flux curve is then displaced from the bottom half of the panel (down-flow region) to the upper half (up-flow region) by some amount (e.g., 0.2 meter), then the top half will have a change in total heat input of

$$\Delta Q_u = (+1.87 - 0.055)\ \frac{MW}{m^2} \times 0.2\,m \times 2.0944\,m$$

$$= +0.76027\ MW_t \text{ (gain in heat)} \qquad \text{(M-1)}$$

The numbers +1.87 and -0.046 MW_t/m^2 result from Figure M-2 when the entire abscissa is shifted to the right by 0.2 meter.

The corresponding change in total heat to the down-flow half of the panel is found in a similar manner using centerline symmetry.

$$\Delta Q_D = (-1.87 + 0.046)\ \frac{MW}{m^2} \times 0.2\,m \times 2.0944\,m$$

$$= -0.76404\ MW_t \text{ (loss in heat)} \qquad \text{(M-2)}$$

The overall panel change ΔQ_T in incident energy is:

$$\Delta Q_T = \Delta Q_u + \Delta Q_D$$

$$= -0.00377\ MW_t \qquad \text{(M-3)}$$

For each increment of gross aiming error, a similar procedure can be followed to produce the data shown in Figure M-3. This figure shows that although the energy shifts for a given gross aiming error are large between the top and bottom half of the panel, the effect on total panel power is small.

FLUX PLOT (MW_t/m^2)
CYLINDRICAL RECEIVER

℄ NORTH — ℄ SOUTH

2.0944m

PANEL No.	1	2	3	4	5	6	7	8	9	10	11	12
1 meter	.065	.061	.059	.055	.053	.049	.048	.044	.042	.040	.036	.034
TOP EDGE	.112	.107	.103	.097	.093	.088	.084	.078	.074	.068	.065	.059
	.204	.194	.186	.177	.167	.160	.150	.143	.133	.124	.116	.107
	.337	.321	.306	.293	.278	.264	.249	.234	.221	.205	.192	.177
	.542	.517	.495	.472	.449	.424	.401	.378	.356	.331	.308	.285
	.890	.852	.812	.774	.736	.698	.660	.622	.584	.547	.506	.468
	1.387	1.328	1.267	1.208	1.147	1.088	1.029	.968	.909	.850	.789	.730
	1.799	1.721	1.643	1.567	1.489	1.411	1.333	1.257	1.179	1.101	1.025	.947
MID LINE	5.336	5.101	4.871	4.643	4.412	4.182	3.954	3.724	3.498	3.266	3.037	2.807

48.831

Figure M-1. Flux Plot (MW/m^2)-Cylindrical Reveiver

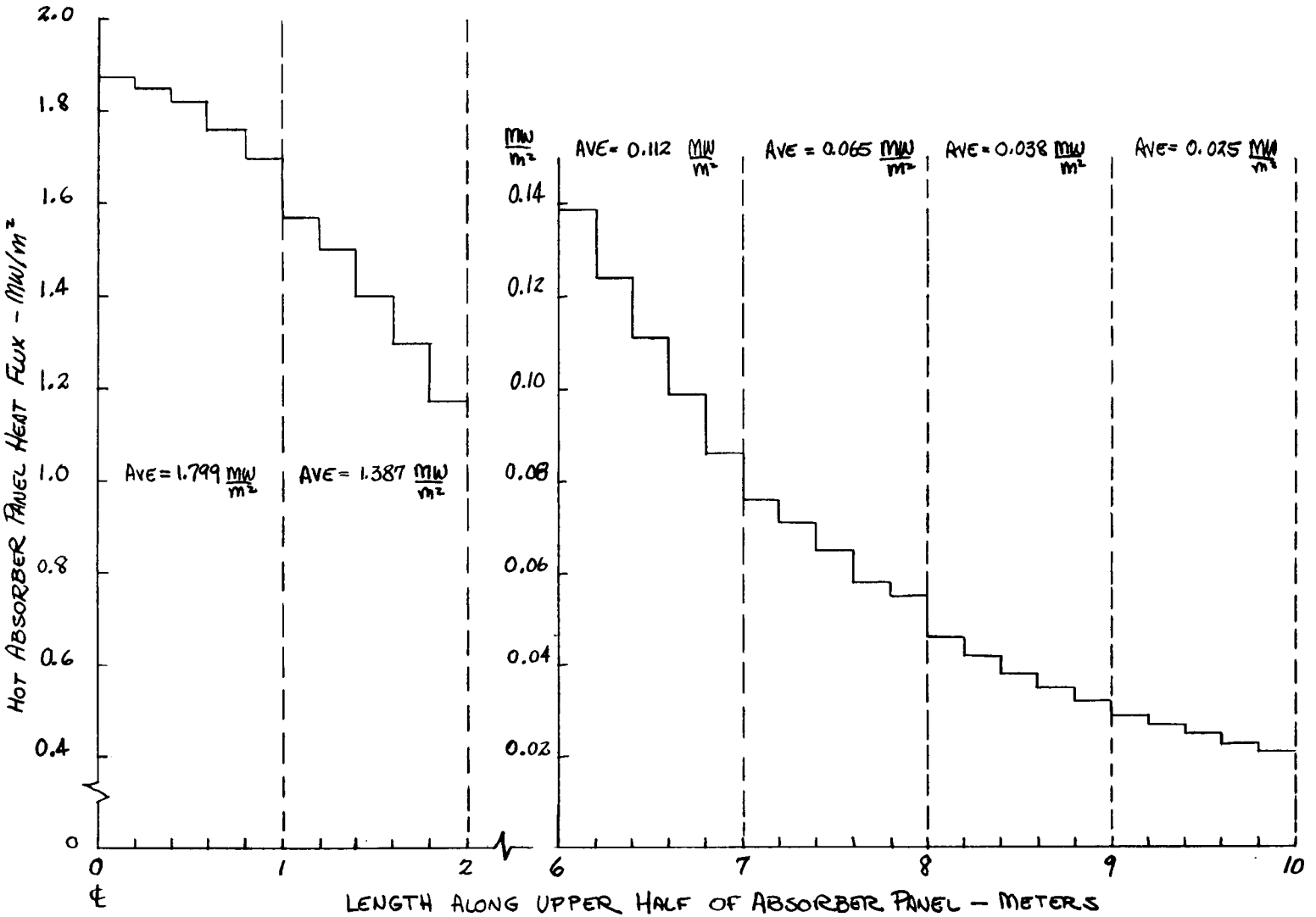

Figure M-2. Detailed Heat Flux Plot for Hot Absorber Panel

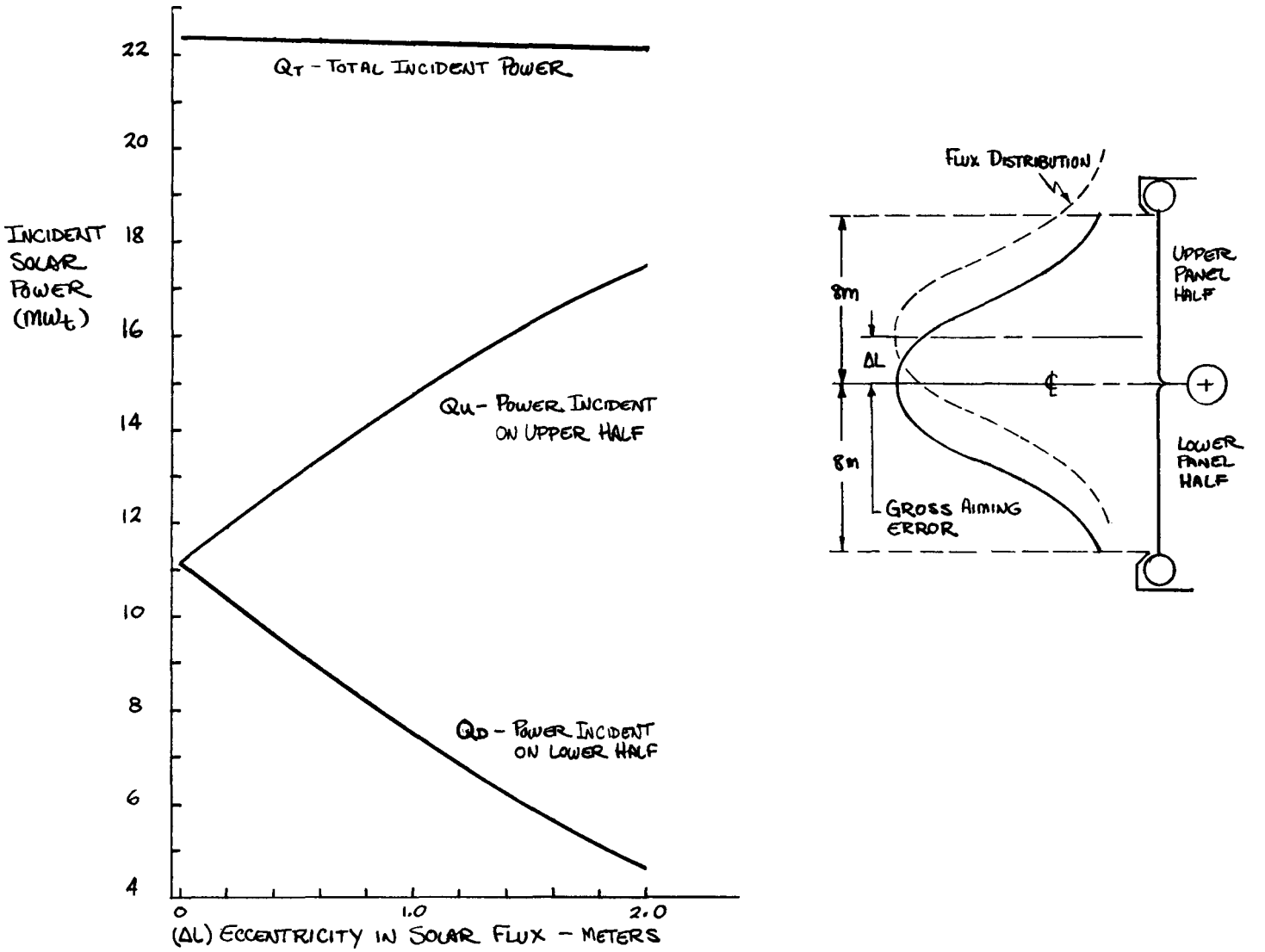

Figure M-3. Effect of Gross Aiming Errors on Incident Solar Energy Distribution on the Hot Panel

Note that the ratio between the absorbed energies top and bottom is

$$\frac{Q_u}{Q_D} = \frac{\eta_u W_u C_P (T_u - 613)}{\eta_D W_D C_P (T_D - 613)}$$

where: T_u, T_D = respective panel outlet temperatures for the upper and lower panel halves (^oF) (M-4)

η_u, η_D = panel efficiencies

W_u, W_D = up-flow and down-flow in the panel (lb/hr)

Letting $W_u = W_D$ and assuming for simplicity that $\eta_u = \eta_D$, Figure M-4 was developed to show how a gross eccentricity in the solar flux might affect the outlet temperatures from the two halves of the hot panel. The difference in the two temperatures constitutes a heliostat error control signal which is used to hold the heat flux profile centered on the solar panel. This illustrates the extreme sensitivity of the control to small eccentricities in solar flux.

HOT BACKFLOW IN LOWER HALF PANELS

Since the flow direction in the lower half panel is against the free convection, there is a possibility at low flows of hot fluid flowing upward toward the center of the panel. This would cause the controller to sense a false low outlet temperature; it would react by reducing flow still further and overheating the panel which would shut down the absorber.

To assess the possibility of having hot backflow, a zeroth order estimate was made of the magnitude of buoyant vs. viscous forces acting on the hot fluid.

If a spherical globule of hot fluid escaped from the panel outlet region and started moving upward, it would experience a drag force given by

$$F_D = \frac{\rho_F U_F^2}{2} (\pi R^2) C_D \qquad \text{(M-5)}$$

where: ρ_F = density of surrounding fluid

U_F = speed of fluid with respect to globule

R = radius of globule

C_D = drag coefficient ($\sim$0.4)

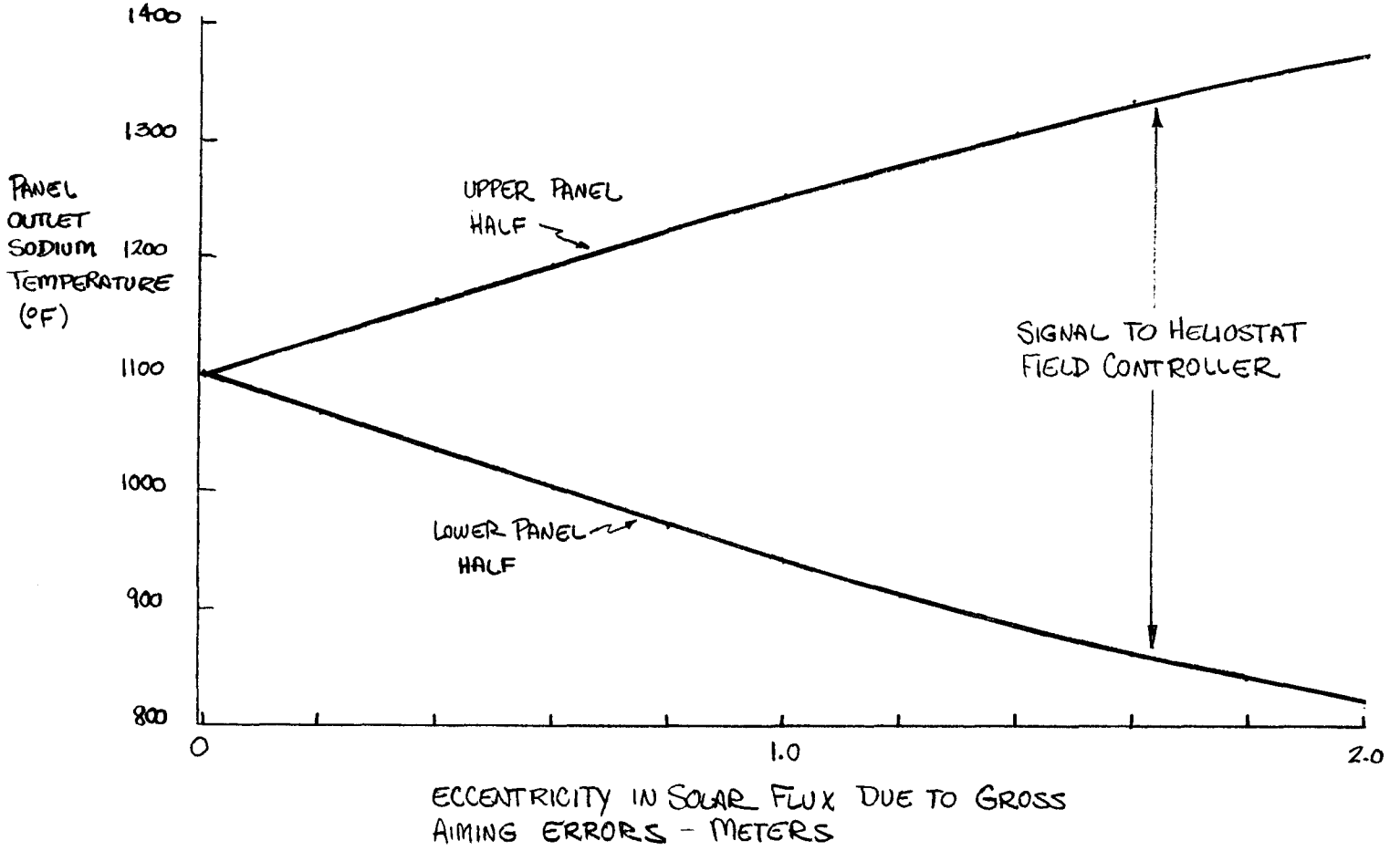

Figure M-4. Effect of Gross Aiming Errors on Incident Solar Energy Distribution on the Hot Panel

The buoyant force driving it upward would be

$$F_B = (\rho_F - \rho_s)\frac{4\pi}{3}R^3 g \qquad \text{(M-6)}$$

where: ρ_s = density of fluid in globule

g = acceleration due to gravity

To prevent upward movement of the globule, the drag force must be greater than the buoyant force. Thus

$$\frac{F_D}{F_B} = \left(\frac{3}{8R}\right)\frac{\rho_F U_F^2 C_D}{(\rho_F - \rho_s)g} > 1 \qquad \text{(M-7)}$$

This ratio was computed for three flow levels in the high flux panel (north side) and the results are plotted in Figure M-5. Since the globule temperature was taken to be 1100 F and the fluid temperature was set at 612 F, these calculations overestimate the buoyant force and are considered conservative. Since under normal conditions the flow in any panel is unlikely to go below 20 percent of its design point value, we concluded on the basis of this calculation that hot backflow is unlikely to occur in any of the panels on the absorber at even the lowest operating flow rates.

OBTAINING A BALANCE BETWEEN UP-FLOW AND DOWN-FLOW IN THE ABSORBER PANELS

The density heads in the absorber panels cause down-flow pressure heads in both halves of the panel. Since this augments flow in one half and retards flow in the other, it is necessary to address the problems of (a) how much flow unbalance this causes (b) what should be done to balance the two flows over the full range of operation.

The flow differential pressure calculations for the top of the tower are presented in Table 5.3-12 of Section 5.3.4 for a case where full tower flow was used and the hot panel pressure loss was evaluated. Using the data contained in this table, it is possible to work around the up-flow and down-flow circuits, where $P_{37} = P_{25}$ is imposed as a control requirement, and obtain an expression of the form:

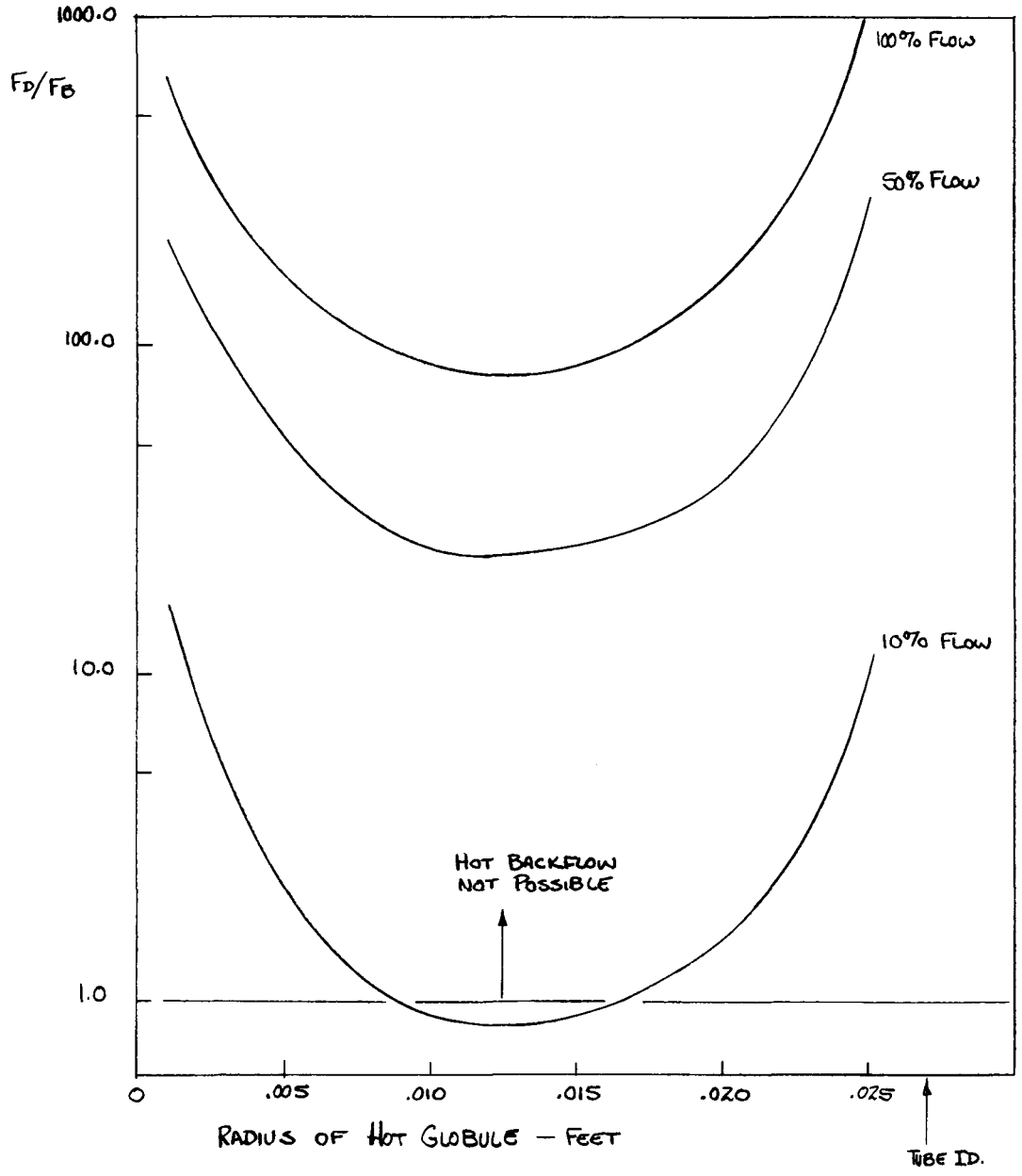

Figure M-5. Analysis of Hot Backflow on North Absorber Panel

$$7.24(W_u/W_R)^2 + 6.35(W_u/W_R)^{1.8} - (7.24+R_o)(W_D/W_R)^2 - 5.38(W_D/W_R)^{1.8} + 0.790 = 0 \quad \text{(M-8)}$$

W_u = up-flow in panel (lb/hr)

W_D = down-flow in panel (lb/hr)

W_R = reference hot panel up-flow or down-flow at 100% power - where $W_D = W_U = W_R$ (lb/hr)

R_o = resistance term for an orifice placed in the down-flow leg to balance the flow at 100% power

The key segment numbers and their respective pressure loss component as used in Equation (M-1) are repeated in Table M-1. Note, however, that the friction losses associated with local resistances (W^2 dependent) and pipe resistances ($W^{1.8}$ dependent) are separated. Equation (M-8) results from summing the resistances around the respective circuits for up-flow and down-flow and can be used universally to evaluate any panel referenced to hot panel flow, W_R.

Pressure Loss In Flow Balancing Orifice

The term R_o in Equation (M-8) represents the resistance in an orifice placed in the down-flow side of the panel to balance the two panel flows. The pressure drop across this orifice is given by:

$$\Delta P_D = R_o (W_D/W_R)^2 \quad \text{(M-9)}$$

Solving for R_o in Equation (M-8) and substituting in Equation (M-9):

$$\Delta P_D = 7.24(W_u/W_R)^2 + 6.35(W_u/W_R)^{1.8} - 5.38(W_D/W_R)^{1.8} - 7.24(W_D/W_R)^2 + 0.790 \quad \text{(M-10)}$$

Assuming a flow unbalance, ΔW exists in the panel favoring the bottom half over the top half:

Table M-1

HOT PANEL FLOW BALANCE EVALUATION

Segment A	Segment B	Velocity-Head	Static-Head	$\Delta P_{friction}$ W^2	$\Delta P_{friction}$ $W^{1.8}$
14	13	-1.602	0.0	0.93	-
13	12	0.0	1.265	-	1.77
12	11	2.702	0.0	0.33	-
11	10	-0.132	0.0	0.08	-
10	9	0.0	10.319	-	1.632
9	8	+0.115	0.0	0.02	-
16	8	+0.115	0.0	0.02	-
17	16	0.0	-10.500	-	1.632
18	17	-0.132	0.0	0.08	-
19	18	2.702	0.0	0.33	-
20	19	0.0	-1.757	-	1.77
21	20	-1.602	0.0	0.93	-
22	21	2.051	0.0	-	0.61
23	22	0.0	0.0	-	1.98
25	23	-0.0563	0.0	2.19	-
15	14	2.0569	0.0	0.61	-
24	15	0.0	-23.051	-	2.95
25	24	-0.0563	0.0	2.19	-

$$W_U/W_R = (W/W_R)(1 - \Delta W/W) \quad \text{(M-11)}$$

$$W_D/W_R = (W/W_R)(1 + \Delta W/W) \quad \text{(M-12)}$$

Substituting Equations (M-11) and (M-12) into Equations (M-8) and (M-10) produces the following two equations, which can be used to evaluate flow unbalance in the panels.

$$7.24(W/W_R)^2(1-\Delta W/W)^2 + 6.35(W/W_R)^{1.8}(1-\Delta W/W)^{1.8}$$
$$-(7.24+R_o)(W/W_R)^2(1+\Delta W/W)^2 - 5.38(W/W_R)^{1.8}(1+\Delta W/W)^{1.8} \quad \text{(M-13)}$$
$$+ 0.790 = 0$$

$$\Delta P_D = 7.24(W/W_R)^2(1-\Delta W/W)^2 + 6.35(W/W_R)^{1.8}(1-\Delta W/W)^{1.8} \quad \text{(M-14)}$$
$$-5.38(W/W_R)^{1.8}(1+\Delta W/W)^{1.8} + 0.790$$

Panel Flow Unbalance With a Fixed Size Orifice

The use of a fixed size orifice in the panel would be the simplest solution to balancing the panel flows. An analysis was made to determine the magnitude of the flow unbalance.

Using the hot panel (No. 1) at 100 percent power ($W/W_R = 1$) where $W_U = W_D = W$, it was found in Table 5.3-12 that $\Delta P_D = 1.76$ psid. Therefore R_o in Equation (M-13) can be set equal to 1.76 and held constant for this evaluation. Also note that

$$Q/Q_R = (WC_p\Delta T)/(W_R C_p \Delta T_R) \cong W/W_R \quad \text{(M-15)}$$

Using Equations (M-14) and (M-15), the following flow unbalances were calculated:

W/W_R	Q/Q_R	$\Delta W/W$
1.0	1.0	0.0
0.9	0.9	0.00392
0.8	0.8	0.00906
0.7	0.7	0.01599
0.6	0.6	0.02710

W/W_R	Q/Q_R	$\Delta W/W$ (Cont'd)
0.5	0.5	0.0444
0.4	0.4	0.0750
0.3	0.3	0.1390
0.2	0.2	0.3130
0.15	0.15	0.5480
0.12	0.12	0.8450

These data are plotted in Figure M-6. Notice that between 40 percent and 100 percent power the flow unbalance is relatively small, but below 40 percent power it becomes severe. The effect of this type of flow unbalance with a control system which maintains constant outlet temperatures in the two panel halves would be to introduce a heat flux eccentricity through the heliostat control. Figure M-3 shows that small gross heat flux eccentricities produce large heat input unbalances between the two halves without degrading the total incident energy on the panels. This indicates that large values of $\Delta W/W$ could be accomodated. However, the plant may be operated with partial cloud cover where the cold panel (No. 12) power may be quite low; therefore, it was concluded that a fixed orifice was inadequate for balancing the flows in the panels.

Attempts were made to correct the problem by over-orificing at 100 percent power (ΔP_D > 1.76 psid) without success. Also, orificing was added to the up-flow side of the panel to make the density head effect a smaller fraction of the total pressure drop. This helps but requires much more pumping without totally eliminating the flow unbalance at very low power levels.

Variable Orifice

By varying the orifice resistance as power changes, it is possible to maintain the up-flow equal to the down-flow in a panel. With the flows balanced, the solar flux is centered on the panel and the two outlet temperatures are equal. Equation (M-14) was used to evaluate the orifice pressure loss where $\Delta W/W = 0$ and $Q/Q_R = W/W_R$. The results are tabulated below:

W/W_R	Q/Q_R	ΔP_D
1.0	1.0	1.760
0.8	0.8	1.439
0.6	0.6	1.177
0.4	0.4	0.976
0.3	0.3	0.901
0.2	0.2	0.844
0.1	0.1	0.805
0.05	0.05	0.7994
0.01	0.01	0.79024
0.005	0.005	0.79007
0.0	0.0	0.79000

These data are plotted in Figure M-7.

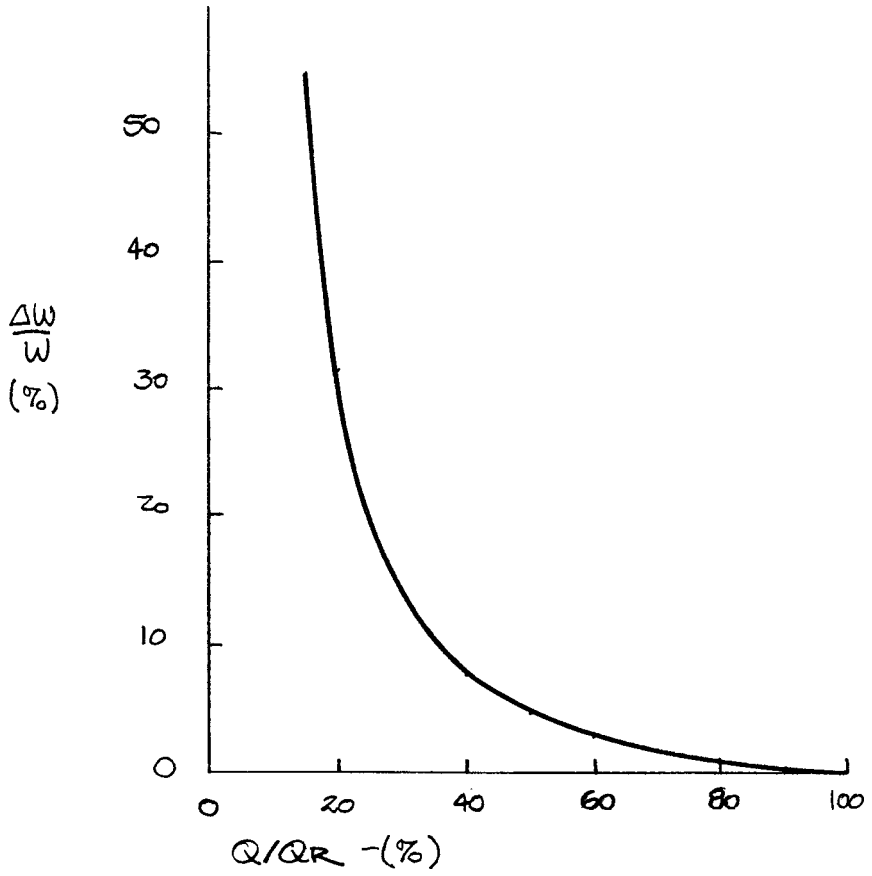

Figure M-6. Effect of Fixed Orifice on Flow Mismatch Between Upper and Lower Panel Halves

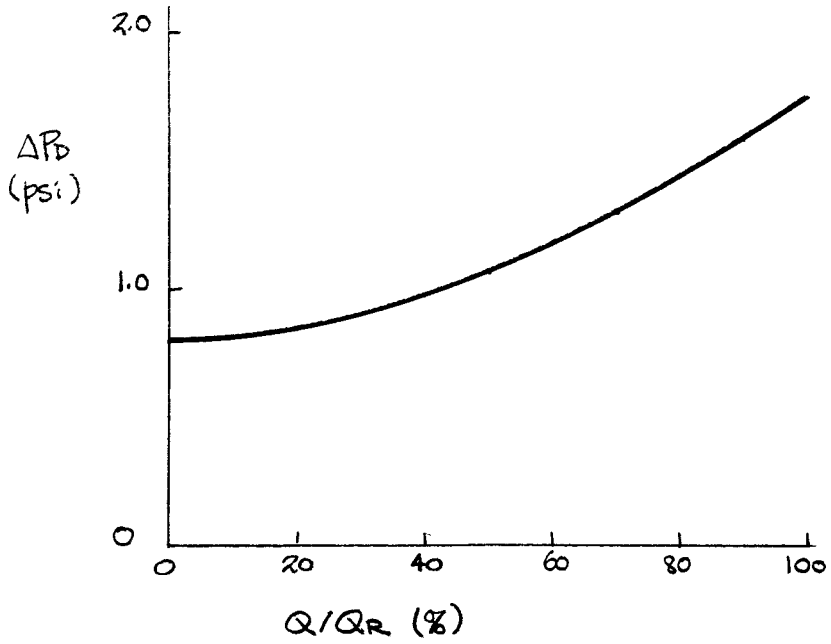

Figure M-7. Variable Orifice Pressure Differentials Required to Balance Flows in Two Panel Halves

To maintain equal up-flow and down-flow in a panel over the full power range, it is necessary to devise a variable orifice with the flow characteristics outlined above. If this is done, the heat flux eccentricity will be zero and the maximum possible power will be realized.

DESIGN OF VARIABLE ORIFICE

The analytical model used in designing the variable orifice for balancing flows in the solar panel is shown in Figure M-8. This orifice is fitted with two springs. The first spring is designed to allow the orifice area to open rapidly at low flow rates. The second spring takes over and adjusts the pressure drop as required at the higher flow rates.

The orifice pressure loss characteristic as shown in Figure M-7 can be expressed as:

$$\Delta P_D = 0.790 + K \frac{V^2}{2g} \rho = 0.790 + \frac{K(W_D/3600)^2}{2g(A/144)^2 \rho \times 144} \qquad \text{(M-16)}$$

But ΔP_D = 1.76 psid when the orifice is wide open ($A = A_0$) and the flow rate is equal to the full flow in the hot panel ($W_u = W_R = 0.2341 \times 10^6$ pounds/hour). Using this information in Equation (M-16), A_0 and D_0 can be obtained:

$$A_0 = 10.75 \text{ square inches; } D_0 = 3.70 \text{ inches}$$

Again from Figure M-7, the pressure loss can also be expressed as:

$$\Delta P_D = 0.790 + 0.970 (W_D/W_R)^2 (A_0/A)^2 \qquad \text{(M-17)}$$

Designing First Spring

Contact with the second spring was arbitrarily set such that the annular area $\pi D_0(X_1 - X_0) = A_0$. Solving for $(X_1 - X_0)$:

$$X_1 - X_0 = D_0/4 = 0.925 \qquad \text{(M-18)}$$

The pressure drop across the variable orifice applied over the area of the plug, A_0 produces a force which compresses the first spring:

$$\Delta P_D A_0 = K_{S1} X$$

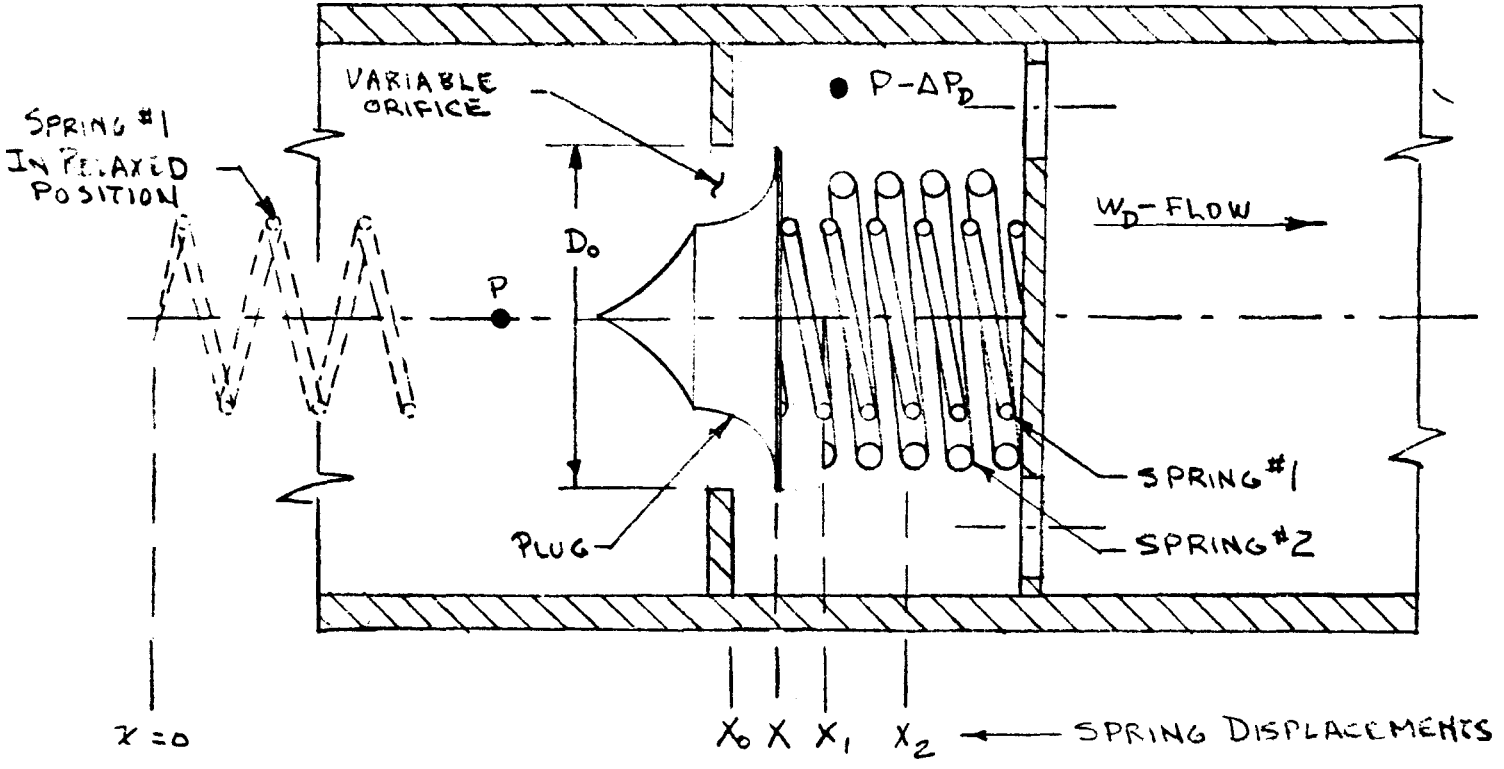

Figure M-8. Analytical Model for the Design of a Variable Orifice

But $\Delta P_D = 0.790$ at $X = X_0$ (at $Q/Q_R = 0.0$ in Figure M-7, the orifice is closed).

$$K_{S1} = \frac{0.790 \times A_o}{X_o} \qquad \text{(M-19)}$$

$$\Delta P_D = K_{S1}/A_o X = 0.790\,(X/X_o) \qquad \text{(M-20)}$$

The following table can be generated using Equations (M-17) and (M-20) and Figure M-7.

W/W_R	ΔP_D	A	X/X_0	X
0	0.790	0	1.000	13.533
0.01	0.7902	4.279	1.0003	13.537
0.05	0.7944	5.911	1.0056	13.609
0.10	0.8050	6.952	1.01899	13.790
0.20	0.844	7.724	1.06835	14.458

The last column X was determined from Equation (M-18) and the ratio X/X_0. Note that at $W/W_R = 0.20$, $X - X_0 = 14.458 - 13.533 = 0.925$ inch. This value of W/W_R was arbitrarily chosen as the cut-off flow rate where contact is made with the second spring. The orifice plug would be shaped to the A vs. X values listed above.

The spring constant for spring No. 1 is from Equation (M-10):

$$K_{S1} = 0.790 \times 10.75/13.533 = 0.6275\ \#/in. \qquad \text{(M-21)}$$

Designing the Second Spring

After the second spring starts to compress, the drag force of the orifice plug must equal the compressive force of both springs in parallel.

$$\Delta P_D = (K_{S1} X + K_{S2}(x - X_1))/A_o \qquad \text{(M-22)}$$

When $\Delta P_D = 1.76$ at 100 percent flow rate, assume that spring No. 2 will compress another 1.0 inch or $X_2 = X_0 + 0.925 + 1.0$,

$$X_2 = 13.533 + 0.925 + 1.0 = 15.458$$

Solving Equation (M-13) for K_{S2}

$$K_{sz} = 9.220 \ \#/in.$$

Equation (M-13) becomes

$$\Delta P_D = 0.916\ X - 12.400 \qquad \text{(M-23)}$$

Using Equations (M-17) and (M-23), a second table can be generated:

W/W_R	ΔP_D	A	X
0.20	0.844	7.724	14.458
0.30	0.901	8.455	14.521
0.40	0.976	8.970	14.603
0.50	1.069	9.344	14.704
0.60	1.177	9.700	14.822
0.70	1.300	10.019	14.956
0.80	1.439	10.283	15.108
0.90	1.592	10.532	15.275
1.00	1.760	10.750	15.458

The above relationship between A and X describes the shape of the remainder of the plug required to balance the flow in the two halves of the panel for panel powers Q/Q_R between 20 percent and 100 percent.

Determining the Shape of the Plug

To find the shape of the plug (D vs. L) is a complex geometry problem beyond the scope of this study. However, the rough shape can be determined from applying the following relationships:

$$A = A_o - \frac{\pi}{4} D^2$$

$$D = \sqrt{4/\pi\,(A - A_o)} \qquad \text{(M-24)}$$

$$L = X - X_o \qquad \text{(M-25)}$$

The plug diameter D at depth L will be given by Equations (M-24) and (M-25). Figures M-9 and M-10 are plots of the plug characteristic.

The plug shape illustrated in Figure M-8 was drawn using the D vs. L coordinates from Table M-2. This shape is not exact since, for the plug position

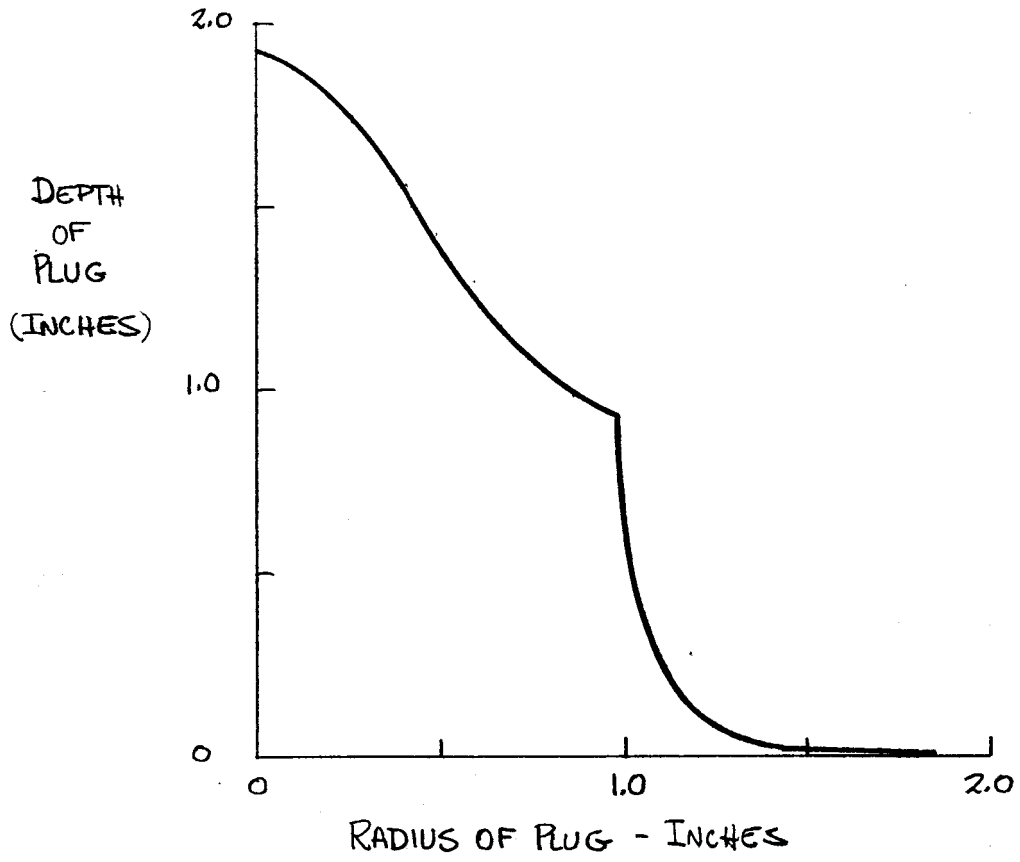

Figure M-9. Approximate Shape of Plug for Variable Orifice Used to Balance Panel Flows

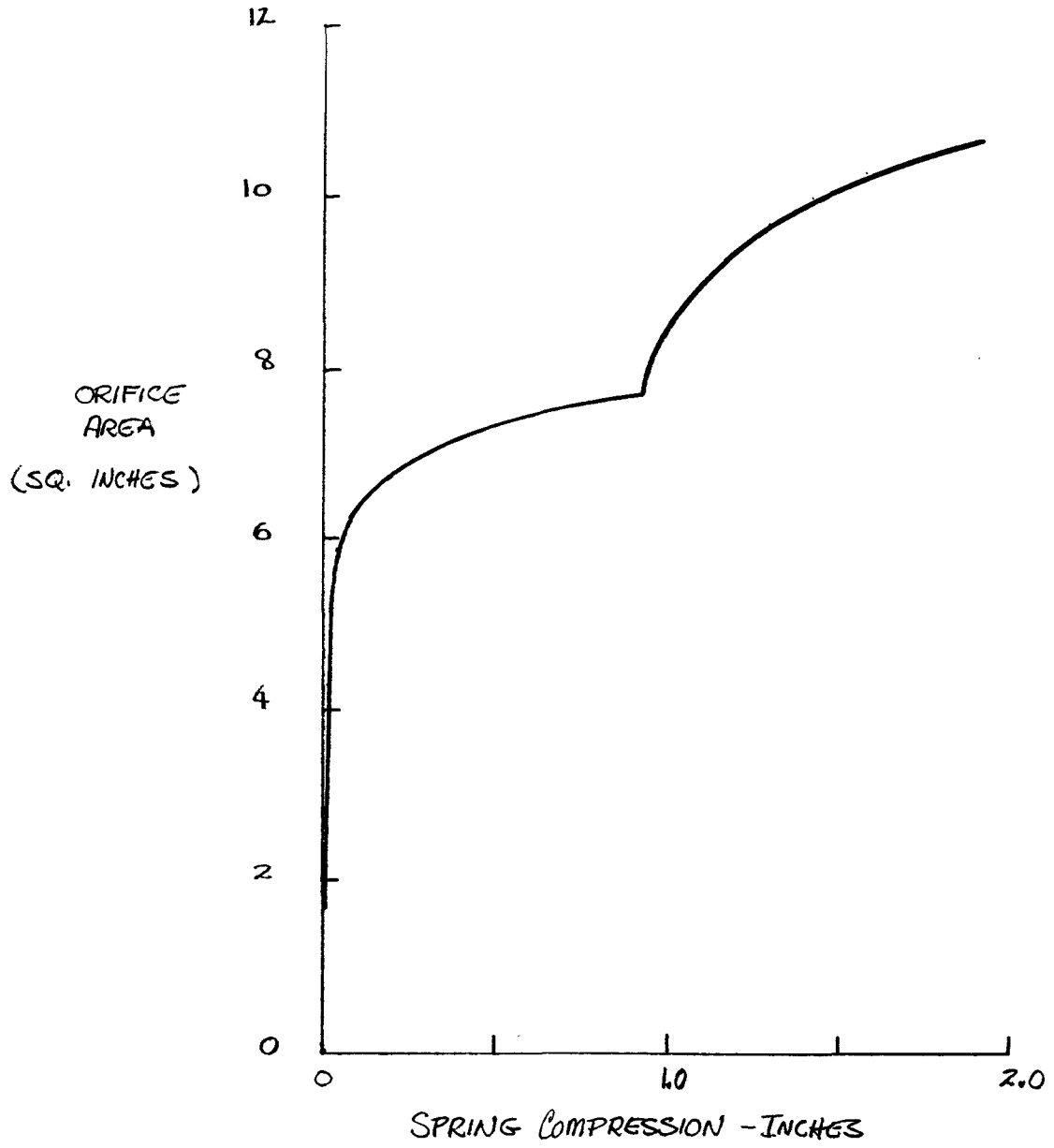

Figure M-10. Required Orifice Flow Area Vs. Spring Compression

Table M-2

SHAPE CHARACTERISTIC FOR PLUG USED IN THE VARIABLE ORIFICE

Orifice Flow Area-A ($in.^2$)	Spring Compression-X ($in.^2$)	Plug Depth $X-X_0$* (in.)	Plug Diameter D (in.)
0.0	13.533	0.00	3.700
4.279	13.537	0.004	2.870
5.911	13.609	0.076	2.482
6.952	13.790	0.257	2.199
7.724	14.458	0.925	1.962
8.455	14.521	0.988	1.709
8.970	14.603	1.070	1.505
9.344	14.704	1.171	1.338
9.700	14.822	1.299	1.156
10.019	14.956	1.423	0.965
10.283	15.108	1.575	0.771
10.532	15.275	1.742	0.527
10.750	15.458	1.925	0.000

*X_0 = 13.537

shown in Figure M-8, the minimum flow area for the orifice is not necessarily in the plane of the orifice opening as was assumed in Equation (M-24). Before building such a plug, a more rigorous geometric evaluation is required.

Mechanical Design of the Variable Orifice

The two spring constants can be supplied either by coil springs (Figure M-8) or by a cantilever beam with the plug mounted on the end. The cantilever beam design would be very similar to a drag flowmeter and could be easily designed for a dual function, i.e., balancing the panel flows and measuring the flow rate. For this reason the cantilever design was selected as the reference. Figure M-11 shows one possible configuration. Cantilever spring No. 1 would be installed with a heavy preload to provide the characteristics calculated above. Spring No. 2 would take over above 20 percent power and carry most of the drag load on the plug.

This device would require a development program to ensure that the desired characteristics were present.

Flow induced vibrations are a possibility in a design of this type. Careful attention must be given to this possibility in the final design.

At near zero flow, the flow balance will be very sensitive. To avoid the possibility of operating with no down-flow in the panel, it may be desirable to drill a small hole through the centerline of the plug to ensure a low flow at very low powers.

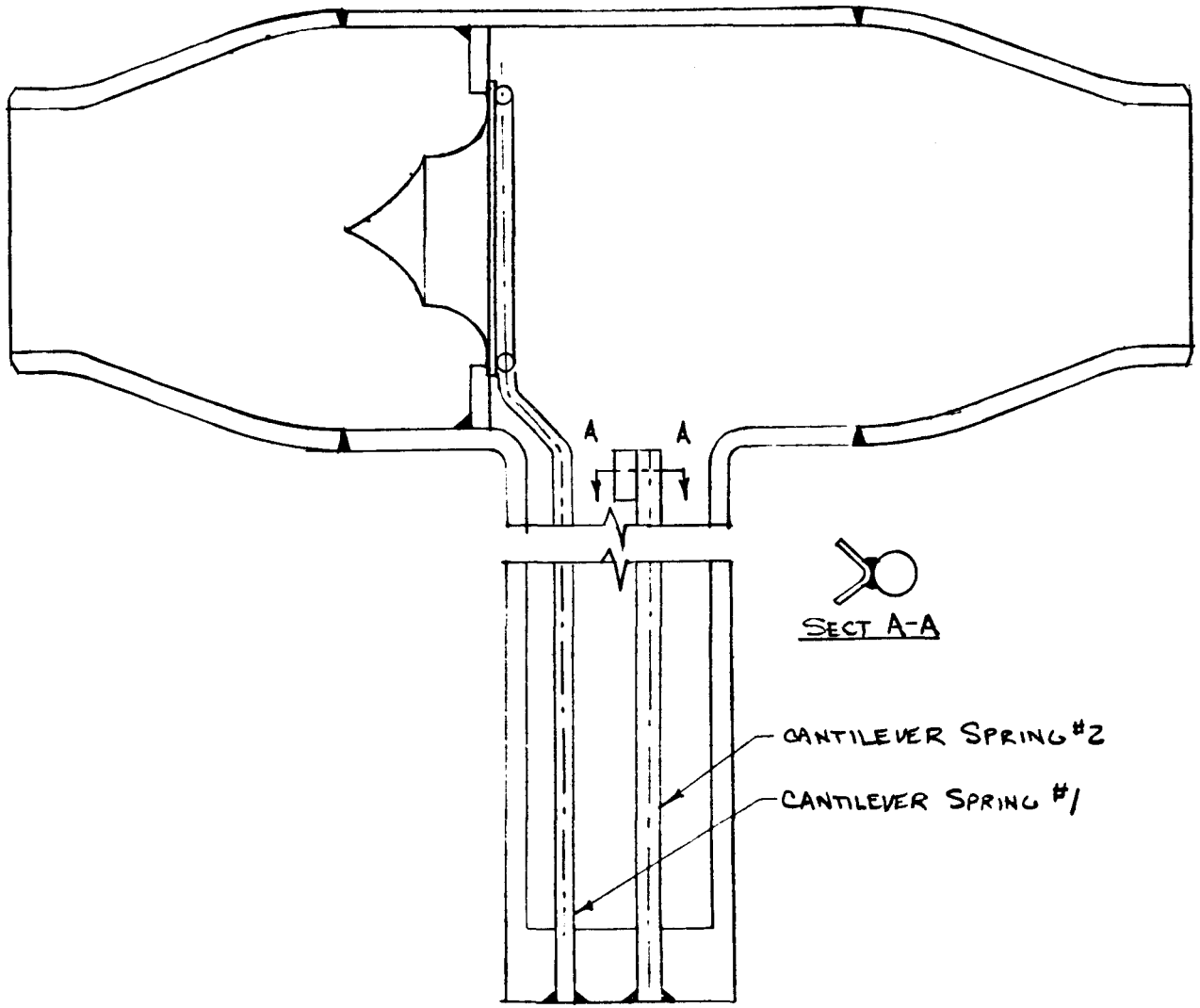

Figure M-11. Reference Design of Variable Orifice Using Cantilevers for Springs

Appendix N

TECHNIQUE FOR ESTIMATING AIR SIDE CONVECTION COEFFICIENT ON ABSORBER

Table N-1 describes the method used to compute the convection coefficient for the receiver loss estimates given in Section 5.3.2. The method accounts for mixed free and forced convection effects and includes corrections for the effect of roughness. The data and arguments used in developing this estimation technique are summarized below.

COMBINED CONVECTION

A measure of the relative importance of forced and free convection is given by the quantity Gr/Re^2. This ratio is about 5 for the advanced central receiver, indicating that free convection cannot be ignored in estimating the best transfer coefficient.*

The effects of combined natural and forced convection on various surfaces have been studied by several authors. Among the relevant investigations are papers by Churchill (Ref. N-1), Churchill and Chu (Ref. N-2), and Oosthuizen and Taralis (Ref. N-3). Unfortunately the results of these studies are not applicable to the combined natural and forced convection problems on vertical cylinders in the range of Reynolds and Grashof numbers needed for the present study. Therefore, Churchill and Usagi's correlation (Ref. N-4), which utilizes the asymptotic behaviors of a function at limiting values of the independent variable z at $z \to 0$ and $z \to \infty$ is employed here to compute the combined natural and forced flow effect. In the present case, the function under question is the Nusselt number. The limiting value of the Nusselt number when the independent variable Re (Reynolds number) tends to zero is given by the natural-convection situation for which several correlations are available (Ref. N-2). For the asymptotic behavior at large Re, the variation of Nusselt number is given by the purely forced convection flow, for which very good correlations and experimental data are available for smooth and rough cylinders (Refs. N-5, N-6, and N-7). Therefore, the combined natural and forced convection problem is expressed as

$$Nu^n = Nu_F^n + Nu_N^n \qquad \text{(N-1)}$$

where Nu is the Nusselt number and the subscripts F and N represent respectively the limiting conditions of purely forced flow (no natural convection) and purely natural convection (no forced flow). The exponent n usually has values in the range $1 \leq n \leq 4$, although it can take on other values as well. According to Churchill and Usagi (Ref. N-4), Equation N-1 can be used whenever the functions Nu_F and Nu_N are uniform functions of the independent variable (in this case, the Reynolds number) with second derivatives that do not change sign. For the combined natural and forced convection problem for a

*Ref. N-1A, p. 358

Table N-1

CALCULATION OF CONVECTION COEFFICIENT
FOR CONCEPTUAL DESIGN RECEIVER

RECEIVER : 16 x 16 m (D x H)
TUBES : 0.75 INCH O.D.
1150°F (AVERAGE)
AMBIENT : 83°F
5.46 m/s WIND (194.3 m)
FILM : 616°F
$\nu = 0.554 \times 10^{-3}$ Ft^2/sec
$\frac{\rho^2 \beta g}{\mu^2} = 0.1 \times 10^6$ $1/°F/Ft^3$
$P_r = 0.686$
$k = 0.253$ Btu/hr/ft/°F

Re	REYNOLDS NUMBER	1.70×10^6
Gr	GRASHOF NUMBER	1.54×10^{13}
E/D	ROUGHNESS	60×10^{-5}

FORCED CONVECTION

SMOOTH CYLINDER $Nu = 1921$ (equation N-3)
ENHANCEMENT BY ROUGHNESS $\times 1.74$ (figure N-2)
ROUGH CYLINDER $Nu_F = 3342$

NATURAL CONVECTION

$Nu_N = 2382$ (equation N-2)

COMBINED CONVECTION

$$Nu = \sqrt{Nu_F^2 + Nu_N^2} = 4104$$

$$h = Nu \frac{k}{D} = 1.98 \frac{Btu}{hr \cdot ft^2 \cdot °F}$$

horizontal cylinder, Churchill (Ref. N-1) has found the value n = 3 to be appropriate. Professor Oosthuizen (Ref. N-3) in a verbal communication with General Electric recommended the use of n = 2 for the correlation.

Smooth Cylindrical Surface

For a vertical cylinder, the equation determining Nu_N as a function of the Grashof number is the same as for a smooth vertical surface. The latest available correlation is that given by Churchill and Chu (Ref. N-2):

$$Nu_N = \left\{ 0.825 + \frac{0.387\,(Gr\,Pr)^{1/6}}{\left[1 + (0.492/Pr)^{9/16}\right]^{8/27}} \right\}^2 \qquad \text{(N-2)}$$

where Gr and Pr are the Grashof and Prandtl numbers respectively. This correlation fits all available data accurately up to Gr $\sim 4 \times 10^{12}$. Since no data at all are available for higher Grashof numbers, the errors involved in using this correlation to extrapolate to the advanced central receiver case cannot be assessed at this time.

In purely forced convection flow over circular cylinders, the correlation that fits all available data including those of Achenbach (Ref. N-6) and Zdanavichiyus (Ref. N-8) most accurately is that of Churchill and Bernstein (Ref. N-5):

$$Nu_F = 0.3 + \frac{0.62\sqrt{Re}\,Pr^{1/3}}{\left[1 + (0.4/Pr)^{2/3}\right]^{1/4}} \left\{ 1 + \left(\frac{Re}{282000} \right)^{5/8} \right\}^{4/5} \qquad \text{(N-3)}$$

This equation provides a lower bound on the observed values of Nu_F for all Re·Pr > 0.4. In the range of Re·Pr of present interest, it fits the data accurately, with deviations of less than ±3 percent.

By using Equations N-2 and N-3, the values of Nu as computed from Equation N-1 have been plotted in Figure N-1, with Groshof number as a parameter. Since n is not known, calculations have been carried out for three assumed values n = 2,3, and 4. These results are shown on the graph. The combined natural and forced convection effect is largest in the range of operating Reynolds numbers for the receiver. Since the heat transfer coefficients predicted by using the various values of n do not differ from one another very much, any of the three values could be used. In the present study we have chosen n = 2, which predicts the largest loss from the receiver.

Rough Cylindrical Surface

The only data on rough cylindrical surfaces in forced flow are those of Achenbach (Refs. N-6, N-7). These data were obtained by measurements on a cylinder (0.15 meter diameter) in a wind tunnel (0.9 meter in width).

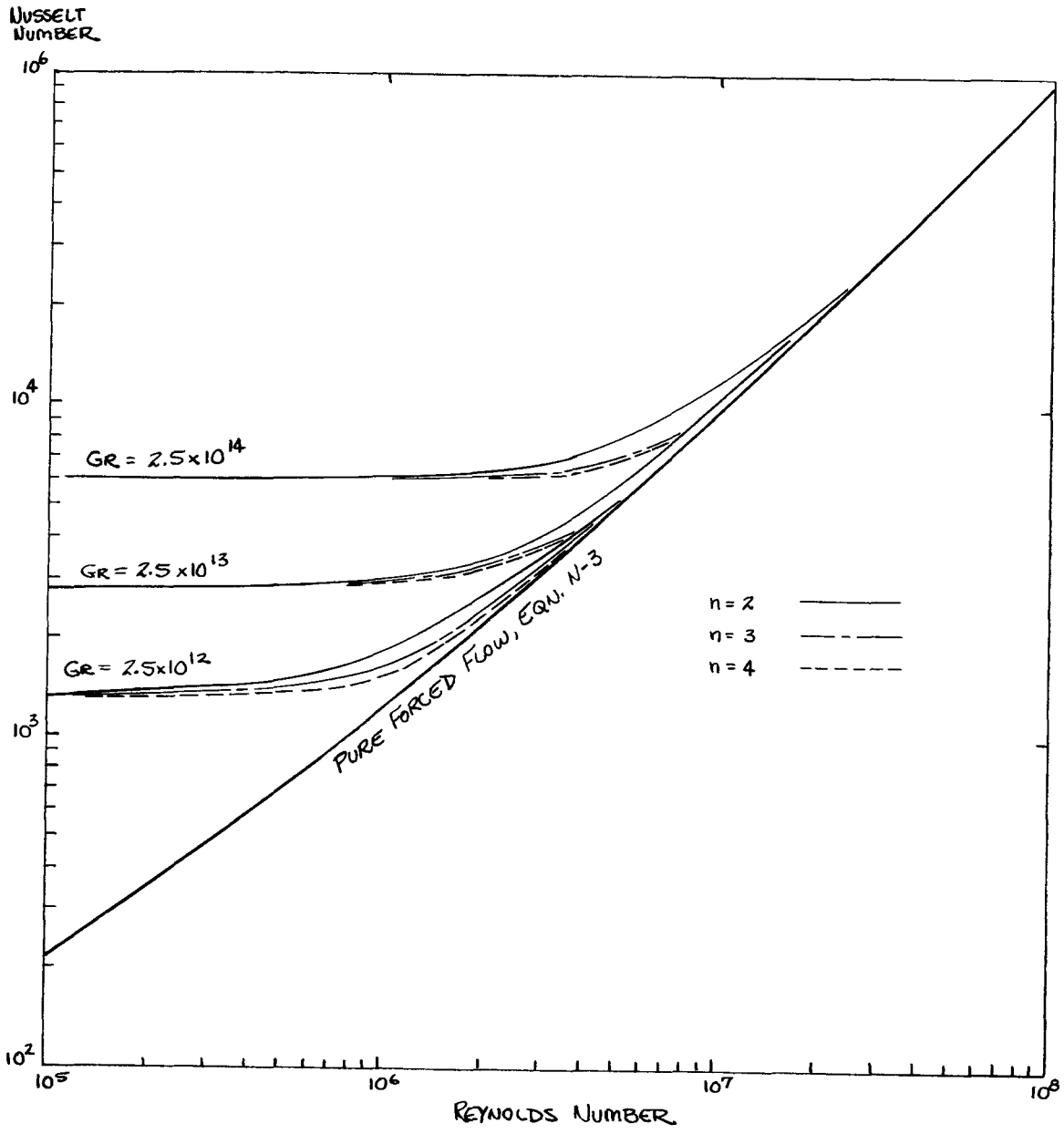

Figure N-1. Application of Equation (N-1) to Convection on Smooth Cylinders

Figure N-2 shows Achenbach's data* replotted to show the enhancement due to roughness as a ratio of the rough Nusselt number to the smooth one. Since the orignal data did not include a curve for the roughness ($\varepsilon/D = 60 \times 10^{-5}$), this curve has been determined by interpolation and is also shown in Figure N-2. The design point Reynolds number is 1.7×10^6 and the enhancement of heat transfer is shown to be 1.74 in the figure. To obtain the forced convection coefficient for the advanced central receiver, these enhancement factors were applied to a smooth cylinder Nusselt number derived from Equation N-3.

The surface presented to natural convection due to the tubes welded on the receiver surface is not rough in the usual sense of the term. It has been assumed that Equation N-2 is still applicable for the evaluation of the Nusselt number without a roughness correction, even though the surface has depressions and elevations. No experimental data relating to such a surface have been found in the literature.

The use of Equation N-1 for the combined effect of free and forced convection now becomes questionable since Nu_F is no longer a smooth function of Re. Nevertheless, Equation N-1 provides results of reasonable accuracy because Nu_F is a uniform function of Re in a piece-wise manner. So, the equation should be usable for calculating Nu in each region of continuity of Nu_F.

---

*Reference N-7, Figure 4.

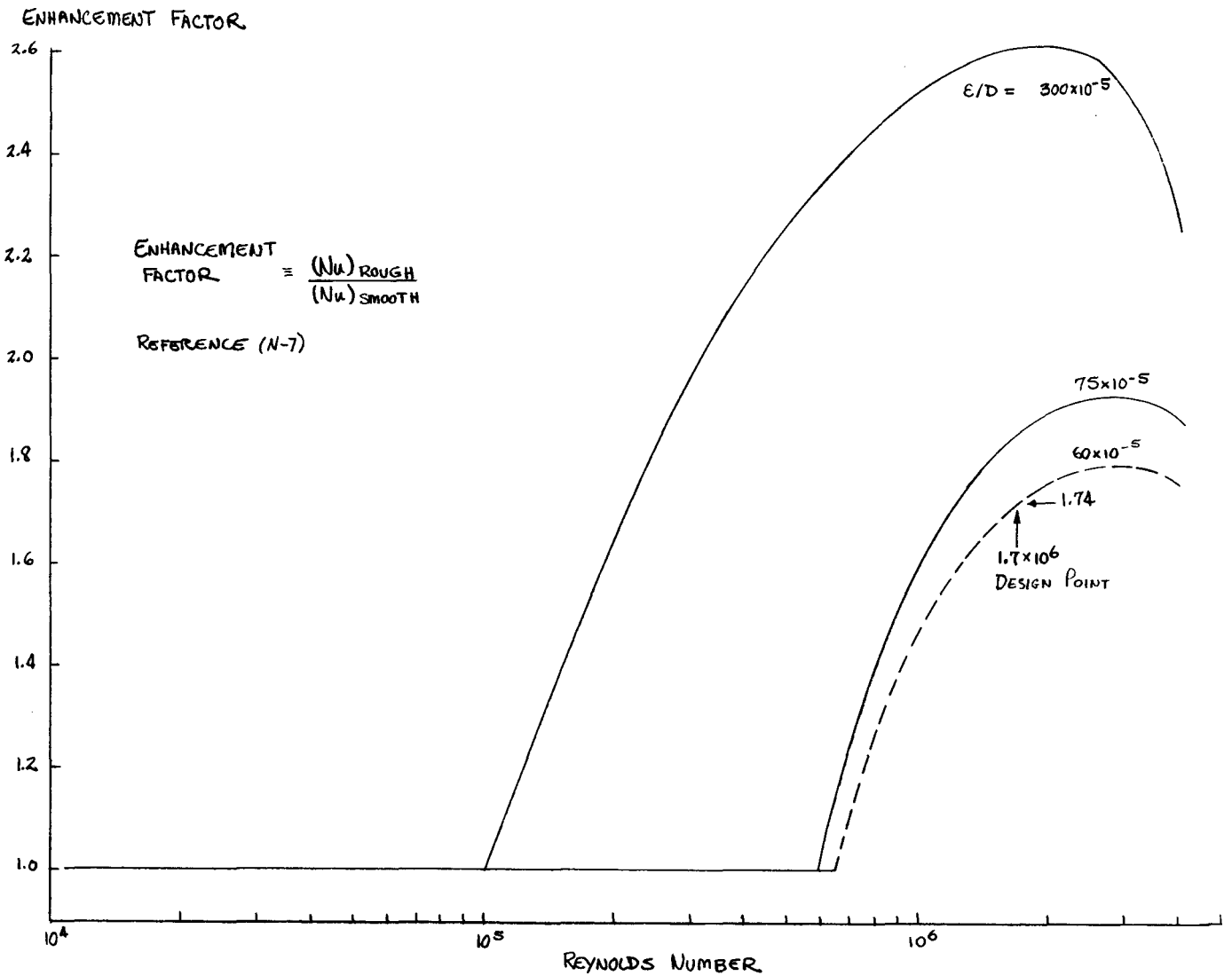

Figure N-2. Forced Convection - Enhancement of Heat Transfer Due to Roughness

REFERENCES

N-1. R.W. Churchill, "A Comprehensive Correlating Equation for Laminar, Assisting Forced and Free Convection," AIChE Jour., Vol. 23, No. 1, 1977, pp. 10-16.

N-1A. F. Kreith, Principles of Heat Transfer, Second Edition, International Textbook Company, Scranton, Pa., 1965.

N-2. R.W. Churchill and H.H.S. Chu, "Correlating Equations for Laminar and Turbulent Free-Convection from a Vertical Plate" Int. J. Heat Mass Trans., Vol. 18, 1975, pp. 1323-1329.

N-3. P.H. Oosthuizen and D.N. Taralis, "Combined Convective Heat Transfer from Vertical Cylinders in a Horizontal Fluid Flow," Paper No. 76 - HT-41, ASME-AIChE Heat Trans. Conf., St. Louis, August 9-11, 1976.

N-4. S.W. Churchill and R. Usagi, "A General Expression for the Correlation of Rates of Transfer and Other Phenomena," AIChE-Jour., Vol. 18, No. 6, November 1972, pp. 1121-1128.

N-5. S.W. Churchill and M. Bernstein, "A Correlating Equation for Forced Convection from Gases and Liquids to a Circular Cylinder in Cross-Flow," J. Heat Trans., ASME, Series C, Vol. 99, May 1977, pp. 300-305.

N-6. E. Achenbach, "Heat Transfer from Smooth and Rough Surfaced Circular Cylinders in Cross-Flow," Fifth Int. Heat Trans. Conf., Tokyo, Vol. 1, FC 6.1, 1974, pp. 229-233.

N-7. E. Achenback, "Evaluation of Measurements of the Local and Total Heat Transfer from Smooth and Rough Cylinders in Cross-Flow," Heat and Mass Transfer Source Book, Fifth All-Union Conference, Minsk, John Wiley and Sons, 1976.

N-8. G.B. Zdanavichyus, et al., "Local Heat Transfer in an Air Stream Flowing Laterally to a Circular Cylinder at High Re Numbers," Int. Ch. Engrg, Vol. 16, No. 1, January 1976, pp. 121-127.

Appendix O

ABSORBER LOSS COMPUTER PROGRAM

A computer program based on the analysis described in Section 5.3.2 is listed in Table O-1. The program is written for the General Electric MARK III time sharing system. A variable list defining the symbols used in this program is given in Table O-2, and sample output for the conceptual design is listed in Table O-3.

Table O-1

ABSORBER LOSS COMPUTER PROGRAM

```
 100 REAL KN,KT,N,NU
110 DIMENSION W(12),QS(12,8),ET(12,8),TNA(12,8),TN(8),HN(12,8),KT(12,8),U(12,8),
120 &          TT(12,8),QR(12,8),QC(12,8),EFP(12),QIP(12),QRP(12),QCP(12),WP(12),TTP(12,8)
130 FILENAME FLUX
140 DATA DX,DY,CN,TH,TC,PI/1.0,2.0944,.30353,1097.22,612.95,3.14159/
150 DATA ET/96*0.90/
160 DATA TT/96*1100./
170 DATA DL,D,N,SIG,EPS,ALPHA/.75,.65,108.,.1714E-8,.90,.95/
180 PRINT, "AIR TEMP.,CONV. COEFF.,C1"
190 READ, TA,HT,C1
200 PRINT,"FLUX PLOT FILENAME"
210 READ, FLUX
220 READ(FLUX,500) ((QS(I,J),I=1,12),J=1,8)
230 500 FORMAT(4X,12F6.3)
240 20 PRINT,"FULL PRINT(YES=1,NO=0)"
250 READ,L
260 DO 160 M=1,5
270 WR=0.
280 QIR=0.
290 QRR=0.
300 QCR=0.
310 DO 150 I=1,12
320 SUM=0.
330 DO 120 J=1,8
340 SUM= SUM + QS(I,J)*ET(I,J)
350 120 CONTINUE
360 W(I)= SUM*DX*DY*3.413E6/CN/(TH-TC)
370 WP(I)=2*W(I)
380 TN(1)= TC + QS(I,1)*ET(I,1)*DX*DY*3.413E6/W(I)/CN
390 TNA(I,1)= (TC + TN(1))/2.
400 DO 130 J=2,8
410 TN(J)= TN(J-1) + QS(I,J)*ET(I,J)*DX*DY*3.413E6/W(I)/CN
420 TNA(I,J)= (TN(J-1)+TN(J))/2.
430 130 CONTINUE
440 QIP (I)=0.
450 QRP(I)=0.
460 QCP(I)=0.
470 DO 140 J=1,8
480 KN= 125.3-12.74*ALOG(TNA(I,J))
490 PE= 48.*W(I)*CN/(PI*D*KN*N)
500 NU= 7.0 + .025*(PE**(.8))
510 HN(I,J)= KN*NU*12./D
520 KT(I,J)= 6.7 + .004705 *(TNA(I,J)+TT(I,J))/2.
530 U(I,J)= DL/HN(I,J)/D + DL/24./KT(I,J)*ALOG(DL/D)
540 U(I,J)= 1./U(I,J)
550 QT= C1*QS(I,J)*ET(I,J)*3.413E6/10.7636
560 TT(I,J)= TNA(I,J) + QT/U(I,J)
570 TTP(I,J)= TNA(I,J) + QT/U(I,J)/C1
580 QR(I,J)= SIG*EPS*DX*DY*10.7636*((TT(I,J) + 460.)**4 - (TA + 460.)**4)/3.413E6
590 QC(I,J)= HT*DX*DY*10.7636*(TT(I,J) - TA)/3.413E6
600 ET(I,J)= ALPHA - (QR(I,J)+QC(I,J))/QS(I,J)/DX/DY
610 QIP(I)= QIP(I) + QS(I,J)*DX*DY
620 QRP(I)= QRP(I) + QR(I,J)
630 QCP(I)= QCP(I) + QC(I,J)
640 140 CONTINUE
650 QIP(I)= 2.*QIP(I)
660 QRP(I)= 2.*QRP(I)
670 QCP(I)= 2.*QCP(I)
680 EFP(I)= ALPHA - (QRP(I)+QCP(I))/QIP(I)
690 WR=WR + WP(I)*2.
700 QIR=QIR+QIP(I)*2.
710 QRR=QRR+QRP(I)*2.
```

Table O-1 (Cont'd)

```
720 QCR=QCR+QCP(I)*2.
730 150 CONTINUE
740 QREF= QIR*.05
750 EFR= ALPHA-(QRR +QCR)/QIR
760 160 CONTINUE
770 PRINT 510,WR,QIR,QRR,QCR,QREF,EFR
780 510 FORMAT(1X,"RECEIVER SUMMARY"/1X,"FLOW=",E13.6,"LB/HR"/
790 &          1X,"INCIDENT=",F8.2,"MW"/
800 &          1X,"RAD. LOSS=",F8.2,"MW"/
810 &       1X,"CONV. LOSS=",F8.2,"MW"/
820 &          1X,"REFL. LOSS=",F8.2,"MW"/
830 &       1X,"EFFICIENCY=",F6.4/"O")
840 PRINT 520
850 520 FORMAT(1X,"PANEL",2X,"FLOW",9X,"INCIDENT",2X,"RADIATION",2X,"CONVECTION",2X,"EFFICIENCY"/
860 &          8X,"LB/HR",8X,"MW",8X,"MW",9X,"MW")
870 PRINT 530,(I,WP(I),QIP(I),QRP(I),QCP(I),EFP(I),I=1,12)
880 530 FORMAT(1X,I2,5X,F8.0,5X,F8.3,2X,F8.3,3X,F8.3,4X,F7.4)
890 PRINT 540
900 540 FORMAT("OOUTSIDE TUBE TEMPERATURES(DEG. F)")
910 PRINT 550,((TT(I,J),I=1,12),J=1,8)
920 550 FORMAT(1X,12F8.1)
930 PRINT 560
940 560 FORMAT("ONODE EFFICIENCIES(P.U.)")
950 PRINT 570,((ET(I,J),I=1,12),J=1,8)
960 570 FORMAT(1X,12F8.4)
970 IF (L.EQ.0) GO TO 200
980 PAUSE
990 PRINT 580
1000 580 FORMAT("OINCIDENT FLUX(MW/SQ.M)")
1010 PRINT 590,((QS(I,J),I=1,12),J=1,8)
1020 590 FORMAT(1X,12F7.3)
1030 PRINT 600
1040 600 FORMAT ("ORADIATION LOSS(MW)")
1050 PRINT 570,((QR(I,J),I=1,12),J=1,8)
1060 PRINT 620
1070 620 FORMAT("OCONVECTION LOSS(MW)")
1080 PRINT 570,((QC(I,J),I=1,12),J=1,8)
1090 PRINT 640
1100 640 FORMAT("ONODE SODIUM TEMPERATURES(DEG. F)")
1110 PRINT 550 , ((TNA(I,J),I=1,12),J=1,8)
1120 PAUSE
1130 PRINT 660
1140 660 FORMAT("OSODIUM HEAT TRANSFER COEFFICIENTS(BTU/HR*F*FT**2)")
1150 PRINT 550,((HN(I,J),I=1,12),J=1,8)
1160 PRINT 680
1170 680 FORMAT("OTUBE CONDUCTANCE(BTU/HR*F*FT**2)")
1180 PRINT 550,((U(I,J),I=1,12), J=1,8)
1190 PRINT 700
1200 700 FORMAT("OTUBE WALL CONDUCTIVITY(BTU/HR*F*FT)")
1210 PRINT 710,((KT(I,J),I=1,12), J=1,8)
1220 710 FORMAT(1X,12F7.1)
1230 PRINT 720
1240 720 FORMAT("OPEAK TUBE TEMPERATURE (DEG. F)")
1250 PRINT 550,((TTP(I,J),I=1,12),J=1,8)
1260 200 CONTINUE
1270 PRINT,"CONTINUE ITERATION?(YES=1,NO=0)"
1280 READ,LI
1290 IF(LI.EQ.1) GO TO 20
1300 STOP
1310 END
```

Table 0-2

VARIABLE LIST FOR ABSORBER LOSS PROGRAM

ALPHA	= absorptivity
CI	= heat flux factor to account for two dimensional tube wall conduction
CN	= average specific heat of sodium
D	= tube i.d.
DX	= panel width
DX	= node length
EFP(I)	= efficiency of panel i
EFR	= efficiency of receiver
EPS	= emissivity
ET(I,J)	= efficiency of node i in panel j
HN(I,J)	= sodium side heat transfer coefficient
HT	= air side convective heat transfer coefficient
KN	= sodium thermal conductivity
KT(I,J)	= tube wall thermal conductivity
N	= number of tubes per panel
NU	= Nusselt number of sodium
PE	= Peclet Number of sodium
QC(I,J)	= convection loss from node i in panel j
QR(I.J)	= radiative loss from node i in panel j
QS(I,J)	= incident solar flux on node i in panel j
QCP(I)	= convective loss from panel i
QCR(I)	= radiative loss from panel i
QIP(I)	= incident power on panel i
QIR	= solar incident power on receiver
QRP(I)	= radiative loss on panel i
QRR	= radiative loss from receiver
SIG	= Stefan Boltzmann Constant
TA	= ambient air temperature
TC	= sodium inlet temperature
TH	= sodium outlet temperature
TN(I)	= sodium temperature at outlet of node i, TN(0) = TC
TNA(I,J)	= average sodium temperature in node i of panel j
TT(I,J)	= average tube wall temperature in node i of panel j

Table 0-2 (Cont'd)

U(I,J) = tube conductance
W(I) = sodium flowrate in one half of panel i
WP(I) = sodium flowrate in panel i
WR = receiver sodium flowrate

Table 0-3

DESIGN POINT ABSORBER LOSS OUTPUT

```
RECLOSS      11:39EST     11/27/78

AIR TEMP.,CONV. COEFF.,C1?83.,2.0,.6366

FLUX PLOT FILENAME?FLUX1

FULL PRINT(YES=1,NO=0)?1

RECEIVER SUMMARY
FLOW= 0.856792E+07LB/HR
INCIDENT=  414.14MW
RAD. LOSS=   19.60MW
CONV. LOSS=   4.83MW
REFL. LOSS=  20.71MW
EFFICIENCY=0.8910
```

HEAT TO SODIUM 369.00 MW_t

PANEL	FLOW LB/HR	INCIDENT MW	RADIATION MW	CONVECTION MW	EFFICIENCY
1	474851.	22.628	0.841	0.204	0.9038
2	452795.	21.623	0.837	0.204	0.9019
3	431586.	20.655	0.832	0.203	0.8999
4	410449.	19.692	0.827	0.203	0.8977
5	388861.	18.707	0.822	0.202	0.8952
6	367449.	17.731	0.818	0.202	0.8925
7	346319.	16.768	0.813	0.201	0.8895
8	324987.	15.796	0.809	0.201	0.8861
9	303940.	14.837	0.805	0.200	0.8823
10	282316.	13.852	0.801	0.200	0.8777
11	260880.	12.876	0.798	0.199	0.8726
12	239525.	11.905	0.795	0.199	0.8665

OUTSIDE TUBE TEMPERATURES(DEG. F)

897.5	889.8	881.9	874.2	866.3	858.4	850.3	842.6	834.6	826.5	818.8	810.7
995.9	990.7	985.0	979.5	973.8	968.3	962.9	957.3	951.8	946.7	941.6	936.5
1045.5	1042.7	1039.1	1036.0	1032.7	1029.8	1026.6	1023.7	1020.6	1018.4	1015.5	1013.3
1072.5	1070.9	1069.1	1067.6	1066.0	1064.2	1062.6	1061.3	1059.8	1059.0	1057.9	1057.4
1088.9	1088.1	1086.9	1086.4	1085.4	1084.6	1083.7	1083.1	1082.6	1082.4	1082.1	1082.3
1097.1	1096.6	1096.0	1095.7	1095.1	1095.0	1094.3	1094.4	1094.0	1094.1	1094.1	1094.5
1098.9	1098.7	1098.4	1098.3	1098.0	1098.0	1097.7	1097.7	1097.6	1097.6	1098.0	1098.1
1098.9	1098.6	1098.5	1098.2	1098.1	1097.8	1097.8	1097.6	1097.4	1097.3	1097.2	1097.2

NODE EFFICIENCIES(P.U.)

0.9383	0.9381	0.9377	0.9374	0.9370	0.9366	0.9361	0.9356	0.9349	0.9342	0.9334	0.9324
0.9306	0.9300	0.9294	0.9286	0.9278	0.9269	0.9259	0.9248	0.9235	0.9220	0.9203	0.9182
0.9160	0.9147	0.9133	0.9118	0.9101	0.9083	0.9062	0.9038	0.9012	0.8982	0.8943	0.8902
0.8905	0.8878	0.8853	0.8825	0.8793	0.8754	0.8714	0.8670	0.8620	0.8556	0.8489	0.8410
0.8505	0.8458	0.8411	0.8364	0.8303	0.8242	0.8170	0.8088	0.8008	0.7894	0.7779	0.7634
0.7830	0.7738	0.7666	0.7575	0.7464	0.7376	0.7240	0.7130	0.6957	0.6775	0.6565	0.6318
0.6428	0.6287	0.6166	0.5963	0.5814	0.5608	0.5427	0.5118	0.4885	0.4484	0.4251	0.3725
0.4240	0.3904	0.3720	0.3310	0.3083	0.2574	0.2434	0.1809	0.1454	0.0853	-0.0106	-0.0670

```
PAUSE

LINE  CALLING-ROUTINE

980   RECLOSS
```

Table 0-3 (Cont'd)

```
INCIDENT FLUX(MW/SQ.M)
  1.821   1.742   1.663   1.586   1.507   1.428   1.349   1.272   1.194   1.115   1.038   0.959
  1.404   1.344   1.283   1.223   1.161   1.101   1.042   0.980   0.920   0.860   0.799   0.739
  0.901   0.862   0.822   0.784   0.745   0.707   0.668   0.630   0.591   0.554   0.512   0.474
  0.549   0.523   0.501   0.478   0.455   0.429   0.406   0.383   0.360   0.335   0.312   0.289
  0.341   0.325   0.310   0.297   0.281   0.267   0.252   0.237   0.224   0.208   0.194   0.179
  0.207   0.196   0.188   0.179   0.169   0.162   0.152   0.145   0.135   0.126   0.117   0.108
  0.113   0.108   0.104   0.098   0.094   0.089   0.085   0.079   0.075   0.069   0.066   0.060
  0.066   0.062   0.060   0.056   0.054   0.050   0.049   0.045   0.043   0.040   0.036   0.034

RADIATION LOSS(MW)
  0.0337  0.0329  0.0321  0.0314  0.0306  0.0299  0.0291  0.0284  0.0277  0.0270  0.0264  0.0257
  0.0449  0.0442  0.0435  0.0429  0.0422  0.0415  0.0409  0.0402  0.0396  0.0390  0.0384  0.0379
  0.0515  0.0511  0.0506  0.0501  0.0497  0.0493  0.0489  0.0485  0.0481  0.0478  0.0474  0.0471
  0.0553  0.0551  0.0548  0.0546  0.0544  0.0541  0.0539  0.0537  0.0535  0.0534  0.0532  0.0531
  0.0578  0.0576  0.0575  0.0574  0.0572  0.0571  0.0570  0.0569  0.0568  0.0568  0.0567  0.0568
  0.0590  0.0589  0.0588  0.0588  0.0587  0.0587  0.0586  0.0586  0.0585  0.0586  0.0586  0.0586
  0.0593  0.0593  0.0592  0.0592  0.0592  0.0591  0.0591  0.0591  0.0591  0.0591  0.0591  0.0592
  0.0593  0.0592  0.0592  0.0592  0.0592  0.0591  0.0591  0.0591  0.0591  0.0590  0.0590  0.0590

CONVECTION LOSS(MW)
  0.0108  0.0107  0.0106  0.0105  0.0103  0.0102  0.0101  0.0100  0.0099  0.0098  0.0097  0.0096
  0.0121  0.0120  0.0119  0.0118  0.0118  0.0117  0.0116  0.0115  0.0115  0.0114  0.0113  0.0113
  0.0127  0.0127  0.0126  0.0126  0.0125  0.0125  0.0125  0.0124  0.0124  0.0124  0.0123  0.0123
  0.0131  0.0131  0.0130  0.0130  0.0130  0.0130  0.0129  0.0129  0.0129  0.0129  0.0129  0.0129
  0.0133  0.0133  0.0133  0.0133  0.0132  0.0132  0.0132  0.0132  0.0132  0.0132  0.0132  0.0132
  0.0134  0.0134  0.0134  0.0134  0.0134  0.0134  0.0134  0.0134  0.0134  0.0134  0.0134  0.0134
  0.0134  0.0134  0.0134  0.0134  0.0134  0.0134  0.0134  0.0134  0.0134  0.0134  0.0134  0.0134
  0.0134  0.0134  0.0134  0.0134  0.0134  0.0134  0.0134  0.0134  0.0134  0.0134  0.0134  0.0134

NODE SODIUM TEMPERATURES(DEG. F)
   697.7   697.9   698.0   698.3   698.5   698.7   698.8   699.2   699.4   699.8   700.4   700.9
   847.2   847.9   848.2   848.7   849.2   849.8   850.3   851.1   851.8   852.9   854.2   855.5
   953.0   954.0   954.2   954.9   955.5   956.4   957.1   958.0   958.9   960.5   962.0   963.7
  1018.1  1019.1  1019.4  1020.1  1020.8  1021.6  1022.3  1023.4  1024.2  1025.9  1027.2  1029.1
  1056.8  1057.6  1057.8  1058.6  1059.2  1059.8  1060.4  1061.3  1062.1  1063.6  1064.7  1066.4
  1079.2  1079.8  1079.9  1080.6  1080.9  1081.5  1081.8  1082.7  1083.3  1084.4  1085.3  1086.6
  1090.8  1091.2  1091.3  1091.7  1091.9  1092.4  1092.5  1093.1  1093.4  1094.1  1094.8  1095.5
  1095.8  1096.0  1096.0  1096.2  1096.2  1096.4  1096.4  1096.6  1096.7  1096.9  1097.3  1097.4
PAUSE

LINE  CALLING-ROUTINE

1120  RECLOSS
```

Table 0-3 (Cont'd)

```
SODIUM HEAT TRANSFER COEFFICIENTS(BTU/HR*F*FT**2)
  7625.4  7542.2  7461.7  7380.5  7296.6  7212.5  7128.8  7042.6  6956.7  6867.0  6776.2  6684.6
  7278.9  7195.8  7116.0  7035.2  6951.9  6868.1  6784.7  6698.9  6613.3  6523.4  6432.3  6340.4
  7068.4  6985.6  6906.4  6826.1  6743.2  6659.8  6576.7  6491.4  6406.4  6316.4  6226.2  6134.4
  6949.8  6867.4  6788.7  6708.6  6626.1  6543.3  6460.7  6375.7  6291.1  6201.5  6112.2  6020.7
  6882.9  6801.1  6722.6  6642.8  6560.7  6478.4  6396.2  6311.7  6227.4  6138.7  6049.8  5959.0
  6845.2  6763.9  6685.7  6606.1  6524.6  6442.5  6360.9  6276.6  6192.8  6104.8  6016.5  5926.5
  6825.9  6745.1  6667.0  6587.9  6506.7  6424.8  6343.6  6259.8  6176.6  6089.3  6001.4  5912.4
  6817.7  6737.2  6659.3  6580.7  6499.7  6418.3  6337.3  6254.1  6171.2  6084.7  5997.4  5909.3

TUBE CONDUCTANCE(BTU/HR*F*FT**2)
  1726.7  1719.6  1712.5  1705.4  1698.1  1690.6  1683.0  1675.4  1667.6  1659.5  1651.4  1643.0
  1773.9  1767.0  1759.9  1752.8  1745.4  1738.0  1730.5  1722.7  1714.9  1706.8  1698.6  1690.2
  1800.3  1793.6  1786.6  1779.8  1772.5  1765.3  1757.9  1750.3  1742.5  1734.7  1726.4  1718.0
  1815.1  1808.4  1801.7  1794.9  1787.8  1780.5  1773.2  1765.7  1758.0  1750.1  1741.8  1733.5
  1823.8  1817.1  1810.4  1803.7  1796.6  1789.3  1782.0  1774.4  1766.7  1758.7  1750.4  1742.0
  1828.5  1821.7  1815.0  1808.3  1801.1  1794.0  1786.5  1779.0  1771.2  1763.1  1754.7  1746.2
  1830.2  1823.5  1816.8  1810.1  1802.9  1795.7  1788.3  1780.7  1772.9  1764.7  1756.3  1747.6
  1830.8  1824.0  1817.4  1810.5  1803.4  1796.1  1788.7  1781.0  1773.1  1764.8  1756.3  1747.6

TUBE WALL CONDUCTIVITY(BTU/HR*F*FT)
   10.5    10.4    10.4    10.4    10.4    10.4    10.3    10.3    10.3    10.3    10.3    10.3
   11.0    11.0    11.0    11.0    11.0    11.0    11.0    11.0    10.9    10.9    10.9    10.9
   11.4    11.4    11.4    11.4    11.4    11.4    11.4    11.4    11.4    11.4    11.4    11.4
   11.6    11.6    11.6    11.6    11.6    11.6    11.6    11.6    11.6    11.6    11.6    11.6
   11.7    11.7    11.7    11.7    11.7    11.7    11.7    11.7    11.7    11.7    11.8    11.8
   11.8    11.8    11.8    11.8    11.8    11.8    11.8    11.8    11.8    11.8    11.8    11.8
   11.9    11.9    11.9    11.9    11.9    11.9    11.9    11.9    11.9    11.9    11.9    11.9
   11.9    11.9    11.9    11.9    11.9    11.9    11.9    11.9    11.9    11.9    11.9    11.9

PEAK TUBE TEMPERATURE (DEG. F)
  1011.5   999.3   986.8   974.7   962.2   949.5   936.7   924.4   911.7   898.9   886.4   873.4
  1080.8  1072.2  1063.0  1054.2  1044.9  1036.0  1027.1  1017.9  1008.9  1000.2   991.5   982.8
  1098.3  1093.4  1087.5  1082.3  1076.8  1071.7  1066.3  1061.2  1055.8  1051.5  1046.1  1041.6
  1103.6  1100.5  1097.5  1094.6  1091.8  1088.5  1085.6  1083.0  1080.1  1077.9  1075.4  1073.5
  1107.2  1105.5  1103.5  1102.2  1100.4  1098.7  1097.0  1095.6  1094.3  1093.2  1092.1  1091.3
  1107.3  1106.2  1105.1  1104.4  1103.2  1102.6  1101.4  1101.1  1100.1  1099.7  1099.2  1099.0
  1103.4  1103.0  1102.5  1102.0  1101.5  1101.2  1100.6  1100.3  1100.0  1099.6  1099.8  1099.5
  1100.7  1100.2  1099.9  1099.4  1099.1  1098.7  1098.5  1098.1  1097.9  1097.5  1097.2  1097.0
CONTINUE ITERATION?(YES=1,NO=0)?0


PROGRAM STOP AT 1300
```

Appendix P

STEAM GENERATOR CONCEPTUAL DESIGN ANALYSIS — COMPUTER PROGRAM OUTPUT

Tables P-1, P-2, and P-3 list the output from computer program "STMGEN" used to design the steam generator modules described in Section 5.3.5.

Table P-1

EVAPORATOR DESIGN CALCULATIONS -- COMPUTER PROGRAM "STMGEN" OUTPUT

```
 CASE NO.  1              ** SOLAR STEAM GENERATOR SIZING **
                       CASE 1 ** EVAPORATOR

             INPUT DATA


NAMELIST    DATAA
NPRINT=             1,
XLNGTH=    0.69000000E 02,      DXL    =    0.10000000E 00,      DOTUBE=    0.62500000E 00,      PITCHO=    0.12200000E 01,
TNAIN =    0.85910000E 03,      TNAOUT=    0.61200000E 03,      TSTMIN=    0.52890000E 03,      TSTMOT=    0.67390000E 03,
PSTMIN=    0.27000000E 04,      HFOUL =    0.57140000E 04,
MAT   =             2,    HXTYPE=             1,
MWUNIT=    0.12660000E 03,
NTUBES=           600,
ECARB =    0.52500000E 00,      CORR   =    0.19000000E-01,      XKIN   =    0.78000000E 02,      XKOUT  =    0.10000000E 01,
XLOUT =    0.12650000E 02,      XLMARG=    0.11000000E 02,      XLIN   =    0.58000000E 01,      SUBDOW=    0.10000000E 01,
WTSTMO=    0.83812000E 06,      WTNAO  =    0.57120000E 07,
NCASES=            15,
HSTMOT=    0.10381000E 04,      DRODSC=    0.              ,    DRODNB=    0.              ,    DRODFB=    0.              ,
DRODSH=    0.              ,    DRODIN=    0.              ,    DRODOT=    0.              ,
NBAF  =             2,
WBAF  =    0.83334000E-02,      BAFSPA=    0.25000000E 01,
NDOUB =             0,
PDNAO =    0.63000000E 01,      DPDNAO=    0.90000000E 02,      DITUBO=    0.39700000E 00,      HSTMII=    0.52290000E 03,
NDEMO =             0,
ROUGH1=    0.64000000E-04,      ROUGH2=    0.64000000E-04,
NBUND =             1,
XDPRAT=    0.              ,    PHE    =    0.              ,    PNA    =    0.              ,    DMID   =    0.              ,
GAPO  =    0.              ,    GROVE  =    0.              ,    PSTMOU=    0.              ,    DPSTMT=    0.              ,
RECIRC=    0.              ,    PDRUM  =    0.              ,    TFW    =    0.              ,    DOSHD  =    0.              ,
XLSHD =    0.              ,
MATSHD=             0,
XDNBOO=    0.              ,
$ END
          MM INDEX=  50
          MM INDEX=  50
          MM INDEX=  50
          MM INDEX=  50

   TNAIN      TNAOUT    TSTM(1)   TSTMOUT   TUBE L   PSTMIN    DP-STM    DP-NA TUBE NO. PITCH     STM-FLOW      NA-FLOW
 859.100    612.00000   530.377   674.138   80.563 2700.000   105.416   15.501       600 1.2200   0.8381E 06   0.5712E 07
          MM INDEX=  50
          MM INDEX=  50
          MM INDEX=  50
          MM INDEX=  50
 859.100    612.00000   530.384   675.539   71.990 2700.000    74.500   10.131       700 1.2200   0.8381E 06   0.5712E 07
          MM INDEX=  50
          MM INDEX=  50
          MM INDEX=  50
          MM INDEX=  50
 859.100    612.00000   530.385   675.881   69.483 2700.000    67.014    8.924       734 1.2200   0.8381E 06   0.5712E 07
          MM INDEX=  50
          MM INDEX=  50
          MM INDEX=  50
          MM INDEX=  50
 859.100    612.00000   530.386   675.935   69.096 2700.000    65.833    8.778       740 1.2200   0.8381E 06   0.5712E 07
          MM INDEX=  50
          MM INDEX=  50
          MM INDEX=  50
          MM INDEX=  50
```

Table P-1 (Cont'd)

CASE NO. 1 ** SOLAR STEAM GENERATOR SIZING **
CASE 1 ** EVAPORATOR

INPUT DATA

EVAPOR		
HEAT LOAD PER UNIT	126.5768	MWT
TUBE LENGTH ACTIVE	69.00	FEET
ALLOWABLE LENGTH VARIATION	0.100	FEET
TUBE OD	0.62500	INCHES
TUBE CENTER PITCH	1.22000	INCHES
TEMPERATURE,SODIUM INLET	859.10	F
,SODIUM OUTLET	612.00	F
,STEAM INLET	530.40	F
,STEAM OUTLET	0.	F
ENTHALPY,STEAM OUTLET	1038.35	BTU/LBM
PRESSURE ,STEAM INLET	2700.00	PSI
FOULING FACTOR	5714.00	BTU/HR-F-FT**2
DECARBONIZATION FACTOR E ON TUBE STRENGTH	0.52500	FACTION
TUBE CORROSION ALLOWANCE	0.01900	INCHES

Table P-1 (Cont'd)

** SOLAR STEAM GENERATOR SIZING **
CASE 1 ** EVAPORATOR

OUTPUT DATA

J	SECT TYPE	ACTIVE LENGTH FT	T-NA F	T-OD WALL F	T-ID WALL F	T-WAL FOUL ID. F	T-STM F	U-OVER BTU/HR-FT**2-F	H-NA	H-WAL	H-STM	QUAL	P-STM PSI	DP-STM PSI	VELO FT/SEC	H-STEAM BTU/LBM	HEAT FLUX BTU/HR-FT**2
1	SUBC	0.	612.0	603.4	572.0	556.5	530.4	1083.6	10262.0	2815.2	3388.1	0.	2673.8	24.2	7.57	522.9	88439.8
2	SUBC	1.33	617.0	608.8	578.7	563.9	539.2	1085.9	10247.8	2812.6	3415.7	0.	2673.2	24.4	7.66	533.5	84469.5
3	SUBC	2.73	622.0	614.1	585.4	571.3	547.9	1088.0	10233.6	2809.9	3442.6	0.	2672.5	24.6	7.74	544.0	80614.5
4	SUBC	4.19	627.0	619.5	592.1	578.6	556.5	1090.1	10219.5	2807.3	3468.9	0.	2671.8	24.9	7.83	554.6	76883.1
5	SUBC	5.72	632.0	624.8	598.7	585.9	564.9	1092.0	10205.5	2804.6	3494.6	0.	2671.0	25.1	7.92	565.1	73287.4
6	SUBC	7.33	637.0	630.1	605.2	593.0	573.2	1093.9	10191.4	2801.9	3519.6	0.	2670.3	25.4	8.02	575.6	69838.7
7	SUBC	9.01	642.0	635.5	611.7	600.0	581.3	1095.7	10177.4	2799.1	3544.0	0.	2669.5	25.6	8.12	586.2	66548.0
8	SUBC	10.78	647.0	640.8	618.1	607.0	589.2	1097.3	10163.5	2796.4	3567.7	0.	2668.6	25.9	8.23	596.7	63429.3
9	SUBC	12.63	652.0	646.0	624.4	613.8	597.0	1098.9	10149.5	2793.6	3590.7	0.	2667.7	26.2	8.35	607.2	60458.0
10	SUBC	14.57	657.0	651.3	630.6	620.5	604.6	1100.4	10135.6	2790.8	3613.0	0.	2666.8	26.6	8.46	617.7	57713.4
11	SUBC	16.60	662.0	656.5	636.8	627.1	611.9	1101.8	10121.8	2788.0	3634.5	0.	2665.9	26.9	8.59	628.2	55181.5
12	SUBC	18.72	667.0	661.8	642.8	633.5	619.1	1103.1	10108.0	2785.2	3655.3	0.	2664.9	27.3	8.72	638.7	52874.5
13	SUBC	20.93	672.0	667.0	648.7	639.8	626.0	1104.3	10094.2	2782.4	3675.2	0.	2663.9	27.7	8.87	649.2	50811.4
14	SUBC	23.22	677.0	672.1	654.5	645.9	632.7	1105.4	10080.4	2779.7	3694.4	0.	2662.8	28.1	9.02	659.7	49007.4
15	SUBC	25.59	682.0	677.3	660.2	651.9	639.1	1106.4	10066.7	2776.9	3712.7	0.	2661.7	28.5	9.18	670.2	47481.2
16	SUBC	28.02	687.0	682.4	665.7	657.6	645.2	1107.4	10053.0	2774.1	3730.0	0.	2660.6	28.9	9.35	680.7	46254.4
17	SUBC	30.52	692.0	687.5	671.1	663.2	651.0	1108.2	10039.4	2771.4	3746.4	0.	2659.5	29.4	9.53	691.1	45383.0
18	SUBC	33.05	697.0	692.5	676.3	668.5	656.6	1108.9	10025.7	2768.7	3761.9	0.	2658.3	29.8	9.73	701.6	44838.9
19	SUBC	35.59	702.0	697.5	681.4	673.6	661.7	1109.6	10012.2	2766.0	3776.3	0.	2657.2	30.3	9.94	712.1	44673.3
20	SUBC	38.13	707.0	702.5	686.1	678.2	666.3	1110.5	9998.6	2766.0	3788.9	0.	2656.0	30.8	10.17	722.5	45203.2
21	NSUB	38.52	707.8	703.2	686.9	678.9	667.0	1110.2	9996.5	2763.0	3790.8	0.	2655.9	30.9	10.20	724.2	45303.6
22	NSUB	41.01	712.8	707.5	688.3	679.0	671.1	1272.2	9983.0	2763.0	6714.7	0.	2654.8	31.4	10.46	734.6	52982.3
23	NSUB	43.13	717.8	711.7	689.7	679.1	674.9	1414.3	9969.5	2759.9	14408.1	0.	2653.8	31.8	10.74	745.1	60638.5
24	NUCL	44.23	720.7	714.2	690.6	679.2	676.9	1488.0	9961.6	2759.9	29130.3	0.	2653.3	32.0	10.92	751.3	65221.5
25	NUCL	45.88	725.7	718.4	692.0	679.2	676.9	1491.8	9948.1	2759.9	30780.5	0.0324	2652.5	32.5	11.94	761.7	72900.1
26	NUCL	47.36	730.7	722.6	693.4	679.3	676.8	1493.7	9934.8	2755.9	32331.5	0.0648	2651.7	33.0	12.97	772.1	80531.9
27	NUCL	48.71	735.7	726.9	694.8	679.4	676.8	1496.5	9921.4	2755.9	33820.6	0.0971	2650.9	33.5	13.99	782.6	88223.8
28	NUCL	49.95	740.7	731.1	696.3	679.5	676.8	1497.9	9908.1	2752.7	35233.7	0.1294	2650.2	33.9	15.02	793.0	95856.2
29	NUCL	51.09	745.7	735.3	697.7	679.5	676.7	1500.0	9894.8	2752.7	36600.1	0.1616	2649.6	34.4	16.04	803.4	103545.4
30	NUCL	52.15	750.7	739.5	699.1	679.6	676.7	1500.9	9881.6	2749.6	37903.3	0.1938	2648.9	34.9	17.07	813.8	111164.5
31	NUCL	53.13	755.7	743.7	700.5	679.7	676.6	1502.5	9868.4	2749.6	39172.6	0.2259	2648.3	35.4	18.09	824.2	118847.8
32	NUCL	54.06	760.7	747.9	701.9	679.7	676.6	1503.0	9855.2	2746.4	40387.5	0.2580	2647.8	35.8	19.11	834.6	126448.5
33	NUCL	54.93	765.7	752.1	703.3	679.8	676.6	1504.3	9842.1	2746.4	41577.3	0.2900	2647.2	36.2	20.13	845.0	134125.3
34	NUCL	55.75	770.7	756.3	704.7	679.9	676.6	1504.4	9829.0	2743.2	42717.6	0.3220	2646.6	36.7	21.16	855.4	141712.5
35	NUCL	56.53	775.7	760.5	706.1	679.9	676.5	1505.5	9815.9	2743.2	43838.9	0.3539	2646.0	37.2	22.18	865.8	149388.2
36	FILM	57.25	780.6	769.5	729.7	710.6	676.5	1045.5	9803.2	2732.1	3189.9	0.3851	2645.5	37.7	23.18	875.9	108876.9
37	FILM	58.26	785.6	773.9	731.7	711.6	676.4	1054.6	9790.2	2732.1	3277.6	0.4169	2644.7	38.4	24.21	886.3	115143.7
38	FILM	59.22	790.6	778.3	734.1	713.0	676.4	1054.9	9777.2	2728.1	3288.0	0.4487	2643.9	39.1	25.24	896.7	120499.4
39	FILM	60.14	795.6	782.7	736.5	714.4	676.4	1057.8	9764.3	2728.1	3317.9	0.4805	2643.1	39.8	26.26	907.1	126167.4
40	FILM	61.02	800.6	787.1	738.7	715.6	676.3	1061.5	9751.4	2724.2	3362.0	0.5122	2642.4	40.4	27.29	917.4	131958.7
41	FILM	61.86	805.6	791.5	740.9	716.8	676.3	1065.7	9738.5	2724.2	3406.0	0.5439	2641.8	40.9	28.31	927.8	137845.4
42	FILM	62.66	810.6	795.9	743.2	718.1	676.2	1067.3	9725.7	2720.3	3430.3	0.5755	2641.2	41.5	29.33	938.1	143425.9
43	FILM	63.43	815.6	800.3	745.4	719.3	676.2	1070.8	9712.9	2720.3	3469.0	0.6071	2640.6	42.0	30.36	948.5	149293.4
44	FILM	64.17	820.6	804.6	747.5	720.3	676.2	1074.4	9700.1	2716.3	3514.8	0.6386	2640.0	42.5	31.38	958.8	155197.7
45	FILM	64.89	825.6	809.0	749.8	721.7	676.1	1075.5	9687.4	2716.3	3528.5	0.6701	2639.3	43.1	32.41	969.2	160775.4
46	FILM	65.58	830.6	813.4	751.9	722.6	676.1	1079.9	9674.7	2712.1	3585.7	0.7016	2638.7	43.7	33.43	979.5	166873.7
47	FILM	66.24	835.6	817.8	754.3	724.1	676.1	1079.9	9662.1	2712.1	3587.0	0.7330	2638.2	44.2	34.45	989.9	172300.3
48	FILM	66.89	840.6	822.1	756.1	724.8	676.0	1086.6	9649.5	2708.0	3671.9	0.7644	2637.6	44.7	35.48	1000.2	178844.5
49	FILM	67.51	845.6	826.5	758.6	726.4	676.0	1084.4	9636.9	2708.0	3647.9	0.7958	2637.1	45.1	36.50	1010.5	183925.6
50	FILM	68.11	850.6	830.9	760.6	727.4	676.0	1087.7	9624.3	2704.1	3694.4	0.8271	2636.6	45.7	37.53	1020.9	189953.5
51	FILM	68.69	855.6	835.3	762.9	728.6	676.0	1089.7	9611.8	2704.1	3719.7	0.8584	2636.0	46.2	38.54	1031.2	195788.2
52	FILM	69.09	859.1	838.3	764.1	729.1	675.9	1093.1	9603.1	2700.4	3768.3	0.8801	2635.6	46.5	39.24	1038.3	200216.2

Table P-1 (Cont'd)

```
   ** SOLAR STEAM GENERATOR SIZING **
 CASE 1 ** EVAPORATOR

OUTPUT DATA

 TUBE OD                          0.62500 INCHES
 TUBE WALL THICKNESS              0.114000 INCHES
 REQUIRED TUBE WALL               0.       INCHES
 TUBE ID                          0.39700 INCHES
 NUMBER OF TUBES                      740
 ACTIVE TUBE LENGTH                 69.09 FEET
 ACTIVE HT. TRANSFER AREA,ID      5313.62 FT**2
 STEAM FLOW RATE              0.8381E 06 LBM/HR
 STEAM MASS VELOCITY              365.989 LBM/SEC-FT**2
 FOULING FACTOR                  5714.00BTU/FT**2-HR
 DNB QUALITY                      0.38506 FRACTION
 DNB MARGIN                      -128.56 PERCENT
 HYDAULIC DIAMETER,SODIUM        0.166744 FEET
 SODIUM INLET VELOCITY              5.98 FT/SEC
 SODIUM OUTLET VELOCITY             5.76 FT/SEC
 SODIUM FLOW RATE PER UNIT  0.5712E 07 LBM/HR
 SODIUM PRESSURE DROP               8.778 PSI
 NA PRES DROP IN SUPPORTS           7.542 PSI
 STEAM SIDE PRESSURE DROP          65.828 PSI
 INLET PRESSURE DROP               24.224 PSI
 SUBCOOLED PRESSURE DROP ,          7.821 PSI
 NUCLEATE BOILING PRES DROP,        5.623 PSI
 FILM BOILING PRESSURE DROP,        8.853 PSI
 SUPERHEAT PRESSURE DROP            0.    PSI
 OUTLET PRESSURE DROP              19.307 PSI


 SODIUM SIDE DATA
 TUBE SUPPORT MINIMUM WEB THICKNESS        0.1000INCHES,
 DISTANCE BETWEEN SUPPORTS                 2.5000 FEET
 SODIUM PRESSURE DROP COEF PER SUPPORT      1.35349
 TUBE SUPPORT USE NA FLOW HOLES THAT ARE MIX OF BOTH TYPES
   WITH BROKEN EDGES
 DIAMETER OF EQUIVALENT HOLE IN SUPPORT       0.611 INCHES
 MAXIMUM SODIUM VELOCITY IN SUPPORTS        9.83944 FT/SEC

 TEMPERATURE,STEAM INLET          530.40 F
 TEMPERATURE,STEAM OUTLET         674.84 F
 TEMPERATURE,SODIUM INLET         859.10 F
 TEMPERATURE,SODIUM OUTLET        612.00 F
 ENTHALPY, STEAM INLET            522.90 BTU/LBM
 ENTHALPY, STEAM OUTLET          1038.35 BTU/LBM
 ENTHALPY, SODIUM INLET           414.36 BTU/LBM
 ENTHALPY,SODIUM OUTLET           338.73 BTU/LBM


  SECTION AVERAGE PROPERTIES
SECTION     LOG MEAN TEMP       OVERALL U       TUBE SEC. LENGTH
              DEGREES F       BTU/FT**2-HR-F        FEET

  SUBC           60.78            925.69             44.23
  NUCL           69.69           1497.29             13.02
  FILM          139.96           1068.22             11.84
  SUPH              0.                0.                0.
```

Table P-2

SUPERHEATER DESIGN CALCULATIONS -- COMPUTER PROGRAM "STMGEN" OUTPUT

```
 CASE NO.  1              ** SOLAR STEAM GENERATOR SIZING **
                        CASE 2 ** SUPERHEATER

             INPUT DATA


 NAMELIST    DATAA
 NPRINT=           1,
 XLNGTH=   0.33650000E 02,     DXL    =   0.10000000E 00,     DOTUBE=   0.62500000E 00,     PITCHO=   0.12200000E 01,
 TNAIN =   0.11000000E 04,     TNAOUT=   0.85910000E 03,     TSTMIN=   0.67390000E 03,     TSTMOT=   0.10039000E 04,
 PSTMIN=   0.25800000E 04,     HFOUL =   0.10000000E 21,
 MAT   =           3,   HXTYPE=           2,
 MWUNIT=   0.60830000E 02,
 NTUBES=         600,
 ECARB =   0.52500000E 00,     CORR   =   0.19000000E-01,     XKIN   =   0.50000000E 00,     XKOUT  =   0.10000000E 01,
 XLOUT =   0.12650000E 02,     XLMARG=   0.21700000E 01,     XLIN   =   0.58000000E 01,     SUBDOW=   0.10000000E 01,
 WTSTMO=   0.72880000E 06,     WTNAO  =   0.38030000E 07,
 NCASES=          15,
 HSTMOT=   0.14604000E 04,     DRODSC=   0.             ,     DRODNB=   0.             ,     DRODFB=   0.             ,
 DRODSH=   0.             ,     DRODIN=   0.             ,     DRODOT=   0.             ,
 NBAF  =           2,
 WBAF  =   0.83334000E-02,     BAFSPA=   0.25000000E 01,
 NDOUB =           0,
 PDNAO =   0.63000000E 01,     DPDNAO=   0.90000000E 02,     DITUBO=   0.39700000E 00,     HSTMII=   0.10820000E 04,
 NDEMO =           0,
 ROUGH1=   0.64000000E-04,     ROUGH2=   0.64000000E-04,
 NBUND =           1,
 XDPRAT=   0.             ,     PHE    =   0.             ,     PNA    =   0.             ,     DMID   =   0.             ,
 GAPO  =   0.             ,     GROVE  =   0.             ,     PSTMOU=   0.             ,     DPSTMT=   0.             ,
 RECIRC=   0.             ,     PDRUM  =   0.             ,     TFW    =   0.             ,     DOSHD  =   0.             ,
 XLSHD =   0.             ,
 MATSHD=           0,
 XDNBOO=   0.             ,
 $BEND
     TNAIN      TNAOUT    TSTM(1)  TSTMOUT   TUBE L   PSTMIN   DP-STM   DP-NA TUBE NO. PITCH     STM-FLOW      NA-FLOW
  1100.000   859.10000  672.393 1005.204   32.652 2580.000   98.687   3.047       600  1.2200   0.7288E 06   0.3803E 07
  1100.000   859.10000  672.372 1004.964   33.314 2580.000  105.917   3.241       582  1.2200   0.7288E 06   0.3803E 07
  1100.000   859.10000  672.359 1004.820   33.681 2580.000  110.242   3.356       572  1.2200   0.7288E 06   0.3803E 07
```

Table P-2 (Cont'd)

CASE NO. 1 ** SOLAR STEAM GENERATOR SIZING **
CASE 2 ** SUPERHEATER

INPUT DATA

SUPERH		
HEAT LOAD PER UNIT	80.7996	MWT
TUBE LENGTH ACTIVE	33.65	FEET
ALLOWABLE LENGTH VARIATION	0.100	FEET
TUBE OD	0.62500	INCHES
TUBE CENTER PITCH	1.22000	INCHES
TEMPERATURE, SODIUM INLET	1100.00	F
, SODIUM OUTLET	859.10	F
, STEAM INLET	672.77	F
, STEAM OUTLET	0.	F
ENTHALPY, STEAM OUTLET	1460.39	BTU/LBM
PRESSURE , STEAM INLET	2580.00	PSI
FOULING FACTOR	0.10E 21	BTU/HR-F-FT**2
DECARBONIZATION FACTOR E ON TUBE STRENGTH	0.52500	FACTION
TUBE CORROSION ALLOWANCE	0.01900	INCHES

Table P-2 (Cont'd)

** SOLAR STEAM GENERATOR SIZING **
CASE 2 ** SUPERHEATER

OUTPUT DATA

J	SECT TYPE	ACTIVE LENGTH FT	T-NA F	T-OD WALL F	T-ID WALL F	T-WAL FOUL ID. F	T-STM F	U-OVER BTU/HR-FT**2-F	H-NA	H-WAL	H-STM	QUAL	P-STM PSI	DP-STM PSI	VELO FT/SEC	H-STEAM BTU/LBM	HEAT FLUX BTU/HR-FT**2
1	FILM	0.	859.1	839.1	708.6	708.6	672.4	972.2	9074.5	1391.3	5009.5	0.9931	2572.9	6.8	50.65	1082.0	181550.4
2	SUPH	0.18	860.8	841.6	716.9	716.9	672.3	923.4	9070.4	1395.5	3904.0	1.0000	2572.7	7.0	50.95	1084.7	174037.4
3	SUPH	0.73	865.8	846.4	720.5	720.5	673.9	915.6	9058.3	1395.5	3770.4	1.0000	2572.1	7.6	52.23	1092.6	175702.4
4	SUPH	1.28	870.8	851.2	724.4	724.4	675.7	910.6	9046.3	1401.2	3650.9	1.0000	2571.5	8.1	53.60	1100.5	177628.3
5	SUPH	1.82	875.8	856.0	728.5	728.5	677.8	902.7	9034.3	1401.2	3528.1	1.0000	2570.9	8.7	54.98	1108.4	178746.2
6	SUPH	2.36	880.8	860.9	733.0	733.0	680.0	896.3	9022.3	1407.4	3396.9	1.0000	2570.3	9.3	56.39	1116.3	179941.2
7	SUPH	2.89	885.8	865.8	737.7	737.7	682.6	887.2	9010.4	1407.4	3271.7	1.0000	2569.7	9.9	57.79	1124.2	180278.5
8	SUPH	3.42	890.8	870.7	742.9	742.9	685.5	879.9	8998.5	1413.9	3143.7	1.0000	2569.0	10.5	59.23	1132.0	180681.1
9	SUPH	3.96	895.8	875.7	748.2	748.2	688.5	871.7	8986.6	1417.3	3027.1	1.0000	2568.4	11.1	60.67	1139.9	180708.5
10	SUPH	4.49	900.8	880.7	753.7	753.7	691.7	863.2	8974.8	1420.8	2914.1	1.0000	2567.7	11.7	62.13	1147.8	180462.9
11	SUPH	5.02	905.8	885.7	759.2	759.2	695.2	855.4	8963.0	1424.3	2813.7	1.0000	2567.0	12.4	63.59	1155.7	180160.9
12	SUPH	5.56	910.8	890.7	764.9	764.9	698.8	847.8	8951.2	1427.9	2721.7	1.0000	2566.4	13.0	65.05	1163.6	179727.1
13	SUPH	6.09	915.8	895.8	770.7	770.7	702.7	840.0	8939.4	1431.5	2631.0	1.0000	2565.6	13.7	66.53	1171.4	179018.5
14	SUPH	6.63	920.8	900.8	776.6	776.6	706.7	833.1	8927.7	1435.1	2554.3	1.0000	2564.9	14.4	68.01	1179.3	178340.2
15	SUPH	7.17	925.8	905.9	782.5	782.5	711.0	826.6	8916.0	1438.8	2484.3	1.0000	2564.2	15.1	69.50	1187.2	177549.6
16	SUPH	7.71	930.8	911.0	788.5	788.5	715.5	820.5	8904.4	1442.5	2420.2	1.0000	2563.4	15.9	70.99	1195.1	176652.4
17	SUPH	8.26	935.8	916.1	794.7	794.7	720.3	814.5	8892.8	1446.2	2359.4	1.0000	2562.6	16.6	72.50	1202.9	175567.5
18	SUPH	8.81	940.8	921.2	801.0	801.0	725.2	808.5	8881.2	1450.0	2300.7	1.0000	2561.8	17.4	74.01	1210.8	174290.1
19	SUPH	9.36	945.8	926.3	807.4	807.4	730.5	802.7	8869.6	1453.9	2246.0	1.0000	2561.0	18.2	75.53	1218.6	172860.4
20	SUPH	9.92	950.8	931.5	814.0	814.0	735.9	797.2	8858.1	1457.8	2195.5	1.0000	2560.2	19.0	77.06	1226.5	171299.8
21	SUPH	10.48	955.8	936.6	820.6	820.6	741.7	792.0	8846.6	1461.7	2148.7	1.0000	2559.3	19.9	78.60	1234.4	169594.5
22	SUPH	11.05	960.8	941.8	827.4	827.4	747.7	787.1	8835.1	1465.7	2105.4	1.0000	2558.4	20.7	80.15	1242.2	167748.2
23	SUPH	11.63	965.8	947.0	834.2	834.2	754.0	782.7	8823.7	1469.7	2066.3	1.0000	2557.5	21.6	81.71	1250.1	165789.2
24	SUPH	12.21	970.8	952.2	841.1	841.1	760.5	778.5	8812.3	1473.7	2030.2	1.0000	2556.6	22.6	83.29	1257.9	163698.6
25	SUPH	12.80	975.8	957.5	848.2	848.2	767.3	774.7	8800.9	1477.8	1997.9	1.0000	2555.6	23.5	84.87	1265.8	161500.9
26	SUPH	13.40	980.8	962.7	855.3	855.3	774.4	771.3	8789.6	1481.9	1968.7	1.0000	2554.6	24.5	86.46	1273.6	159190.5
27	SUPH	14.01	985.8	967.9	862.5	862.5	781.8	768.3	8778.3	1486.1	1942.7	1.0000	2553.5	25.5	88.07	1281.5	156754.8
28	SUPH	14.63	990.8	973.2	869.7	869.7	789.4	765.7	8767.0	1490.2	1920.0	1.0000	2552.5	26.6	89.67	1289.3	154252.2
29	SUPH	15.25	995.8	978.5	877.0	877.0	797.2	763.6	8755.8	1494.4	1900.2	1.0000	2551.3	27.7	91.29	1297.2	151657.9
30	SUPH	15.89	1000.8	983.8	884.4	884.4	805.3	761.9	8744.6	1498.6	1883.4	1.0000	2550.2	28.8	92.91	1305.0	148970.9
31	SUPH	16.54	1005.8	989.1	891.8	891.8	813.6	760.5	8733.4	1502.9	1869.3	1.0000	2549.0	30.0	94.54	1312.9	146196.0
32	SUPH	17.21	1010.8	994.4	899.3	899.3	822.1	759.7	8722.2	1507.1	1858.0	1.0000	2547.8	31.2	96.18	1320.7	143336.9
33	SUPH	17.88	1015.8	999.7	906.8	906.8	830.9	759.2	8711.1	1511.4	1849.3	1.0000	2546.5	32.5	97.83	1328.5	140393.5
34	SUPH	18.58	1020.8	1005.0	914.4	914.4	839.9	759.1	8700.0	1515.7	1843.0	1.0000	2545.1	33.8	99.48	1336.4	137366.3
35	SUPH	19.28	1025.8	1010.4	922.0	922.0	849.0	759.5	8689.0	1520.0	1839.2	1.0000	2543.7	35.2	101.14	1344.2	134254.0
36	SUPH	20.01	1030.8	1015.7	929.7	929.7	858.4	760.2	8677.9	1524.4	1837.7	1.0000	2542.3	36.6	102.80	1352.0	131054.9
37	SUPH	20.75	1035.0	1021.1	937.5	937.5	868.0	761.3	8667.0	1528.8	1838.4	1.0000	2540.7	38.1	104.47	1359.9	127766.8
38	SUPH	21.51	1040.8	1026.4	945.3	945.3	877.7	762.8	8656.0	1533.1	1841.2	1.0000	2539.2	39.7	106.15	1367.7	124387.0
39	SUPH	22.30	1045.8	1032.4	956.8	956.8	887.7	735.1	8645.1	1539.0	1680.9	1.0000	2537.5	41.3	107.83	1375.5	116234.0
40	SUPH	23.14	1050.8	1037.8	965.1	965.1	897.8	733.6	8634.2	1543.5	1668.1	1.0000	2535.7	43.1	109.52	1383.4	112253.6
41	SUPH	24.01	1055.8	1043.3	973.4	973.4	908.0	732.2	8623.3	1548.1	1656.2	1.0000	2533.8	45.0	111.21	1391.2	108189.1
42	SUPH	24.91	1060.8	1048.7	981.7	981.7	918.5	731.0	8612.5	1552.7	1645.1	1.0000	2531.8	47.0	112.91	1399.0	104043.4
43	SUPH	25.85	1065.8	1054.2	990.1	990.1	929.0	729.9	8601.6	1557.3	1634.8	1.0000	2529.7	49.0	114.62	1406.9	99818.9
44	SUPH	26.83	1070.8	1059.7	998.5	998.5	939.8	728.9	8590.9	1562.0	1625.3	1.0000	2527.4	51.3	116.34	1414.7	95518.8
45	SUPH	27.86	1075.8	1065.2	1007.0	1007.0	950.6	728.1	8580.1	1566.6	1616.5	1.0000	2525.1	53.6	118.06	1422.5	91146.2
46	SUPH	28.94	1080.8	1070.7	1015.5	1015.5	961.6	727.3	8569.4	1571.3	1608.3	1.0000	2522.5	56.1	119.79	1430.3	86703.8
47	SUPH	30.08	1085.8	1076.2	1024.0	1024.0	972.7	726.7	8558.7	1576.0	1600.8	1.0000	2519.8	58.8	121.54	1438.2	82194.4
48	SUPH	31.28	1090.8	1081.7	1032.6	1032.6	983.9	726.2	8548.1	1580.6	1593.9	1.0000	2516.9	61.7	123.29	1446.0	77621.3
49	SUPH	32.55	1095.8	1087.3	1041.2	1041.2	995.2	725.8	8537.5	1585.4	1587.5	1.0000	2513.8	64.8	125.03	1453.8	72987.8
50	SUPH	33.68	1100.0	1091.9	1048.5	1048.5	1004.8	725.5	8528.6	1589.3	1582.6	1.0000	2511.0	67.6	126.35	1460.4	69054.1

DIV CHECK AT LOCATION 076216

Table P-2 (Cont'd)

```
   ** SOLAR STEAM GENERATOR SIZING **
 CASE 2 ** SUPERHEATER

OUTPUT DATA

 TUBE OD                          0.62500 INCHES
 TUBE WALL THICKNESS              0.114000 INCHES
 REQUIRED TUBE WALL               0.       INCHES
 TUBE ID                          0.39700 INCHES
 NUMBER OF TUBES                      572
 ACTIVE TUBE LENGTH                 33.68 FEET
 ACTIVE HT. TRANSFER AREA,ID      2002.46 FT**2
 STEAM FLOW RATE              0.7286E 06 LBM/HR
 STEAM MASS VELOCITY              411.724 LBM/SEC-FT**2
 FOULING FACTOR               0.10E 21BTU/FT**2-HR
 DNB QUALITY                      0.      FRACTION
 DNB MARGIN                       0.      PERCENT
 HYDAULIC DIAMETER,SODIUM      0.166744 FEET
 SODIUM INLET VELOCITY            5.36 FT/SEC
 SODIUM OUTLET VELOCITY           5.15 FT/SEC
 SODIUM FLOW RATE PER UNIT  0.3803E 07 LBM/HR
 SODIUM PRESSURE DROP             3.356 PSI
 NA PRES DROP IN SUPPORTS         2.898 PSI
 STEAM SIDE PRESSURE DROP       110.244 PSI
 INLET PRESSURE DROP              6.796 PSI
 SUBCOOLED PRESSURE DROP          0.    PSI
 NUCLEATE BOILING PRES DROP,      0.    PSI
 FILM BOILING PRESSURE DROP,      0.212 PSI
 SUPERHEAT PRESSURE DROP         60.573 PSI
 OUTLET PRESSURE DROP            42.663 PSI


 SODIUM SIDE DATA
 TUBE SUPPORT MINIMUM WEB THICKNESS        0.1000INCHES,
 DISTANCE BETWEEN SUPPORTS                 2.5000 FEET
 SODIUM PRESSURE DROP COEF PER SUPPORT      1.34873
 TUBE SUPPORT USE NA FLOW HOLES THAT ARE MIX OF BOTH TYPES
   WITH BROKEN EDGES
 DIAMETER OF EQUIVALENT HOLE IN SUPPORT       0.611 INCHES
 MAXIMUM SODIUM VELOCITY IN SUPPORTS        8.80834 FT/SEC

 TEMPERATURE,STEAM INLET          672.77 F
 TEMPERATURE,STEAM OUTLET        1002.69 F
 TEMPERATURE,SODIUM INLET        1100.00 F
 TEMPERATURE,SODIUM OUTLET        859.10 F
 ENTHALPY, STEAM INLET           1082.00 BTU/LBM
 ENTHALPY, STEAM OUTLET          1460.39 BTU/LBM
 ENTHALPY, SODIUM INLET           486.87 BTU/LBM
 ENTHALPY,SODIUM OUTLET           414.36 BTU/LBM


  SECTION AVERAGE PROPERTIES
SECTION     LOG MEAN TEMP       OVERALL U       TUBE SEC. LENGTH
              DEGREES F       BTU/FT**2-HR-F         FEET

  SUBC             0.              0.                0.
  NUCL             0.              0.                0.
  FILM           187.61          972.32              0.18
  SUPH           136.56         1006.70             33.50
```

Table P-3

REHEATER DESIGN CALCULATIONS -- COMPUTER PROGRAM "STMGEN" OUTPUT

```
CASE NO.  1            ** SOLAR STEAM GENERATOR SIZING **
                  CASE 2 ** REHEATER

          INPUT DATA


NAMELIST    DATAA
NPRINT=          1,
XLNGTH=   0.35450000E 02,     DXL    =   0.10000000E 00,     DOTUBE=   0.10500000E 01,     PITCHO=   0.20500000E 01,
TNAIN =   0.11000000E 04,     TNAOUT=   0.85910000E 03,     TSTMIN=   0.57250000E 03,     TSTMOT=   0.10003000E 04,
PSTMIN=   0.41700000E 03,     HFOUL =   0.10000000E 21,
MAT   =          3,   HXTYPE=          3,
MWUNIT=   0.40570000E 02,
NTUBES=        266,
ECARB =   0.52500000E 00,     CORR   =  0.19000000E-01,     XKIN   =  0.50000000E 00,     XKOUT  =  0.10000000E 01,
XLOUT =   0.12650000E 02,     XLMARG=   0.22700000E 01,     XLIN   =  0.58000000E 01,     SUBDOW=   0.10000000E 01,
WTSTMO=   0.59110000E 06,     WTNAO  =  0.19088000E 07,
NCASES=         15,
HSTMOT=   0.15238000E 04,     DRODSC=   0.            ,     DRODNB=   0.            ,     DRODFB=   0.            ,
DRODSH=   0.            ,     DRODIN=   0.            ,     DRODOT=   0.            ,
NBAF  =          2,
WBAF  =   0.83334000E-02,     BAFSPA=   0.25000000E 01,
NDOUB =          0,
PDNAO =   0.63000000E 01,     DPDNAO=   0.90000000E 02,     DITUBO=   0.95000000E 00,     HSTMII=   0.12896000E 04,
NDEMO =          0,
ROUGH1=   0.64000000E-04,     ROUGH2=   0.64000000E-04,
NBUND =          1,
XDPRAT=   0.            ,     PHE    =  0.            ,     PNA    =  0.            ,     DMID   =  0.            ,
GAPO  =   0.            ,     GROVE  =  0.            ,     PSTMOU=   0.            ,     DPSTMT=   0.            ,
RECIRC=   0.            ,     PDRUM  =  0.            ,     TFW    =  0.            ,     DOSHD  =  0.            ,
XLSHD =   0.            ,
MATSHD=          0,
XDNBOO=   0.            ,
$BEND
```

TNAIN	TNAOUT	TSTM(1)	TSTMOUT	TUBE L	PSTMIN	DP-STM	DP-NA	TUBE NO.	PITCH	STM-FLOW	NA-FLOW
1100.000	859.10000	571.919	1000.625	36.259	417.000	36.310	0.226	266	2.0500	0.5911E 06	0.1909E 07
1100.000	859.10000	571.941	1000.685	36.018	417.000	34.626	0.216	272	2.0500	0.5911E 06	0.1909E 07
1100.000	859.10000	571.986	1000.809	35.484	417.000	31.133	0.196	286	2.0500	0.5911E 06	0.1909E 07

Table P-3 (Cont'd)

CASE NO. 1 ** SOLAR STEAM GENERATOR SIZING **
CASE 2 ** REHEATER

INPUT DATA

REHEAT		
HEAT LOAD PER UNIT	40.5549	MWT
TUBE LENGTH ACTIVE	35.45	FEET
ALLOWABLE LENGTH VARIATION	0.100	FEET
TUBE OD	1.05000	INCHES
TUBE CENTER PITCH	2.05000	INCHES
TEMPERATURE, SODIUM INLET	1100.00	F
,SODIUM OUTLET	859.10	F
,STEAM INLET	572.44	F
,STEAM OUTLET	0.	F
ENTHALPY, STEAM OUTLET	1523.76	BTU/LBM
PRESSURE ,STEAM INLET	417.00	PSI
FOULING FACTOR	0.10E 21	BTU/HR-F-FT**2
DECARBONIZATION FACTOR E ON TUBE STRENGTH	0.52500	FACTION
TUBE CORROSION ALLOWANCE	0.01900	INCHES

Table P-3 (Cont'd)

** SOLAR STEAM GENERATOR SIZING **
CASE 2 ** REHEATER

OUTPUT DATA

J	SECT TYPE	ACTIVE LENGTH FT	T-NA F	T-OD WALL F	T-ID WALL F	T-WAL FOUL ID. F	T-STM F	U-OVER BTU/HR-FT**2-F	H-NA	H-WAL	H-STM	QUAL	P-STM PSI	DP-STM PSI	VELO FT/SEC	H-STEAM BTU/LBM	HEAT FLUX BTU/HR-FT**2
1	SUPH	0.	859.1	832.8	801.5	801.5	572.0	292.9	3194.3	2690.7	366.5	1.0000	414.0	3.0	160.17	1289.6	84108.8
2	SUPH	0.49	864.1	838.0	807.1	807.1	580.1	293.2	3189.7	2695.1	366.7	1.0000	413.8	3.1	161.95	1294.5	83271.2
3	SUPH	0.98	869.1	843.2	812.8	812.8	588.2	293.4	3185.1	2705.9	367.0	1.0000	413.7	3.3	163.72	1299.4	82414.9
4	SUPH	1.47	874.1	848.5	818.4	818.4	596.5	293.7	3180.5	2712.8	367.4	1.0000	413.5	3.5	165.50	1304.3	81540.4
5	SUPH	1.97	879.1	853.7	824.1	824.1	604.8	294.0	3175.9	2719.6	367.8	1.0000	413.3	3.7	167.29	1309.1	80647.9
6	SUPH	2.48	884.1	859.0	829.7	829.7	613.2	294.3	3171.3	2726.5	368.2	1.0000	413.1	3.8	169.08	1314.0	79738.7
7	SUPH	2.99	889.1	864.2	835.4	835.4	621.6	294.6	3166.8	2733.4	368.7	1.0000	412.9	4.0	170.87	1318.9	78812.9
8	SUPH	3.51	894.1	869.5	841.1	841.1	630.1	295.0	3162.2	2740.3	369.2	1.0000	412.7	4.2	172.66	1323.8	77871.1
9	SUPH	4.03	899.1	874.7	846.7	846.7	638.7	295.4	3157.7	2747.2	369.7	1.0000	412.5	4.4	174.46	1328.7	76914.3
10	SUPH	4.56	904.1	880.0	852.4	852.4	647.3	295.7	3153.1	2754.2	370.2	1.0000	412.3	4.6	176.26	1333.5	75942.9
11	SUPH	5.10	909.1	885.3	858.1	858.1	656.0	296.1	3148.6	2761.1	370.8	1.0000	412.1	4.8	178.07	1338.4	74957.5
12	SUPH	5.64	914.1	890.6	863.9	863.9	664.7	296.6	3144.1	2768.0	371.4	1.0000	411.9	5.0	179.88	1343.3	73959.1
13	SUPH	6.20	919.1	895.9	869.6	869.6	673.5	297.0	3139.6	2775.0	372.0	1.0000	411.7	5.2	181.69	1348.2	72947.7
14	SUPH	6.76	924.1	901.2	875.3	875.3	682.3	297.4	3135.1	2781.9	372.6	1.0000	411.5	5.5	183.50	1353.0	71924.4
15	SUPH	7.32	929.1	906.5	881.0	881.0	691.1	297.9	3130.7	2788.9	373.3	1.0000	411.2	5.7	185.32	1357.9	70889.1
16	SUPH	7.90	934.1	911.8	886.8	886.8	700.0	298.4	3126.2	2795.9	373.9	1.0000	411.0	5.9	187.15	1362.8	69843.1
17	SUPH	8.48	939.1	917.1	892.5	892.5	708.9	298.8	3121.8	2802.8	374.6	1.0000	410.8	6.2	188.97	1367.6	68786.9
18	SUPH	9.07	944.1	922.4	898.3	898.3	717.9	299.3	3117.3	2809.8	375.3	1.0000	410.5	6.4	190.80	1372.5	67720.0
19	SUPH	9.68	949.1	927.7	904.0	904.0	726.8	299.8	3112.9	2816.8	376.1	1.0000	410.3	6.6	192.63	1377.4	66644.1
20	SUPH	10.29	954.1	933.0	909.8	909.8	735.8	300.3	3108.5	2823.8	376.8	1.0000	410.0	6.9	194.47	1382.2	65559.1
21	SUPH	10.91	959.1	938.3	915.6	915.6	744.8	300.8	3104.1	2830.8	377.6	1.0000	409.8	7.2	196.31	1387.1	64465.4
22	SUPH	11.54	964.1	943.7	921.3	921.3	753.8	301.4	3099.7	2837.8	378.3	1.0000	409.5	7.4	198.15	1392.0	63363.6
23	SUPH	12.19	969.1	949.0	927.1	927.1	762.9	301.9	3095.3	2844.8	379.1	1.0000	409.2	7.7	200.00	1396.8	62254.2
24	SUPH	12.84	974.1	954.3	932.9	932.9	771.9	302.4	3090.9	2851.8	379.9	1.0000	408.9	8.0	201.85	1401.7	61137.6
25	SUPH	13.51	979.1	959.7	938.7	938.7	781.0	303.0	3086.5	2858.8	380.7	1.0000	408.6	8.3	203.71	1406.5	60013.5
26	SUPH	14.19	984.1	965.0	944.4	944.4	790.1	303.5	3082.2	2865.9	381.5	1.0000	408.3	8.6	205.57	1411.4	58883.6
27	SUPH	14.88	989.1	970.3	950.2	950.2	799.2	304.1	3077.8	2872.9	382.3	1.0000	408.0	8.9	207.44	1416.2	57746.8
28	SUPH	15.59	994.1	975.7	956.0	956.0	808.3	304.6	3073.5	2879.9	383.1	1.0000	407.7	9.2	209.31	1421.1	56604.3
29	SUPH	16.31	999.1	981.0	961.8	961.8	817.4	305.2	3069.2	2887.0	383.9	1.0000	407.3	9.6	211.19	1426.0	55455.9
30	SUPH	17.04	1004.1	986.4	967.6	967.6	826.5	305.7	3064.8	2894.0	384.8	1.0000	407.0	9.9	213.07	1430.8	54302.5
31	SUPH	17.80	1009.1	991.7	973.4	973.4	835.6	306.3	3060.5	2901.0	385.6	1.0000	406.6	10.3	214.96	1435.7	53143.6
32	SUPH	18.56	1014.1	997.1	979.2	979.2	844.7	306.9	3056.2	2908.1	386.5	1.0000	406.3	10.6	216.86	1440.5	51980.1
33	SUPH	19.35	1019.1	1002.5	985.0	985.0	853.8	307.4	3052.0	2915.1	387.3	1.0000	405.9	11.0	218.76	1445.4	50811.9
34	SUPH	20.15	1024.1	1007.8	990.8	990.8	862.9	308.0	3047.7	2922.2	388.2	1.0000	405.5	11.4	220.68	1450.2	49639.1
35	SUPH	20.97	1029.1	1013.2	996.6	996.6	872.1	308.6	3043.4	2929.2	389.0	1.0000	405.1	11.8	222.60	1455.1	48462.4
36	SUPH	21.82	1034.1	1018.5	1002.4	1002.4	881.2	309.2	3039.2	2936.3	389.9	1.0000	404.6	12.2	224.52	1459.9	47281.6
37	SUPH	22.68	1039.1	1023.9	1008.2	1008.2	890.3	309.7	3034.9	2943.3	390.7	1.0000	404.2	12.7	226.46	1464.8	46097.0
38	SUPH	23.57	1044.1	1029.3	1014.1	1014.1	899.4	310.3	3030.7	2950.4	391.6	1.0000	403.8	13.1	228.41	1469.6	44909.1
39	SUPH	24.48	1049.1	1034.7	1019.9	1019.9	908.5	310.9	3026.5	2957.4	392.5	1.0000	403.3	13.6	230.37	1474.5	43717.4
40	SUPH	25.41	1054.1	1040.0	1025.7	1025.7	917.6	311.5	3022.3	2964.5	393.4	1.0000	402.8	14.1	232.35	1479.3	42522.3
41	SUPH	26.37	1059.1	1045.4	1031.5	1031.5	926.7	312.1	3018.1	2971.6	394.2	1.0000	402.3	14.6	234.33	1484.1	41324.3
42	SUPH	27.36	1064.1	1050.8	1037.3	1037.3	935.8	312.7	3013.9	2978.6	395.1	1.0000	401.8	15.1	236.33	1489.0	40123.4
43	SUPH	28.38	1069.1	1056.2	1043.1	1043.1	944.8	313.2	3009.7	2985.7	396.0	1.0000	401.2	15.6	238.35	1493.8	38919.6
44	SUPH	29.43	1074.1	1061.6	1049.0	1049.0	953.9	313.8	3005.5	2992.8	396.9	1.0000	400.7	16.2	240.38	1498.7	37713.1
45	SUPH	30.52	1079.1	1066.9	1054.8	1054.8	963.0	314.4	3001.4	2999.8	397.7	1.0000	400.1	16.8	242.43	1503.5	36504.0
46	SUPH	31.64	1084.1	1072.3	1060.6	1060.6	972.1	315.0	2997.2	3006.9	398.6	1.0000	399.5	17.4	244.50	1508.4	35292.5
47	SUPH	32.80	1089.1	1077.7	1066.4	1066.4	981.1	315.6	2993.1	3014.0	399.5	1.0000	398.8	18.0	246.59	1513.2	34078.7
48	SUPH	34.01	1094.1	1083.1	1072.2	1072.2	990.1	316.1	2989.0	3021.0	400.4	1.0000	398.1	18.7	248.70	1518.1	32862.6
49	SUPH	35.25	1099.1	1088.5	1078.0	1078.0	999.2	316.7	2984.8	3028.1	401.3	1.0000	397.4	19.4	250.45	1522.9	31644.4
50	SUPH	35.48	1100.0	1089.5	1079.1	1079.1	1000.8	316.8	2984.1	3028.1	401.4	1.0000	397.3	19.5	250.75	1523.8	31423.6

DIV CHECK AT LOCATION 076216

Table P-3 (Cont'd)

** SOLAR STEAM GENERATOR SIZING **
CASE 2 ** REHEATER

OUTPUT DATA

TUBE OD	1.05000	INCHES
TUBE WALL THICKNESS	0.050000	INCHES
REQUIRED TUBE WALL	0.	INCHES
TUBE ID	0.95000	INCHES
NUMBER OF TUBES	286	
ACTIVE TUBE LENGTH	35.48	FEET
ACTIVE HT. TRANSFER AREA,ID	2524.03	FT**2
STEAM FLOW RATE	0.5911E 06	LBM/HR
STEAM MASS VELOCITY	116.633	LBM/SEC-FT**2
FOULING FACTOR	0.10E 21	BTU/FT**2-HR
DNB QUALITY	0.	FRACTION
DNB MARGIN	0.	PERCENT
HYDAULIC DIAMETER,SODIUM	0.280274	FEET
SODIUM INLET VELOCITY	1.90	FT/SEC
SODIUM OUTLET VELOCITY	1.83	FT/SEC
SODIUM FLOW RATE PER UNIT	0.1909E 07	LBM/HR
SODIUM PRESSURE DROP	0.196	PSI
NA PRES DROP IN SUPPORTS	0.156	PSI
STEAM SIDE PRESSURE DROP	31.133	PSI
INLET PRESSURE DROP	2.978	PSI
SUBCOOLED PRESSURE DROP ,	0.	PSI
NUCLEATE BOILING PRES DROP,	0.	PSI
FILM BOILING PRESSURE DROP,	0.	PSI
SUPERHEAT PRESSURE DROP	16.538	PSI
OUTLET PRESSURE DROP	11.616	PSI

SODIUM SIDE DATA

TUBE SUPPORT MINIMUM WEB THICKNESS	0.1000	INCHES,
DISTANCE BETWEEN SUPPORTS	2.5000	FEET
SODIUM PRESSURE DROP COEF PER SUPPORT	0.53659	

TUBE SUPPORT USE NA FLOW HOLES THAT ARE MIX OF BOTH TYPES
WITH BROKEN EDGES

DIAMETER OF EQUIVALENT HOLE IN SUPPORT	1.131	INCHES
MAXIMUM SODIUM VELOCITY IN SUPPORTS	2.57844	FT/SEC

TEMPERATURE,STEAM INLET	572.44	F
TEMPERATURE,STEAM OUTLET	1000.17	F
TEMPERATURE,SODIUM INLET	1100.00	F
TEMPERATURE,SODIUM OUTLET	859.10	F
ENTHALPY, STEAM INLET	1289.60	BTU/LBM
ENTHALPY, STEAM OUTLET	1523.76	BTU/LBM
ENTHALPY, SODIUM INLET	486.87	BTU/LBM
ENTHALPY,SODIUM OUTLET	414.36	BTU/LBM

SECTION AVERAGE PROPERTIES

SECTION	LOG MEAN TEMP DEGREES F	OVERALL U BTU/FT**2-HR-F	TUBE SEC. LENGTH FEET
SUBC	0.	0.	0.
NUCL	0.	0.	0.
FILM	0.	0.	0.
SUPH	176.81	310.15	35.48

Appendix Q

CRITIQUE OF CYLINDRICAL STORAGE TANKS

It has been suggested that a cylindrical tank design might be more cost effective than the spherical concept. The proposed cylindrical concept would have very low cover gas pressure (inches of water) to allow a thin top, with sides designed for the pressure of the liquid head, and a thin bottom which would take advantage of backfill to support the pressure loading. Several questions must be answered to determine whether this concept is feasible:

- How can low cover gas pressure be maintained during all operating modes?
- Is a low net positive suction head (NPSH) pump available for the tower loop?
- Can a cylindrical vessel of this type be designed to meet the ASME code?
- Does the cylindrical concept meet the advanced central receiver specifications?
- Is the cylindrical vessel actually more cost effective?

LOW COVER GAS PRESSURE

Consider the change in cover gas pressure as the hot tanks are emptied of liquid and the cold tanks are simultaneously filled. The initial pressure may be selected at a low value, e.g., 15 psia. If the gas is confined (i.e., none is extracted or added), the pressure when this process is complete is given by the ideal gas relation

$$P_H = P_C \left(\frac{V_C}{V_H}\right)\left(\frac{T_H}{T_C}\right) = 15 \text{ psia } \left(\frac{356{,}500}{385{,}300}\right)\left(\frac{1100+460}{610+460}\right) = 20.2 \text{ psia}$$

To prevent this pressure rise, gas must be extracted during the process and added during the reverse process. If the extracted gas is simply vented and imported gas used for makeup, the plant would consume about 43,000 standard cubic feet of gas per day. Argon costs about \$0.04/standard cubic foot in bulk quantities, so this represents an expenditure of \$1720/day or about \$19 million over the life of the plant. This is obviously too expensive. An alternative approach is to compress the vented gas and store it until it can be reintroduced on the reverse cycle. To store it at 500 psia would require a tank about 13 feet in diameter with walls about 1.3 inches thick. The electric energy required for compression would be about 0.4 $MW_e h$/day, which translates into a 1.1 $MW_t h$/day equivalent thermal loss from the system. In addition about 0.3 $MW_t h$/day are lost in cooling the gas before compression and heating it before injecting it for makeup. Thus, the total thermal loss is about 1.4 $MW_t h$ or 0.2% of the 750 $MW_t h$ put through storage on the design point day. This is a small penalty, and the cost of the compressor and gas storage tank would also be small; therefore, this appears to be a feasible solution to the gas control problem.

LOW NPSH PUMP

The Clinch River Breeder Reactor pump design can be made to fit this application by increasing its speed from 1116 rpm to 1760 rpm and cutting back the impellor diameter. At this speed the NPSH required is about 3 psig (suction specific speed = 10,000), which is consistent with a low pressure tank concept. It is not necessary to use an advanced screw-type, two-stage impellor to achieve this low NPSH.

ASME CODES

This is a difficult area since the codes can be interpreted in various ways to cover a multitude of possible concepts, and the effect on cost is not always clearly discernible. Section VIII of the ASME code does not describe rules for designing a cylindrical tank such as we are considering here. To qualify under Section VIII, a detailed stress analysis would most likely be required to demonstrate that the tank had at least a safety factor of 4. If liquid metal equipment experience to date may be taken as a guide, it seems likely that this analysis would cost enough to negate the potential savings in material costs.

The American Petroleum Institute has a design procedure (API 620) for oil storage tanks of this type, but it is unlikely that a utility would ever purchase a tank for 30 year service at 1100 F which bore only the API code stamp.

ASME Section III Class 3 (ND-3900) adapts the API 620 rules to the design of radioactive waste storage vessels and adds the requirement of nuclear quality control and assurance. Although ND-3900 is limited to operating temperatures below 200 F, the opinion of one code committee member is that higher temperature vessels could qualify if the allowable stresses from Section VIII were used in the ND3900 equations. Additional analysis would be required to account for thermal expansion effects, especially in the tank bottom. It is our opinion that a tank bearing the ASME Section III stamp would probably be acceptable to utilities.

ADVANCED CENTRAL RECEIVER

Section 3.1.2 of the Advanced Central Receiver Program Requirements (Rev. B, 3-16-78) states: "The energy storage subsystem shall be designed to provide safe and reasonable access for proper inspection, maintenance, and repair of the structure. . ."

The bottom of the cylindrical tank would rest on a layer of block type insulation* which rests in turn on sand backfill or a concrete pad. Thus the bottom could only be inspected from inside the tank. To accomplish this, the tank must be drained and cooled so that inspectors can enter; this requires a lengthy plant shutdown. Workers would have to wear protective suits due to sodium residues and would require an air supply since the tank must be kept filled with argon. It is our opinion that this is not a safe operating practice, and that it is inconsistent with a timely inspection and maintenance program as called for in the Advanced Central Receiver Program specifications.

---

*Example: Kaowool insulation block, 5 percent compression at 3500 psi.

COST EFFECTIVENESS

An example of the cylindrical tank design calculated using ASME Section III rules is provided at the end of this appendix.

If all of the hot fluid were contained in one cylindrical tank, this tank would be 79.12 feet high and 79.12 feet in diameter. The conical top and flat bottom would both be 0.198 inch thick, which is the minimum allowed by the code. The vertical sides would taper from 0.260 inch thick at the top to 1.259 inches at the bottom. The weight of stainless steel in this tank, excluding top and bottom retaining rings, would be about 622,000 pounds. By comparison, a spherical tank designed to ASME Section VIII rules would weigh about 496,000 pounds if its walls were continuously tapered from 0.260 inch thick at the top to 0.835 inch at the bottom. Thus it appears that the cylindrical tank concept does not offer a cost advantage over the spherical concept.

CONCLUSIONS

The cylindrical tank concept does not appear to offer any cost advantage and it introduces maintenance problems and a slightly more complex gas control system. We conclude that spherical tanks designed to ASME Section VIII rules are superior for this application.

CYLINDRICAL TANK (HOT)

$V = 3 \times \frac{4\pi}{3}\left(\frac{62.8}{2}\right)^3 = 389{,}044\ ft^3$

$D = H = \sqrt[3]{\frac{4V}{\pi}} = 79.12\ ft$

$R = 39.56\ ft$

$A_T = \pi R^2 = 4916\ ft^2$

$\rho_s = 500\ lb/ft^3$ (stainless Steel)

$T = 1100F \quad S_{ts} = 12{,}400\ psi \quad E = .85$

$C = .010"$ Corrosion allowance

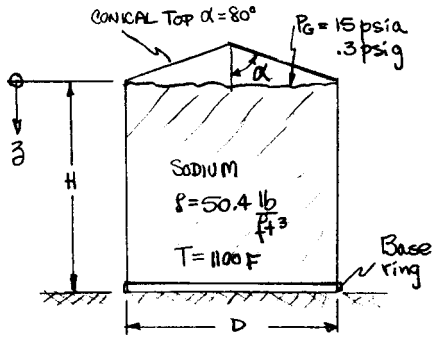

ASME SECTION III, ND-3900 DESIGN

1st Iteration

Weights – use minimum allowable thicknesses

TOP $W_T = \frac{\pi R^2}{\sin\alpha} t_{min} \rho_s = \frac{\pi (39.56)^2}{\sin 80°} \times \frac{3}{16}" \times \frac{1}{12} \times 500 = 39{,}000\ lb$

SIDES $W_S = \pi D H\, t_{min} \rho_s = \pi (79.12)^2 \times \frac{1}{4}" \times \frac{1}{12} \times 500 = 205{,}000\ lb$

Unit Forces

TOP $T_1 = \frac{39.56}{2\cos 80°}\left(.3 \times 144 - \frac{39{,}000}{4916}\right)\times\frac{1}{12} = 9.49\,(43.20 - 7.93)$

$= 334.68\ lb/in$ (tension, at top joint)

$T_2 = \frac{.3 \times (39.56/12)}{\cos 80°} = 5.70\ lb/in$ (tension, at top joint)

SIDES $T_1 = \frac{39.56}{2\times 12}\left(.3\times 144 + 0^* - \frac{39{,}000 + 205{,}000(z/79.12)}{4916}\right)$

$= 1.65\,(43.20 + 0^* - 7.93 - z)$

$= 58.20 - .869\,z = \begin{cases} 58.20\ lb/in & z=0 \\ -10.54\ lb/in & z=79.12' \end{cases}$ tension / compression

$T_2 = (50.4\,z + .3\times 144)\frac{39.56}{12} = 13.10 + 166.2\,z$

$= \begin{cases} 13.10\ lb/in & z=0 \\ 13162\ lb/in & z=79.12 \end{cases}$ tension / tension

* weight of liquid = A_T × liquid head pressure

CYLINDRICAL TANK - CONT'D

Required Thickness - both T_1 & T_2 are positive almost everywhere

$$\therefore \quad t = \frac{T_{MAX}}{S_{ts} \cdot E} + c \quad \text{at each section}$$

TOP

$$t = \frac{334.68 \text{ lb/in}}{12{,}400 \text{ lb/in}^2 \times .85} + .010 = .032 + .010$$

The minimum allowable thickness* is 3/16" without corrosion adder ∴ the thickness of the top is

$$t = .188 + .010 = .198"$$

SIDES Near the top of the tank T_1 dominates, beyond $\bar{z}$, T_2 dominates

$$T_1 = T_2 \quad \text{at } \bar{z}$$

$$58.2 - .869\,\bar{z} = 13.10 + 166.2\,\bar{z}$$

$$\bar{z} = .27 \text{ ft}$$

		t (in.)	t^*_{MIN} (in.)
$z = 0$	$\frac{58.20}{12{,}400 \times .85} + .010$	$= .006 + .010 = .016$	.260
$z = .27$	$\frac{57.96}{12{,}400 \times .85} + .010$	$= .005 + .010 = .015$	.260
$z = 15.78$	$\frac{2635}{12{,}400 \times .85} + .010$	$= .250 + .010 = .260$	.260
$z = 79.12$	$\frac{13162}{12{,}400 \times .85} + .010$	$= 1.249 + .010 = 1.259$	—

BOTTOM $t = .188 + .010 = .198"$ min. allowable assume stress supported by base structure under tank

* see paragraph ND 3932.4

CYLINDRICAL TANK - CONT'D

2nd Iteration

Weights

TOP $W_T = \frac{\pi(39.56)^2}{\sin 80^\circ} \frac{.198"}{12} \times 500 = 41\,187$ lb

SIDES $W_S = \pi(79.12) \times \frac{500}{12}\left(.260 \times 15.78 + \frac{.260+1.259}{2} \times (79.12 - 15.78)\right)$

$= 540{,}723$ lb

Unit Forces

TOP $T_1 = \frac{39.56}{12 \times 2\cos 80^\circ}\left(.3 \times 144 - \frac{41187}{4916}\right) = 330.5$ lb/in

$T_2 = 5.70$ lb/in

SIDES $T_1 = \frac{39.56}{2 \times 12}\left(.3 \times 144 + 0 - \frac{41187 + 540{,}723(3/79.12)}{4916}\right)$

$= 57.40 - 2.292\,3 = \begin{cases} 57.40 & 3 = 0 \\ -123.90 & 3 = 79.12 \end{cases}$

$T_2 = 13.10 + 166.2\,3 = \begin{cases} 13.1 \\ 13162 \end{cases}$

Required Thickness

TOP $t = .198"$ base on min. allowable t, hoop stress

SIDES

	t (inches)	Based on
$3 = 0$	.260	min. allowable
$3 = 15.78$	.260	hoop stress
$3 = 79.12$	1.259	" " $\frac{123.9}{13162} < 5\%$ ND 3922.2 (6)

Bottom $t = .198"$ $W_B = \pi(39.56)^2 \times \frac{.198}{12} \times 500 = 40{,}562$ lb

TOTAL WEIGHT OF STEEL = $W_T + W_S + W_B$ = **622,472 lb**
USED IN TANK WALLS

SPHERICAL TANK (HOT)

$V = 389{,}044\ ft^3$

$R = \sqrt[3]{\frac{3V}{4\pi}} = 45.27\ ft$

$T = 1100F \quad S_{ts} = 12{,}400\ psi$ (316 SS)

$E = .85$

$C = .010"$ corrosion

$\rho_s = 500\ lb/ft^3$

$P_G = .3\ psig$

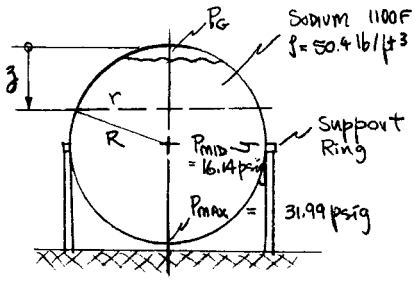

ASME SECTION VIII, UG-27 DESIGN

Opinion of committee member is that section VIII permits design with graded thickness of wall. A conservative approach is to use

$$t = \frac{P(z)\,R}{2SE - .2P_{MAX}} + C \qquad \text{but } t-c \geq .25" \text{ in the spirit of section III class 3}$$

where $P(z)$ varies with elevation but R is the sphere diameter not the cross section diameter.

$$P(z) = P_G + \rho z \qquad P_{MAX} = P_G + 2\rho R \qquad P_{MID} = P_G + \rho R$$

$$t(z) = \left[\frac{P_G R}{2SE - .2P_{MAX}} + c\right] + \left[\frac{\rho R}{2SE - .2P_{MAX}}\right] z \qquad = \alpha + \beta z \geq .260"$$

$$W_T = \int_0^{2R} \rho_s\, t(z)\, 2\pi r(z)\, \frac{dp}{dz}\, dz \quad = \text{weight of metal in tank walls}$$

$$r(z) = \sqrt{R^2 - (R-z)^2}$$

$$\frac{R}{r} = \frac{dp}{dz}$$

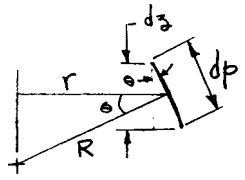

$$W_T = 2\pi R \rho_s \int_0^{2R} t(z)\, dz$$

$$t(z) = \left[\frac{.3 \frac{lb}{in^2} \times 45.27 ft \times 12 \frac{in}{ft}}{2 \times 12{,}400 \frac{lb}{in^2} \times .85 - .2 \times 31.99 \frac{lb}{in^2}} + .010 \, in \right]$$

$$+ \left[\frac{50.4 \frac{lb}{ft^3} \times 45.27 ft \frac{ft^2}{144 in^2}}{2 \times 12{,}400 \times .85 - .2 \times 31.99} \right] z \, ft \times 12 \frac{in}{ft}$$

$$= .018'' + 9.022E\text{-}3 \; z(ft)$$

$$.260 = .018 + 9.022E\text{-}3 \; \bar{z} \quad \rightarrow \quad \bar{z} = 26.82 \, ft$$

$$t(z) = \begin{cases} .260'' & 0 \le z \le 26.82 \, ft \quad \text{based on min. allowed thickness} \\ .018 + 9.022E\text{-}3 \; z & 26.82 < z < 2R \quad \text{based on stress.} \end{cases}$$

$$W_T = 2\pi (45.27 ft) \, 500 \frac{lb}{ft^3} \left\{ \int_0^{26.82 ft} \left(\frac{.260}{12}\right) ft \, dz + \int_{26.82}^{90.54 ft} \frac{.018 + 9.022E\text{-}3 \, z}{12} \, dz \right\}$$

$$= 1.422E5 \frac{lb}{ft^2} \left\{ \frac{.260 \times 26.82}{12} + \frac{(90.54 - 26.82) \times .018}{12} \right.$$

$$\left. + \frac{9.022E\text{-}3}{12 \times 2} \left(90.54^2 - 26.82^2 \right) \right\}$$

$W_T = \boxed{496{,}042 \, lb}$ Weight of metal in tank walls.

Two Stage Tank

Top half $t_T = t(R) = .426''$
Bottom half $t_B = t(2R) = .835''$

$W_T = 2\pi R^2 (t_T + t_B) = 676{,}557 \, lb.$

Appendix R

SODIUM COMPONENT DESIGN SUPPLEMENTAL CALCULATIONS

R-1 Storage Tank Size Calculations - Pilot Plant

Based on one hour of full power operation of the steam generators from thermal storage, the sodium volumes required in hot and cold storage were V_{TH} = 13941 ft^3 and V_{TC} = 12919 ft^3 respectively (See Section 7.2.2.3). The corresponding tank diameter (assuming the use of spherical storage tanks) can be calculated from:

$$d = \sqrt[3]{\frac{6V_T}{\pi}}$$

For the hot tank (1100°F sodium):

$$d_H = \sqrt[3]{\frac{6 \times 13941}{\pi}} = 29.86 \text{ ft.}$$

For the cold tank (612°F sodium):

$$d_C = \sqrt[3]{\frac{6 \times 12919}{\pi}} = 29.11 \text{ ft.}$$

Since the tanks will be fabricated in the ambient condition (~82°F), both tanks will contract to:

$$d_H = 29.86\ (1\text{-}10.8 \times 10^{-6}(1100\text{-}82))$$

$$d_H = 29.53 \text{ ft. (hot tank)}$$

$$d_C = 29.11\ (1\text{-}10.8 \times 10^{-6}(612\text{-}86))$$

$$d_C = 28.92 \text{ ft. (cold tank)}$$

These diameters will be the shop fabricated sizes.

The hot and cold tanks are joined by a pressure equalization line into the two cover gas spaces. Whatever mass of sodium is removed from one tank must be compensated for by an equal mass addition to the other tank. The analytical model used for the analysis is shown in Figures R-1 and R-2.

The mass of gas is assumed trapped in the tops of the tanks and moves from one tank to the other as the sodium is displaced ΔV_C in cold tank and ΔV_H in hot tank. It is further assumed that the gas in the tanks is always in thermal equilibrium with the sodium in the tank (T_C and T_H respectively for the cold and

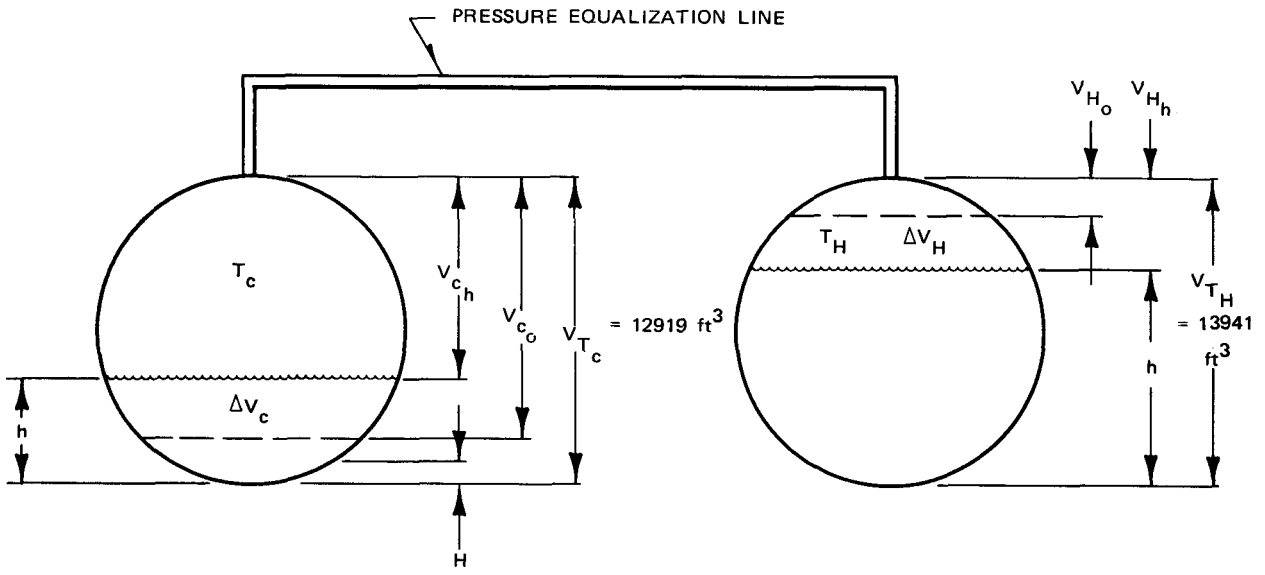

COLD STORAGE TANK

Figure R-1.

HOT STORAGE TANK

Figure R-2.

Analytical Model Used in Establishing Storage Tank Pressures

hot tanks). Since the mass of gas is held constant,

$$V_{c_h}\rho_c + V_{H_h}\rho_H = W_T = \text{CONST.} \tag{1}$$

But from the gas law:

$$\rho_c = P_c/RT_c \text{ and } \rho_H = P_H/RT_H \tag{2}$$

Introducing (2) into (1) and noting that $P_c = P_H = P_g$ as a result of the pressure equalization line:

$$P_g = RW_T/(V_{c_h}/T_c + V_{H_h}/T_H) \tag{3}$$

The initial conditions in the tanks are cold tank empty (V_{CO}) and hot tank full (V_{HO}) from which the initial gas pressure can be derived using eq. (3)

$$P_{g_o} = RW_T/(V_{CO}/T_C + V_{HO}/T_H \tag{4}$$

As sodium is displaced from one tank over to the other, mass is conserved:

$$\Delta V_c\rho_{N_c} = \Delta V_H\rho_{N_H} \tag{5}$$

From figure R-1 note that $V_{c_h} = V_{c_o} - \Delta V_c$ and $V_{H_h} = V_{H_o} + \Delta V_H$ from which equation (3) becomes:

$$P_g = RW_T/[(V_{CO} - \Delta V_C)/T_C + (V_{HO} + \Delta V_H)/T_H] \tag{6}$$

$$P_g = (RW_TT_C/V_{CO})/[(1 + (\frac{V_{HO}}{V_{CO}})\frac{T_C}{T_H}) + \frac{\Delta V_C}{V_{CO}}(\frac{\Delta V_H}{\Delta V_C}\frac{T_C}{T_H} - 1)] \tag{7}$$

Substituting (4) and (5) into (7)

$$P_g = \frac{P_{g_o}(1 + \frac{V_{HO}}{V_{CO}}\frac{T_C}{T_H})}{(1 + \frac{V_{HO}}{V_{CO}}\frac{T_C}{T_H}) + \frac{\Delta V_C}{V_{CO}}(\frac{P_{NC}}{P_{NH}} - 1)} \tag{8}$$

But $\Delta V_c = V_{co} - V_{ch}$ (See Figure R-1). Thus:

$$P_g/P_{g_o} = 1/[1 + (1 - \frac{V_{ch}}{V_{co}})(\frac{\rho_{NC}}{\rho_{NH}}\frac{T_C}{T_H} - 1)/(1 + \frac{V_{HO}}{V_{CO}}\frac{T_C}{T_H})] \tag{9}$$

Assuming both tanks operate between 5% and 95% full, and referring to Figures R-1 and R-2:

$$V_{CO} = 12919 \times .95 = 12273 \tag{10}$$

$$V_{HO} = 13941 \times .05 = 697.05 \tag{11}$$

$$\frac{V_{HO}}{V_{CO}} = 0.05680 \tag{12}$$

$$\frac{T_C}{T_H} = \frac{612 + 460}{1100 + 460} = .68846 \tag{13}$$

$$\frac{\rho_{NC}}{\rho_{NH}} = \frac{54.6}{50.6} = 1.07905 \tag{14}$$

Substituting (10) through (14) into (9) gives

$$P_g/P_{g_o} = 1/[\ 75256 + 2.01615 \times 10^{-5}\ V_{ch}] \tag{15}$$

The volume V_{ch} corresponding to tank depth "h" is given by:

$$V_{ch} = V_{TC} - \frac{\pi}{3} h^2(3r_c - h) \tag{16}$$

Equations (15) and (16) can be used to determine the gas pressure in the tanks at any tank depth "h" in the cold tank.

The pressure on the tank wall at any elevation "H" (See Figure R-1) is obtained from:

$$P_H = P_g + (h - H)\ \rho_{NC}/144 \tag{17}$$

The volume in the hot tank can be calculated from noting the conservation of sodium mass between tanks:

$$V_{CN}\rho_{NC} + V_{HN}\rho_{NH} = V_{TC}\rho_{NC} \tag{18}$$

The total tank volumes in each case are:

$$V_{TC} = V_{CN} + V_{ch} \text{ and } V_{TH} = V_{HN} + V_{Hh} \tag{19}$$

From (18) and (19)

$$V_{ch} = V_{TH} \frac{\rho NH}{\rho NC} - V_{Hh} \frac{\rho NH}{\rho NC} \quad (20)$$

Substituting (20) into (15)

$$Pg/Pgo = 1/(1.01304 - 1.86845 \times 10^{-5} V_{Hh}) \quad (21)$$

Equation 21 permits an evaluation of the gas pressures for the hot tank, whereas, equation 15 only applies to the cold tank.

R-2 PUMP PERFORMANCE EVALUATIONS

The pump head was calculated in psi and the pump flow rate in lbs/hr. Respective conversions to pump head in ft. of sodium and flow rate in GPM can be obtained from:

$$H = 144\ \Delta P/\rho \tag{22}$$

$$GPM = 0.12468\ W/\rho \tag{23}$$

The pump mechanical power required can be calculated as follows:

$$MW_p = 3.02058 \times 10^{-9}\ (GPM)(H)(\rho) \tag{24}$$

The electrical power expenditure is:

$$MW_e = MW_p/ \tag{25}$$

and $\eta = \eta_M \eta_p \eta_{MG}$

For the tower pump $\eta_{MG} = 1.0$ since there is no speed control. The nomenclature for all of the calculations above is listed below:

GPM = Pump flow rate in gallons per minute

W = Pump flow rate in lbs/hr

ρ = Density of liquid pumped, lbs/ft^3

ΔP = Pump head expressed in psid

H = Pump head expressed in feet of liquid

MW_p = Mechanical energy expended in raising the fluid pressure, MW_t

MW_e = Electrical energy supplied to the pump drive motor, MW_e

η_M = Electrical to mechanical energy conversion efficiency in drive motor

η_{MG} = Combined efficiency of motor generator set and hydraulic coupling used in controlling pump speed

η_p = Mechanical efficiency of pump

η = Combined overall efficiency of pump, motor and speed controller

The specific speed of the pumps was calculated from:

$$N_S = \frac{RPM\ \sqrt{GPM/N}}{(H/N_{ST})^{3/4}} \qquad (26)$$

Where: N_S = Specific speed of pump

RPM = Rotational speed, RPM

N = Single flow N = 1, double flow N = 2

N_{ST} = Number of stages used in pump

The suction speed of the pumps was calculated from:

$$S = \frac{RPM\ \sqrt{GPM/N}}{(H_S/N_{ST})^{3/4}} \qquad (27)$$

Here the term H_S is the net positive suction head given by:

$$H_S = 144\ P_{IN}/\rho + (V^2/2g)/144 - 144\ P_{SAT}/\rho$$

where: S = Suction specific speed

H_S = Net positive suction head, ft

P_{IN} = Pump inlet pressure, psia

V = Flow velocity at pump inlet nozzle, ft/sec

P_{SAT} = Saturation pressure of fluid at pump inlet temperature, psia

R-3 EM PUMP HEAD

In order to generate pump head data for each EM pump it is necessary to do a detailed analysis of the absorber system piping and the associated pressure losses. Using Figure R-3 as a rough analytical model the following calculations were made for the pressure differential across each pair of points in the system:

$$\Delta P_{FRICT} = f \frac{L_{eq}}{D} \frac{V^2}{2g} \frac{\rho}{144} \quad \text{(Friction pressure loss)} \tag{28}$$

$$\Delta P_{VEL} = \frac{0.02517}{\rho} \left[\frac{W_A^2}{d_A^4} \quad \frac{W_B^2}{d_B^4}\right] \frac{1}{144} \quad \text{(Pressure loss due to area change)} \tag{29}$$

$$\Delta P_Z = (Z_A - Z_B) \frac{\rho}{144} \tag{30}$$

Adding the three pressure loss components

$$P_B - P_A = \Delta P_{VEL} + \Delta P_Z + \Delta P_{FRICT} \tag{31}$$

In order to avoid sign errors the flow must always move from point "B" to point "A" when setting up individual calculations. The resulting system pressure calculations are shown in Table 7.2.2-14 (see Section 7.2.2.4.5).

In equation (28) there is an equivalent pipe length "L_{eq}" which in the case of pipe flow consists of the summation of all straight lengths of pipe plus equivalent adders for elbows, valves, etc. In the case of area changes or tee connectors, the equivalent length approach was also used. Therefore, the ΔP_{FRICT} column in Table 7.2.2-14 (Section 7.2.2.4.5) can be divided into elements that vary as the flow rate raised to the 1.8 power and others which vary as the square of the flow rate.

Using Table 7.2.2-14, it is possible to separate out specific pressure losses. For example, between points 3 and 5

$$P_3 - P_5 = \underbrace{1.0878 \left(\frac{W}{W_R}\right)^2}_{\Delta P_{VEL}} + \underbrace{0.3881 \left(\frac{W}{W_R}\right)^2}_{\Delta P_{FRICT}\ (\text{AREA CHANGES})} + \underbrace{1.1642 \left(\frac{W}{W_R}\right)^{1.8}}_{\Delta P_{FRICT}\ (\text{STRAIGHT PIPES})} \tag{32}$$

where: W = Flow rate in any panel, #/HR

W_R = Flow rate in the hot panel, #/HR

using the same principle between points 6 and 14

$$P_6 - P_{14} = -0.79760 \left(\frac{W}{W_R}\right)^2 + 1.0995 \left(\frac{W}{W_R}\right)^2 + 3.9327 \left(\frac{W}{W_R}\right)^{1.8} + 8.0361 \tag{33}$$

adding egs (15) and (16) together:

$$(P_6-P_5) + (P_3-P_{14}) = 5.0969 \left(\frac{W}{W_R}\right)^{1.8} + 1.7778 \left(\frac{W}{W_R}\right)^2 + 8.0361 \quad (34)$$

But from Table 7.2.2-14 (Section 7.2.2.4.5)

$$(P_3-P_{14}) = 6.1038 - 2.7415 = 3.3623 \quad (35)$$

At full power for which this analysis was performed the pressure in the three headers 3,14, and 21 (see Figure R-3) remain constant for all panels. Therefore, the value above $(P_3-P_{14}) = 3.3623$ is constant for all panels operating at full power. Note, however, that this number must be adjusted as power changes since the flows in the remainder of the receiver piping will change with power level.

Since the EM pump head is by definition (P_6-P_5) as defined in Figure R-3:

$$\Delta P_{EM} = (P_6-P_5) \quad (36)$$

Substituting (35) and (36) into (34) produces the final expression for pump head

$$P_{EM} = 5.0969 \left(\frac{W}{W_R}\right)^{1.8} + 1.7778 \left(\frac{W}{W_R}\right)^2 + 4.6738 \quad (37)$$

If $W = W_R$ in equation (37) as would be the case for the hot panel flow rate then ΔP_{EM} from equation (37) (where $W/W_R = 1$) should agree with (P_6-P_5) from Table 7.2.2-14 (see Section 7.2.2.4.5). Both values agree at 11.5485 psid.

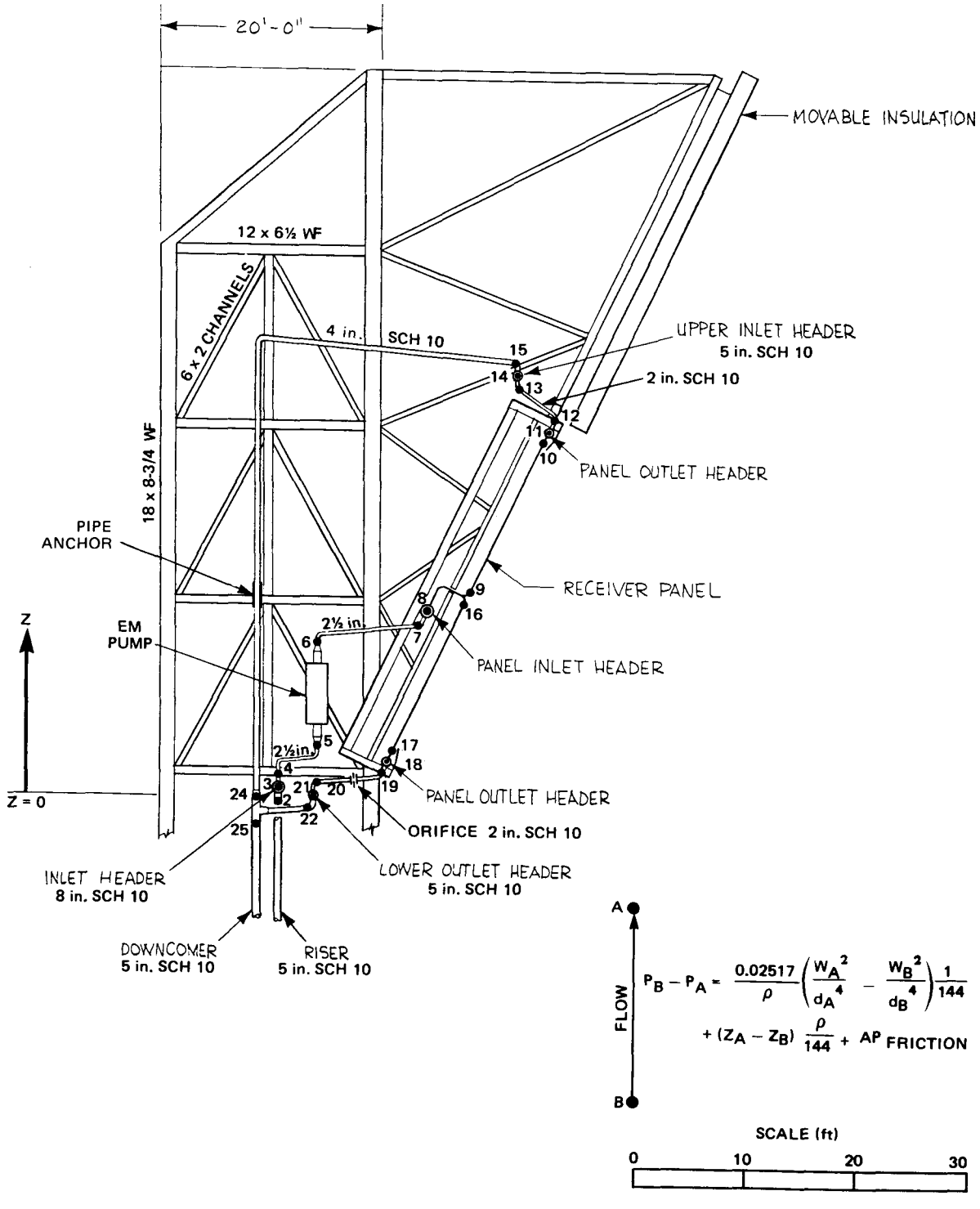

Figure R-3. Receiver Assembly

R-4 REHEATER DESIGN CALCULATIONS

In the reheater the low value for the steam side heat transfer coefficient is the controlling parameter in setting the overall heat transfer coefficient. The tube wall coefficient in both plants will be almost identical except for temperature effects since the same tubing is used for both plants.

The steam side coefficients (based on tube I.D.) for the commercial plant reheater were (in BTU/HR/FT^2/°F units based on tube I.D.)

$$h_{inlet} = 366.5,\ h_{outlet} = 401.4,\ h_{ave} = 384$$

The equation used to calculate these steam side coefficients is:

$$h_i = \frac{Ks}{di}\ (0.0133\ Re^{0.84}\ P_R^{0.333})$$

$$V = W/(N\ \tfrac{\pi}{4}\ d_i^{\,2}\rho)$$

$$Re = Vd_i\ \rho/\mu$$

$$P_r = C_p\ \mu/K_s$$

where: h_i = Steam side coefficient based on tube I.D., BTU/HR/FT^2/°F

K_s = Conductivity of steam, BTU/HR/FT/°F

μ = Viscosity of steam, lbs/ft-hr

ρ = Density of steam, lbs/ft^3

C_p = Specific heat of steam, BTU/lb/°F

N = Number of tubes in reheater

W = Steam flow rate in all the tubes, lbs/hr

V = Steam flow velocity, ft/hr

Re = Reynolds Number

P_r = Prandtl Number

Table R-1 shows a tabulation of h_{inlet}, h_{outlet}, and h_{ave} as a function of the number of tubes in the pilot plant reheater. Thirty tubes were found to have an average coefficient of 385.1 BTU/HR/FT^2/°F which agrees well with the 384 BTU/HR/FT^2/°F for the commercial plant. Therefore, the pilot plant reheater will have thirty tubes.

The tube wall conductance will be almost the same for the two plants since the tubing is identical and only the effect of temperature on thermal conductivity will change it. Listed below are the average steam temperatures and average

sodium temperatures for the two plants. The tubing will operate somewhere between the steam and sodium temperatures.

TABLE R-1

Steam Side Heat Transfer Coefficients
In The Pilot Plant Reheater
As A Function Of Number Of Tubes

Number of Tubes	h_{inlet} *	h_{outlet} *	$h_{ave.}$ *
25	434.3	463.5	448.9
30	372.6	397.7	385.1
35	327.4	349.4	338.4
40	292.6	312.3	302.5

*BTU/HR/FT^2/°F values based on Tube I.D.

	Commercial Plant	Pilot Plant
Average Steam Temp. °F	786.38	804.6
Average Sodium Temp. °F	979.55	990.02

It was concluded that the average wall conductance from the commercial plant STMGEN computer runs would be sufficiently accurate for use on the pilot plant reheater.

$$h_W = \frac{2690.7 + 3028.1}{2} = 2859.4 \text{ BTU/HR/FT/°F (Based on I.D.)}$$

The sodium side heat transfer coefficient was evaluated from the Graber and Rieger correlation:

$$Nu = A + B\,(Pe)^n$$

where:

$A = 0.25 + 6.2\,(P/d)$

$B = -0.007 + 0.032\,(P/d)$

$n = 0.8 - 0.024\,(P/d)$

P/d = Pitch to diameter ratio for the tubing array

Pe = Peclet No. = Reynold's No. x Prandtl's No.

$Nu = h_o d/K$ = Nusselt's No.

The values of the sodium heat transfer coefficient h_o, calculated for the pilot plant are as follows, where the units are BTU/HR/FT^2/^{8}F based on the tube O.D.

$$h_o = 3237.2 \text{ Inlet}; \quad h_o = 2961.0 \text{ outlet}$$

The average value is $h_o = 3099$.

The overall coefficient can now be calculated from

$$U_o = \frac{1}{\frac{do}{di}\left[\frac{1}{h_i} + \frac{1}{h_w}\right] + \frac{1}{h_o}}$$

$$U_o = \frac{1.05}{0.95}\left[\frac{1}{385.1} + \frac{1}{2859.4}\right] + \frac{1}{3099} = 279.41 \text{ BTU/HR/FT}^2/^\circ\text{F}$$

The active length of the reheater can be determined by solving for "L" in the following overall heat balance expression for the reheater.

$$Q = U_o A_o \text{LMTD} = U_o(\pi d_o L N)\ \text{LMTD}$$

$$L = \frac{Q}{U_o(\pi d_o N)\text{LMTD}}$$

where:
- Q = Heat duty for the reheater, BTU/HR
- LMTD = Log mean temperature difference for the reheater, °F
- N = Number of tubes in the reheater
- U_o = Overall heat transfer coefficient based on tube O.D., BTU/HR/FT^2/°F
- d_o = Tubing O.D., ft.
- L = Nominal active length required, ft.

Substituting values:

$$L = \frac{2.946\ (3.413 \times 10^6)}{279.41\ (\pi \frac{1.05}{12}\ 30)\ 182.2} = 23.95 \text{ feet}$$

This length is the nominal length requirement based on nominal heat transfer conditions which have error tolerances. A 7% margin for heat transfer uncertainties was added to the commercial plant reheater; therefore, the pilot plant should be similarly treated:

$$L_A = 23.95\ (1.07) = 25.6 \text{ feet}$$

The LMTD approach to heat exchanger design is based on fluids on both shell and tube side which have constant specific heats. Normally superheated steam varies greatly in specific heat as can be seen from Figure R-4. However, for the reheater, the steam follows line A-B which is sufficiently near to being constant as to justify the use of the LMTD design method.

In the case of the superheater design, C_p changes radically and the use of LMTD leads to inaccurate results. However, where used for small extrapolations, and where accuracy is not paramount, the use of LMTD can be excused. This was the approach used to size the pilot plant superheater.

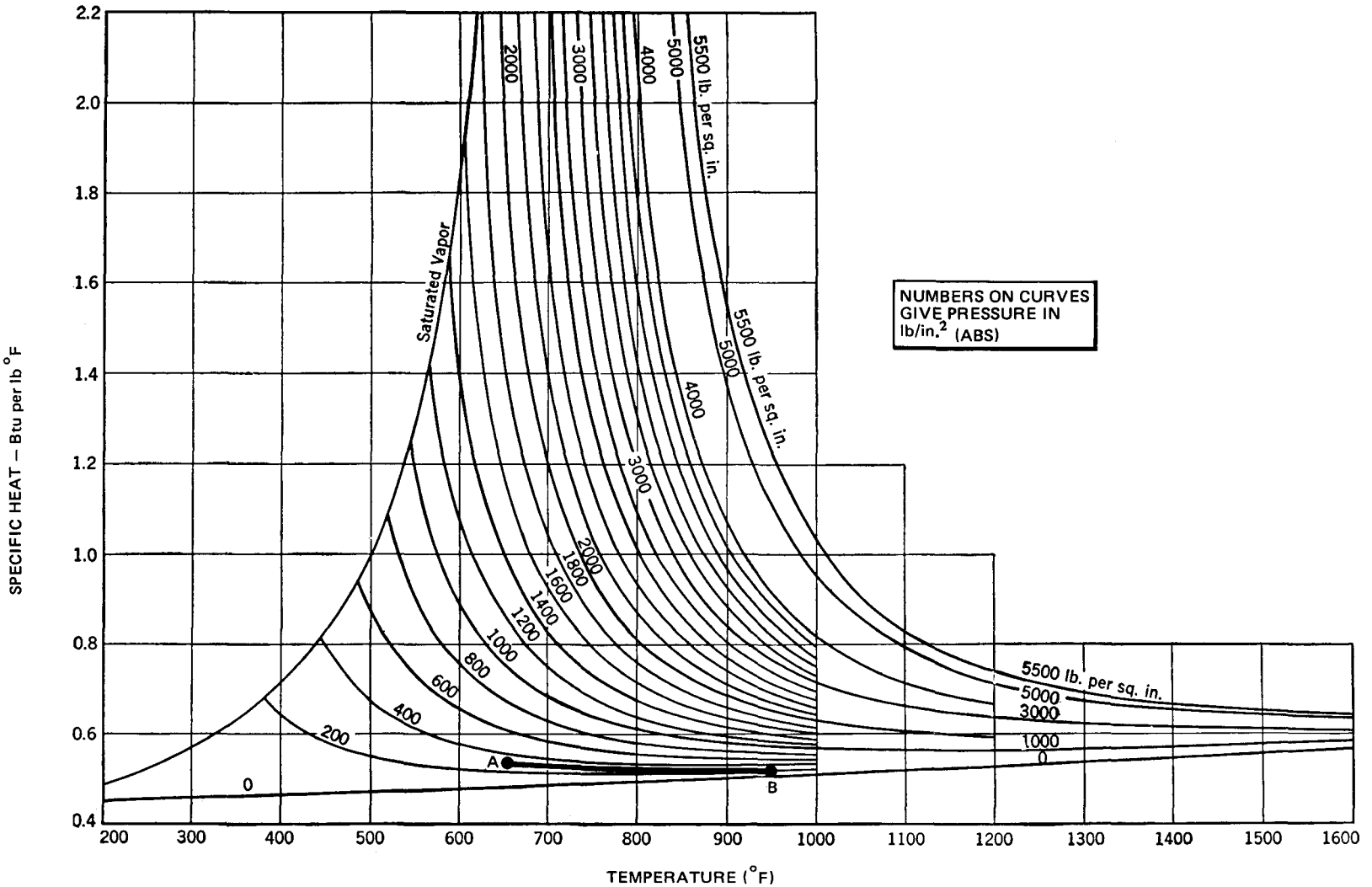

(*Keenan & Keyes, Thermodynamic Properties of Steam*)

Figure R-4. Specific Heats of the Vapor For Constant Pressure

Appendix S

PILOT PLANT HEAT BALANCE EVALUATIONS

To compensate for the lower turbine throttle conditions in the pilot plant the steam was throttled (independently from the turbine throttle) in the line between the superheater and the turbine. Figure S-1 details this constant enthalpy process where the superheater steam outlet temperature is unknown. By interpolating the steam tables the temperature was established at 1004.0°F.

It should be noted that all the evaluations presented here are for full power operation. No part-load calculations were made.

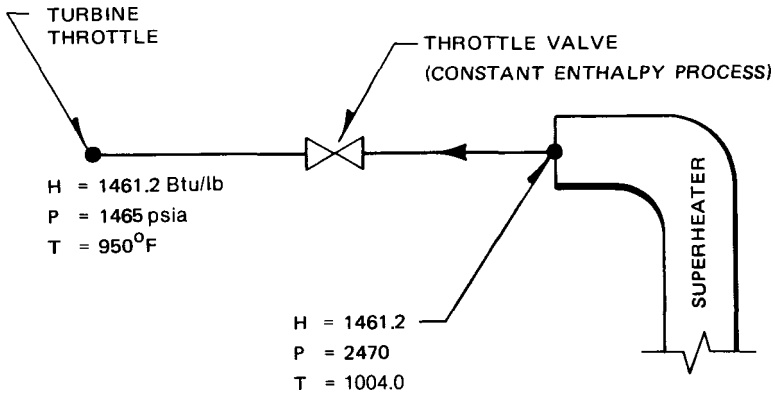

S/H STEAM OUTLET TEMPERATURE FOR H = 1461.2 AND 2470 psia

Figure S-1. Constant Enthalpy Throttling Process Between Superheater and Turbine Throttle

The turbine heat balance shows the feedwater return conditions without the effect of the 10% steam drum blowdown as being:

W = 85400 #/HR flow rate

P = 1831 psi pressure

H = 461.9 BTU/# water enyhalpy

T = 477.6°F feedwater temperature

The blowdown flow is taken from the steam drum and routed to the condenser hot well through a regenerative heat exchanger with return feedwater as a coolant. After joining the condensate stream it passes through a full flow dimeneralizer and the feedwater heaters. Since the overall heat lost from the system in this process is negligibly small, a simple heat balance of the type detailed in Figure S-2 will suffice for the evaluation of the final feedwater return temperature. After

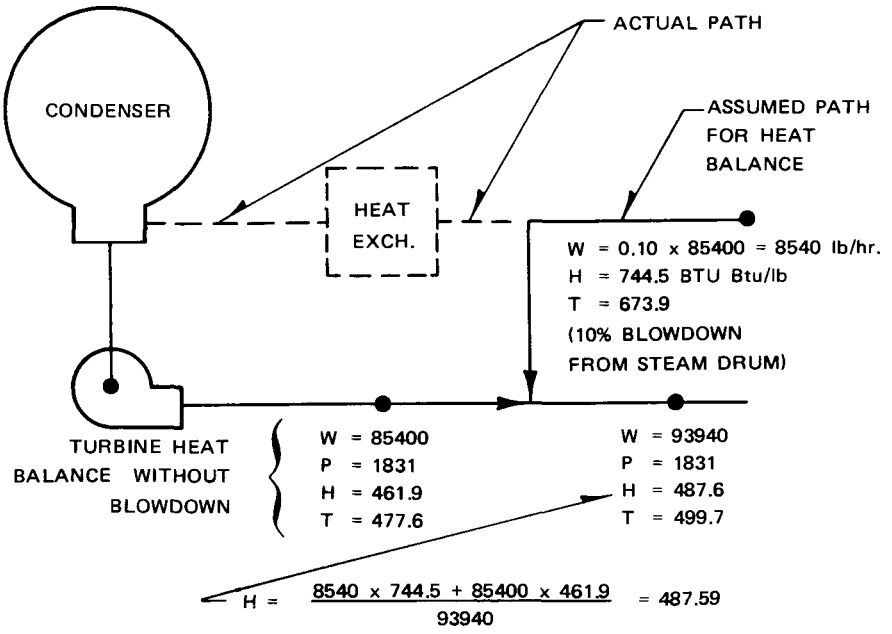

Figure S-2. Calculation of Impact of 10 Percent Drum Blowdown and Cleanup On Feedwater Thermal ConditionF

calculating the new enthalpy (H = 487.59) from a mixing heat balance the corresponding return temperature to the steam generator subsystem was found to be 499.7°F.

Figure S-3 shows the feedwater stream as it interfaces with the recirculation pump and the steam drum. The recirculation ratio will be held at R = 1.15 which is prototypic of the commercial plant. Recirc. ratio is defined here as the ratio (evaporator flow rate/steam flow rate) and is the reciprocal of the steam quality exiting the evaporator. Thus the exit steam quality is 1/1.15 = 0.8696 from the evaporator. Of the flow passing through the evaporator 15% (with respect to steam flow) exits as water which is separated from the steam in the steam drum. Of this 10% is blown down to the condenser for cleanup and 5% is recirculated as indicated in Figure S-3. Since the steam drum is operated at 2600 psia to be prototypic of the commercial plant it is necessary to throttle the 5% recirculated flow stream (point B to point C) as indicated in Figure S-3 in order to match the return feedwater pressure at 1831 psia. This constant enthalpy process occurs at H = 744.5 BTU/lb as indicated. Since the water was initially saturated the steam quality after throttling was calculated to be X = 0.1853. This stream (point C) then mixes with the cold feedwater (point A) and enters the pump (point D) with a mixture enthalpy of H = 498.8 BTU/# and a corresponding subcooled temperature of T = 509.0°F. Details of the calculation are shown in Figure S-3.

In passing through the recirculation pump energy is added to the fluid. A pump efficiency of 80% and a motor efficiency of 95% were assumed giving an overall efficiency of 76%. Since the pressure must be raised from 1820 psia to 2716 psia the head required is ΔP = 896 psid or 2661.8 ft of head. This combined with the flow rate and efficiency allows the pump power (MW_p = 0.09845) and the electrical power (MW_e = 0.12954) to be calculated. Of the electrical energy entering the motor 5% is lost to the cooling air. Of the remainder 20% is dissipated as frictional heat in the pump itself and raises the water temperature. The remaining 80% of the energy is potential energy which is dissipated throughout the system as frictional pressure drop. Since the system is heavily insulated all but 5% of the electrical energy represents heat added to the system. For simplification all of this added heat energy was considered as added to the fluid as it passes through the pump. The details of this calculation are shown in Figure S-4. It was found that the temperature rose from T = 509°F to T = 512.3°F in the process. Thus the temperature and enthalpy of the fluid entering the evaporator are 512.3°F and 503.1 BTU/#.

Figure S-5 details the heat balance on the water side of the evaporator. Conditions at the evaporator inlet have been fully defined. At the outlet end only the flow rate and pressure level are known. But the exit steam quality is also known from the recirculation ratio set earlier. Steam quality and exit pressure are used to calculate the exit enthalpy. With steam/water flow rate, inlet enthalpy, and outlet enthalpy known the evaporator power can be calculated as detailed in Figure S-5. The result is a power level of 15.395 MW_t.

From the steam drum the separated steam flows over to the superheater inlet under constant enthalpy conditions as detailed in Figure S-6. The exit steam conditions were established earlier (see Figure S-1). The power level generated by the superheater can now be calculated as detailed in Figure S-7.

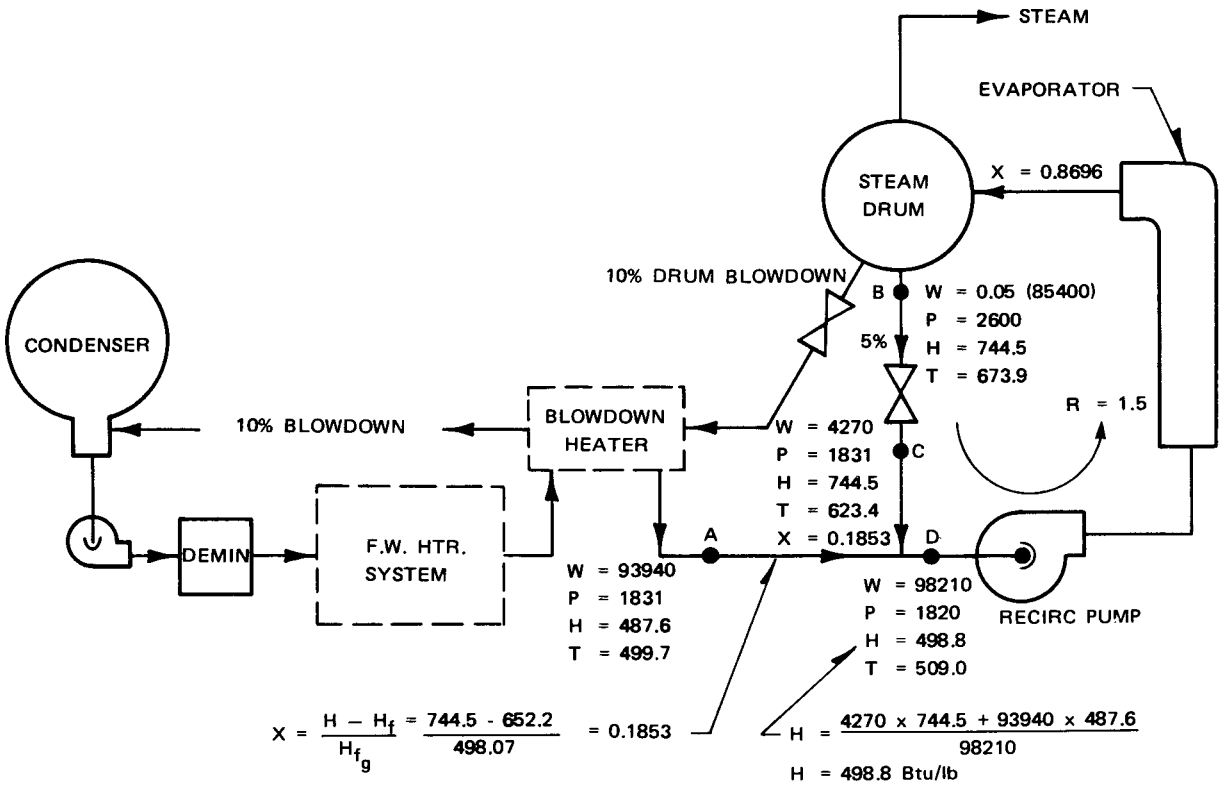

Figure S-3. Mixing Tee Heat Balance for Evaluation of Recirculation Pump Inlet Operation

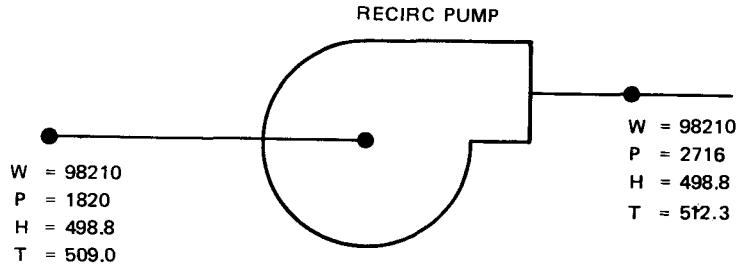

*Assumes all MWe pump energy is recovered in fluid pumped except 5% motor loss to atmosphere. Part of this absorbed energy in fluid would be distributed in recirc loop friction, but is concentrated here for simplicity.

v_f =
ΔP = 896 psi
η = 0.76
GPM = 252.6
H_D = 2661.8 ft
MW_P = 0.09845 PUMP
MW_c = 0.12945 ELECT.
MW_s = 0.12306 (95% RETURN TO SYSTEM = 4.20×10^5 Btu/hr)
ΔH = $4.20 \times 10^5 / 98210$ = 4.28 Btu/lb

Figure S-4. Recirculation Pump Heat Balance

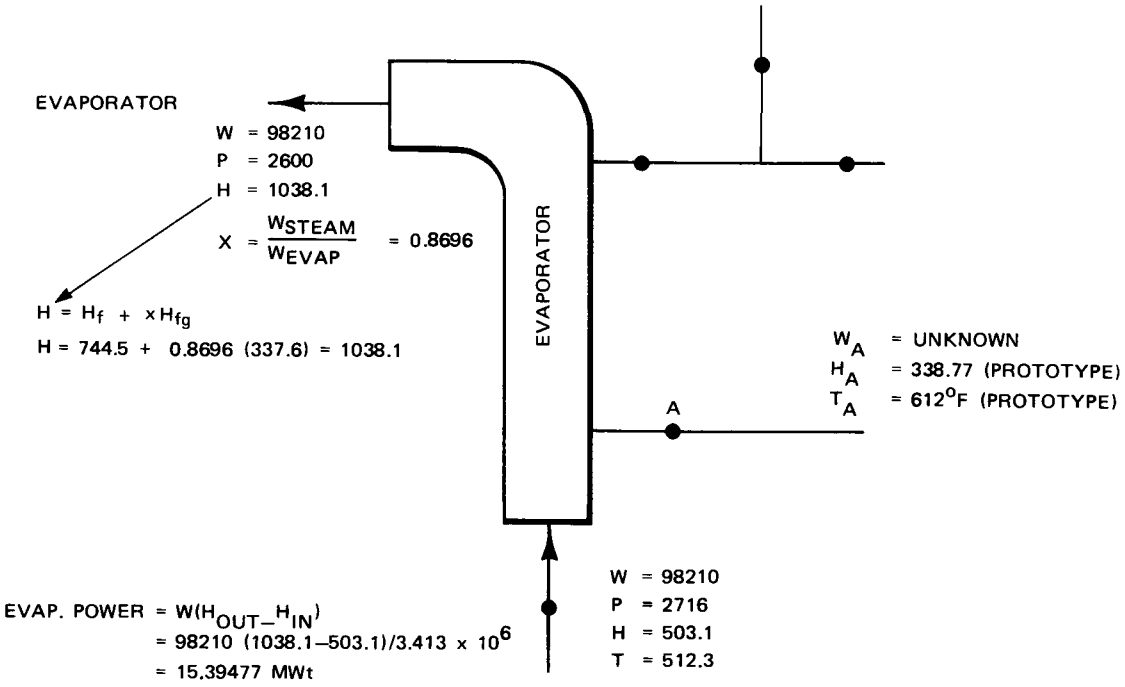

Figure S-5. Water Side Heat Balance on the Evaporator

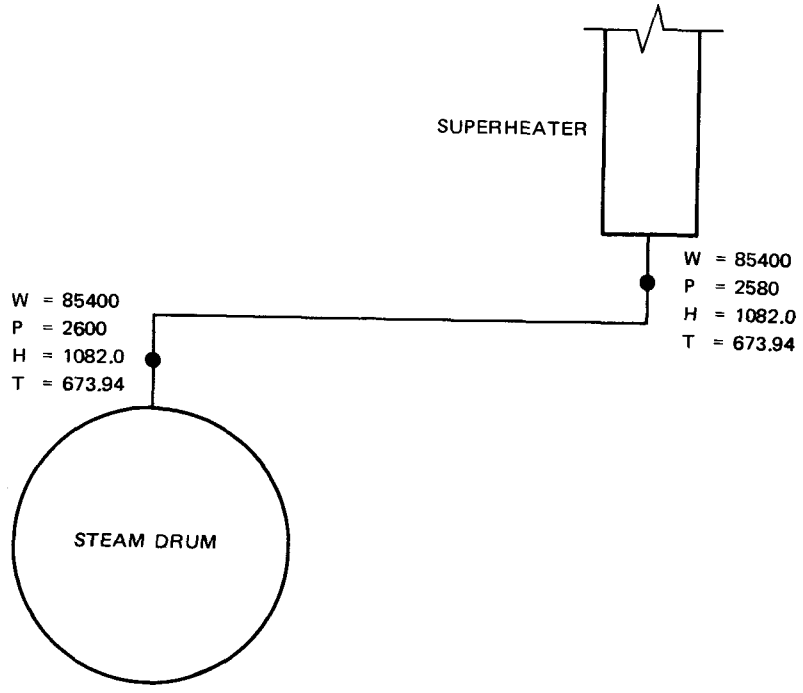

Figure S-6. Constant Enthalpy Expansion From Steam Drum to Superheater

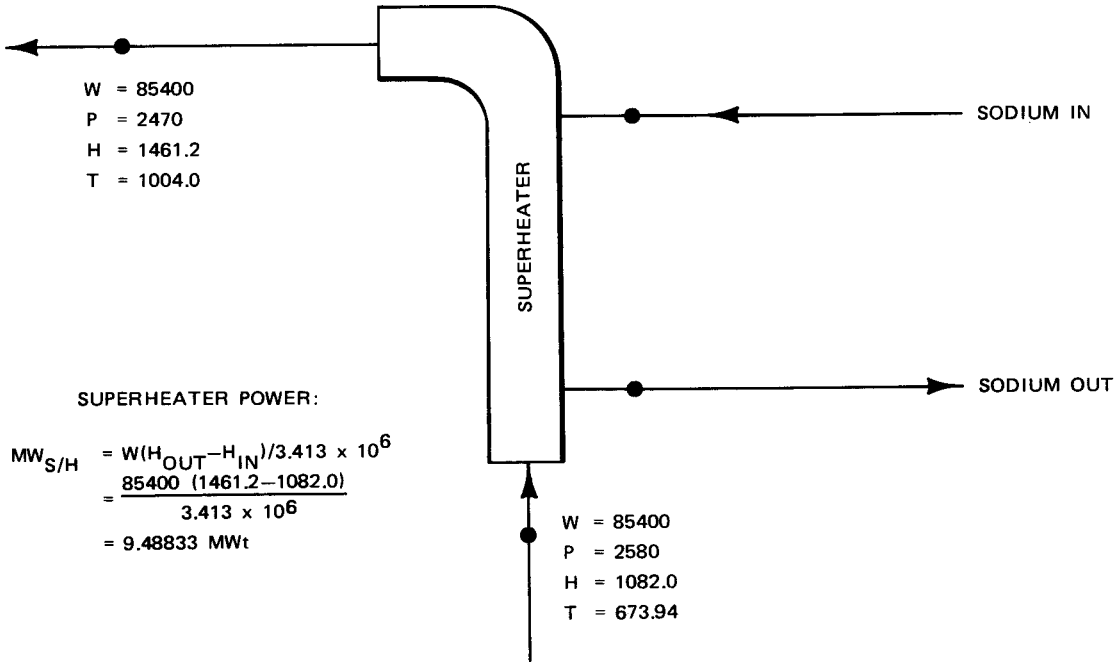

Figure S-7. Superheater Water Side Heat Balance

Before leaving the evaporator and superheater it is a good idea to perform an overall heat balance on the steam drum as a final accuracy check. This check is detailed in Figure S-8. The results were close enough to provide confidence that the earlier calculations were correct.

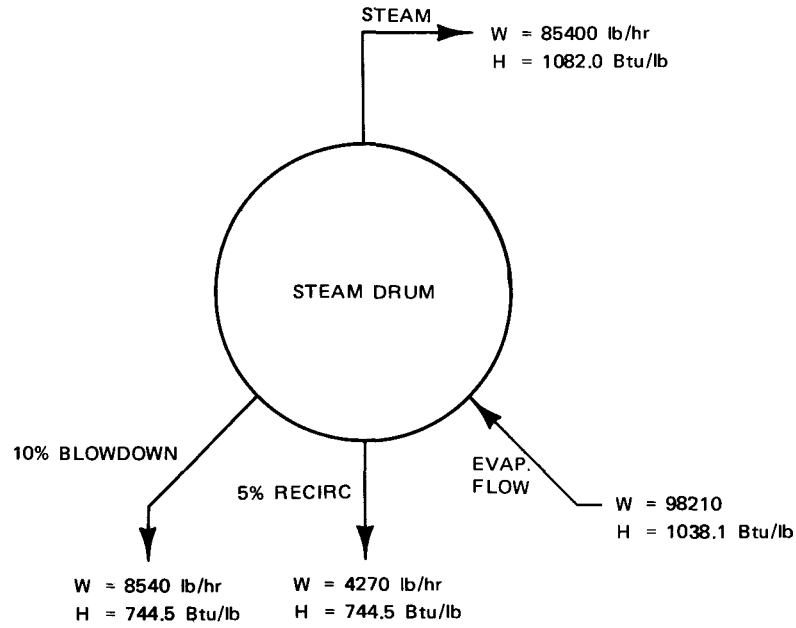

85400 + 8540 + 4270 = 98210 lb/HF FLOW CONTINUITY CHECKS

8540 x 744.5 + 4270 x 744.5 + 85400 x 1082.0 = 98210 x 1038.1

$1.0194 \times 10^8 = 1.0195 \times 10^8$ HEAT BALANCE CHECKS

Figure S-8. Calculation Check on Steam Side Heat Balance

Figure S-9 shows the heat balance on the steam side of the reheater module. The conditions at points "A" and "B" were given by the turbine heat balance. Due to line losses $P_A > P_D$ and $P_C > P_B$. In passing through the reheater there is another pressure loss where $P_C < P_D$. These pressures at points "C" and "D" were estimated based on Task 4 data. As the design progresses these pressures must be adjusted. They do not affect the heat balance since the processes A-D and C-B are constant enthalpy throttling. However, the temperatures at "C" and "D" will be affected by the pressure level and this in turn affects the required surface area in the reheater. Using the estimated pressures and using constant enthalpy throttling the temperatures T_C and T_D were determined. From the steam flow rate and enthalpy change across the reheater the power level was calculated to be 2.946 MW_t as shown in Figure S-9. Combining this power level with the evaporator (15.395 MW_t) and the superheater (9.488 MW_t) the total power transmitted through the steam generator system is 27.829 MW_t.

Table S-1 shows the inlet and outlet sodium temperatures and enthalpies to the steam generator subsystem. Also detailed is the calculation of the total flow through the steam generators which was found to be 6.413 x 10^5 lbs/hr.

TABLE S-1

SODIUM SIDE HEAT BALANCE INPUT DATA

	Sodium Temperature (°F)	Sodium Enthalpy (BTU/LB)
Sodium Cold Leg	612°F	338.77
Sodium Hot Leg	1100°F	486.89

$$W_{Na} = \frac{MW_T \times 3.413 \times 10^6}{(H_{HOT} - H_{COLD})} = \frac{27.829 \times 3.413 \times 10^6}{(486.89 - 338.77)}$$

$$W_{Na} = 6.4127 \times 10^5 \text{ lbs/hr}$$

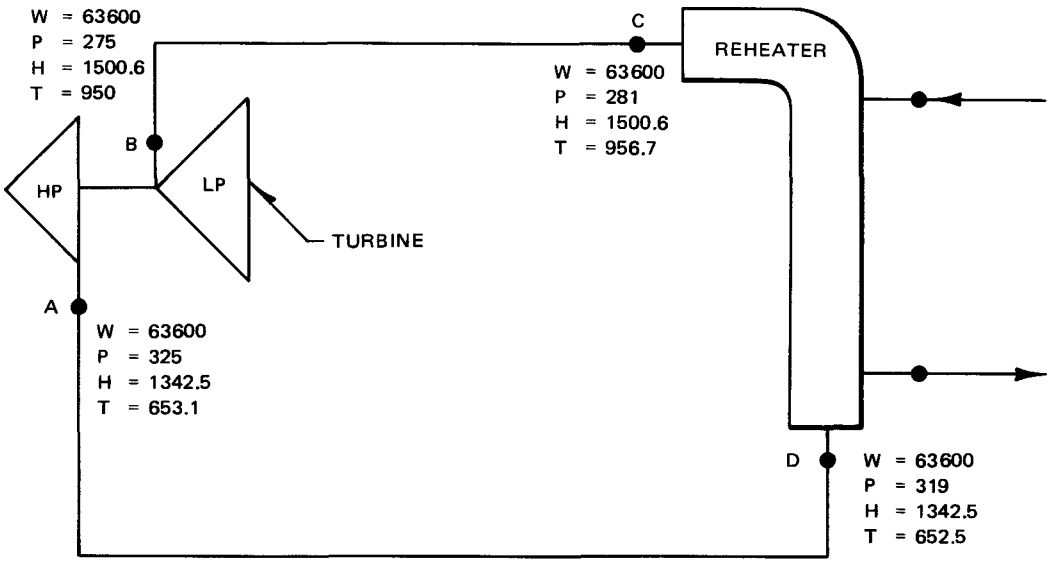

REHEATER POWER LEVEL

$$MW_{R/H} = W(H_{OUT}-H_{IN})/3.413 \times 10^6$$

$$= 63600\ (1500.6-1342.5)/3.413 \times 10^6$$

$$= 2.946\ MWt$$

Figure S-9. Reheater Heat Balance

The flow rate split between the superheater and reheater can be arbitrarily set at any value as long as the sum of the two flows equals the flow rate in the evaporator. However, most flow splits will produce a mismatch in the three temperatures at the mixing tee connecting all three steam generator modules. This can be avoided, however, by adjusting the flow split to a value that makes the evaporator inlet temperature equal to the exit temperature at both the superheater and reheater. This avoids a potentially serious mixing tee design problem at the design point and provides the conditions for completing the heat balance. The temperatures may become mismatched, however, at off-design power condition. The sodium side heat balance in the evaporator (designated E/V) is given by:

$$MW_{E/V} = W_{E/V} (H_{IN} - H_{OUT}) / 3.413 \times 10^6$$

Noting that all the sodium flow (6.4127×10^5) passes through the evaporator and solving for H_{IN}.

$$H_{IN} = H_{OUT} + \frac{MW_{E/V} \times 3.413 \times 10^6}{W_{E/V}}$$

$$= 338.77 + \frac{15.395 \times 3.413 \times 10^6}{6.4127 \times 10^5}$$

$$= 420.72 \text{ BTU/lb}$$

The corresponding temperature is 880.03°F. The sodium inlet and outlet enthalpies and power levels are now known for all three modules. The flow rates in the superheater and reheater are calculated from:

$$W_{S/H} = \frac{MW_{S/H} \times 3.413 \times 10^6}{(H_{OUT} - H_{IN})} = \text{Superheater flow rate}$$

$$= \frac{9.488 \times 3.413 \times 10^6}{(486.89 - 420.72)} = 4.8942 \times 10^5 \text{ lbs/hr}$$

and $$W_{R/H} = \frac{MW_{R/H} \times 3.413 \times 10^6}{(H_{OUT} - H_{IN})} = \text{Reheater flow rate}$$

$$W_{R/H} = \frac{2.946 \times 3.413 \times 10^6}{(486.89 - 420.72)} = 1.5197 \times 10^5 \text{ lbs/hr}$$

As a final calculational check, flow continuity at the mixing tee must be assured:

$$W_{E/V} = W_{S/H} + W_{R/H}$$

$$6.4127 \times 10^5 = 1.5197 \times 10^5 + 4.8942 \times 10^5$$

$$6.4127 \times 10^5 \cong 6.4139 \times 10^5 \text{ lbs/hr}$$

This final accuracy check was considered sufficiently close to consider the heat balance correct.

Appendix T

BACKUP DETAILS FOR COST ESTIMATE

This appendix contains additional details for the first commercial plant cost estimate. Because of the large volume of backup information generated in preparing this estimate, it has not been possible to include in-depth details for all cost categories. Only those categories which include advanced equipment have been reported here.

SODIUM AND STEAM PIPING (Accounts 4250.3, 4250.23, 4520.1, 4520.2, 4520.3)

Tables T-1 and T-2 give the steam and feedwater piping cost breakdown. Note that account 4250.3 also includes the sodium piping which inter-connects the steam generators. Table T-3 lists the sodium piping runs for which cost estimates were prepared. Tables T-4, T-5, and T-6 describes the cost estimates for the sodium piping items in account 4250. Table T-7 lists the sodium valve costs used in these estimates.

MASTER CONTROL SUBSYSTEM (Account 4350)

Table T-8 presents a breakdown of the master control subsystem cost estimate. These numbers were based on a verbal quote by the Honeywell Corporation for the solar plant concept.

ABSORBER PANELS (Account 4511)

Table T-9 shows the breakdown of absorber panel manufacturing costs. The total does not include the cost of special fixtures and furnaces that might be required to braze the panels. This cost estimate was made on a cost-plus-fixed-fee basis. It includes $6000 for quality control, which is normal for a quotation of this size, but does not include nuclear-type quality control, which could be very costly.

Table T-10 gives details of the material costs for each absorber panel. Weld inspection costs are about $240,000 for 24 panels. This includes 100 percent X-ray inspection of the critical outlet header welds, and 10 percent X-ray inspection of the less critical inlet header welds, as shown in Table T-10. The outlet header is more critical because it may cycle rapidly between 1100 F and 612 F during cloud passing incidents. The tube/header joints used in this cost estimate are described as "current method" in Figure T-1. Alternate methods (2 and 3) were considered to reduce the number of weld and inspection points. Neither of these methods were selected, however, because they both require one-inch-thick forged headers, which add about $100,000 to the absorber cost and about 24,000 pounds to the weight.

SODIUM PUMPS (Accounts 4513.1, 4513.5, and 4562)

Table T-11 gives a cost breakdown for the electromagnetic pumps used on the absorber panels. Note that the duct is designed to ASME Section VIII, Division 1 rules; however, the cost is not very sensitive to the code selection in this case because the pressure parts in the duct represent only a small proportion of the cost.

Table T-12 gives a similar breakdown for the two centrifugal pump cost estimates. Factory labor and material costs were estimated on the basis of a vendor quote for similar pumps built to ASME Section III, Class 1 (plus RDT) specifications which yielded a cost of $41/pound. These nuclear-type pumps were quite heavy due to requirements for radiation shielding and a long shaft to accommodate the shielding. The approach used here to remove the nuclear cost penalties was to re-estimate the pump weight based on a Section VIII, Division 1 design and apply the $41/pound to this lower weight. The costs listed in Table T-12 also include vendor engineering and motors to drive the pumps. The steam generator pump has a motor-generator set to provide variable speed operation and a pony motor for very low flows.

STEAM GENERATORS (Account 4561)

Table T-13 gives a breakdown of the steam generator costs. Cost data for these estimates were obtained by scaling current costs for nuclear-type units of similar design. The nuclear units are designed to the ASME Code, Section III, Class 1 (plus RDT standards); this imposes significant cost penalties due to the stringent quality assurance and analysis requirements of these standards. For the solar application, it will be sufficient to obtain an ASME Section VIII stamp. However, due to the sodium/water reaction hazard, it will be necessary to perform quality assurance procedures and thermal stress analyses not required by Section VIII. The effort and cost involved will be roughly equivalent to that required by Section III, Class 3.

STORAGE VESSELS (Accounts 4611, 4612, 4660)

Table T-14 describes the storage tank specifications used in preparing this cost estimate. Tables T-15 and T-16 give a detailed breakdown of the cost estimates for the cold and hot tanks respectively.

Figure T-2 shows the tank foundation concept used in preparing the estimate in account 4660. This foundation was designed to support the tank static load and to resist earthquake overturning movements. The soil bearing capacity was assumed to be 2000 pounds/square foot.

Table T-1

STEAM AND FEEDWATER PIPING - STEAM GENERATORS
(Account 4250.3)

Component	Pipe Quantity* Diameter (in.)	Pipe Quantity* Length (ft)	Field Man-Hours	Field Labor Cost ($)	Field Material Cost** ($)	Total ($)
Sodium Piping						
Reheater Inlet Pipe	8	—	58	1,043	4,434	5,477
Superheater Inlet Pipe	9	—	173	3,111	15,634	18,745
RH to Mix Tee	10	—	114	2,050	78,262	80,312
SH to Mix Tee	11	—	150	2,699	9,695	12,394
Mix Tee to Evap. Inlet	12	—	469	8,435	30,401	38,836
SG Vent Lines	23	—	206	3,705	66,991	70,696
SG Pump Dump Line	25	—	83	1,493	34,251	35,744
SG Dump Line	26	—	379	6,816	106,427	113,243
Evap. to Cold Tank	13	—	1,720	30,934	80,048	110,982
SG to RP Tank	31	—	498	8,957	25,610	34,567
Steam/Water Piping						
RH to LP Turbine	15.5	280	845	15,197	44,734	59,931
HP Turbine to RH	14	240	649	11,672	30,621	42,293
SH to HP Turbine	13.5	280	747	13,435	83,444	96,879
Steam Drum to SH	10	260	411	7,392	13,881	21,273
Evap. to Steam Drum	9.2	100	240	4,316	15,373	19,689
Recirc. Pump to Evap.	12	200	413	7,428	28,307	35,735
Steam Drum to Recirc. Suct.	2	140	95	1,709	1,695	3,404
Pipe Cleaning and Testing	—	—	145	2,608	892	3,500
4250.3 Totals			7,395	133,000	670,700	803,700

*If no length is given, the number under "Diameter" refers to the piping run number in Table T-3. If a length is given, the number under "Diameter" is the weighted average diameter of pipe in the segment quoted.
**Includes insulation, weld metal, pipe, valves and fittings.

Table T-2

STEAM AND FEEDWATER PIPING - HIGH PRESSURE STEAM AND FEEDWATER TRAIN (Account 4250.23)

Component	Pipe Quantity Diameter* (in.)	Pipe Quantity Length (ft)	Field Man-Hours	Field Labor Cost ($)	Field Material Cost** ($)	Total ($)
Cooling Water Make-up	12	100	572	10,288	145,453	155,741
Heater #4 to Recirc. Pump	12	600	1,098	19,750	99,823	119,573
Blowdown-Steam Drum to Heater #8	10	150	371	6,673	16,101	22,774
Cooling Water-Cond. to Cool. Tower	54	10,292	54,539	980,987	809,813	1,790,800
Heater #1 Through Heater #4-FW Pipe	8	200	762	13,706	13,034	26,740
LP Turb. to Heater #1	10	20	95	1,709	3,440	5,149
Cond. to Heater #1	10	300	1,785	32,106	49,489	81,595
LP Turb. to Heater #2	10	20	95	1,709	3,440	5,149
Drain, Heater #1	4	25	48	863	1,378	2,241
Drain, Heater #2	4	25	48	863	1,378	2,241
Drain, Heater #3	3	150	214	3,849	4,158	8,007
Drain, Heater #5	6	150	428	7,698	8,604	16,302
Drain, Heater #6	6	100	286	5,144	5,873	11,017
Drain, Heater #7	4	100	190	3,417	3,785	7,202
Drain, Heater #8	6	150	428	7,698	8,604	16,302
HP Turb. to Heater #4	10	150	893	16,062	24,916	40,978
HP Turb. to Heater #5	10	150	893	16,062	24,916	40,978
HP Turb. to Heater #6	10	150	893	16,062	24,916	40,978
HP Turb. to Heater #7	10	150	893	16,062	24,916	40,978
Blowdown Ht. Ex. Piping	4	300	714	12,843	15,300	28,143
Pipe Cleaning and Testing	--	--	214	3,849	1,063	4,912
4250.23 Totals			65,459	1,177,400	1,290,400	2,467,800

*Weighted average diameter of pipe in the segment quoted.
**Includes insulation, weld metal, pipe, valves, and fittings.

Table T-3

SODIUM PIPING DATA

RUN NO.	FROM	TO	MAX. TEMP. (°F)	DESIGN PRESS. (psig)	MAX. VELOCITY (ft/sec)	PIPE SIZE	RUN LENGTH (ft)	FITTINGS TEES	FITTINGS ELBOWS	FITTINGS VALVES*	COMMENTS
1	Tower Base	Receiver (Riser)	630	350	21.9	20" Sch 20	750	-	1	1-20" check	
2	Receiver	Throttle Station (Downcomer)	1150	325	24.2	20" Sch 20	800	-	1	-	
3	Throttle Station	Hot Storage Tank Inlet Header	1150	50	23.5	20" Sch 20	160	7	4	2-8", 2-2" Cont 2-8", 2-2" S.O.	
4	Hot Tank Inlet Header	Hot Tank Inlet Nozzle	1150	15	19.4	12" Sch 20	470	3	-	3-12" S.O.	3 Branch Lines
5	Hot Tank Outlet Nozzle	Hot Tank Outlet Header	1150	425	19.4	12" Sch 40	275	3	3	3-12" S.O.	3 Branch Lines
6	Hot Tank Outlet Header	S.G. Pump Suction	1150	425	10.8	24" Sch 40	140	4	4	-	
7	S.G. Pump	Steam Gen. (S.G.)	1150	475	19.3	18" Sch xs	350	2	6	-	
8	Hot S.G. Supply Line	Reheater Inlet	1150	450	18.5	10" Sch 40	30	-	1	-	
9	Hot S.G. Supply Line	Superheater Inlet	1150	450	21.6	14" Sch 40	80	-	1	-	
10	Reheater Outlet	Evaporator Inlet Line	900	450	17.6	10" Sch 20	70	-	1	1-10" Cont.	
11	Superheater Outlet	Evaporator Inlet Line	900	450	20.6	14" Sch 20	40	-	1	-	
12	Evaporator Inlet Line	Evaporator Inlet Nozzle	900	450	18.3	18" Sch xs	75	2	4	-	
13	Evaporator Outlet Nozzle	Cold Tank Inlet Line	630	425	17.9	18" Sch 20	500	5	12	-	
14	Cold Tank Inlet Line	Cold Tank Inlet Nozzle	630	400	17.2	10" Sch 10	290	-	12	3-10" S.O.	3 Branch Lines
15	Cold Tank Outlet Nozzle	Cold Tank Outlet Line	630	35	11.4	16" Sch 20	230	-	12	3-12" S.O.	
16	Cold Tank Outlet Line	Tower Pump Suction	630	35	9.6	30" Sch 20	120	2	4	-	
17	Tower Pump Discharge	Tower Base	630	300	22.5	20" Sch 20	400	-	12	1-20" S.O.	
18	Hot Tank Inlet Line	Cold Tank Inlet HDR	630	35	13.5	10" Sch 20	220	-	2	1-10" S.O.	Receiver return to Cold Tanks for Startup and Standby
19	Cold Tank Outlet Line	Hot Tank Outlet Line	630	35	20.3	10" Sch 20	220	-	2	1-10" Cont	S.G. Standby and Startup Bypass
20	Throttle Station	Cold Tank Inlet Header	630	35	15.9	2" Sch 40	1200	-	6	1-2" S.O.	Receiver Vent Line
21	Tower Pump Discharge	Cold Tank Inlet	630	300	11.7	4" Sch 80	120	-	4	1-4" Cont.	
22	Tower Pump Suction	Tower Pump Discharge	650	300	11.7	4" Sch 80	60	4	4	4-4" S.O.	Cold Trap System
23	S.G. Vent	Evaporator Outlet	1150	75	15.9	2" Sch 40	500	3	6	3-2" Cont.	3 S.G. Vent Lines
24	Tower Pump	Dump Tank	650	50	11.7	4" Sch 40	30	-	4	1-4" S.O.	
25	S.G. Pump	Dump Tank	1150	50	12.6	4" Sch 40	30	-	4	1-4" S.O.	
26	S.G.'s	Dump Tank	900	50	12.1	4" Sch 40	500	3	4	3-4" S.O.	
27	Cover Gas Main	Between Storage Tanks	650	50	82.0	10" Sch 40	300	6	-	1-10" S.O.	
28	Cover Gas Branch	Storage Tanks	650	50	45.0	8" Sch 40	290	-	6	6-8" S.O.	
29	Cover Gas Header		100	100	--	4" Sch 40	360	6	-	-	
30	Cover Gas Supply Lines		100	100	45.0	2" Sch 40	600	-	-	2-2" S.O.	6 Total
31	S.G. Rupture Discs	RP Tank	900	200	15.0	10" Sch 40	225	3	5	-	Carbon Steel
32	Fill Line		600	100	12.0	4" Sch 40	200	-	4	1-4" S.O.	
33	Riser	Downcomer (Tower Base Shunt)	1150	325	-	4" Sch 40	20	2	-	1-4" S.O.	

*S.O. = shutoff valve, Cont. = control valve
**Selection is consistent with ASME Section VIII, Division 1 code and (or) ANSI B16.34 power piping code.

Table T-4

RISER/DOWNCOMER, THROTTLE VALVES,
EM PUMP, COOLING AIR DUCTS
(Account 4520.1)

Component	Run Number*	Field Man-Hours	Field Labor Cost ($)	Field Material Cost ($)**	Total ($)
Downcomer	2	6,772	121,822	465,888	587,710
Throttle Valve Station	3	1,643	29,556	456,913	486,469
R/D Shunt	33	24	432	17,210	17,642
Riser	1	4,107	73,881	923,924	997,805
Pump to Riser	17	1,437	25,851	190,946	216,797
Vent Line on Tower Pump	20	257	4,623	35,369	39,992
Cold Trap Piping	22	134	2,411	38,425	40,836
Receiver Piping Installation	—	—	—	27,804	27,804
Blower and Duct, EM Cooling Air	—	1,102	19,824	148,521	168,345
4520.1 Totals		15,476	278,400	2,305,000	2,583,400

*See Table T-3
**Includes insulation, weld metal, pipe, valves, and fittings.

Table T-5

ABSORBER HEADERS AND PIPE (ACCOUNT 4520.2)

	Description					Installed Cost											
						Material*		Labor		Insulation**		Trace Heaters**		Hangers		Cost	
	Material	Size (in.)	Wall Thickness (in.)	Length (ft)	Quantity	Unit ($/ft)	Subtotal ($)	Unit ($/ft)	Subtotal ($)	Unit ($/ft)	Subtotal ($)	Unit ($/ft)	Subtotal ($)	Unit ($/ft)	Subtotal ($)	Subtotal ($)	Total ($)
Outlet Header	316	18	0.312	190.80	2	252.0	48,080.70	23.1	4,407.40	72.2	13,775.50	79.5	15,168.32	21.8	4,159.36	85,591.29	171,183
Inlet Header	A106B	24	0.375	151.05	1	63.8	9,636.91	39.4	5,951.37	78.6	11,872.43	105.4	15,920.54	29.0	4,380.41	47,761.62	47,762
Panel Outlet	316	3	0.120	10.00	48	44.0	440.0	3.40	34.00	13.5	135.00	15.0	150.00	3.8	38.00	797.00	38,256
EM Pump Inlet	A106B	5	0.134	20.00	24	8.8	176.0	5.4	108.0	16.6	332.00	24.0	480.00	6.0	120.00	1,216.0	29,184
EM Pump Outlet	A106B	5	0.134	15.00	24	8.8	132.0	5.4	81.0	16.6	249.00	24.0	360.0	6.0	90.00	912.0	21,888
																	$308,273
															4520.2	TOTAL	308,000

* Material based on vendor data.
**Installed cost (material based on vendor data).

Table T-6

TOWER TO STEAM GENERATORS INCLUDING STORAGE (Account 4520.3)

Component	Run Number*	Field Man-Hours	Field Labor Cost ($)	Field Material Cost ($)**	Total ($)
Hot Tank Inlet Piping	4	717	12,898	252,422	265,320
Hot Tank Outlet Piping	5	542	9,751	226,885	236,636
Hot Tank to SG Pump	6	1,448	26,050	71,988	98,038
SG Pump to SG	7	1,267	22,793	91,827	114,620
Cold Tank Inlet Piping	14	388	6,980	111,115	118,095
Cold Tank Outlet Piping	15	828	14,896	162,079	176,975
Cold Tank to Tower Pump	16	1,234	22,200	39,944	62,144
Hot to Cold Tanks Inlet Shunt	18	209	3,760	43,695	47,455
Hot to Cold Tanks Outlet Shunt	19	209	3,760	43,695	47,455
Tower Pump Bypass (Low Flow)	21	97	1,745	14,023	15,768
Tower Pump Dump Line	24	56	1,007	19,032	20,039
Sodium Fill Line	32	117	2,105	16,603	18,708
Cover Gas Lines:					
Hot to Cold Tanks, Main	27	473	8,509	24,835	33,344
Hot and Cold Tanks, Branch	28	434	7,808	29,871	37,679
Hot and Cold Tanks, Headers	29	243	4,372	4,782	9,154
Hot and Cold Tanks, Supply lines	30	1,032	18,566	27,404	45,970
4520.3 Totals		9,294	167,200	1,180,200	1,347,400

*See Table T-3.
**Includes insulation, weld metal, pipe, valves, and fittings.

Table T-7

SODIUM VALVE COSTS

Pipe Size (in.)	Control Valves		Shutoff Valves	
	Service 860 F	Temperature 1100 F	Service 650 F	Temperature 1100 F
20	--	--	100,000	--
12	--	--	35,000	50,000
10	40,000	--	25,000	--
8	--	34,000	15,000	27,000
4	--	15,600	17,000	--
2	--	12,350	5,000	10,650

NOTES:

1. Commercial valves, designed to ANSI B16.34.
2. Materials:
   - 1100 F 316SS
   - 860 F 2-1/4 Cr-1 Mo
   - 650 F Carbon Steel
3. All valves have provision for remote operator control.
4. All valves have freeze-type stem seals.

Table T-8

MASTER CONTROL SUBSYSTEM

	Component	Cost ($)
1.	Core, Working Memory and Bulk Memory, 500 Analog/500 Digital Channels, Video Displays	600,000
2.	Performance Calculation (software)	60,000
3.	Control Implementation and Definition (software)	300,000
4.	Project Management and Staging for Factory Test	40,000
5.	Power Supply (uninterruptable)	40,000
	Total (material)*	1,040,000
6.	Field Installation (30%)**	300,000
	4350 Total	1,340,000

*Based on verbal quote for "SEER" system by Process Computer Systems, Honeywell Corp., Phoenix, Arizona.

**Based on process computer installation cost for a Pressurized Water Reactor plant.

Table T-9

ABSORBER PANEL COST DETAIL
(24 Panels)

Shop Material	$ 586,800	
Shop Labor and Overhead	1,069,160	
Incoming Freight	2,880	
Total Shop Cost	$1,658,840	$1,658,840
Design Drafting	58,800	
Blueprints	5,000	
Contract Control	100,000	
Engineering Dept.	12,300	
Estimating Dept.	7,000	
Contract Reserve (4%)	74,500	
Purchasing Dept. and QC Manuf.	6,000	
Total Main Office Cost	$ 263,600	$ 263,600
Subtotal		$1,922,440
SGA and Overhead		135,579
Fee (8%)		165,793
4511 Total		$2,223,812

Table T-10

ABSORBER PANEL MATERIALS AND FACTORY LABOR (ONE PANEL)

	Weight* (lb)	Material Cost ($)	Factory Man-Hours
Panel Fabrication			
Tubing, 0.75-in. dia x 0.049-in. wall 6230 ft @ $1.85/ft, Incoloy 800H	2,490	11,530	644
100% X-ray of Tube-to-Stub Welds	--	--	324
Header Fabrication			
(a) Inlet Header Plate, 0.25-in. Thick, 320 lb @ 2.52/lb Incoloy 800H	320	815	308
Stubs	85	425	--
End Caps, Vents, Drains, Nipples, Straight Stops, and Saddles	175	690	--
Dye Penetrant Weld Inspection	--	--	10
10% X-ray Stubs and Headwelds	-	-	11
(b) Outlet Header Plate, 0.25-in. Thick, 485 lb @ $2.52/lb, Incoloy 800H	485	1,225	360
Stubs	85	425	--
End Caps, Vents, Drains Nipples, and Straight Stops	240	1,010	--
Dye Penetrant Weld Inspection	--	--	13
100% X-ray Stubs and Head Welds	--	--	114
Support Structure			
Carbon Steel @ $0.22/lb	10,360	2,300	414
Insulation			
Stainless Steel Pins, Fiberfrax, Aluminum Cover	2,900	840	70
Expansion Roller Assemblies			
Cor-ten, T-22, Incoloy Parts @ $1.75/lb	800	1,000	45
Paint			
Black and White Pyromark	50	130	--
Brazing Operations and Materials			
Nicrobraz Metal, 24 lb @ $25/lb	--	600	--
Furnace Charges	--	2,500	--
Purge Gases			
N_2 32,000 ft^3 @ $6.60/1000 ft^3	--	240	--
H_2 32,000 ft^3 @ $11.00/1000 ft^3	--	360	--
Gas Preheat Charge	--	360	--
Totals (per panel)	17,990	24,450	2,313
For 24 panels		586,800	

*Includes an allowance for scrap. Completed panel weight is 16,443 lb.

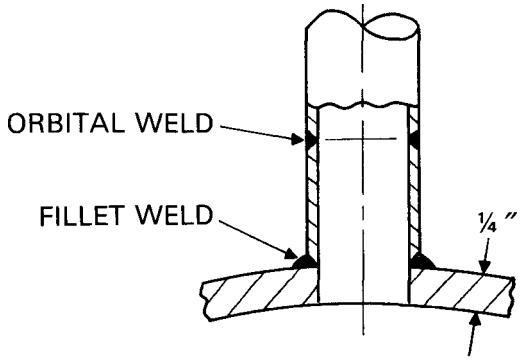

FABRICATION PROCEDURE
1. WELD STUBS TO HEADER
2. DRILL HOLES IN STUBS
3. MAKE ORBITAL WELDS

1. CURRENT METHOD

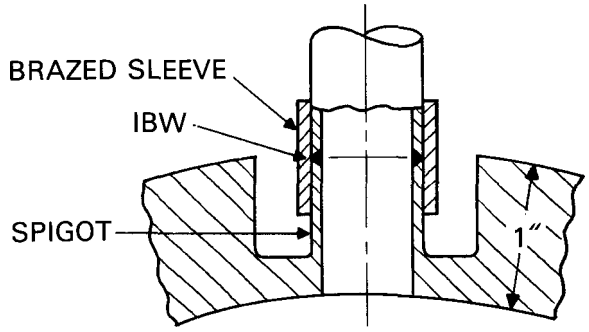

FABRICATION PROCEDURE
1. MACHINE SPIGOTS
2. SLIDE SLEEVES OVER TUBES
3. MAKE IBW
4. BRAZE SLEEVES

2. WELD REDUNDANCY METHOD

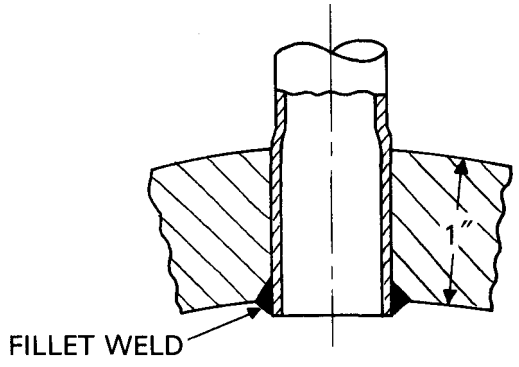

FABRICATION PROCEDURE
1. DRILL HOLES
2. INSERT TUBES
3. EXPAND TUBE
4. FILLET WELD

3. ALTERNATE METHOD

Figure T-1. Absorber Panel Tube-Header Welds

Table T-11

ELECTROMAGNETIC PUMPS - COST BREAKDOWN

Pump Component	Preproduction Cost 1000 $	Production Cost 1000 $	Total 1000 $
Stator	38.5	1358.4	1396.9
Duct	75.8	1591.2	1667.0
Power Supply	8.0	1075.2	1083.2
Subtotal			4147.1
Fee			386.5
4513.1 Total			4533.6

NOTE: Above costs are based on utilization of the same pump design for all pumps although duct geometry will be different for different flow ratings; different duct geometry does not significantly affect the cost. Costs are based on a 600 gpm pump recently manufactured by General Electric.

Table T-12

CENTRIFUGAL PUMPS - COST BREAKDOWN

Cost Category	Main Tower Pump Cost ($)	Steam Generator Pump Cost ($)
Factory Labor and Materials*	2,337,000	1,968,000
Vendor Engineering (15%)	351,000	295,000
Constant Speed Motor Drive	170,000	--
Motor-Generator Set Drive	--	245,000
Pony Motor	--	92,000
4513.5 Total	$2,858,000	
4562 Total		$2,600,000

Pump Part	Weight** (lb)	Weight** (lb)
Tank	26,000	22,000
Hydraulics	8,000	6,000
Structure	23,000	20,000
	57,000	48,000

*Cost per pound to manufacture production pumps (estimated by Byron Jackson in 1976 dollars) = $35/lb. Cost in 1978 dollars (escalated at 8% per year) = $41/lb.

**Based on ASME Section VIII, Division 1 design concept.

Table T-13

STEAM GENERATOR COST BREAKDOWN

Cost Component	Cost ($1000) Evaporator	Superheater	Reheater
Vendor Engineering (15%)	536	360	447
Fabrication and Inspection[a] [b]	1,829	1,206	1,513
Materials[b] [c]	1,285	888	1,084
Tooling[d]	260	175	217
Handling[d]	197	132	164
4561 Totals	4,107	2,761	3,425

NOTE: These costs vary with the number of units produced. Costs quoted are for the fourth units in the series.

(a) 60% reduction from current cost data on nuclear-type units.

(b) Current nuclear units based on 2-1/4Cr-1Mo construction. Incoloy 800 for solar application was assumed to cost twice as much per unit weight of material. Fabrication effort and costs for the two materials were assumed to be comparable.

(c) 57% reduction from current cost data on nuclear type units.

(d) Assumed the same for nuclear and solar applications.

Table T-14

STORAGE TANK SPECIFICATIONS USED IN COST ESTIMATE

	Hot Tanks	Cold Tanks
Vessel Weight* - tons	170	90
Vessel Material	SA240 GR316	SA515 GR70
Support Legs		
Number	20	20
Length*/Diameter - feet/inches	36/24	36/24
Pipe Schedule/Grade	160/B	160/B
Weight* (including bracing) - tons	215	215
Material	ASTM A312 TP316	ASTM A53
Stairs, Material	Carbon Steel	Carbon Steel
Weight* - tons	35	35
Vessel Insulation		
Material (inner)	Kaowool	Thermal Wool
Thickness/Area* - inches/ft^2	8/13,000	24/13,000
Material (outer)	Thermal Wool	--
Thickess/Area* - inches/ft^2	15/14,000	--
Aluminum Jacket Area* - ft^2	15,000	14,000
Weight* of Ins. and Jacket - pounds	120,000	110,000
Insulation on Legs		
Material	Calcium Silicate w/Alum. Jacket	Calcium Silicate w/Alum. Jacket
Length of Preformed Tube* - Feet	720	720
Vessel Trace Heating		
Heater Type	Tubular 1/2-in. Diameter	Tubular 1/2-in. Diameter
Length* - Feet	2,320	2,320

*Quantities quoted include about 10% scrap allowance.

Table T-15

COLD STORAGE TANK COST ESTIMATE

	Unit Cost	Labor ($)	Material ($)
Vessel			
Raw Plate	$ 300/ton	--	27,000
Factory Fabrication	$ 500/ton	--	45,000
Shipping	$ 100/ton	--	9,000
Rig at Factory	$ 20/ton	--	1,800
Field Fabrication	$ 600/ton	54,000	--
Field Rig	$ 150/ton	13,500	--
Legs			
Raw Pipe and Plate	$1,054/ton	--	226,600
Factory Fabrication	$ 250/ton	--	53,800
Shipping	$ 100/ton	--	21,500
Rig at Factory	$ 20/ton	--	4,300
Field Fabrication	$ 100/ton	21,500	--
Field Rig	$ 100/ton	21,500	--
Stairs			
Material	$1,400/ton	--	49,000
Field Erection	$ 530/ton	18,500	--
Total (Metal, Fab., Ship., and Inst.)		129,000	438,000
Total - 3 Tanks		387,000	1,314,000
Insulation - Vessel			
Thermal Wool	$ 2.00/ft^2	--	26,000
Aluminum Jacket	$ 0.60/ft^2	--	8,400
Shipping	$ 0.05/lb	--	5,500
Factory Rig	$ 0.01/lb	--	1,100
Field Inst. - Insulation	$ 2.00/ft^2	208,000	--
Jacket	$ 1.50/ft^2	21,000	--
Field Rig	$ 0.25/lb	27,500	--
Insulation - Legs			
Calcium Silicate	$13.00/ft	--	9,400
Aluminum Jacket	$ 5.00/ft	--	3,600
Factory Rig	$ 0.25/ft	--	200
Field Inst. - Insulation	$16.00/ft	11,500	--
Jacket	$ 2.10/ft	1,500	--
Field Rig	$ 1.25/ft	900	--
Total (Insulation)		270,400	54,200
Total - 3 Tanks		811,200	162,600
Trace Heating			
Heaters	$10.15/ft	--	23,600
Shipping	5%	--	1,200
Field Installation	$ 7.60/ft	17,600	--
Total (Trace Heating)		17,600	24,800
Total - 3 Tanks		52,800	74,400
4612 Total - 3 Tanks		1,251,000	1,551,000

Table T-16

HOT STORAGE TANK COST ESTIMATE

	Unit Cost	Labor ($)	Material ($)
Vessel			
Raw Plate	$3,300/ton	--	561,000
Factory Fabrication	$2,500/ton	--	475,000
Shipping	$ 100/ton	--	17,000
Rig at Factory	$ 20/ton	--	3,400
Field Fabrication	$2,803/ton	476,500	--
Field Rig	$ 150/ton	25,500	--
Legs			
Raw Pipe and Plate	$3,300/ton	--	709,500
Factory Fabrication	$1,702/ton	--	366,000
Shipping	$ 100/ton	--	21,500
Rig at Factory	$ 20/ton	--	4,300
Field Fabrication	$1,000/ton	215,000	--
Field Rig	$ 100/ton	21,500	--
Stairs			
Material	$1,400/ton	--	49,000
Field Erection	$ 530/ton	18,500	--
Total (Metal, Fab., Ship., and Inst.)		757,000	2,156,700
Total - 3 Tanks		2,271,000	6,470,100
Insulation - Vessel			
Kaowool	$ 7.20/ft^2	--	93,600
Thermal Wool	$ 1.25/ft^2	--	17,500
Aluminum Jacket	$ 0.60/ft^2	--	9,000
Shipping	$ 0.05/lb	--	6,000
Factory Rig	$ 0.01/lb	--	1,200
Field Inst. - Insulation	$ 2.00/ft^2	192,000	--
Jacket	$ 1.50/ft^2	22,500	--
Field Rig	$ 0.25/lb	30,000	--
Insulation - Legs			
Calcium Silicate	$13.00/ft	--	9,400
Aluminum Jacket	$ 5.00/ft	--	3,600
Factory Rig	$ 0.25/ft	--	200
Field Inst. - Insulation	$16.00/ft	11,500	--
Jacket	$ 2.10/ft	1,500	--
Field Rig	$ 1.25/ft	900	--
Total (Insulation)		258,400	140,500
Total - 3 Tanks		775,200	421,500
Trace Heating			
Heaters	$10.15/ft	--	23,600
Shipping	5%	--	1,200
Field Installation	$ 7.60/ft	17,600	--
Total (Trace Heating)		17,600	24,800
Total - 3 Tanks		52,800	74,400
4611 Total - 3 Tanks		3,099,000	6,966,000

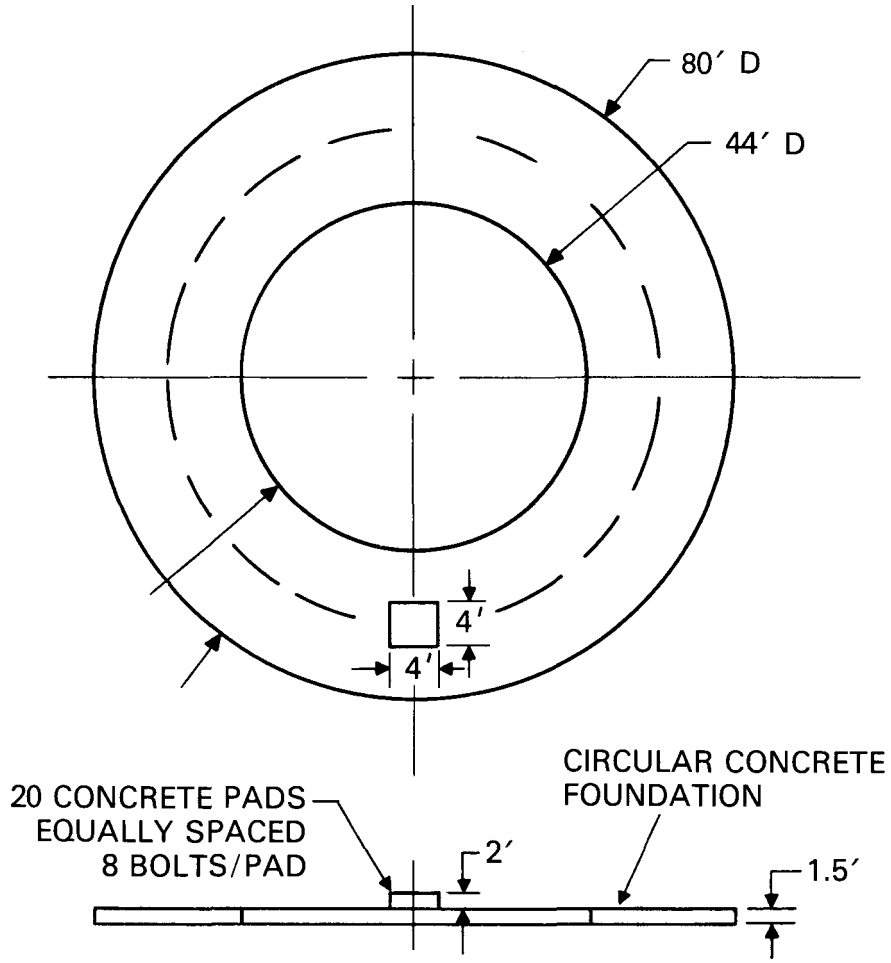

NOTE: 45 LB OF REBAR/YD³ OF CONCRETE

Figure T-2. Storage Vessel Foundations

Appendix U

ALTERNATIVE STEAM GENERATOR CONFIGURATIONS

REFERENCE HOCKEY-STICK CONCEPT

The sodium-heated steam generator system is one of the most critical elements of the plant because of the need for extremely high reliability of the sodium-to-steam/water boundary and the necessity to make the system capable of safely accommodating any failure of this boundary. Consistent with these needs and in consideration of the relatively short schedule currently contemplated for development of the Advanced Central Receiver plant (commerical plant operation in the late-1980s), the hockey-stick single-wall tube steam generator concept, nearing completion of development for the Clinch River Breeder Reactor Plant (CRBRP), was selected as the reference approach.

Development of the hockey-stick concept for sodium-heated steam generator application was initiated by Atomics International (AI) in the 1960s, culminating in a test of a 158-tube nominally 30 MW_t model at the U.S. Liquid Metal Engineering Center (now ETEC) for over 4000 hours of sodium-heated steaming at tube powers, sodium temperatures, and steam pressures and temperatures approaching those planned for the Advanced Central Receiver plant. The results from this test, completed in November 1973, affirmed the basic feasibility and soundness of the design concept. On the basis of the success of this test, along with completion of other significant developments and an assessment of acceptable cost potential, the hockey-stick design was selected in early 1974 as the reference concept for CRBRP.

Following selection of the hockey stick as the reference for CRBRP, a comprehensive program of development and testing was implemented, including: (a) materials properties testing and fabrication development, (b) full-scale shell-side (water) flow distribution and tube vibration test (completed), (c) large-leak sodium-water reaction tests (currently about 50% complete), (d) departure from nucleate boiling temperature fluctuation and corrosion tests (completed), (e) few-tube segment model thermal performance, stability, and long-term endurance tests (initiated in 1978), (f) part-power performance and structural integrity test of full-sized prototype plant unit (testing to begin at ETEC in 1980-81).

By completion of the prototype test at ETEC in the early 1980s, the hockey-stick concept will have been under continuous development and testing in the U.S. for over fifteen years. The hockey-stick design is now at the most advanced stage of development of any design available from U.S. manufacturers, with a strong commitment from DoE to complete its development as outlined above. For these reasons, the hockey-stick concept was selected for use in the Advanced Central Receiver plant.

COILED-TUBE ALTERNATIVE CONCEPT

Although lagging behind the hockey-stick steam generator development, two other sodium-heated steam generator designs are under active development by DoE: the coiled-tube, single-wall design by B&W and the straight-tube, double-wall design by Westinghouse.

The coiled single-wall design is of particular interest because its development resumes an effort on coiled-tube designs that was actively pursued under AEC sponsorship for approximately ten years until termination in about 1972. The planned program now being implemented is similar in scope to the CRBRP hockey-stick steam generator program and is the next earliest development underway in the U.S. Correspondingly comprehensive development programs for the coiled-tube, single-wall concept are underway by Holland/Germany, Japan, and France on a schedule ahead of the U.S. program.

Prototype tests of coiled-tube single-wall steam generator designs, roughly equivalent to the early AI test at 30 MW_t of the hockey-stick steam generator, have been carried out at 50 MW_t in the Dutch facility at Hengelo, at 45 MW_t in the French facility at Les Renardier, and at 50 MW_t in the Japanese facility at Oaraii, all at temperatures and pressures approaching those for the Advanced Central Receiver plant. From the information available to the U.S., it appears that, in general, the coiled-tube design has been shown by these tests to perform satisfactorily.

Development of the coiled-tube steam generator concept is continuing intensively abroad because one of the three loops of the SNR-300 LMFBR under construction at Kalkar, Germany, will use coiled-tube units, the MONJU LMFBR plant to be brought into operation in the mid-1980s in Japan will use coiled-tube units entirely, and the SUPER-PHENIX LMFBR plant under construction in France for operation in the early 1980s, will use coiled-tube units.

A 70 MW_t prototype of the coiled-tube design, made of 2-1/4 Cr - 1 Mo, is being designed now and is planned for installation at ETEC for tests beginning in 1983 under DoE sponsorship, after the hockey-stick prototype tests.

Although development of the coiled-tube concept is now at the second level of completion relative to the hockey-stick concept in the U.S., the fact that an intensive DoE-sponsored development has been implemented, on a schedule that is currently only two years behind the hockey stick, plus the major commitment to the coiled-tube steam generator concept by other nations in the LMFBR community, demand that consideration be given to the coiled-tube, single-wall concept as a potentially acceptable alternative to the single-wall hockey-stick concept. The basic feasibility of the coiled-tube concept seems to have been demonstrated and assessment of its economic potential for application to the Advanced Central Receiver plant is now needed.

STRAIGHT-TUBE ALTERNATIVE CONCEPT

The apparent simplicity of the straight-tube, single-wall concept suggests that it may have economies of manufacture relative to both the hockey stick and the coiled-tube concepts. Tests of a straight-tube, single-wall steam generator design using a bellows in the shell to provide for differential expansion between the tubes and the shell were successfully completed at 50 MW_t in the Dutch facility at Hengelo, and two of the three loops in SNR-300 LMFBR will use this design. The French have also tested to some degree a 45 MW_t straight-tube model steam generator at Les Renardier, but have abandoned this design approach in favor of the coiled-tube design concept.

In the U.S., the chief experience with sodium-heated steam generators using straight-tubes was by AI in the 1960s, before it abandoned this approach in favor of the hockey-stick design; by the EBR II in Idaho, which has successfully employed a double-wall, straight-tube design for more than ten years of power operation; and the double-wall, straight-tube steam generator development now in progress at Westinghouse under DoE sponsorship. The only straight-tube steam generator development currently active in the U.S. is the work by Westinghouse on the double-wall concept. The plan for this program includes design and manufacture of a 70 MW_t prototype for test at ETEC. The current plan for the prototype is to begin testing in the ETEC facility in 1985, which places the U.S. schedule for straight-tube, double-wall development about two years behind the coiled-tube development and four years behind the hockey-stick development, assuming an equivalently comprehensive effort on the respective designs.

The promise of the double-wall, straight-tube design is an increase in reliability, specifically in terms of decreasing the likelihood of a sodium-water reaction. It is expected that this would be achieved at the expense of increased manufacturing cost compared to the single-wall designs. Also, it is not evident that such an increase in reliability over the reference single-wall approach will be necessary for the Advanced Central Receiver plant. For these reasons, use of the double-wall concept has not been seriously contemplated for this application.

Although U.S. straight-tube concept development is oriented toward the double-wall concept, it has some general applicability to the single-wall concept also. This applicability, along with the fact that the hockey-stick design under active development is essentially a straight-tube concept (with the bent region rather than a shell bellows used for accommodating differential thermal expansion), places the straight-tube, single-wall concept as a potentially viable candidate for the Advanced Central Receiver plant. This is further substantiated by the successful 50 MW_t test of this concept at Hengelo and the use of it in the SNR-300 LMFBR. Therefore, any comprehensive reevaluation of the steam generator concept selection for the Advanced Central Receiver plant should include consideration of the straight-tube, single-wall design.

☆ U.S. GOVERNMENT PRINTING OFFICE: 1980-640-258/2151